Universidade de Aveiro Departamento de Biologia,
2011

Cornelia Rinn

Grânulos de zimogénio do pâncreas: novas proteínas em locais inesperados

Pancreatic zymogen granules: new proteins in unexpected places

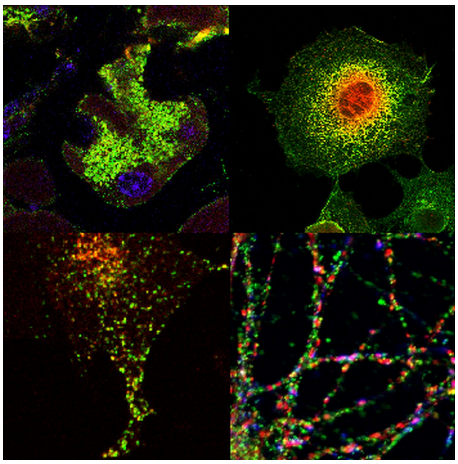

Universidade de Aveiro Departamento de Biologia
Ano 2011

Cornelia Rinn

Grânulos de zimogénio do pâncreas: novas proteínas em locais inesperados

Pancreatic zymogen granules: new proteins in unexpected places

Universidade de Aveiro Departamento de Biologia
Ano 2011

Cornelia Rinn

Grânulos de zimogénio do pâncreas: novas proteínas em locais inesperados

Pancreatic zymogen granules: new proteins in unexpected places

Dissertação apresentada à Universidade de Aveiro para cumprimento dos requisitos necessários à obtenção do grau de Doutor em Biologia, realizada sob a orientação científica do Doutor Michael Schrader, Investigador Principal do Centro de Biologia Celular e do Departamento de Biologia da Universidade de Aveiro

Apoio financeiro da FCT (FCT; SFRH/BD/38629/2007), Centro de Biologia Celular & Departamento de Biologia da Universidade de Aveiro e Universidade de Aveiro

o júri

presidente

Prof. Doutor António Ferreira Pereira de Melo,
Professor Catedrático do Departamento Electronico da Universidade de Aveiro.

Prof. Doutor Amadeu Mortagua Velho da Maia Soares,
Professor Catedrático do Departamento de Biologia da Universidade de Aveiro.

Prof. Doutor Carlos Jorge Alves Miranda Bandeira Duarte,
Professor Associado com Agregação da Faculdade de Ciências e Tecnologia da Universidade de Coimbra.

Prof. Doutora Odete Abreu Beirão da Cruz e Silva,
Professora Auxiliar com Agregação da Universidade de Aveiro.

Prof. Doutora Ana Luísa Monteiro de Carvalho,
Professora Auxiliar da Faculdade de Ciências e Tecnologia da Universidade de Coimbra.

Prof. Doutor Michael Schrader,
Professor Auxiliar convidado Convidado com Agregação da Universidade de Aveiro. (Orientador)

agradecimentos

First of all I would like to thank deeply to PD Dr. Michael Schrader for his trust and support through all my work and for giving me the opportunity to participate in such an interesting and versatile project. I thank him for his patient, supervision and for the many discussions in which he shared his very detailed knowledge about cell biology and microscopy always connecting his knowledge to some little anecdotes making it easy to remember the newly acquired techniques and other details.

Furthermore, I would like to thank Prof. Odete da Cruz e Silva and Prof. Edgar da Cruz e Silva and all members of the Centro de Biologia Celular and the Departamento de Biologia in Aveiro for their big support. I also thank to the University of Aveiro and FCT for their accommodating collaboration and financial support (FCT; SFRH/BD/38629/2007).

Moreover, I would like to thank very much Prof. Dr. Ana Luísa Carvalho and Prof. Dr. Carlos Duarte and also to Dr. Sandra Santos from the University of Coimbra for their cooperation, the kind opportunity to get an inside view into the work of neurosciences and for the very nice atmosphere every time I got to work in their laboratories.

I would like to thank very much Brigitte Agricola and Volkwin Kramer from the University of Marburg for their cooperation in electron microscopy and professional advices.

I would like to thank very much to Maria Gómez-Lázaro and Nina Bonekamp for spending so many hours together with me on the confocal microscope and to Monica Almeida for her help in some tricky experiments.

I very much would like to thank my dear colleagues and friends: Markus Islinger, Daniela Ribeiro, Fatima Camões, Sandra Grille, and Judith Prüssing for a very nice working atmosphere, a lot of very helpful advices and just being themselves.

I very much thank to those friends standing always on my side during all this time in Portugal especially to Aneesh Chauhan, Bruno Pimentel and Inês Castro for many philosophical discussions and making me smile; and to my friends in Germany, especially to Miriam Lauz and Sonja Eckhardt, Sabiene Kloske, Carina Blatt and Zeljka Stojicic.

Finally, I would like to thank very much to my family and to Eduardo's family for so much support and love you have given me through all the time! And of course to Eduardo I thank in love, for always standing by my side, not giving up on me, fighting for me, challenging me, loving me and never losing patience with me!

palavras-chave Proteómica, secreção exócrina e (neuro)endócrina, grânulos de zimogénio do pâncreas, vesículas sinápticas, cérebro, Piccolo, RMCP-1, ZG16p, AR42J

resumo

Os mecanismos de biogénese, distribuição apical e secreção regulada de enzimas digestivas dos grânulos de zimogénio são, atualmente, pouco conhecidos. De modo a esclarecer e descrever estes processos de elevada importância biológica e clínica, é necessária uma melhor compreensão dos componentes da membrana granular e as funções e interações destes. Neste trabalho, através de uma abordagem proteómica, foi possível identificar novas proteínas granulares previamente associadas ao transporte vesicular sináptico. Para estudar as funções destas proteínas na génese e secreção de grânulos, foram realizados estudos de sobre-expressão, assim como estudos bioquímicos (1D, 2D, and LC-MS/MS) e morfológicos, utilizando céluas de mamífero. Entre as proteínas descobertas, cinco foram selecionadas e analisadas: RMCP-1, Piccolo, Synaptojanin-1, APP e ZG16p. Destas proteínas, confirmou-se a presença da RMCP-1 e APP nos grânulos de zimogénio. Interessantamente, o lectin ZG16p da secreção pâncreatico, encontra-se expressa no cérebro de rato, estando localizada nos terminais pós-sinápticos e em grânulos de RNA, indicando uma possível função desta proteína na formação das vesículas sinápticas.

Finalmente, demonstrei que a formação de grânulos de zimogénio pode ser modulada, no modelo de células pancreáticas AR42J, pelas condições de cultura. Em contraste com as proteínas de carga neuroendocrinas, a sobre-expressão de proteínas de carga ou da membrana dos grânulos de zimogénio não foi suficiente para induzir a formação de grânulos ou de estruturas granulares em células constitutivamente secretoras, indicando diferenças na biogénese de grânulos neuroendócrinos e exócrinos.

keywords

Proteomics, exocrine, (neuro)endocrine secretion, pancreatic zymogen granules, synaptic vesicles, brain, Piccolo, RMCP-1, ZG16p, AR42J cells

abstract

The mechanisms of secretory granule biogenesis, apical sorting and regulated secretion of digestive enzymes in pancreatic acinar cells are not yet well understood. In order to shed light on these biologically and clinically important processes, a better molecular understanding of the components of the granule membrane, their functions and interactions is required. Using a proteomics-based approach, novel granule proteins were identified, which have been previously described to be involved in synaptic vesicle biogenesis and trafficking. To elucidate the yet unknown functions of these proteins in zymogen granule biogenesis and secretion, overexpression studies as well as biochemical (1D, 2D, and LC-MS/MS) and morphological methods were applied to mammalian cells. Five proteins identified were selected for further evaluation: RMCP-1, Piccolo, Synaptojanin-1, APP and ZG16p. While RMCP-1 and APP were confirmed to be new zymogen granule proteins, the existence of Synaptojanin-1 and Piccolo in ZGs could not be verified. Interestingly, the pancreatic secretory lectin ZG16p was demonstrated to be expressed in rat brain, localizing to post-synapses and RNA granules suggesting a potential function in synaptic vesicle formation.

I also demonstrated that ZG formation in AR42J cells, a pancreatic model system, can be modulated by altering the growth conditions in cell culture. In contrast to neuroendocrine cargo proteins, overexpression of ZG cargo and membrane proteins was not sufficient to induce ZG formation or granule-like structures in constitutively secreting cells pointing to differences in neuroendocrine and exocrine granule biogenesis.

TABLE OF CONTENTS

List of Figures:

List of Tables:

Abbreviations

Amy	Amylase
APS	ammonium-persulfate
bp	base pairs
BSA	bovine serum albumin
°C	degree Celsius
CBP	carboxypeptidase
cDNA	complementary DNA
Chymo	chymotrypsin
Chym	chymase, rat mast cell chymase1
Coomassie	coomassie brilliant blue
crtl	control
Cyt.	cytosol
d	day
Dexa	dexamethasone
+D	cells stimulated with 10 nM dexamethasone
-D	unstimulated control cells
ddH_2O	double distilled Water (MilliQ grade)
DMEM	Dulbecco's Modified Eagle Medium
DMSO	dimethyl-sulfoxide
DNA	deoxyribonucleic acid
dNTP	2`desoxy-nukleosid-5`-triphosphat
ECL	enhanced chemiluminescence
E. coli	*Escherischia coli*
EDTA	ethylendiamintetraacetic acid
EM	electron microscopy
ER	endoplasmatic reticulum
et. *al*	and others
EtBr	ethidium bromide
FBS	fetal bovine serum
FOY-305	ethyl-4-(6-Guanidinobenzoyloxy)-benzoate
g	Gramm
×g	$\times 9{,}81 m/s^2$
GAPDH	glyceraldehyd-3-Phosphat-dehydrogenase
GFP	green-fluorescent-protein
GPI	glykosyl-phosphatidyl-inositol
h	hours
HEPES	4-(2-hydroxyethyl)-1-piperazineethane sulfonic acid
HMW	high molecular weight
H_2O_2	hydrogen peroxide
HRP	horse radish peroxidase
IMF	immunofluorescence
kDa	kilodalton
L	litre

LB	luria bertani
Lys	lysate
M	molar
m	milli
μ	micro
μm	micro meter
MMLV	*Moloney Murine Leukemia Virus*
mc	monoclonal
min	minutes
MOPS	3-(N-morpholino)-propan-sulfonic acid
mRNA	messenger RNA
NC	nitrocellulose
nm	nano meter
OD	optical density
P	pellet
p. a.	*por analysis*
PAA	poly-acryl-amide
PAGE	poly-acryl-amide gel electrophoreses
PBS	phosphate buffered saline
PBS-T	phosphate buffered saline –Tween-20
pc	polyclonal
PCR	polymerase chain reaction
PEI	poly-ethylene-imine
PFA	*para*-formaldehyde
pH	negative decative logarithm of the H^+ concentration
PMSF	phenyl-methyl-sulfonyl-fluorid
Poly-A	poly-adenylate
rev	reverse
RT	room temperature
RT-PCR	reverse transcription PCR
s	seconds
SDS	sodium dodecyl sulfate
Sh	sheep
SN	supernatant
Snj1	synaptojanin-1
SQ	semi-quantitative
Synphys	synaptophysin
SV	synaptic vesicle
t	time
TAE	tris/acetate/EDTA
Taq	*termophilus aquaticus*
TCA	trichloro acidic acid
TEMED	tetramethylenediamine
TGN	trans-Golgi network
TRITC	tetra-methyl rhodamine isothiocyanate

Tris	tris-(hydroxyl)-aminomethan
Tryp	trypsin
U	unit
UV	ultra violet
V	volt
v/v	volume per volume
WB	western blot
w/v	weight per volume
ZG	zymogen granule
ZGC	zymogen granule content
ZGM	zymogen granule membrane

Chapter 1 INTRODUCTION

1.1 The Pancreas as a Model for Exocrine Secretion

The pancreas is a composite gland of the digestive and endocrine system of vertebrates. The endocrine cells are grouped in the islets of Langerhans occupying approximately 1.5% of the pancreatic tissue being surrounded by the exocrine cells (Figure 1). The endocrine cells produce hormones (*e.g.* insulin, glucagon and somatostatin) and the pancreatic peptide, which are secreted upon stimuli directly into the blood stream, influencing carbohydrate metabolism (Junqueira, Carneiro 1996). The exocrine pancreas, producing mainly digestive enzymes, is structured in lobules which consist of several acinar units of around 20-30 exocrine cells. Attached to a basement membrane, the polarized acinar cells surround the acinar lumen with their apical pole (Figure 1 and Figure 2). As the acinar cells accommodate the typical inventory of secretory cells, the pancreas served as a model to unravel the role of individual intracellular compartments in the secretory pathway (Palade 1975). In particular, acinar cells harbor a constitutive vesicular secretion system directed to both the basal and the apical cellular membrane and a regulated secretion system for the controlled secretion of the digestive enzymes (Burgoyne and Morgan 2003). The basolateral membrane, facing neighboring cells, is responsible for intercellular communication while the apical membrane in acinar cells is responsible for the regulated secretion of digestive enzymes (Barthel, Nickel et al. 1995; Nelson and Yeaman 2001). Thus, to discriminate between proteins destined for the individual secretion systems acinar cells possess elaborated sorting systems to ensure the correct packaging of individual constituents into the proper vesicles.

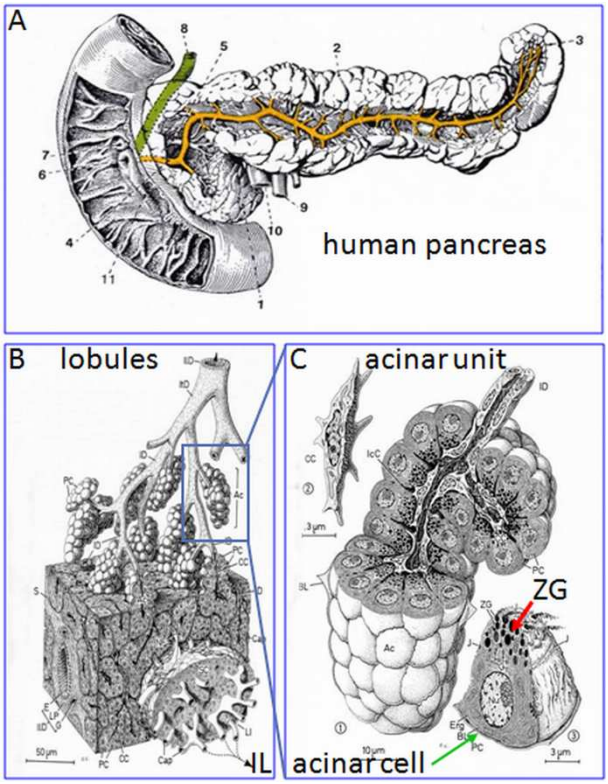

Figure 1: Human pancreas.
(**A**) Human pancreas attached to the duodenum, showing the pancreatic duct system in (yellow). (**B**) Lobules of the pancreas showing acinar units surrounding an islet of Langerhans (IL). (**C**) Acinar units consistent of acinar cells surrounding a lumen. A single acinar cell is marked with a green arrow and the ZG at the apical pole of this acinar cell are marked with a red arrow. (Taschenbuch der Histologie, Georg Thieme Verlag 2009)

Like most secreted proteins the digestive enzymes in acinar cells are synthesized at the strongly developed rough endoplasmic reticulum (rER), pass through the prominent Golgi apparatus and are finally packaged into secretory vesicles termed zymogen granules (ZG) (Figure 3). The ZG contain around 15 to 20 different inactive pro-enzymes with a molecular mass between 13-90 kDa. These hydrolytic enzymes are termed zymogens and can be divided into five functional groups: lipases (pancreatic lipase, pro-phospholipase A2), glycosidases (α-Amylase), endo- and exoproteases (Trypsinogen 1-4, Carboxypeptidase A-D, Chymotrypsinogen 1 and 2, pro-Elastase 1), RNase and DNase. Consequently, acinar cells are highly specialized in the production, sorting and packaging of digestive enzymes and isoenzymes, which are packaged and stored in a condensed and inactive form in relatively large (~1 μm in diameter, Figure 2) granules (Scheele 1993; Borgonovo, Ouwendijk et al. 2006; Dikeakos and Reudelhuber 2007).

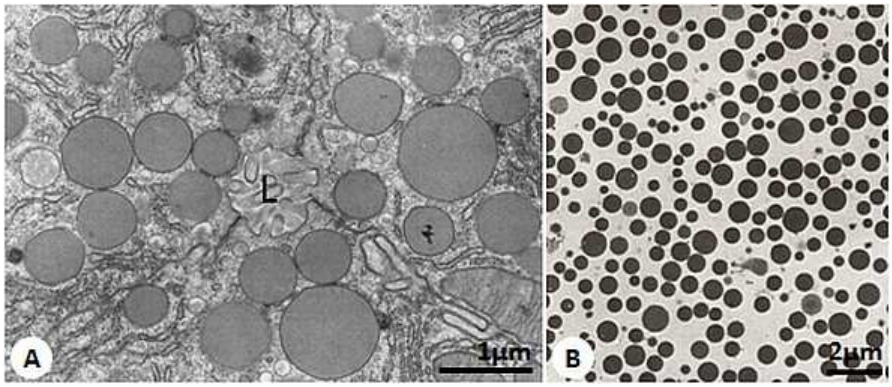

Figure 2: Ultrastructure of zymogen granules.
(**A**) Electron micrograph of ZGs in the apical region of pancreatic acinar cells surrounding an acinar lumen (L). (**B**) Electron micrograph of a crude ZG fraction isolated from rat pancreas.

When required, the zymogens are secreted upon a stimulus via cholinergic neurons of the parasympatic system and the gastrointestinal hormones cholecystokinin (CCK), or secretin (Jamieson and Palade 1971; Williams 2001; Williams, Chen et al. 2009). In pancreatic acinar cells CCK activates multiple signaling pathways through the G protein-coupled receptor, CCK1 (Schnefel, Profrock et al. 1990; Yule, Baker et al. 1999). Activation of CCK1 induces conformational changes in the α-subunit of the associated heterotrimeric G protein thus promoting the exchange of GDP for GTP. GTP-bound Gα dissociates from the complex and activates downstream effectors which stimulate phospholipase C and adenylate cyclase (Sabbatini 2010, Graziano 1987). Finally, phosphoplipase catalyzes the formation of inositol-1, 4, 5-trisphosphate causing an increase in intracellular Ca^{2+} levels (Sabbatini, Bi et al. 2010). Synaptotagmin, which is proposed to act as a clamp, preventing the fusion of docked vesicles and also zymogen granules in the absence of relevant stimuli, ensures that secretion does not occur spontaneously (Poo, Dan et al. 1995; Falkowski, Thomas et al. 2011). Synaptotagmin does that via the inhibition of membrane fusion through an interaction with the SNARE complex (Falkowski, Thomas et al. 2010; Falkowski, Thomas et al. 2011). It is proposed that, (among other factors) upon Ca^{2+} binding, Synaptotagmin dissociates from the SNARE complex, allowing SNAP/NSF interaction to lead to membrane fusion triggering exocytosis (Popov and Poo 1993; Morimoto, Popov et al. 1995).

Proteins secreted at the apical membrane enter the pancreatic duct system and are conveyed to the intestinal lumen. Solubilized in an aqueous, bicarbonate solution secreted by pancreatic duct cells, the enzymes reach the duodenum, where the gastric acid is neutralized by the alkaline secret thus creating an environment allowing effective enzyme activation. First, enterokinase cleaves Trypsinogen into active Trypsin which again converts all remaining enzyme precursors into their active forms thereby priming the break down of carbohydrates, proteins and lipids in the chyme to ensure nutrient absorption by the enterocytes of the small intestine. The physiological importance of this secretion process is illustrated by fact, that along with hepatocytes, the pancreatic acinar cells exhibit the highest rate of protein synthesis among all cells in higher organisms. In the pancreatic acinar cell of the exocrine pancreas, more than 90% of the synthesized proteins are targeted to the secretory pathway (Figure 3) (Scheele, Palade et al. 1978).

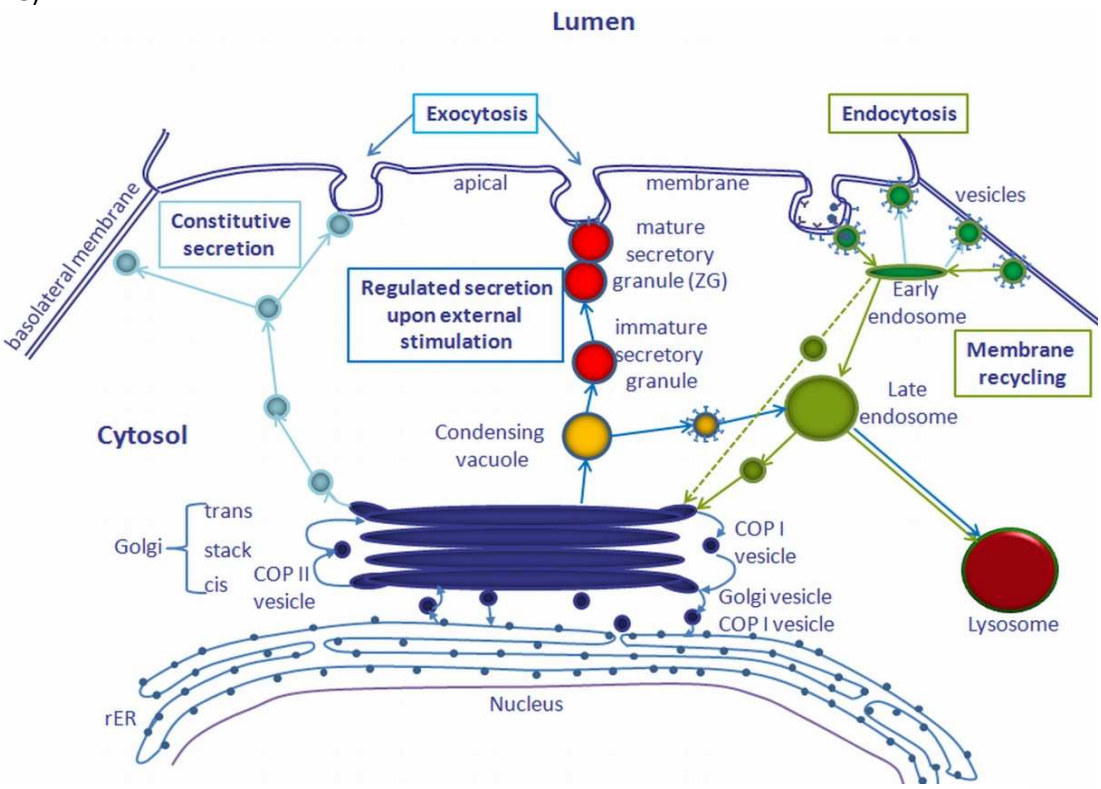

Figure 3: Secretory pathways, exocytosis and endocytosis in eukaryotic cells
The way a protein takes from the rER (blue line, with dots representing ribosomes) through the Golgi complex (blue filled structure) where it is packaged in vesicles and sent to the plasma membrane, is called secretory pathway. A protein can be secreted constitutively (light blue vesicles) but sorted to a specific membrane compartment (apical or basolateral), here indicated by the arrows pointing towards both types of membranes, or it is destined for regulated secretion. In this case, proteins are sorted into condensing vacuoles (yellow) which through a maturation process of selective aggregation bud off vesicles with remote proteins not destined for regulated secretion (constitutive-like secretion, little yellow vesicle) in a clathrin-dependent manner. On its way to the apical membrane, the secretory granule matures to a large dense core granule (red vesicles, ZG) and is stored there until secretion upon an external stimulus. Upon stimulation and increase in Ca^{2+}, a ZG fuses with the plasma membrane. Other ZG may fuse with the first one to discharge their content (compound exocytosis). Rejected proteins are sent to late endosomes (big greenish vesicle) from where they can be transported towards different locations *e.g.* lysosomes (big brown vesicle), or back to the Golgi complex (small greenish vesicles), depending on the protein itself. Membranes can then be recycled via clathrin-dependent endocytosis (little dark green vesicles) from both membrane compartments and are sent back to the Golgi via early endosomes (oval dark green vesicle).

Untimely, pancreatitis a severe and painful inflammation disorder can arise by the activation of digestive enzymes emerging from the pancreatic acinar cells thereby leading to an autodigestion of the organ and eventually surrounding tissue. Pancreatitis has a mortality rate of around 5% in milder versions which, however, can rise to 70% for severe inflammations. Moreover, chronic pancreatitis promotes the development of pancreatic cancer which is one of the most aggressive forms with survival rates between 25% when discovered at an early stage and 6%, depending on the disease state at the time of diagnosis. Missorting to lysosomes or the basolateral membrane are other reasons for pancreatic injury (Gaisano and Gorelick 2009; Husain and Thrower 2009) such as pancreatitis. Thus, understanding how ZG packaging and secretion is controlled and regulated may be a prerequisite to fully understand the etiology of this disorder and to improve and develop new treatments, or to discover and define risk factors which can be explored for diagnosis.

1.2 Protein Sorting: From the TGN to Zymogen Granules

Proteins following the secretory pathway contain a specific ER-sorting signal at the N-terminus of the peptide chain, which is the first part of the protein to be synthesized. Leaving the ribosome, this short sequence is recognized by a protein complex called signal recognition particle (SRP) which then binds to a SRP receptor in the rER membrane by hydrolyzing GTP to GDP. This whole complex transports the growing protein chain to a membrane channel in the rER called translocon. At the translocon, the peptide is fed into the rER lumen where the signal sequence is cleaved and post-translational modifications (*e.g.* formation of disulfide bonds, addition and processing of carbohydrates, folding) are initiated and later completed in the Golgi complex. The sorting of proteins to their destined vesicles takes place at the Trans-Golgi-Network (TGN) according to sorting signals contained in the protein sequence; *e.g.,* the majority of lysosomal proteins are recognized by specific signal patches at the proteins surface and subsequently marked by fusion of mannose 6-phosphate (M6P) residues, allowing their recognition by M6P receptors in the Golgi complex and transport to the endosomal/lysosomal compartment through the involvement of clathrin (Olson, Sun et al. 2010). Others lysosomal proteins are recognized by alternative receptors like LIMP-2 or Sortilin, and lysosomal transmembrane proteins require a specific cytosolic sorting signal (Gough, Zweifel et al. 1999; Braulke and Bonifacino 2009).

The sorting of zymogen proteins into secretory granules diverges from such a common scheme: Sorting starts for most proteins in the TGN through a selective aggregation at a slightly acidic pH (6.5) (Leblond, Viau et al. 1993; Colomer, Kicska et al. 1996; Castle and Castle 1998; Dartsch, Kleene et al. 1998) and high Ca^{2+} levels (Siekevitz and Palade 1966; Chanat and Huttner 1991; Freedman and Scheele 1993) while a few proteins already form complexes in the ER lumen (Tooze, Kern et al. 1989; Kleene, Kastner et al. 1999). It is assumed that the so-formed dense core aggregates associate to specific TGN membrane domains. The aggregates exhibit a distinct protein composition and contain certain zymogens in association with non-enzymatic proteins, which have been proposed to act as “helper” proteins in complex formation, aggregation and/or sorting to the membrane (Kleene, Kastner et al. 1999; Kleene, Classen et al. 2000). While the

selective aggregation is well documented, the interaction with the TGN/ZG membrane mediating the sorting of regulated secretory proteins is poorly understood at the molecular level. In fact, at present neither a sorting signal, nor a sorting receptor has been identified. Two models, an active one known as „Sorting by entry“ and a passive one known as „Sorting by retention“, are discussed but could as well complement each other (Tooze 1998; Borgonovo, Ouwendijk et al. 2006). In the active „Sorting by entry“ model, membrane binding of aggregated secretory proteins is assumed to depend on a “sorting receptor” within the TGN, so that the entry into forming granules is restricted to receptor-mediated trafficking (Figure 4). In the passive „sorting by retention“ model the sorting event is the formation of the aggregates itself. Here, the ZG present the sorting site to which also non-secretory proteins can enter (Figure 4). Non-regulated secreted proteins are then selectively removed from the immature secretory granules (condensing vacuole, CV) through the constriction of small clathrin-coated vesicles (constitutively-like secretion), which leads to zymogen granule (ZG) maturation (Castle 1990; Arvan and Castle 1998; Dahan, Anderson et al. 2005). In addition, it was shown that a proper assembly of lipid microdomains and cholesterol biosynthesis are crucial for the ZG formation at the TGN (Schmidt, Schrader et al. 2001; Gondre-Lewis, Petrache et al. 2006).

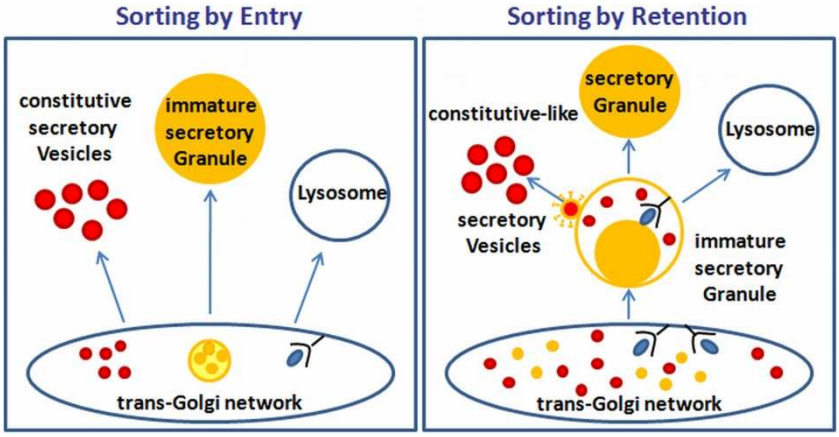

Figure 4: Protein sorting models.

In the active “Sorting by entry” model, aggregated proteins are sorted in the TGN and bind to the ZGM via a specific sorting receptor. In the passive “Sorting by retention” model the ZG present the sorting site in which non-secretory proteins can enter and are selectively removed by constriction of clathrin-coated secretory vesicles (constitutive-like secretion). (Figure taken from Tooze et al. 1998 and modified)

1.3 Sorting and Packaging of Zymogens with the Help of a Submembranous Matrix

As mentioned above, two hypotheses for the sorting of zymogens into ZG are currently discussed: the active “Sorting by entry“ and the passive “Sorting by retention” model. To clarify this issue more information on the interaction between aggregated zymogens and the membranes of the TGN/ZGM is required. Receptors for some major zymogens were postulated (*e.g*. Amylase) but have yet not been identified. As a consequence, the aggregated secretory

proteins may more likely interact with specialized membrane domains or submembranous structures instead with receptors specific for individual enzymes. A network-like structure on the luminal side of the ZGM was already observed by freeze-fracture and deep-etching studies (Cabana, Hugon et al. 1981). Since around 90% of sulfated proteoglycans were found associated with the ZGM and could be released by alkaline sodium carbonate treatment, Scheele et al (1994) postulated the existence of a submembranous matrix at the luminal surface of the ZG. Later studies from Dartsch and colleagues demonstrated that zymogen granule content (ZGC) proteins condense upon an acidic pH of 5.9 and bind to ZG membranes in a condensation-sorting assay (Dartsch, Kleene et al. 1998). More recent findings indicate that membranous or submembranous proteoglycans indeed interact with the zymogens via electrostatic interactions: Muclin, a strongly glycosylated and sulfated membrane protein, was suggested as a potential sorting receptor for aggregated zymogens in ZG (De Lisle 2005). Most likely, muclin binding is mediated via interactions between its negatively charged sulfate groups and positively charged patches on the zymogens in the TGN (Boulatnikov and De Lisle 2004). Moreover, negatively charged proteoglycans in secretory granules of haematopoietic and mast cells have been shown to be involved in the binding and sorting of small positively charged molecules, such as histamine (Brion, Miller et al. 1992; Grimes and Kelly 1992; Castle and Castle 1998) and proteases (Lutzelschwab, Pejler et al. 1997; Huang, Sali et al. 1998), and proteoglycans were found aggregated to the secretory proteins after exocytosis in the pancreatic duct system (Tartakoff, Jamieson et al. 1975; Reggio and Palade 1978). Furthermore, alterations in the glycosylation and sulfation lead to problems in proper zymogen condensation and packaging (De Lisle 2002). Thus, a submembranous matrix was hypothesized to be essential for the shape and stability of ZG (Schrader 2004), mediating protein sorting, packaging and ZG biogenesis (Matsumoto, Sali et al. 1995; Forsberg and Kjellen 2001).

To fully understand how the export proteins are selected and discriminated from Golgi-resident proteins it is indispensable to identify the molecular components of the submembranous matrix and characterize their linkage to the granule-surrounding membrane. Peripheral membrane proteins identified in ZG are: the secretory lectin ZG16p, ZG29p (Kleene, Zdzieblo et al. 1999), Syncollin (Kalus, Hodel et al. 2002), the serpin ZG46p (Chen, Cronshagen et al. 1997) and GP3, a glycoprotein which is secreted into the pancreatic juice (Wagner, Wishart et al. 1994). In a condensation-sorting assay these components have been identified as sulfated proteoglycans and glycin-rich glycoproteins, which *in vitro* are able to link aggregated zymogens to the ZGM (Schmidt, Dartsch et al. 2000; Schmidt, Schrader et al. 2001). In a recent proteomics study, the proteoglycans glypican-4-heparansulfate-proteoglycan, proteoglycan-2 and Syndecan 4 were identified in a ZG fraction (Rindler, Xu et al. 2007). Sulfated proteoglycans were also found in many other cellular compartments (endosomes, lysosomes and the nucleus) but especially in storage granules of immunosecretory cells (Gallagher, Hall et al. 1986; Kolset and Gallagher 1990; Prydz and Dalen 2000). (Glycosylphosphatidylinositol) GPI- anchored membrane proteins like *e.g.* GP2 were found to be associated to a scaffold of sulfated proteoglycans (Kleene, Dartsch et al. 1999; Schmidt, Dartsch et al. 2000; Schmidt, Schrader et al. 2001). The GPI-anchor is supposed to integrate into lipid microdomains of the ZGM (Figure 5, Schmidt, Schrader et al. 2001). It was found that the submembranous matrix is associated with lipid microdomains, which are rich in cholesterol and sphingolipids (Schmidt, Schrader et al. 2001; Kalus, Hodel et al. 2002). Apparently,

the depletion of cholesterol leads to a disturbance in lipid microdomain formation which in turn inhibits granule formation (Schmidt, Schrader et al. 2001) and is leading to a miss-sorting of zymogens into the constitutive secretion pathway (Schmidt, Schrader et al. 2001; Kalus, Hodel et al. 2002). These findings were supported by a study in a mouse model with a cholesterol synthesis deficiency leading to a strong reduction in the number of secretory granules in the pancreas (Gondre-Lewis, Petrache et al. 2006). The few remaining granules, however, had an abnormal morphology and a reduced regulated secretion which could be restored through the addition of exogenous cholesterol. Further, the insertion of cholesterol precursors in artificial membranes led to a decreased membrane curvature, emphasizing the importance of cholesterol in granule biogenesis (Gondre-Lewis, Petrache et al. 2006).

In summary, there is increasing evidence that the submembranous matrix is involved in the sorting of zymogens in the TGN due to electrostatic interactions with the proteins to be exported and may act as a mechanic support for the generally formation of membrane curvature at the TGN thereby stabilizing the granule structure.

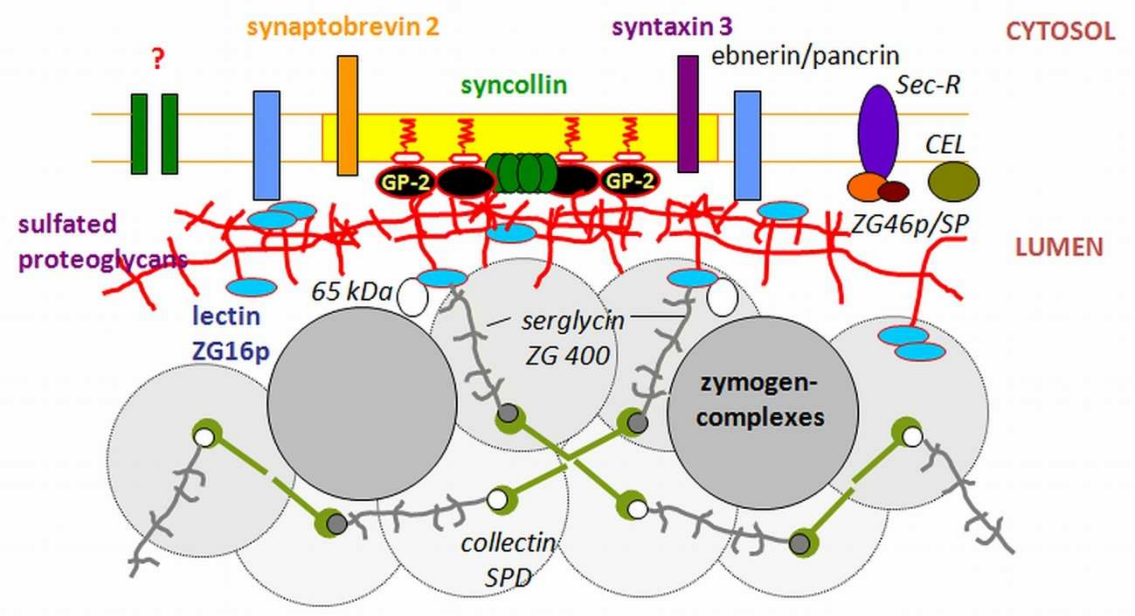

Figure 5: Submembranous matrix model (Kalus et al 2002, Schrader 2004)
Lipid microdomains (yellow) in the ZGM and associated components like the GPI-anchored glycoprotein GP2 (black ovals), may be involved in the binding of a submembranous protein matrix (red) composed of proteoglycans, glycoproteins and lectins (*e.g.,* ZG16p in light blue). Additional components are the SNARE proteins syntaxin 3 and synaptobrevin 2. Syncollin binds to membranes in a cholesterol-dependent manner and forms homo-oligomers. A hypothetical 'core' domain containing highly-ordered lipids is indicated.

1.4 Zymogen Granule Exocytosis

Mature ZG are transported along microtubules towards the apical plasma membrane and then transferred to a subapical actin network guiding to the fusion site (Ishihara, Sakurai et al. 2000; Ueda, Ohnishi et al. 2000; Valentijn, Valentijn et al. 2000). This step requires dynein,

dynactin and myosin motor proteins that were recently identified by proteomics studies of zymogen granule membrane (ZGM) fractions (Chen, Walker et al. 2006; Rindler, Xu et al. 2007). Until a hormonal or neuronal stimulus leads to an increase of intracellular Ca^{2+} concentrations which triggers the exocytosis of the ZG content into the pancreatic duct system (Williams 2001; Williams, Chen et al. 2009), the ZGs are stored underneath the apical plasma membrane. Despite intensive studies, the exact mechanism for ZG exocytosis is not yet clear since *e.g.* no Ca^{2+} sensor has been identified. However, some information about proteins mediating the ZG fusion with the plasma membrane starts to emerge (Wasle and Edwardson 2002; Williams, Chen et al. 2009; Falkowski, Thomas et al. 2011). Several soluble N-ethylmaleimide-sensitive factor-activating protein receptor (SNARE) proteins, as well as Rab GTPases and aquaporins are suggested to be involved in granule docking, priming, swelling and exocytosis (Chen, Edwards et al. 2002; Cho, Sattar et al. 2002; Riedel, Antonin et al. 2002; Chen, Li et al. 2004; Faust, Gomez-Lazaro et al. 2008; Williams, Chen et al. 2009; Gomez-Lazaro, Rinn et al. 2010). Partially, the localization of these proteins to ZG was confirmed in recent proteomic studies (Chen, Walker et al. 2006; Rindler, Xu et al. 2007; Chen, Ulintz et al. 2008) but further functional evaluation is required to clarify the role in the excretion process. It was proposed that the ZG membrane connects and fuses temporally to specific plasma membrane structures called “Porosomes” (Jeftinija 2006) and that the ZG release their content upon an increase of intra-vesicular pressure after vesicle swelling (Cho, Sattar et al. 2002; Kelly, Abu-Hamdah et al. 2005; Sugiya, Matsuki-Fukushima et al. 2008). Furthermore, in a process called compound exocytosis, granules with a more basal location may fuse with more apically positioned granules that are intermittently in contact with the plasma membrane (Thorn, Fogarty et al. 2004; Pickett and Edwardson 2006). This homotypic fusion is supposed to be mediated by the SNARE protein Syntaxin 3 on the ZG membrane (Hansen, Antonin et al. 1999). The fusion of ZG with the plasma membrane is transmitted by an actin meshwork and lasts several minutes (Nemoto, Kojima et al. 2004; Thorn, Fogarty et al. 2004). ZG membranes are then recycled in two steps: first by constriction of patches from the primary ZG fused to the plasma membrane (Thorn, Fogarty et al. 2004) and then by endocytosis of integrated ZGM material in the plasma membrane through clathrin-coated vesicles.

1.5 Biogenesis and Secretion of Secretory Granules in (Neuro)Endocrine Cells

In (neuro)endocrine cells, regulated secretory proteins (RSP) can be divided into soluble, aggregating proteins and membrane-bound proteins (Pimplikar and Huttner 1992; Yoo 1993) which are packed in secretory granules (SG). The accepted model of SG biogenesis comprises four distinct steps ultimately leading to the formation of mature secretory granules (MSGs). These are (1) aggregation of the RSP and its sorting at the TGN membrane, (2) budding from the TGN, (3) homotypic fusion of immature SGs, and (4) remodeling of the immature SG membrane and contents as depicted in Figure 6, (Tooze, Martens et al. 2001; Inomoto, Umemura et al. 2007). The interaction of the soluble RSPs with specialized membrane domains of the TGN and membrane bound RSPs induces an association into oligomers which subsequently leads to the formation of immature secretory granules (ISG) at the TGN (Arvan and Castle 1998; Tooze 1998). Like in ZG

maturation this aggregation process is pH-dependent (secretory granules provide a pH of 5.5) and occurs in a calcium-dependent manner (Ozawa and Takata 1995; Yoo 1995). In contrast to ZG, however, a submembranous matrix based on a proteoglycan scaffold seems to lack in secretory granules. Instead, several different sorting domains were identified on cargo proteins. Granins (chromogranins and secretogranins) are regulated secretory proteins ubiquitously found in the cores of amine-, peptide hormones and neurotransmitter dense-core secretory granules (Huttner, Gerdes et al. 1991). It is assumed that these acidic proteins support the formation of aggregates and assist in the sorting of pro-hormones (Huttner and Natori 1995). Granins exist as membrane bound forms, interacting with soluble proteins probably as "nucleation receptors" during aggregation (Tooze, Martens et al. 2001). In addition, it was also demonstrated that overexpression of CgA and B as well as of Secretogranin II and POMC induces the formation of granule-like dens-core structures in non-(neuro)endocrine cells such as COS-1 and COS-7 (Kim, Tao-Cheng et al. 2001; Huh, Jeon et al. 2003; Beuret, Stettler et al. 2004; Inomoto, Umemura et al. 2007; Stettler, Beuret et al. 2009). For chromogranin A (CgA) and B (CgB) and for the pro-opiomelanocortin (POMC), a disulfide-bonded loop at the N-terminus has been identified as a signal for sorting into ISGs (Chanat, Weiss et al. 1993; Cool, Fenger et al. 1995; Kromer, Glombik et al. 1998). Disruption of these loops leads to mistargeting into the constitutive pathway as was described for CgB (Chanat, Weiss et al. 1993). The capacity of granins to sort proteins by their incorporation into aggregates is supporting the model of "Sorting by entry", previously explained in section 1.2.

SGPs such as CBP-E or Secretogranin III bind to cholesterol-rich membrane domains at the TGN/SG. Both proteins were shown to function as sorting receptors for peptide hormones (Loh, Snell et al. 1997; Rindler 1998; Han, Suda et al. 2008; Takeuchi and Hosaka 2008), via recruition of granins to the SG membrane (Cool, Normant et al. 1997; Normant and Loh 1998; Park, Koshimizu et al. 2009; Hosaka and Watanabe 2010). Based on these informations, it was suggested that neuroendocrine cells combine "Sorting by entry" and "Sorting by retention"-like mechanisms for the sorting of peptide hormones and the biogenesis of secretory granules (Takeuchi and Hosaka 2008).

Besides the role of cholesterol rich membrane domains and lipid microdomains as anchor regions for SG membrane receptors, these domains were also shown to be involved in membrane curvature, budding, fission and apical targeting (Ikonen and Simons 1998; Thiele and Huttner 1998; Huttner and Zimmerberg 2001; Tooze, Martens et al. 2001). It was demonstrated that the depletion of cholesterol by lovastatin inhibits the formation of POMC containing ISGs and constitutive vesicles from the TGN (Wang, Thiele et al. 2000). At present, it is still not clear if SG possess only a single or multiple types of lipid microdomains. However, findings of Blazquez and Thiele (2000) point to the existence of multiple lipid domains as they demonstrated that the pro-hormone convertase 2 associated with detergent-insoluble rafts together with the granule protein GPIII (Palmer and Christie 1992), whereas CgA did not. Additionally, different sorting domains have been identified on several RSPs such as on the pro-peptide somostatin (Stoller and Shields 1989) and PC5-A (De Bie, Marcinkiewicz et al. 1996) but no common structural sorting motif emerged from these studies.

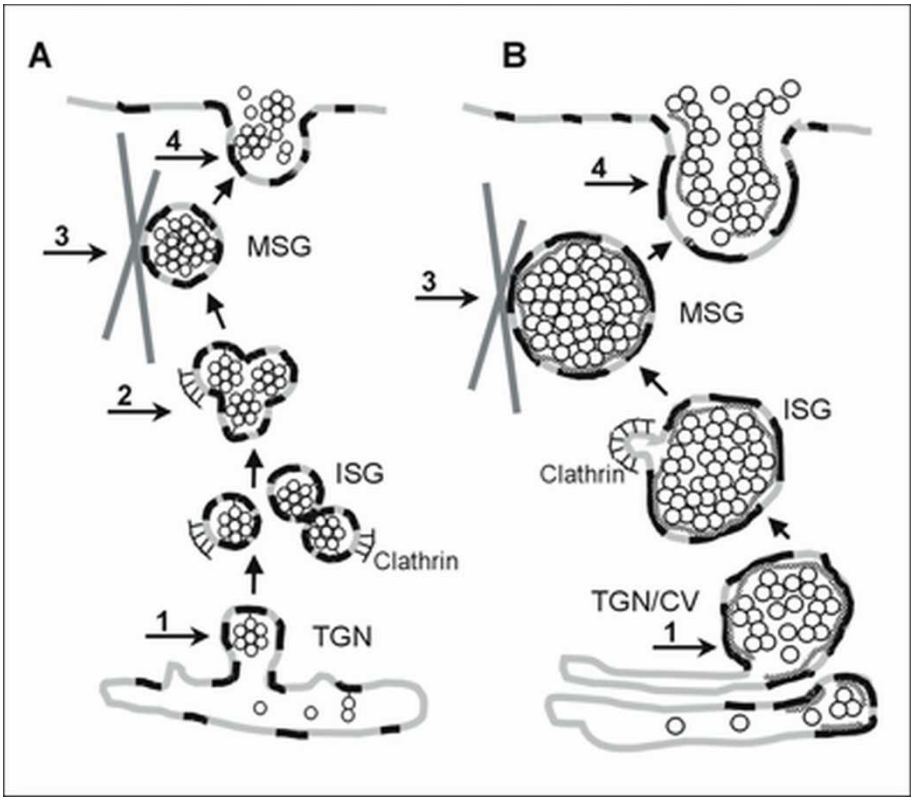

Figure 6: Biogenesis of secretory granules in neuroendocrine and exocrine cells.
(**A**) Formation, homotypic fusion, maturation/remodelling and exocytosis of secretory granules in neuroendocrine cells. In neuroendocrine cells immature secretory granules (ISG) mature (MSG) through "homotypic fusion" (2) and removal of clathrin coated vesicles (CCV) containing non-regulated secretory proteins. (**B**) Formation, maturation/remodelling and exocytosis of secretory granules in the acinar cells of the exocrine pancreas. In exocrine cells maturation of ISG to MSG occurs only through constriction of CCV. The sorting and association of the regulated secretory proteins (RSP) succeeds most likely over a submembranous matrix (dark gray line). In both cell types, „lipid rafts"(black lines) participate in the sorting of the RSP, the transport of secretory granules (by binding to the cytoskeleton (3)) and in the fusion with the plasma membrane (4). (Taken from Schrader 2004)

In contrast to ZGs, SGs fuse homotypically with each other to mature after leaving the TGN. The (t)-SNARE (*s*oluble N-ethylmaleimide-sensitive-factor attachment receptor) protein Syntaxin 6 (Syn6) was identified as a component of the core machinery of the homotypic fusion of ISG (Wendler, Page et al. 2001) but is not incorporated into mature SGs. Interestingly, Syn6 associates to the (t)-SNAREs SNAP25, SNAP29/GS32 and also to the (v)-SNARE VAMP4, but none of these proteins were found to be involved in the homotypic fusion process. These findings rather point to a fusion mediated by forming t-t SNARE interactions between Syn6 molecules on the opposing vesicles (Wendler, Page et al. 2001). Other proteins found to be involved in this process are Rab3D (Riedel, Antonin et al. 2002) and Synaptotagmin IV (Syt-IV) (Ahras, Otto et al. 2006). It was found that the cytoplasmic domain of Syt-IV binds specifically to Syn6 on ISGs but not to MSGs, inhibiting homotypic fusion. Moreover, the depletion of Syt-IV prevents the activation of PC2 thus reducing the processing of secretogranin II (Ahras, Otto et al. 2006). The next step of SG maturation is the formation of clathrin-coated vesicles (CCVs) from immature SGs

(ISGs) to remove non-secretory proteins. The clathrin adaptor GGA (Golgi-associated-gamma-ear-containing, ADP-ribosylation factor-binding protein) was found to be essential for the budding of CCVs from ISGs (Kakhlon, Sakya et al. 2006). Its depletion resulted in the retention of VAMP4 and Syn6 in MSGs and led to the inhibition of the autocatalysis of PC2 and as well prevented the processing of secretogranin II to its product p18.

As a result of the two maturation steps (homotypic fusion and CCV budding), highly ordered dense core granules are formed, which are much smaller than ZG but larger than the initial ISGs. The MSGs are finally transported along microtubules towards the apical cell membrane. MSGs are than stored to fuse with the apical plasma membrane via exocytosis, (Figure 6 A), upon a Ca^{2+} or secretagogeous stimulus (Wendler, Page et al. 2001).

1.6 ZGM Associated Proteins

A group of proteins identified in ZG (which include the glycoprotein GP2, the lipase GP3, the lectin ZG16p, Syncollin, Syntaxin 3 and supposedly also Synaptobrevin 2) interact with lipid microdomains in the ZGM on the submembranous granule matrix. The major ZGM protein GP2 binds to the ZG membrane with the help of its GPI-anker, as shown in Figure 5, but also a soluble form was identified (Rindler and Hoops 1990; Fukuoka, Freedman et al. 1992). Although until now no essential function for GP2 in ZG biogenesis could be confirmed (Dittie and Kern 1992; Schmidt, Schrader et al. 2001; Yu, Michie et al. 2004), a new role in host defense by binding bacterial fimbriae has recently been proposed (Yu and Lowe 2009). GP2 was also identified as a transcytotic receptor on M cells for type-I-piliated bacteria in the process of mucosal immune response (Hase, Kawano et al. 2009). The GP2 homologue uromodulin/Tamm Horsfall protein was also identified as a possible soluble receptor for bacteria in order to remove them from the urogenital system (Bates, Raffi et al. 2004; Mo, Zhu et al. 2004). Similar to GP2, also Syncollin, another membrane-bound ZG protein, was identified in pancreatic juice in a soluble form (Kalus, Hodel et al. 2002; Gronborg, Bunkenborg et al. 2004). Even though Syncollins` function is not yet known, it may be required for sorting/packaging of zymogens as well as for granule formation, since it is part of the submembranous matrix. It was hypothesized that Syncollin might be involved in signal transduction processes across the granule membrane and thus in the regulation of granule maturation (*e.g*. via membrane pores) and/or exocytosis of secretory proteins via lipid microdomains (Schrader 2004).

The Zymogen Granule Protein ZG16p

The secretory lectin ZG16p is a 16 kDa protein that belongs to the Jacalin lectin family due to its sequence similarities to the carbohydrate recognition domain of the plant lectin Jacalin from jack fruit (which specifically binds to Galβ1-3GalNAc) (Cronshagen, Voland et al. 1994; Kleene, Dartsch et al. 1999; Kanagawa, Satoh et al. 2011). Lectins are carbohydrate binding proteins with a high specificity to individual or groups of mono- or oligosaccharides (Barondes 1988; Gabius, Andre et al. 2002). In animals, lectins play important roles in cell adhesion, maintenance of

membrane polarization, the recognition of pathogens (innate immune system), glycoprotein synthesis and in various protein trafficking/sorting processes (Dodd and Drickamer 2001; Delacour, Koch et al. 2008; Pearse and Hebert 2010; Svajger, Anderluh et al. 2010; Tanne and Neyrolles 2010; Butterfield and Owen 2011).

Figure 7 shows a phylogenetic tree, compiled of the ZG16 sequences available at the ncbi protein database. For a better overview, the tree was partially organized in subgroups such as primates or rodents. Branches marked in green represent ZG16p homologues in various species including mammals, reptiles and fishes. The blue branch represents the least related sequence shown in this tree coming from the green sulfur bacteria (*prosthecochloris aestuarii*). The gray branches illustrate the distribution of the ZG16p homologue PAUF/ZG16b. ZG16b/PAUF is to 30% identical to ZG16p; 18% of the amino acids are conserved substitutes and around 14% are functionally conserved amino acids (see alignment in Appendix, Rinn, Aroso et al. 2011). In humans, the paralog ZG16b/PAUF (Pancreatic Adenocarcinoma Up-regulated Factor) was recently reported to play a role in gene regulation and cancer metastasis (Kim, Lee et al. 2009; Lee, Kim et al. 2010).

A multiple sequence alignment restricted to mammalian sequences reveals that ZG16p is highly conserved among mammals: 70% of the amino acids are homologue, 25% are identical and only 5% of the amino acids do not relate to each other (Figure 8). ZG16p shares sequence homologies, specifically at the C-terminus, with two secretory proteins from other exocrine glands, prostatic spermine binding protein and common salivary protein 1, possibly belonging to a group of evolutionary related proteins (Cronshagen, Voland et al. 1994).

For the human proteins ZG16p and ZG16bp, the crystal structure was recently resolved (Kanagawa, Satoh et al. 2011): both proteins harbor a β-prism fold of 3 β-sheets, each consisting of 3-4 β-strands forming three Greek motifs similar to jacalin related mannose-binding type lectins (Kanagawa, Satoh et al. 2011). The N-terminal parts of ZG16p and ZG16bp contain each an ER-targeting signal. Kanagawa et al. (2011) suggested that the sugar-binding capacity of ZG16p originates from three different loops (GG-loop, recognition loop, and binding loop) all situated on top of the β-prism fold which act together as one motif (Figure 9). This motif is well conserved and is shared by all mannose-binding-type Jacalin-related lectins (Kanagawa, Satoh et al. 2011). In addition, a positively charged basic patch of lysine and arginine residues, which may bind sulfated groups of GAGs, is located around the putative sugar-binding site of ZG16p and ZG16bp. ZG16p has also been found to associate with cholesterol-glycosphingolipid-enriched microdomains in the ZGM together with GP2 and sulfated proteoglycans (Schmidt, Schrader et al. 2001). In addition, a tightly membrane-associated form of about 32 kDa, presumably a dimer, has been identified (Kleene, Dartsch et al. 1999; Kalus, Hodel et al. 2002). However, the ZGM association of ZG16p was not influenced in GP2 knock-out mice (Yu, Michie et al. 2004). Pretreatment of ZGM with anti-ZG16p antibody or with chondroitinase ABC in an *in vitro* condensation-sorting assay (Dartsch, Kleene et al. 1998) inhibited the binding of aggregated content proteins to the membrane by about 40-50% whereas pretreatment with anti-Amylase antibody had no significant effect (Kleene, Dartsch et al. 1999). Competition experiments with mono- and disaccharides showed that the addition of 10 mM galactose had only a weak inhibitory effect on condensation-sorting (Kleene, Dartsch et al. 1999).

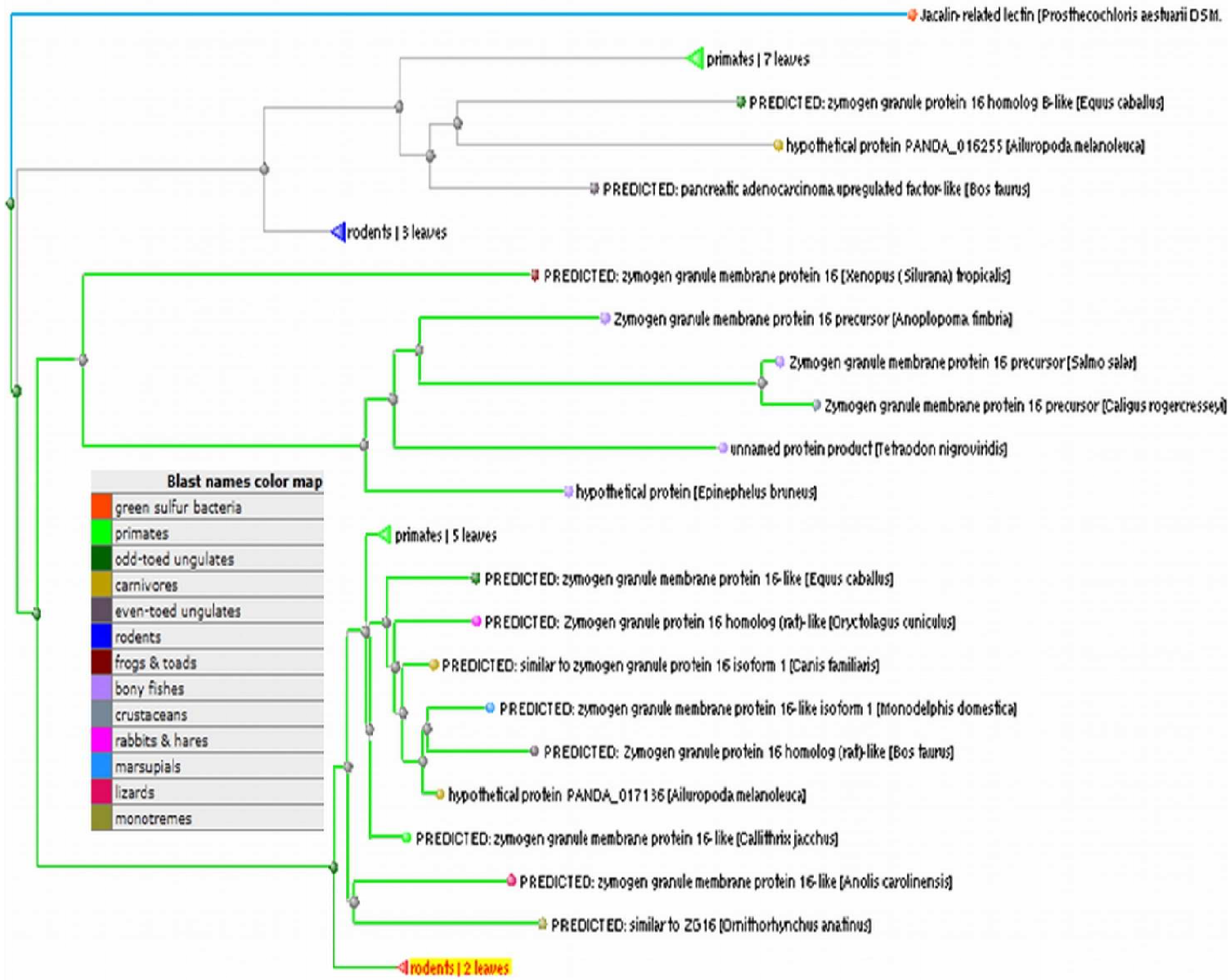

Figure 7: Phylogenetic tree for ZG16p.
In a sequence alignment for ZG16p using the rat ZG16p sequence Q8CJD3, marked in red, as start sequence, 105 sequences similar to rat ZG16p were found using the BLAST pairwise alignments for proteins from NCBI. After removing duplicates, 46 sequences were left, originating in bacteria, plants to reptiles, fishes and mammals. These 46 sequences were chosen to be aligned with each other to compile a Phylogenetic tree using the BLAST tree view tool from NCBI. The green branches mark homologues of ZG16p found in various species. Gray branches mark the ZG16B paralog also found in various species, and blue marks the least related sequence from the green sulphur bacteria. Plant sequences were excluded from the tree due to the chosen parameters (see section 3.11).

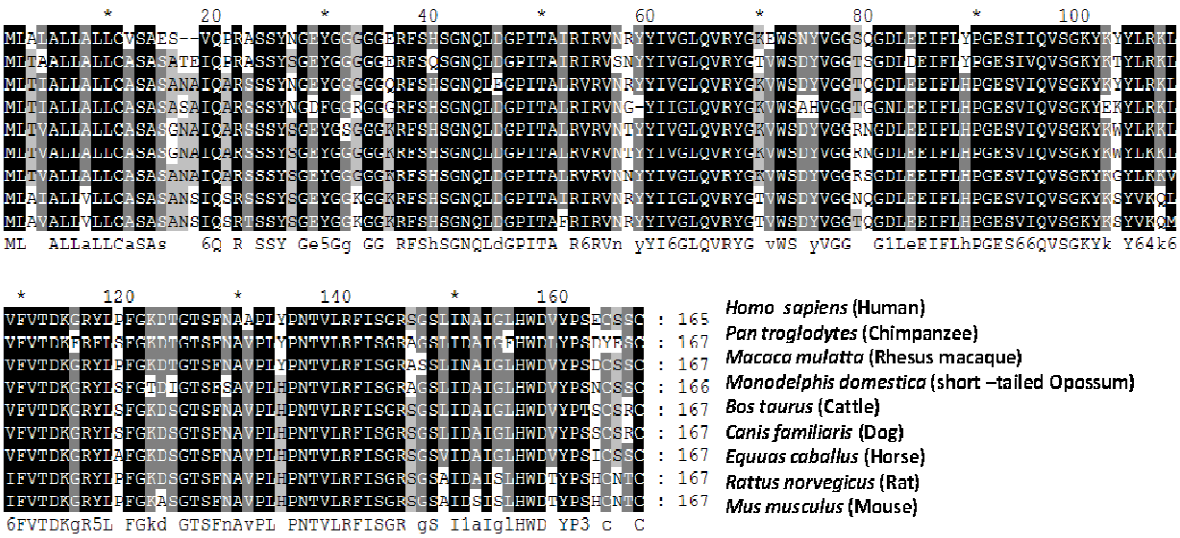

Figure 8: ZG16p is highly conserved in mammals.
The alignment was compiled using Clustal X2, and Genedoc was used for the graphical layout. Selected sequences for human, rat, mouse, chimpanzee, rhesus monkey, opossum cattle dog and horse were aligned with each other. The selected sequences show a 70% homology with each other (black highlighted amino acids) and from the remaining 30%, 25% are highly conserved (amino acids highlighted in gray).

Thévenod and co-workers proposed an additional function of ZG16p in the regulation of a K^+ conductance in ZG (Braun and Thevenod 2000). They suggested a regulatory role for ZG16p in the direct coupling between granule fusion to the plasma membrane and the activation of channels in the ZGM (Thevenod 2002). It was already proposed that anion-cation channels might promote a "flushing out" of the granule content (i.e., enzymes or mucins) during exocytosis in pancreatic acinar cells and in intestinal goblet cells (De Lisle and Hopfer 1986; Guo, Merlin et al. 1997). In fact, goblet cells use two types of secretion (apocrine and merocrine), depending on the type of stimuli they receive. Mucus secretion occurs by fusion of secretory vesicles to the plasma membrane causing the release of the mucins (merocrine) through an exchange of Ca^{2+} for Na^+ and a cellular volume increase up to 600 fold (Perez-Vilar 2007; Rogers 2007). It is speculated that a similar mechanism may take place after an initial, fusion pore-mediated granule swelling by the granule matrix, including ZG16p (Thevenod, Anderie et al. 1994; Thevenod 2002). Furthermore, it was found that the expression of ZG16 mRNA in the rat pancreas is only moderately affected by a hormonal treatment with cholecystokinin (CCK) or cerulein (Cronshagen, Voland et al. 1994). Both peptide hormones are known to evoke a complete release of ZG and to upregulate expression and transport of zymogens (Wang and Cui 2007). On the other hand, a repeated treatment of mice with supraphysiological doses of CCK over 2 weeks, causing pancreatitis, led to a short term down regulation of ZG16 mRNA in the pancreas (Neuschwander-Tetri, Fimmel et al. 2004). In dexamethasone-treated AR42J cells, a pancreatic model system, a strong upregulation of the ZG16 mRNA was observed already after 24 hours (Cronshagen, Voland et al. 1994). Additionally, an immunohistochemical staining and northern blot analysis of several rat organs revealed the presence in duodenum and colon, where ZG16p was found to localize to mucus-producing goblet cells (Cronshagen, Voland et al. 1994). In a study involving biomaterial patches sutured onto rat stomach, ZG16p mRNA was found to be slightly upregulated (together with Amylase and lipase

mRNA) already under control conditions (surgery without implant) and to a higher extent with implant (Lobler, Sass et al. 2002). In a study about differentially expressed genes in the rat ileum used for bladder augmentation, ZG16 was found in a cDNA microarray to be transiently increased compared to normal ileum after 1 and 3 months post-surgery (Miyake, Hara et al. 2004). By RT-PCR and immunoblotting, ZG16p was shown to be expressed in human liver and to be down regulated in hepatocellular carcinoma. Down-regulation appears to be a consequence of the hepatic cancer rather than the cause (Zhou, Cao et al. 2007). Overexpression of ZG16p in some hepatoma cell lines inhibited cell proliferation or cell cycle progression (Zhou, Cao et al. 2007). In a study on hepatotoxicity of pharmaceutical xenobiotics, rat ZG16 mRNA level doubled under the influence of the hepatotoxic substance ANIT (α-napthylisothiocyanate) (Jessen, Mullins et al. 2003). Finally, in a rat cDNA hybridization array, ZG16 was found to be 3 times upregulated after a post commissural fornix transfection, during axonal regeneration, being associated to axonal regeneration failure (Kury, Abankwa et al. 2004). Another study found the ZG16 gene located in an area of chromosomal microduplication (16p11.2), which has been related to several clinical conditions, like childhood neurodevelopmental disorders, mental retardation, schizophrenia and others (Bedoyan, Kumar et al. 2010). Very recently, human ZG16p was demonstrated to bind to pathogenic Candida and Malassezia species heavily coated with mannan. Since ZG16p was detected in mucus-producing cells such as serosanguineous acinar cells of the parotid gland, acinar cells of the pancreas, and goblet cells of the intestine, which are involved in self-defense against invading pathogens, these observation imply a role of ZG16p in the recognition of pathogenic fungi through unique specificity to polyvalent mannose, which is a key signature of non-self microorganisms in the digestive system (Tateno, Yabe et al. 2011). Remarkably, two other structurally different C-type lectins - PSP (Pancreatic Stone Protein) and PAP (Pancreatitis associated Protein) - found in ZG (and pancreatic sections) exert anti-inflammatory, anti-apoptotic, proliferative, and antibacterial effects (Iovanna and Dagorn 2005; Moniaux, Song et al. 2011). Thus, ZG16p may as well be involved in other cellular functions potentially depending on its sugar-binding lectin domain.

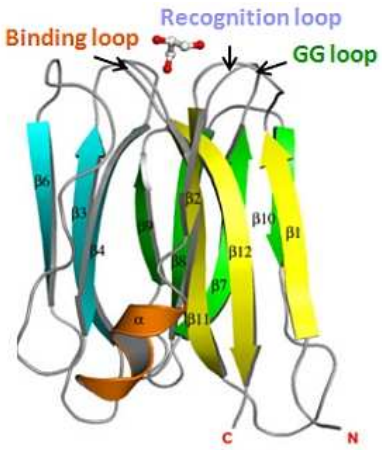

Figure 9: ZG16p protein structure with sugar binding motifs adapted from Kanagawa et al

1.7 The Importance of Proteomics Studies for the Architecture of ZG

Zymogen granules are well-suited for subcellular (and suborganellar) proteomics, as they are abundant organelles of the exocrine pancreas, which can be easily isolated and purified, owing to their large size and density. In addition, their isolation yields large quantities of organelles and proteins (Gomez-Lazaro, Rinn et al. 2010). Furthermore, intact ZGs can be lysed and further separated into a ZG content (ZGC) and ZGM fraction. The ZGM can then be further separated in fractions enriched in peripheral or integral membrane proteins.

Through several different proteomics approaches such as 2D-SDS PAGE, doubled-SDS-PAGE and Shot gun-LC-MS/MS, more and more putative ZGM and ZGM associated proteins have been identified. Chen et al. (2006) applied an experimental approach combining either 2D-SDS PAGE or 2D-liquid chromatography with tandem mass-spectrometry to identify further ZGM proteins. To increase the probability to identify new integral ZG membrane proteins, the membranes were treated with potassium bromide and carbonate. However, neither treatment allowed the identification of hitherto unknown integral membrane proteins; rather ZG content proteins such as Amylase, enzymes of the lipid metabolism and peripheral ZGM proteins (*e.g.* Syncollin) were detected (Chen, Walker et al. 2006). These data were partially confirmed by another LC-MS/MS study, where a similar set of proteins was identified as lipid-microdomain associated proteins (Berkane, Nguyen et al. 2007). Rindler et al (2007) analyzed individual ZG subfractions in a LC-MS/MS approach in order to gain information on the suborganellar distribution of individual ZG proteins thus intending a reconstruction of the ZG architecture. Chen et al (2008) improved this assignment of proteins to individual ZG subfractions by a quantitative MS-approach using the isobaric tag for relative and absolute quantification (iTRAQ) method (Chen and Andrews 2008). With this subtractive proteomic method, protein quantities in individual fractions can be compared enabling to discriminate between enriched proteins and contaminations from other fractions. Comparing normally isolated subfractions with samples digested by trypsin before organelle lysis even enabled to partially distinguish between cytosolic and luminal attached proteins (Chen and Andrews 2008; Chen and Andrews 2009).

These recent proteomics studies generated a huge list of new candidate ZG proteins including GTP-binding and transmembrane proteins, ion channels and transport proteins. Up to now only a very small percentage was confirmed by alternative methods (*e.g*. Carboxypeptidase D, SCAMP 1, Tm63A, Pantophysin, PpiB and Chymase) (Rindler, Xu et al. 2007; Chen and Andrews 2008; Faust, Gomez-Lazaro et al. 2008; Borta, Aroso et al. 2010). Especially the number of small GTPases associated to ZG largely increased (from the previously known eight to approximately twenty three) implying their involvement in ZG biogenesis, trafficking and secretion (Gomez-Lazaro, Rinn et al. 2010). Small G-proteins are supposed to regulate each of the four major steps involved in membrane trafficking: vesicle/granule budding, delivery, tethering and final fusion with the target membrane. The majority of the newly identified small G-proteins have not been subjected to further functional studies, but some have been validated by immunodetection. Functional studies (including expression of mutated proteins, knockdown by siRNA and generation of knockout mice) have so far been performed on Rab3D, Rab27B, Rab8A and Rap1 (reviewed in, Williams, Chen et al. 2009). Rab8A is the only Rab protein so far implicated to act in an early stage of ZG formation (Faust, Gomez-Lazaro et al. 2008).

Furthermore, several integral membrane proteins of ZG have been recently identified in proteomics studies (Chen, Walker et al. 2006; Rindler, Xu et al. 2007; Chen and Andrews 2008), but neither a confirmation nor a clear proof of function for most of them has been provided yet. The integral membrane associated protein-1 (ITMAP) was one of the first integral membrane proteins discovered in ZG by proteomics. It could be demonstrated that ITMAP-1 deficient mice have an increased severity of secretagogue- and diet-induced pancreatitis. Moreover, an effect of ITMAP on trypsin activation was confirmed but no influence on ZG size, appearance or composition could be observed (Imamura, Asada et al. 2002). Other proteins of the ZGM include proton pumps, transporters and channels (Jamieson and Palade 1971; Zachowski, Henry et al. 1989; Roussa, Alper et al. 2001; Cho, Sattar et al. 2002; Kelly, Abu-Hamdah et al. 2005; Lee, Torchalski et al. 2008). Intriguingly, many of these proteins are already known to participate in (neuro)endocrine secretion systems (Table 5.0). As depicted, ongoing proteome and functional studies are gradually improving our understanding of the role of individual components of the ZG membrane and submembranous matrix in the process of granule biogenesis; however, our current knowledge remains still fragmentary and new key players have to be identified in order to fill the gaps in the current models on ZG biogenesis.

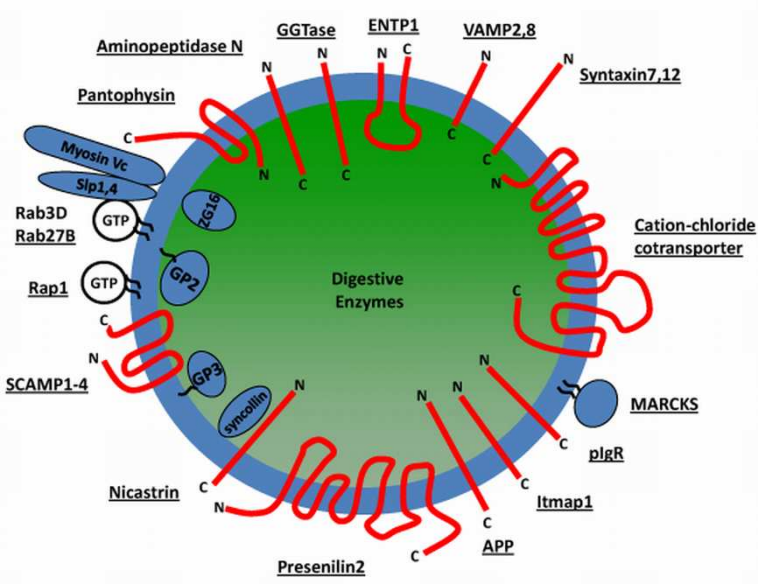

Figure 10: Molecular topology of pancreatic ZGM proteins.
In this model several ZGM proteins are shown which are as well known from synaptic vesicles of the neuroendocrine system, such as, Presinilin, APP, Pantophysin and myosin. (Figure taken from Chen and Ulintz 2008)

Chapter 2 Objectives

Hitherto very few membrane and membrane-associated proteins of the ZG from the acinar cells of the exocrine pancreas have been identified and characterized. However, especially these proteins may contribute to the generation of a submembranous matrix, composed of high molecular weight components (*e.g.* a proteoglycan scaffold and associated (glyco)proteins) which fulfills crucial functions during the sorting and packaging of secretory proteins. Furthermore, these components might as well have a central function in the regulation of apical exocytosis and membrane fusion and in signal transduction. Disturbances in these regulated processes (incorrect compartmentalization, premature activation of the zymogens, incorrect transport, uncontrolled and unspecific fusions) can cause pathological changes of the pancreas, including necrosis and fibrosis, *e.g.* during acute pancreatitis (Adler, Rohr et al. 1982; Raraty, Ward et al. 2000; Gomez-Lazaro, Rinn et al. 2010). Hence, the identification and molecular characterization of these components is highly relevant for both, basic cell biology and clinical research.

The perpetually growing sensitivity of mass spectrometric equipment will increase the potential to identify more and more low-abundance proteins of the ZG. However, in parallel the probability for the detection of contaminating proteins from other cellular compartments or false positives will rise with even higher frequency. Thus, techniques for protein localization complementing proteome studies will grow more and more inevitable to discriminate between actual constituents of the ZG and contaminants (Gomez-Lazaro, Rinn et al. 2010).

In this context, this thesis is designed to identify new low abundant constituent of the ZG and to verify their localization in pancreatic tissue but also in other secreting cell types. As some ZGM and peripheral proteins are already known from (neuro)endocrine secretion systems, implying a functional overlap in secretory vesicle biogenesis in both endocrine and exocrine systems, reciprocally ZG proteins will be also monitored in other secreting tissues. Complementing each other, both immunoblotting with marker proteins typical for the ZG and other cellular organelles such as Golgi, mitochondria, ER, peroxisomes and lysosomes (Faust, Gomez-Lazaro et al. 2008; Borta, Aroso et al. 2010) as well as immunofluorescence (quantification of co-localization by pixel-by-pixel analysis of confocal images) and immunoelectron microscopy will be used for these purposes (Figure 2). Moreover, only functional information will enable to discriminate proteins involved in biogenesis from purely secreted granule content. AR42J cells originally derived from the acinar cells of a rat pancreatic tumor (Longnecker, Lilja et al. 1979) can be used as a model for granule biogenesis and trafficking studies. Treatment of AR42J cells with the synthetic glucocorticoid dexamethasone induces their differentiation into exocrine, acinar-like cells, with *de novo* formation of electron-opaque secretory granules containing the major pancreatic zymogens and exhibiting a regulated secretory state (Logsdon, Moessner et al. 1985). However, AR42J cell still only express an incomplete assembly of known granule proteins which could certainly alter the mechanisms of granule formation. In this respect, a careful adjustment of culture conditions could offer a possibility to improve the value of this model system.

Specific aims/tasks of the thesis:

1. **Identification of new ZG matrix constituents of the rat exocrine pancreas**: To accomplish this task a combination of 1D- and 2D-gel electrophoresis and approaches were applied in order to separate peripheral membrane fractions of the ZG. For protein identification, spots were cut out and analyzed by MALDI-TOF/TOF mass spectrometry.
2. **Validation of new, low abundant ZGM protein candidates identified in the proteomics approach.** Protein candidates for the ZGM with a known distribution in other secretion systems were selected for validation. Immunoblotting and immunofluorescence experiments with pancreatic tissue and cell cultures were used to verify expression and subcellular localization in ZG granules.
3. **Assessment of the presence of ZGM proteins in neuroendocrine secretion systems using the example of ZG16p.** Reciprocal to the existence of neuroendocrine vesicle constituents in ZG, granule proteins may play a role in neuroendocrine tissue. As an example to test this assumption, ZG16 was localized in different brain sections by RT-PCR, immunoblotting and immunofluorescence.
4. **Optimization of the AR42J cell culture system as a model to study ZG biogenesis.** Panserin is a growth factor and serum-free medium for the culture of adherent mammalian cells. Thus, it may be applied to study exogenous regulation of granule formation by defined supplementation of the medium. The influence of Panserin on AR42J differentiation and granule formation was studied by morphological and biochemical methods.
5. **Analysis of the influence of selected ZG constituents on the biogenesis of granules in the AR42J model system.** Several zymogens and ZG membrane proteins were expressed in non-stimulated AR42J cells and in constitutively-secreting COS-7 cells. Their influence on granule formation was studied by immunofluorescence microscopy.

Chapter 3 MATERIALS & METHODS

3.1 Equipment

Cell Culture

- Electro Cell Manipulator ECM 630 (BTX Harvard Apparatus, Holliston, USA)

Centrifuges

- Ultra Centrifuge - Optima™ LE 80K Ultracentrifuge (Beckman Coulter, Fullerton/USA) with a Rotor Type 80 Ti (Beckman Coulter, Ireland)
- High Speed Centrifuge - Avanti™ J-25I (Beckman Coulter, Ireland) with a fixed angle rotor JA 25.50 (USA)

Electrophoresis and blotting equipment

- Horizontal PerfectBlue Gel System Mini M and Maxi S (Peqlab Biotechnology, Erlangen, Germany)
- Hoefer SE 600 Ruby gel chamber (Amersham Biosciences, Uppsala, Sweden)
- Slap mini gel chamber (Keutz, Reiskirchen, Germany)
- Electrophoresis Power supplies: EPS 2A200 and EPS 601 (Amersham Biosciences, Uppsala, Sweden)
- Trans-blot SD Semidry transfer cell (Bio-Rad, Munich, Germany)
- Hoefer TE22 Mini Tank blot system (Amersham Biosciences, Uppsala, Sweden)
- Hoefer TE42 Standard Transfer Tank (Amersham Biosciences, Uppsala, Sweden)
- Ettan IPGphor (GE Healthcare, San Francisco, USA)

Optical Equipment and Microscopes

- Calibrated Imaging Densitometer GS-710 (Bio-Rad, Munich, Germany)
- Leica DMIL microscope (Leitz, Wetzlar, Germany; cell culture)
- Olympus IX81 microscope; PlanApo 100X/1.40 objective (Olympus Optical Co. GmbH, Hamburg, Germany)
    1. Camera F-View II CCD and Soft Imaging software (Soft Imaging Systems, Münster, Germany)
- Zeiss LSM 510; Plan-Apochromat 63× or 100×/1.4 oil objective (Carl Zeiss, Oberkochen, Germany)
    1. Zeiss LSM Image Browser version 4.2.0.121 (Carl Zeiss MicroImaging GmbH 1997-2006, Germany)
- Nanodrop (Nanodrop ND 1000 (Peqlab Biotechnology, Erlangen, Germany)
- Photometer Ultraspec 100 pro (Amersham Biosciences, Uppsala, Sweden)

Other Equipment

- Thermo Cycler MyCycler (Bio-Rad, Munich, Germany)
- LC – MS/MS - Dionex 3000 Ultimate nano LC and a Waters 2690 HPLC with an integrated LcPackings Probot auto sampler. The Probot can spot the eluent directly onto a MALDI target plate, for MALDI MS/MS analysis.

1. Zorbax 300SB-C18 capillary analytical column with 3.5 μm particle size, 150 mm × 75 μm (Agilent Technologies)
2. Zorbax 300SB-C18 trapping column with 5 μm particle size, 5x0.3 mm (Agilent Technologies)

- MALDI-TOF/TOF mass spectrometer (4800 Proteomics Analyzer, Applied Biosystems, Europe)
- Homogenizer (IKA, Jellowline OST 20 digital, Germany)

Most used Software Tools

- Digital images were optimized for contrast and brightness using IrfanView Version 4.23 (Irfan Skiljan, Vienna University of Technology, Austria)
- Programs used for cloning: SECentral Clone Manager 5 (Ed-Sci-Software, NC, USA), OligoCalc 3.26, NCBI Primer-BLAST, NEB Cutter
- Programs used for sequence analysis: Chromas Lite 2.01 (Technelysium Pty Ltd, Brisbane, Australia), Sequence Alignment LaLIGN (Myers and Miller, CABIOS (1989) 4:11-17),
- Clustal W2 and Clustal X2 (Multiple Sequence Alignment, EMBL-EBI)
- BLAST pair wise alignments for proteins (BLASTP 2.2.25+, NCBI) (compilation of Phylogenetic trees)

3.2 Chemicals & Reagents

Table 3-1 Chemicals

Company	Country	Chemical
Applied Biosystems	Foster City, CA, USA	α-Cyano-4-hydroxycinnamic acid
AppliChem	Darmstadt, Germany	Coomassie G250
Bio Rad	München, Germany	Protein Assay-Dye Reagent Concentrate
Fluka	Steinheim, Germany	Ethidiumbromid
		Glucose (D+)
		Glutaraldehyde solution 70 %
		Luminol
		N-propyl gallate
	Buchs, Switzerland	MES
		Sodium acetate
		Trifluoroacetic acid (TFA)
Kodak		Developer
		Fixer
Merck-Schuchardt	Darmstadt, Germany	Chloroform
		Ethanol por analysis
		Hydrogen peroxide 30 % solution
		Isopropanol p. a. (2-propanol)
		Methanol
		Tetramethylethylene diamine
	Hohenheim, Germany	Aceton
Calbiochem/Merck	Darmstadt, Germany	Mowiol 4-88 reagent
Olympus	Japan	Immerson oil type F
Peqlab	Erlangen, Germany	TriFast
Polysciences	Eppelheim, Germany	Hoechst dye 33258
Promega	Madison, Wisconsin, USA	Sequence grade modified porcine Trypsin
Riedel	Seelze, Germany	HPLC-grade acetonitrile
Roth	Karlsruhe, Germany	Acrylamide (Rotiphorese Gel 30)
		Agarose NEEO
		BSA fraction V
		Glycerol
		Magnesium sulfate
		Ponceau S
		Potassium acetate
		Silver nitrate
		Trichloroacetic acid solution 20 %
		Tris – base
Sigma – Aldrich	Steinheim, Germany	Ammoniumperoxodisulfat
		β-Mercaptoethanol

	Boric acid
	Bromophenol blue
	Diethylpyrocarbonat (DEPC)
	Dimethyl sulfoxide
	Dithiothreitol
	Ethylendiamintetraacetic (EDTA)
	Formamide
	Glycine
	HEPES sodium salt
	MES monohydrate
	MOPS sodium salt
	para-Formaldehyde
	p-Coumaric acid
	Potassium carbonate
	Potassium chloride
	Potassium phosphate monobasic
	Potassium phosphate dibasic
	Sodium azid
	Sodium bicarbonate
	Sodium chloride
	Sodium deoxycholate monohydrate
	Sodium dodecyl sulfate (SDS)
	Sodium phosphate dibasic
	Sodium phosphate monobasic
	Sodium thiosulfate solution
	Sucrose
	Triton X – 100

Table 3-2 Medium & Supplements

Medium & Supplements	Company	City, Country
DMEM High Glucose,	PAA	Pasching, Austria
Fetal Bovine Serum "Gold"		
Nutrient Mixture F12 HAM	Sigma-Aldrich	Missouri, USA
Panserin^{TM} 401	Pan Biotech	Aidenbach, Germany
LB Broth	Formedium	Norfolk, UK

Table 3-3 Reagents for Cell & Bacteria Culture

Reagents for Cell & Bacteria Culture	Company	City, Country
Ampicillin	Sigma-Aldrich	Steinheim, Germany
Dexamethasone		
Dimethyl-sulfoxide		
Kanamycine disulfate salt		

Polyethyleneimine (PEI)		Missouri, USA
Lipofectamine	Invitrogen	
Matrigel	Self made	
Penecillin/Streptomycin	PAA	Pasching, Austria
Trypsin – EDTA		

Table 3-4 Molecular Biologically Reagents

Molecular Biologically Reagents and Kits	**Company**	**City, Country**
Restriction & Cloning Enzymes		
EcoRI	New England Biolabs	England
BamHI		
HindIII		
NheI		
PstI		
XhoI		
Antarctic Phosphatase		
T4-Ligase with 10×buffer		

Kits	**Company**	**City, Country**
Gel extraction and PCR purification Kit	Macherey-Nagel	Düren, Germany
Mini and Midi Plasmid preparation Kit		
RNeasy Protect Mini Kit	Quiagen	Hilden, Germany
Quant-iT dsDNA BR Assay Kit	Molecular	Eugene, USA
Quant-iT RNA Assay Kit	Probes/Invitrogen	

PCR and reverse Transcription	**Company**	**City, Country**
DNAse	New England Biolabs	England
dNTP's		
KOD DNA Polymerase with 10×buffer and dNTP's	Novagen, Merck	
Reverse Transcriptase MMLV 10×buffer	New England	Darmstadt, Germany
RNAse Block MMLV		
RNAse	Biolabs	
Tag DNA Polymerase with 10×buffe		England

Protease Inhibitors	**Company**	**City, Country**
Foy-305	Sanol - Schwarz	Reichelsheim, Germany
Phenymethylsulfonyl-fluoride	Sigma - Aldrich	Steinheim, Germany
Trasylol	Bayer	Leverkusen, Germany
Protein & DNA Marker & Loading dye	**Company**	**City, Country**
Kaleidoscop™ Protein Marker	Bio Rad	California, USA

O´GeneRuler^{TM} DNA Ladder Mix	Fermentas	France
6×Orange Loading Dye		
RNA Loading buffer	Sigma-Aldrich	Germany

Table 3-5 Antibodies

Primary Antibodies	Dilution in WB	Dilution in IF	Source	Country
Actin (mouse mc)	1:3000		Prof. Brigitte M. Jockusch	University of Braunschweig, Germany
Amylase (rabbit pc)	1:2000	1:200	Sigma-Aldrich	Missouri, USA
APP (22C11) (mouse mc)	1:200	1:50	Prof. Odete da Cruz e Silva	University of Aveiro, Portugal
Carboxypeptidase A (rabbit pc)	1:800	1:800	Rockland, Immunochemicals	Gilbertsville, PA, USA
Chymase DEAE (pc goat)	1:1000		LB Schwarz, Dep. of Internal Medicine	Virginia Commonwealth University, USA
CEL (pc chicken)	1:88		Isolated from egg yolk (Borta, Aroso et al. 2010)	Marburg, Germany
Chymotrypsin (pc sheep)	1:2000	1:400	Inst. for Cytobiology & Cytopathology	Marburg, Germany
Endolyn78 502 (mc mouse)		1:100	Gudrun Ihrke, Dep. of Cell Biology & Anatomy	Johns Hopkins University, Baltimore, USA
GFP (pc rabbit)		1:200	Invitrogen, Molecular Probes	Eugene, Oregon, USA
GP2 (4A9 mouse mc)	1:2000		A. Lowe	Stanford, USA
MAP2 (pc chicken)		1:5000	Prof. Ana L. Carvalho, Univ. Coimbra	Abcam, Cambridge, England
Myc (mc mouse)		1:200	Santa Cruz Biotechnology	Heidelberg, Germany
p115 (mc mouse)		1:200	Transduction Laboratories	http://www.labome.com/
PDI R-707 (pc rabbit)		1:500	HD Sölling, MPI for Biophysical Chemistry	Göttingen, Germany
Phalloidin Tritc		1:50	Sigma-Aldrich	Missouri, USA
Piccolo (pc rabbit)	1:2500	1:200	Abcam	Cambridge, England
Piccolo (pc rabbit)	1:2500	1:200	Synaptic Systems	Göttingen, Germany

PpiB (pc rabbit)	1:1000	1:600	Abcam	Cambridge, England
PSD95 (mc mouse)		1:200	Prof. Ana L. Carvalho, Univ. Coimbra	Millipore, California, USA
RNaseA (pc rabbit)	1:1000		Sigma-Aldrich	Missouri, USA
Synaptojanin 1 (pc rabbit)		1:200	Synaptic Systems	Göttingen, Germany
Synaptophysin (mc mouse)	1:10000		Prof. Ana L. Carvalho, Univ. Coimbra	Sigma, Missouri, UA
TGN38 (gp)(works only in rat)		1:200	H. F. Kern	Marburg, Germany
VGlut (pc guinea pig)		1:5000	Prof. Ana L. Carvalho, Univ. Coimbra	Millipore, California, USA
ZG16p full length (pc rabbit)	1:5000	1:400	A. Lowe	Stanford, USA
ZG16p N1d1 (pc rabbit)	1:2000	1:200	Cronshagen, Voland et al. 1994	Inst. for Cytobiology & Cytopathology, MR, Germany 1994
Secondary Antibodies	**WB**	**IF**	**Company**	**Country**
TRITC Donkey anti Mouse		1:100	Dianova	Germany
TRITC Donkey anti Rabbit		1:100		
TRITC Donkey anti Sheep		1:400		
Alexa 488 Donkey anti Rabbit		1:500	Invitrogen/ Molecular Probes	Leiden, Netherlands
Alexa 488 Goat anti Mouse		1:500		
Alexa 488 Goat anti Rabbit		1:500		
Alexa 647 Goat anti Guinea Pig		1:500	Prof. Ana L. Carvalho, Univ. Coimbra	
AMCA Rabbit anti Chicken		1:200	Prof. Ana L. Carvalho, Univ. Coimbra	Jackson Immuno Research, USA
Hoechst-dye		1:2000	Polysciences, Inc.	Eppelheim, Germany
HRP Rabbit anti Chicken	1:2000		Sigma-Aldrich Dianova Bio Rad	St. Louis, USA Heidelb., Germany California, USA
HRP Donkey anti Goat	1:2000			
HRP Goat anti Mouse	1:5000			
HRP Goat anti Rabbit	1:5000			

3.3 Oligonucleotides (Primers)

All primers were synthesised by Eurofins MWG|Operon (Ebersberg, Germany). Cleavage sites for restriction enzymes are in italic. All cloning and sequencing primers were designed for genes in *Rattus norvegicus* unless it is noted otherwise.

Table 3-6 Oligonucleotides

Primer	**Primer sequence**	**Gene Name & Accession number**	**Amplified area**
Cloning	*Sequence (5´to 3´)*	*NCBI Pubmed*	*Fragment*
Amylase-Myc up /BamHI	tt *ggatcc* atg aag ttc gtt ctg ctg ct	Amylase 2, pancreatic (Amy2), mRNA NM_031502	bp 16 – 1539 Fragment size 1523 bp
Amylase-Myc down/Hind III	tt *aagctt* caa ctt tga gtc ggc atg ga		
Amylase-YFP up /NheI	tt *gctagc* cat gaa gtt cgt tct gct gct		
Amylase-YFP down /PstI	tt *ctgcag* caa ctt tga gtc ggc atg ga		
Chymase-Myc up /BamHI	tt *ggatcc* atg cag gcc cta cta ttc c	mast cell protease 1 precursor, or chymase (RMCP-1) mRNA U67915.1	bp 27 – 807 Fragment size 780 bp
Chymase-Myc down /EcoRI	tt *gaattc* gct tgg aga ctc tga ctc g		
Chymase-YFP up /EcoRI	tt *gaattc* cca tgc agg ccc tac tat tcc		
Chymase-YFP down /BamHI	tt *ggatcc* ccg ctt gga gac tct gac tcg		
Trypsinogen-Myc up /BamHI	tt *ggatcc* atg aag gcc tta att ttc ctt	protease serine 3, or cationic trypsinogen (Prss3), mRNA NM_0173127	bp 1 – 741 Fragment size 741 bp
Trypsinogen-Myc down/HindIII	tt *aagctt* gtt ggc agc gac ggt ctg ctg		
Trypsinogen-YFP up/NheI	tt *gctagc c*at gaa ggc ctt aat ttt cct t		
Trypsinogen-YFP down/PstI	tt *ctgcag* gtt ggc agc gac ggt ctg ctg		
Sequencing and RT-PCR			
Amylase PCR up	gcc ttc tgg atc ttg cac tc	Amylase 2, pancreatic (Amy2), mRNA NM_031502	bp 542 – 1368 Fragment size 827
Amylase PCR down	agt gct tga caa agc cca gt		
Carboxypeptidase up	tt *ggatcc* atg aag aga cta ctg att ctg ag	Carboxypeptidase A1 (cba1), mRNA NM_016998.	bp 309-1501 Fragment size 1192 bp
Carboxypeptidase down	tt *gatatc* gta ggg gat gat ctg gga gg		
GAPDH1_control	cca gtg agc ttc ccg ttc agc	Glyceraldehyde-3-phosphate dehydrogenase, mRNA	bp 95 – 663 Fragment size 589 bp
GAPDH2_control	acg acc cct tca ttg acc		

		NM_017008.3	
GP2 up GP2 down	tt *ggatcc* atg gtg gct tgt gac ctg ctg tt *gaattc* tca gaa cag cca ggc cag gag g	Pancreatic secretory granule membrane major glycoprotein, mRNA NM_134418.1	bp 102 - 1694 Fragment size 1593 bp
Piccolo up1 bp121 Piccolo down1 bp562 Piccolo up2 bp4429 Piccolo down2 bp 5070 Piccolo up3 bp13921 Piccolo down3 bp14650	gga cgg cta cgg gct tct gca tct ttc aag atg atc gtg gac gaa agt tag tcc aaa aaa gga gtc ttt ttc tga gag gat tct gtc agt cgt gga gaa agg gtc cgg aga tgg cct tca gat gat	piccolo (presynaptic cytomatrix protein) (Pclo), transcript variant 2, mRNA. NM_001110797	Primer Pair1: 440 bp, Primer Pair2: 640 bp, Primer Pair3: 750 bp
rFlZG16fwnosta rFlZG16rvsto	ctc gag taa tgt tgg cca ttg ccc tct tag tat cta gat ctc aac aag tgt tgc agt ggc t	zymogen granule protein 16 (Zg16), rat mRNA NM_134409.2	bp 36-566 Fragment size 531 bp

3.4 Vectors and Plasmids

For the cloning of C-terminal Myc tagged constructs like Amylase-Myc, Chymase-Myc and Trypsinogen-Myc the *pCMV-Tag 5A* vector from Stratagene, USA was used. For the cloning of C-terminal GFP tagged constructs like Amylase-GFP, Chymase-GFP and Trypsinogen-GFP the *pEYFP-N1* vector from Clontech, Saint-Germain-en-Laye, France (Glebov and Nichols 2004) was used. For verification and as controls the following plasmids were used: YFP-ER (kindly provided by R. Jacob, University of Marburg, Germany), ER-Myc-ΔSP-ZG16, cloned by M. Gómez-Lázaro and M. Aroso form our Laboratory, Carboxypeptidase-Myc and Carboxypeptidase untagged both in *pCMV-Tag 5A* and GP2 in *pcDNA3* were cloned by H. Borta and F. Faust from our Laboratory and APP-GFP (kindly provided by Prof. Odete da Cruz e Silva, University of Aveiro, Portugal).

3.5 Molecular Biology Methods

3.5.1 Extraction of total RNA from Tissue and Cells

The isolation of mRNA from cultured cells and animal tissue was generally used for transcription into cDNA. The obtained cDNA served two different purposes: on one hand, for the amplification of a specific gene by PCR and subsequent cloning into an expression vector using the RNeasy Protect Mini Kit (Table 3-4) and on the other hand, for the determination of mRNA

expression levels by RT-PCR in diverse tissues and cell lines using the Trifast extraction method (3.5.1).

For isolation using the RNeasy Protect Mini Kit, cultured cells harvested by trypsination (3.6) were immediately frozen in liquid nitrogen and stored at –80°C or used directly. Cells were homogenized in a 1 mL syringe with a 20 G needle in 1 mL of the provided buffer then following the fabricants protocol. Elution was performed using two times 30 μl RNase-free water. Samples were measured and directly transcribed into cDNA.

For isolation using Trifast, tissue samples of 50 – 100 mg and cells grown in 6 or 10ø cm dishes, harvested by trypsination, were directly frozen in liquid nitrogen and either stored at -80°C or homogenized directly in 1 mL Trifast with a homogenizer (see section 3.1) for tissue and with a 1 mL syringe with a 20 G needle for cells. Following the manufactures protocol, lysates of tissue and cells were incubated at RT for 5 min before 200 μL of chloroform ($CHCl_3$) were added. Samples were shacked vigorously for approximately 15 seconds and kept at RT for 5 – 10 min. During centrifugation at 12000×g for 5 – 15 min the mixtures separated into three phases. The upper colorless aqueous phase contained RNA, the white interphase DNA and the lower red phenol phase proteins. If the upper phase appeared milky, the separation was not completed and the samples were re-centrifuged until a complete separation occurred. The upper aqueous phase, reassembling approximately 60% of the total volume, was transferred into a new 2 mL reaction tube without touching the interphase. RNA was precipitated by adding 1/10 volume of 3 M sodium acetate (pH 4.5) and three volumes of absolute ethanol followed by a 30 min to 1 h incubation at -20°C. From now on all steps occurred on ice. The RNA was spun down for 10 min at 12000×g, 4°C and the supernatant was removed carefully. The pellet was washed twice with 1 mL ice cold 75% ethanol by vortexing and subsequent centrifugation for 8 min at 7500×g. The RNA was air-dried 10 -15 min at RT and dissolved in 30 – 80 μL RNAse free water. RNA concentration was determined as described in section (3.5.6).

3.5.2 RNA Quality Control by Denaturing Agarose Gel Electrophoresis

Prior to the preparation of RNA gels, work space and equipment were cleaned with 70% (v/v) ethanol and 10% (v/v) H_2O_2. For 250 mL of a 1% (w/v) agarose gel 2.5 g agarose powder were boiled in 240 mL 1xMOPS buffer, cooled down to 60-50°C and 3.6 μL of a 1% (10 mg/L) EtBr solution and 10.7 mL of a 37% (v/v) formaldehyde solution were added. The solution was poured into a horizontal gel chamber and well forming combs were added. 5 μL of RNA sample were mixed with 15 μL RNA sample loading buffer (Table 3-4) heated for 10 min at 70°C, shortly chilled on ice, spun down and directly loaded onto the agarose gel. Separation occurred at 95 V for 1 h. Digital images were taken using the Alpha Imager HP (3.1).

5xMOPS running buffer for RNA gel electrophoresis

MOPS	100.0 mM
Na-Acetate	45.0 mM
EDTA	12.0 mM
DEPC	0.1%

In ddH_2O (MilliQ), pH 7.0
The concentrated buffer was agitated for 4 h at 37°C and autoclaved. 1xMOPS buffer was prepared using DEPC water.

3.5.3 Reverse Transcription

By reverse transcription the relatively instable mRNA is reverse transcribed into complementary DNA (cDNA) producing one molecule of cDNA per one molecule of RNA to provide a more stable template for subsequent PCR. Per reaction 3 μg of RNA were transcribed with reverse transcriptase from the *Moloney Murine Leukemia Virus* (MMLV) (Table 3-4) using an oligo dT primer annealing to the polyA tail of the RNA template during 10 min incubation at RT. Transcription occurred at 42°C for 60 - 90 min under softly shaking. The enzyme was inactivated at 65°C for 20 min, the sample was shortly cooled on ice and RNA was digested adding 1 μL RNAse (0.7 μg/μL). The final cDNA was stored at -80°C.

Standard Reaction Mix for 30 µL

mRNA	3 μg (x μL)
dNTP 50×mix (10 mM each)	0.6 μL
Oligo (dT) primer (100 μM)	2.8 μL
MMLV-RT 10×buffer	3.0 μL
MMLV-RT RNase block (40 U/μL)	0.5 μL
MMLV-reverse transcriptase (200 U/μL)	0.5 μL
DEPC or MilliQ grade water	x.x μL (fill up to a final volume of 30 μL)

3.5.4 Semi-Quantitative RT-PCR

Semi-quantitative RT-PCR was applied to determine the mRNA expression levels of genes in different cells and tissues under certain stimuli *e.g.* culture conditions, developmental state, differentiation etc. For this type of PCR generally Taq (*termophilus aquaticus)* polymerase with a low proofreading capacity was used. Before the actual semi-quantitative PCR, the exponential phase for each template was determined by taking samples of 10 μL during and after the PCR reaction at cycle 12, 18, 24, 30 and 35 (after last cycle). Samples were then separated on an agarose gel (3.5.5), compared to an appropriate control (GAPDH) and the optimal cycle number for each template was chosen. For semi-quantitative RT-PCR´s, the same quantity of cDNA (3.5.3) was employed (150 ng in a 50 μL reaction) for all samples. Samples belonging to one set of experiments were run simultaneously. To rule out eventual pipetting errors reactions were repeated with the same set of samples two to three times. To evaluate the sample quality at least three independent sets of samples per experimental approach were performed. For analysis, generally the entire reaction mixture was loaded on an agarose gel (3.5.5), since some templates exhibited very low expression levels under certain conditions.

Standard Reaction Mix for 50 µL

Template cDNA	1.5 µL (150 ng)
Primer forward (0.2 µM/µL)	1.0 µL
Primer reverse (0.2 µM/µL)	1.0 µL
NEB dNTP's (2 mM each)	1.0 µL
Taq Pol 10xBuffer	5.0 µL
Taq DNA polymerase (5 U/µL)	0.5 µL
ddH_2O	x.x µL to fill up to a final volume of 50 µL

Table 3-7 Programs for Semi-Quantitative RT-PCR

Amylase	CBP	GAPDH	GP2	ZG16
94°C 1 min	94°C 1 min	94°C 1 min	94°C 1 min	94°C 1 min
94°C 30 sec 52°C 30 sec } 28 72°C 1 min	94°C 30 sec 55°C 30 sec } 28 72°C 1 min	94°C 30 sec 51°C 30 sec } 28 72°C 1 min	94°C 30 sec 55°C 30 sec } 28 72°C 1 min	94°C 30 sec 60°C 30 sec } 35 72°C 20 sec
72°C 4 min	72°C 4 min	72°C 4 min	72°C 4 min	72°C 2 min
4°C hold	4°C hold	4°C hold	4°C hold	4°C hold
The cycle numbers to each program are written behind the brackets.				

3.5.5 Cloning and Amplification of Plasmids

For the cloning of plasmid constructs, gene specific primer sequences were chosen and used to amplify the coding sequence of selected rat genes. Cloning vectors used are listed in section 3.4, primers, templates; restriction enzymes and fragment size are listed in Table 3-6. For sequence sensitive PCR´s as required for cloning, generally the KOD DNA polymerase from *Thermococcus kodakaraensis* with increased proofreading was used. Annealing temperatures were adjusted to the respective primer pairs, generally 4-7 degrees under the empirical melting temperature of primers given by the fabricant. Elongation times were chosen depending on template length; respecting that the polymerase can amplify approximately 1000 bp/min, even thought the amplification time is as well depending on the type of polymerase. Preparative restriction was carried out at 37°C overnight. An analytical restriction after ligation and plasmid amplification from bacterial clones was completed during 4 h at 37°C. Resulting PCR and restriction products were separated on a 1% (w/v) agarose gel using a 1xTris-Acetate-EDTA (TAE) buffer. Afterwards, selected bands were purified with Gel and PCR purification Kits (Table 3-4). Prior to ligation, digested and purified vectors were dephosphorylated to avoid false positives through re-ligation. For ligation, first DNA concentrations of vector and insert were determined by comparing equal amounts of each to the co-migrated DNA ladder on an agarose gel. The molecule ratios chosen between vector and insert were mostly between 1:3 and 1:5 following the estimated calculation:

$$Mass\ insert\ [ng] = (5 \times Mass\ vector\ [ng] \times lenght\ insert\ [kb])/(lenght\ vector\ [kb]\ )$$

The cDNA was cloned in frame into cloning vectors (3.4). In frame insertion of all constructs was verified by sequencing (MWG). Correct constructs (1 μL plasmid for reproduction or 10 μL ligation mix) were chemically transformed into a 100 μL aliquot of competent bacteria. Therefore, cells were incubated for 30 min on ice followed by a 2 min heat shock at 42°C for DNA uptake. After a 2 min chilling on ice, bacteria were provided with 900 μL LB medium, agitated for 45 min at 37°C for recovery and were spread on antibiotic containing LB-agar plates (100 mg/mL Ampicillin or 30 μg/mL Kanamycin) for selection. Plates were incubated overnight at 37°C. For test cultures, colonies were inoculated in 5 mL LB containing a selective antibiotic and were grown overnight 37°C. Two milliliter of culture were used for plasmid purification with subsequent test digestion. The remaining solution was kept at 4°C for later use or stocks with 50% glycerol were frozen at -80°C. Plasmid isolation occurred at two different scales as mini from 2 mL of a 5 mL overnight culture or as midi from 200 mL overnight culture. Mini preparations for sequencing and midi preparations in general were done with the mini or midi plasmid purification kits from Macherey-Nagel (Table 3-4) following the manufactures protocol. After purification, preparations were air-dried and taken up in ddH_2O_{MilliQ} (35-50 μL for Mini and 400 μL for Midi). For all steps appropriate controls were done simultaneously. Enzymes and Kits were used according to the fabricants instruction.

Standard PCR Reaction Mix for 50 µL

Template DNA	x.x μL mostly 0.2 μL of plasmid DNA or 1 μL of cDNA
Primer forward (0.1 μM /μL)	0.5 μL
Primer reverse (0.1 μM /μL)	0.5 μL
KOD dNTP's (2 mM each)	5.0 μL
KOD $MgSO_4$ (25 mM)	2.0 μL
KOD 10xBuffer	5.0 μL
KOD hot start DNA polymerase (1 U/μL)	1.0 μL
ddH_2O	x.x μL (to fill up to a final volume of 50 μL)

Table 3-8 Programs for Cloning PCR

Amylase-YFP/Myc	Chymase-YFP/Myc	Trypsinogen-YFP/Myc
		94°C 2 min
94°C 2 min	94°C 2 min	94°C 30 sec ⎫
94°C 30 sec ⎫	94°C 30 sec ⎫	62°C 30 sec ⎬ 20 cycles
56°C 30 sec ⎬ 38 cycles	60°C 30 sec ⎬ 38 cycles	72°C 45 sec ⎭
72°C 1.5 min ⎭	72°C 1.5 min ⎭	94°C 30 sec ⎫
72°C 5 min	72°C 5 min	50°C 30 sec ⎬ 20 cycles
4°C hold	4°C hold	72°C 45 sec ⎭
		72°C 4 min
		4°C hold

50xTris-Acetate-EDTA (TAE) buffer

Tris/Base	40 mM
Acetic Acid	20 mM
EDTA	1 mM

In ddH_2O, pH 8.0

3.5.6 Quantification of DNA and RNA

DNA concentrations were measured with the Qubit quantification kit (Table 3-4) following the manufactures protocol. RNA concentrations were determined using a nanodrop ND 1000 (3.1) first calibrated with 1 μL ddH_2O (MilliQ quality) followed by subsequent measuring of 1 μL of each sample.

In between each sample, the optical lens was carefully cleaned with appropriate paper and MilliQ water. From time to time, a blank was measured to ascertain the lens is clean. The nanodrop measures the optical density at a wavelength area from 200 – 350 nm. RNA has equal to DNA an absorption maximum at 260 nm. As proteins absorb light at a wavelength of 280 nm, the ratio of the OD260/280 provides information to determine the purity of a RNA preparation. A clean RNA preparation should have an OD ratio 260/280 of 2.0, although depending on the pH a pure sample can result in values below 2.0 when resuspend in water instead of TE buffer. Furthermore, the OD ratio of 260/230 was determined which should be close to 2.0 as well. At 220-230 nm, three sources of contaminations can produce peaks, these are proteins, chaotropic salts like guanidinium isothiocyanate and phenol coming from the isolation process.

3.6 Cell Culture

Table 3-9 Cell Lines

Cell line and Origin	Characteristics	Source
AR42J; pancreatic exocrine tumor (*Rattus norvegicus*, Wister strain9	Adherent only when plated on matrigel coated surfaces, can be induced with dexamethasone for differentiation to acinar like cells	ATCC, Rockville/USA, CRL-1492
COS-7; kidney, African green monkey (*Ceropithecus aethiops*)	SV40 transformed, produce large T antigen, adherent, fibroblast morphology	ATCC, Rockville/USA, CRL-1651
SH-SY5Y; brain, neuroblastoma taken from bone marrow metastasis, human (*Homo sapiens*)	These cells grow as a mix of floating and adherent cells	ATCC, Rockville/USA; CRL-2266 PhD Miriam Fernandes-Fernandes, Albacete, Spain

The most common buffer applied in cell culture (but also in immunofluorescence, immunoblotting etc.) was 1xPBS buffer with a pH of 7.35. 1×PBS was applied to keep cells in a stable, isotonic and physiological environment.

10xPhosphate buffer saline (PBS)

NaCl	1.37 M
KCl	27 mM
$Na_2HPO_4 * 2H_2O$	80 mM
KH_2PO_4	15 mM

In dH_2O, pH 7.35

For the 1xPBS working solution the pH was readjusted to 7.35.

3.6.1 Maintenance of Mammalian Cells in Culture

AR42J and COS-7 cells were cultured in Dulbecco's modified Eagle medium (DMEM) high glucose (4.5 g/L) supplemented with 10% (v/v) FBS, 100 U/mL Penicillin, and 100 μg/mL Streptomycin (Faust, Gomez-Lazaro et al. 2008).

SH-SY5Y were cultured in a medium mix of 1:1 DMEM and Ham´s F12 medium supplemented with 15% (v/v) FBS, 100 U/mL Penicillin, and 100 μg/mL Streptomycin. The DMEM usually contained 1.5 g/L sodium bicarbonate, 2 mM L-Glutamine.

In general, cells were cultured at 37°C, 5% CO_2, and 95% humidity. Cell culture work was performed in a sterile laminar flow safety cabinet and all materials and solutions were sterilized by filtration, autoclaving or heat sterilization. Routinely, cells were grown in 10ø cm dishes and seeded on coverslips in 6ø cm dishes for immunofluorescence experiments. Cell number was determined using a Fuchs-Rosenthal counting chamber.

3.6.2 Differentiation of AR42J Cells with Dexamethasone

AR42J cells were either cultured as described in section 3.6.1 (Faust, Gomez-Lazaro et al. 2008) or 8 h after seeding cells were washed twice with PBS and the medium was exchanged to the serum free Panserin^{TM} 401 containing 100 U/mL Penicillin, and 100 μg/mL Streptomycin. To improve cell adherence, culture dishes and coverslips were coated with an extract from Engelbreth-Holm-Swarm tumor (matrigel), (Kleinman, McGoodwin et al. 1979). For statistical analysis of growth & induction cells were prior to seeding washed with PBS buffer pH 7.35, trypsinised and counted in DMEM medium under a Leica DMIL microscope (Leitz, Wetzlar, Germany) with a Fuchs-Rosenthal counting chamber. Cells were seeded at a defined number of $0.5*10^6$ cells/dish using 6ø cm dishes containing coverslips for immunofluorescence (IMF) and for counting in the same type of dishes without coverslips. To induce differentiation and zymogen granule formation, cells were incubated with 10 nM dexamethasone (Swarovsky, Steinhilber et al. 1988) for 2-6 days added 24 h after seeding. To optimize culture conditions and maintain equal concentrations of dexamethasone during experiments the medium was exchanged daily and dexamethasone was added freshly. For time-course experiments cells for IMF were fixed at 24, 48, 72, 96, 120 and 144 h and for cell counting cells were trypsinised at the same time points and counted as described before. For immunoblotting cells were seed in a defined number of $1.4*10^6$ cells per 10ø cm and lysed (3.8.4) after 48 and 72 h, or cells were collected for RNA extraction (3.5.1). Medium samples from 48 and 72 h were taken from dishes in which the medium was not exchanged daily to achieve an enrichment of secreted proteins.

3.6.3 Transfection of Cultured Cells

Several methods were applied for the transfection of mammalian cells with plasmid DNA to allow expression of the encoded proteins. The method of choice is depending on cell type, application and the plasmid DNA itself. In this study only transient transfection methods were performed based on different mechanisms of DNA uptake, *e.g.* endocytosis or membrane fusion. The transfection efficiency, cell mortality, and morphological alterations on the cells vary in between the different methods, cell types, and conditions used, thus requiring optimization of the transfection method for each cell line and application.

3.6.3.1 PEI Transfection

For morphological studies like immunofluorescence COS-7 cells were usually transfected using PEI (polyethylenimine). The cationic and branched polymer PEI binds the negatively charged DNA backbone which allows endocytotic uptake of the complex by the cells. Once inside the cell, protonation of the amines results in an influx of counter-ions and water into the vesicle thus lowering the osmotic potential. As a result of the osmotic swelling the vesicles burst and releases the PEI/DNA complex (polyplex) into the cytoplasm where it than can diffuse to the nuclei in a microtubule independent manner. The correct DNA/PEI ratio is crucial for optimal complex formation.

24 hours before transfection cells were seeded in 6ø cm dishes containing coverslips. 10 μg DNA were diluted in 750 μL 150 mM sodium chloride, and 100 μL PEI (0.9-1 mg/mL in dH_2O) were mixed with 650 μL sodium chloride solution. After 15 minutes of incubation at RT the PEI solution was added drop-wise to the DNA solution and the mixture was incubated for additional 20 minutes. 500 μL of the mixture were added drop-wise to 2.5 mL pre-warmed medium into the cell dish and the cells were incubated for 3 to 6 h at 37°C. Afterwards, the cells were washed with PBS and incubated for 24 - 48 h in fresh medium before fixation and processing for immunofluorescence (3.7.1).

3.6.3.2 Electroporation of AR42J and COS-7 Cells

Electroporation is a dynamic phenomenon that depends on the local transmembrane voltage at each point on the cell membrane. For electroporation in a cuvette it is required to have cells in suspension. For some cell types electroporation results in a high mortality rate, but the advantage of this technique is high transfection efficiency and the possibility to transfect cells which are usually difficult to transfect using chemical methods. For electroporation, AR42J or COS-7 cells were grown to 90% confluence and harvested by trypsination, resuspend in 1 mL complete DMEM for AR42J, or in 1 mL HBS buffer (20 mM HEPES, 137 mM NaCl, 5 mM KCl, 6 mM dextrose, 0.7 mM Na_2HPO_4, pH 7.15, sterile) for COS-7. Then 0.5 mL of the cell suspension were transferred to a sterile 0.4 cm gap electroporation cuvette containing 10 μg of DNA. Electroporation was performed in an ECM 630 Electro Cell Manipulator (3.1) at 250 V (AR42J) (Faust, Gomez-Lazaro et al. 2008) or 230 V (COS-7), 1500 μF and 125 Ω. After electroporation, cells were immediately resuspended in complete medium, plated on cover slips, which were uncoated for COS-7 but coated with matrigel for AR42J. To differentiate transfected AR42J cells, 10 nM dexamethasone was added 24 h after electroporation and cells were processed for immunofluorescence after 48 - 72 h. COS-7 cells were used for immunofluorescence 24 - 48 h after electroporation**.**

3.7 Microscopy

In this work an Olympus IX81 (inverted) microscope was used for morphological studies and digital images were taken with the CCD camera F-View II. For co-localization studies a Confocal Zeiss LSM 510 was applied together with associated software. In immunofluorescence (IMF) protocols applied on cells, the non-ionic detergent Triton X-100 (standard detergent) and the surfactant sodium dodecyl sulfate (SDS) were used for permeabilisation and compared with each other. Triton X-100 creates holes in the cell membrane by removing lipids without disturbing protein-protein interactions. In order to reveal epitopes which may be masked for antibodies SDS can used to induce slight denaturation of proteins in fixed cells. For washing in all immunofluorescence and immunohistochemical methods 1xPBS was used.

Mounting medium Mowiol Stock

Mowiol 4-88	12 g
PBS	40 mL, stir overnight
Glycerol	20 mL, stir overnight

The viscous solution was centrifuged for 1 h at 27216×g (15000 rpm) at 4°C (High Speed Centrifuge - Avanti^{TM} J-25I from Beckman Coulter, 3.1). The supernatant was taken and 0.1% (w/v) sodium azide was added. The final working solution consisted of 3 parts Mowiol with 1 part n-propyl gallate solution as bleaching protection.

n-propyl-gallate Stock

N-propyl gallate	2.5% (w/v)	
Glycerol	50% (v/v)	in PBS, pH 7.35

Note: All further mentioned solutions for IMF and IHC were prepared in PBS.

3.7.1 Indirect IMF with Cultured Cells

Cells from rat primary neuronal culture were kindly provided by Prof. A.L. Carvalho and were prepared by S. Santos (Neurosciences, University of Coimbra, Portugal). All other cell types were cultured in our laboratory. All steps occurred at RT and between all steps cells were washed softly 3-6 times with PBS. Cells grown on glass cover-slips (1-14 days, depending on cell type) were fixed for 20 min with 4% (w/v) *para*-formaldehyde (PFA) or in the case of primary neuronal culture, cells were fixed for 15 min with a solution of 4% (w/v) PFA/4% (w/v) sucrose. The samples were permeabilised either for 10 min with 0.2% (w/v) Triton X-100, (neuronal culture with 0.25% Triton X-100 for 5 min), or for 5 min with 1% (w/v) SDS and blocked afterwards with 1% (w/v) BSA for 10 min (neuronal culture for 30 min with 10% BSA). Subsequently, coverslips were incubated for 1 h at RT (neuronal culture for 1-2 h at 37°C) with 30 μL primary and secondary antibodies prepared in 1xPBS buffer or for primary neuronal culture in 3% (w/v) BSA. Antibody dilutions were spun down for 5 min at maximum speed directly before use. During antibody incubation, cells were kept in a humid and dark environment. If several primary or secondary antibodies were

applied the incubation occurred simultaneously. Finally, coverslips were washed in dH_2O to prevent crystal formation through buffer salts, drained carefully, mounted with Mowiol on glass-slides and dried overnight before microscopic examination. For primary culture, coverslips were mounted on glass-slides using Dako and dried for 1 h at RT. In a final step, these coverslips were sealed with nail-polisher and air-dried for 15 min before microscopic examination. For dilution of antibodies see Table 3-5. For occasional visualization of the nuclei Hoechst dye 33528 was used in a concentration of 0.2 μg/mL for 2-5 min after antibody incubation. Hoechst 33528 is a fluorescent dye that is excitable with ultraviolet light at 359 nm and it emits light at 461 nm appearing blue when it is intercalated between the bases of the DNA.

3.7.2 Quantification and Statistical Analysis of Zymogen Granule Formation in AR42J cells

AR42J controls and cells stimulated for zymogen granule (ZG) formation were immunostained with an antibody to Carboxypeptidase A as zymogen granule marker, Nuclei were stained with Hoechst 33528 (Table 3-1 and 3.7.1). For evaluation after Amylase-YFP, Trypsinogen-YFP, Carboxypeptidase-Myc, Myc-ZG16p and GP2 expression cells were co-labelled with an antibody directed to Chymotrypsinogen as ZG marker. For quantitative analysis of granule morphology in AR42J cells, 100-200 cells per coverslip were examined and categorized under the fluorescence microscope and on photographs as cells with 'granular', 'intermediate' or 'vesicular' structures. Analysis was done blind. Cells defined as 'granular' contained numerous heavily stained secretory granules; cells defined as 'intermediate' contained both granule-like/granular and small vesicular structures exhibiting a faint staining; cells defined as 'vesicular' exhibited a fine punctate staining pattern. Four coverslips per preparation were analyzed, and 4-6 independent experiments were performed. Quantitative analysis of ultrastructural alterations of granules after different experimental treatments was performed on EM micrographs. Sections were randomly photographed at a magnification of 3000-12000×. The results of the quantitative analysis presented were from 3-4 independent experiments. Significant differences between experimental groups were detected by analysis of variance for unpaired variables using Microsoft Excel. Data are presented as means ± S.D., with an unpaired t-test used to determine statistical differences. P-values <0.05 are considered as significant, and p-values <0.01 are considered as highly significant. Data analysis and preparation of diagrams were done using Microsoft Excel software.

3.7.3 Immunohistochemical Methods

3.7.3.1 Tissue Fixation

The isolation of mouse tissue was performed through Prof. E. Martin (Department of medical sciences, University of Castalia-La Mancha, Albacete, Spain) via perfusion of mice with 4% (w/v)

PFA. All further steps of tissue fixation until cryo-sectioning were performed under the observation and with help of Dr. M. Fernandez-Fernandez and Dr. M.G. Lazaro.
For post fixation, the isolated organs were first incubated overnight at 4°C in 4% (w/v) PFA afterwards organs were washed several times with 1×PBS and then incubated in 15% (w/v) sucrose at 4°C until they sagged to the bottom of the incubation vial. In a last step the solution was changed to 30% (w/v) sucrose and organs were incubated again until they sagged to the ground.

3.7.3.2 Tissue Freezing & Cryosectioning

Organs were embedded in Tissue-Tek® O.C.T.™ Compound (optimal cutting temperature), a water soluble material consistent of resins and glycols, as follows. Organs were placed in disposable plastic embedding molds with approximately 5 mL O.C.T –compound until total covering and tissue orientations, type of tissue and date were marked on the mold. 2-methylbutane was pre-cooled in liquid nitrogen and samples were immersed until they were totally frozen. Samples were then stored at -80°C. For cryosectioning frozen, O.C.T.-embedded specimens were taken out of the mold, glued to cryostat chucks with O.C.T - compound and chilled in the cryostat chamber until a temperature of -23°C was reached, approximately 1 h. After trimming, 15-20 μm sections were cut, mounted on acid-treated superfrost plus glass slides and were allowed to air dry for approximately 1 h at RT before storing at -20°C. Cryosectioning was performed using a Microm HM 550 Cryostat from Thermo Scientific (Walldorf, Germany).

3.7.3.3 Immunostaining of Tissue (IHC)

Before IHC, cryosections were taken out of -20°C and air-dried for 30 min. Tissue pieces placed on the same slide were surrounded with a wax pen (PAP-PEN) for separation. The entire protocol occurred at RT and except for antibody incubations; slides were softly agitated in all other steps covered with approximately 200 μL of liquid. All solutions used were prepared in 1×PBS. For permeabilisation, samples were incubated three times for 10 min in 0.25% (v/v) Triton X-100 and were then blocked in a solution of 0.25% (v/v) Triton X-100 and 4% (w/v) BSA for 1 h. Tissue pieces were next incubated with 200 μL of primary antibodies diluted in a solution of Triton X-100 0.25% (v/v) and 1% (w/v) BSA for 3 h. Afterwards the specimen were incubated with 200 μL of secondary antibodies for 1 h diluted in 1% (w/v) BSA. Between and after antibody incubation samples were washed three times for 10 min with PBS. For nuclei staining the samples were incubated with Hoechst dye 33528 in a concentration of 0.2 μg/mL in PBS for 10 - 15 min. Afterwards, slides were washed once for 2 min in PBS. Finally, slides were drained carefully, mounted with Mowiol and dried overnight before microscopic examination.

3.7.3.4 Electron Microscopy with Cupromeric Blue

Proteoglycan staining was performed according to the Cupromeronic Blue® (CmB, Seikagaku Corp., Tokyo, Japan) procedure at a critical electrolyte concentration developed by Scott (Scott 1980; Scott 1985). Pancreatic tissue was postfixed with 1% glutaraldehyde for 30 min and stained overnight in 25 mM sodium acetate, pH 5.7, containing 0.5% glutaraldehyde, 0.05% CmB and 0.3 M $MgCl_2$. At this electrolyte concentration highly sulfated acidic glucosaminoglycan side chains of proteoglycans are preferentially stained by CmB (Scott 1985). After three washes in acetate-$MgCl_2$, specimens were contrasted with 0.5% sodium tungstate (Scott, Orford et al. 1981) in water and in 50% ethanol, dehydrated in an ascending series of ethanol and embedded in Epon. For routine electron microscopy (EM), pancreatic lobules were fixed according to Ito and Karnovsky (1968). Isolated ZGM fractions were fixed in 0.1% cacodylate buffer, pH 7.3 containing 1% glutaraldehyde (Serva, Heidelberg, Germany). Specimens were postfixed in 1% osmium tetroxide and embedded in Epon according to standard procedures. Thin sections of 70 nm were stained with uranyl acetate/lead citrate and examined using a Zeiss EM 109 electron microscope, performed by B. Agricola, University of Marburg.

3.7.3.5 Immunoelectron Microscopy

Tissue from rat pancreas and rat tongue was fixed in 0.1 M cacodylate buffer, pH 7.35 containing 2% paraformaldehyde and 0.1% Glutaraldehyde (Serva, Heidelberg, Germany). The samples were dehydrated in a graded series of alcohol, embedded in Lowicryl K4M (Polysciences Ltd., Eppenheim, Germany) and polymerized at 20°C and UV light (360 nm) for 48-72 h. Thin sections (70 nm) were incubated with polyclonal antibodies directed to Chymase (1:200-1:500) and visualized using a 10 nm Protein A-Gold solution (J. Slot, University of Utrecht, The Netherlands) at a dilution of 1:60 or 1:70, both in 0.5% BSA in PBS. Sections were stained with uranyl acetate/lead citrate and examined using a Zeiss EM 109 electron microscope (Oberkochen, Germany), performed by B. Agricola, University of Marburg. The labeling density (gold particles/μm^2) on ZG and control regions was determined manually on images with the same magnification.

3.8 Tissue and Cell Preparation Methods

3.8.1 Isolation of Zymogen Granules

Tissue samples from 200 - 300 g Wister rats were kindly provided by the Instituto de Ciências Biomédicas Abel Salazar (ICBAS), Porto, Portugal or the Medical Faculty and Centre for Neurosciences, Coimbra, Portugal.

Homogenisation buffer for zymogen granule isolation:

Sucrose	250 mM	
MES, pH 6.25	0.5 mM	
$MgSO_4$	0.1 mM	in dH_2O

Protease inhibitors were added in the following final concentrations directly before use: Trasylol 2.5 mM, Foy-305 0.01 mM and PMSF 0.1 mM. All buffers were kept on ice and the entire protocol was conducted at 4°C.

For homogenization, each pancreas was minced manually in 1 mL homogenisation buffer with a scissor. Then homogenization buffer was added up to a final volume of approximately 10 mL and the tissue was homogenized at 2000 rpm with a homogenizer (IKA, Jellowline OST 20 digital, 3.1) making 15-20 strokes against the rotating Teflon-pistil. The initial homogenate was centrifuged at 500×g for 10 min, the resulting post nuclear supernatant (SN1) was transferred into a new tube and centrifuged for 10 min at 2000×g to sediment ZG resulting in (SN2) and (P2). The sedimentation of ZG was repeated with (SN2) resulting in (SN3) and (P3). Each time, the brownish layer of mitochondria on top of the pellet was separated from the white zymogen granules and both fractions were collected in homogenization buffer. To increase the yield SN3 was joined with P1 and the whole procedure starting with the homogenisation was repeated two more times. Since the mitochondrial layer is less compact than the ZG layer, it could easily be removed by a careful wash with homogenisation buffer aspirating the resuspended mitochondria. Both mitochondria and ZG fractions were centrifuged for 20 min at 2000×g. Finally, supernatants were discarded and the mitochondria and ZG layers were separated from each other via careful pipetting. The remaining white ZG pellet was lysed in 0.25 mL to 3 mL of 50 mM Hepes buffer (pH 8.0), depending on the amount of ZG obtained, and was stored at -20°C. All centrifugation steps occurred in an Eppendorf centrifuge 5810R with a swinging bucket rotor (3.1).

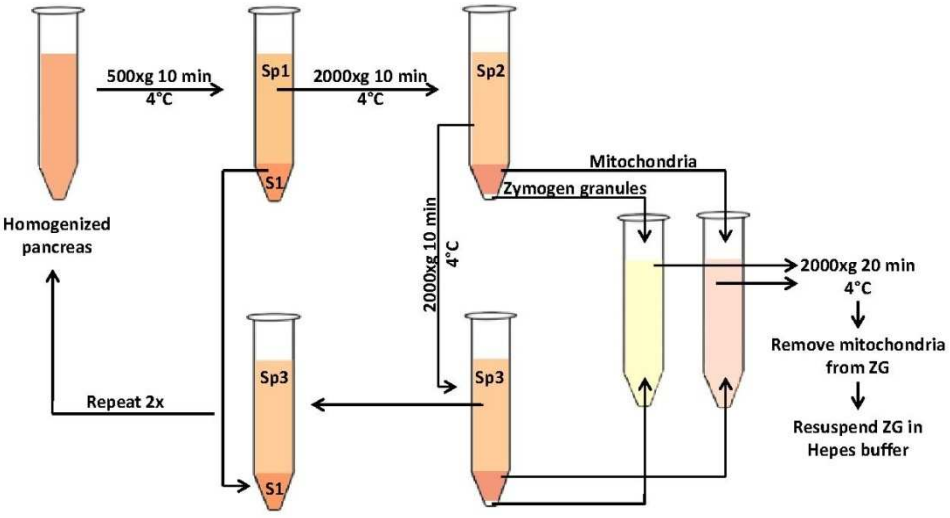

Figure 11: ZG isolation scheme

3.8.2 Zymogen Granule Subfractionation

All steps applied take place at 4°C. Zymogen granules were lysed by a freezing and thawing cycle in 50 mM Hepes buffer, pH 8.0. After lysis ZG content (ZGC) and ZG membranes (ZGM) were separated by centrifugation at 100000×g for 30 min in an Ultracentrifuge Optima^{TM} LE 80K with a Rotor Type 80 Ti (3.1). The supernatant forming the content fraction (ZGC) was collected and frozen at -20°C. To remove ZGC residues from the ZGM pellet, the pellet was carefully washed with a small amount of Hepes buffer. Afterwards the membrane pellet was resuspended in 300 – 1000 μL of Hepes buffer, depending on pellet size. The membranes were rinsed, resuspended in Hepes buffer and treated with 150 mM Na_2CO_3, pH 11.5 for 2 h on ice. Treated membranes (ZGM_{washed}) were recovered by centrifugation at 100000×g for 30 min and thereby separated from peripheral membrane proteins (Wash). The pellet was resuspended in 50 mM Hepes (pH 8.0) and both fractions were stored at -20°C.

3.8.3 Synaptosome Isolation from Rat Brain Tissue

Synaptosomes are the isolated neuronal terminals. They are easy to prepare and rich in synaptic vesicles thus representing an optimal source for synaptic vesicle proteins. The enrichment of synaptic vesicles through isolation of synaptosomes followed a protocol from the group of Prof. P. Gonzalvez (University of Aveiro) based on the method of (Hajos 1975).

SV homogenisation buffer:	0.32 M sucrose
pH 7.4	10 mM Hepes
	10 mM Tris Base

Protease inhibitors were added in the following final concentrations directly before use: Trasylol 2.5 mM, Foy-305 0.01 mM and PMSF 0.1 mM. The centrifuge used for this protocol was an Avanti^{TM} J-25I with a fixed angle rotor JA 25.50 (3.1).

The brain was submerged in 10 mL SV homo buffer minced with a scissor and thereafter homogenized with ca. 25 strokes using a homogenizer (IKA, Jellowline OST 20 digital, 3.1). After a 10 min centrifugation at 1500×g, the nuclear sediment was removed and the supernatant centrifuged at 9616×g for 20 min. While the resulting supernatant was discarded, the pellet fraction was resuspended in 1 mL of SV homogenisation buffer and carefully layered on top of 7.5 mL 0.8 M sucrose in 10 mM Hepes-Tris buffer. If a different volume was used the ratio of 1:7.5 between the brain suspension and the gradient solution was maintained. The gradient solution overlaid by the brain homogenate was centrifuged for 30 min at 9616×g. The resulting gradient had a thin brownish top layer representing myelin, a relatively big middle layer containing the synaptosomes and a pellet mainly consistent of mitochondria. The synaptosome fraction was collected carefully and a 1:1 dilution in 10 mM Hepes-Tris buffer, pH 7.4 (without sucrose) was prepared. Synaptosomes were pelleted in a final centrifugation step at 20000×g for 30 min. The supernatant was discarded while synaptosomes were resuspend in a small amount of SV homogenisation buffer and frozen at -20°C.

3.8.4 Preparation of Cell Lysates

For the preparation of cell lysates, cells grown to confluence on 10ø cm cell culture dishes were washed with 5 mL PBS and placed on ice. Adding 1 mL PBS, cells were detached from the surface with a cell scrapper and pelleted at 500×g for 3 min at 4°C. The cell pellet was suspended in 250 μL lysis buffer and homogenized by 15–20 up and down strokes in a 1 mL syringe with a 26 G x ½, 0.45 x 13 mm needle. The final solution was stored at -20°C. Alternatively, cells were quick lysed with SDS to obtain a whole cell lysate avoiding the degradation of protease-sensitive proteins. A 2% SDS solution (in dH_2O) was heated up to 100°C and 1 mL of the hot solution was pipetted directly into a 10ø cm cell culture dish with cells grown to confluence. The cells were lysed immediately by pipetting the hot solution 5–6 times up and down. The sample was then transferred to a 1.5 mL reaction tube, boiled for 10 min at 95°C and afterwards stored at -20°C for later use.

Lysis Buffer for cell lysates

Tris-HCL	25 mM
NaCl	50 mM
Deoxycholate	0.5% (w/v)
Triton X-100	1.5 mM (0.5%)

In dH_2O, pH 8.0

Protease inhibitors were added in the following final concentrations directly before use: Trasylol 2.5 mM, Foy-305 0.01 mM and PMSF 0.1 mM.

3.8.5 Measurement of Protein Concentrations

Protein concentrations were determined using the Bradford assay (Bradford 1976). For the Bradford assay the Bio-Rad Protein Assay-Dye Reagent concentrate was used following the manufactures protocol. The Bradford assay can be disturbed by Triton X-100 (> 0.5%), SDS (> 0.1%), and sodium deoxycholate (Lottspeich and Engels, 2006). For that reason, protein concentrations of cell lysates obtained with the quick SDS lysing method were measured with the Qubit quantification kit (Table 3-4) following the manufactures protocol.

3.8.6 Protein Precipitation

To purify samples and to diminish their volumes protein solutions were precipitated using either trichchloroactic acid (TCA) or chloroform-methanol (Wessel and Flugge 1984). The chloroform-methanol method of protein precipitation removes SDS, Triton X-100, salts and β-mercaptoethanol from the sample. For the precipitation with chloroform-methanol, one sample volume was mixed with three volumes of methanol plus one volume of chloroform and vortexed thoroughly. Further three volumes of dH_2O were added and the mixture was once more vortexed.

The cloudy solution was centrifuged at 10000×g at RT for 3 min until the emulsion partitioned into three phases. The aqueous upper phase was removed carefully without touching the interface containing the protein. Proteins were precipitated adding three volumes of methanol to the remaining phases. After mixing, a 3 min centrifugation step at 10000×g followed. The pellet was washed once with methanol and air-dried for 10 min. Samples were resuspend in 3×Laemmli buffer and used for SDS-PAGE (3.9.2).

TCA precipitation was carried out as follows: one sample volume was mixed with one volume of 20% (w/v) TCA and incubated on ice for 15 - 20 min. The mix was centrifuged for 10 min at 10000×g and 4°C and the pellet was washed one time with 5% TCA. To remove TCA from the pellet, the pellet was washed two times with 1 mL ice-cold acetone and centrifuged as before. Samples were then air-dried, resuspend in 3×Laemmli buffer and used for SDS-PAGE (3.9.2).

3xSDS-Sample buffer (Laemmli, 1970)

1 M Tris-HCl, pH 6.8	60 mM
Glycerol	10% (w/v)
SDS	2% (w/v)
Bromphenol blue	0.005% (w/v)
Dithiothreitol (DTT)	20 mM
β-Mercaptoethanol	5% (v/v)

In dH_2O

3.9 Biochemical Methods

3.9.1 2D-Gel Electrophoresis

The first dimension of 2D-gel electrophoresis was performed in a horizontal apparatus (Ettan IPGphor, GE Healthcare, San Francisco, USA). Granule subfractions were precipitated with 20% TCA (ratio 1:1). Protein samples (300 μg) were solubilised for 30 min at 30°C in rehydration buffer (Rabilloud 1998). The samples were then applied onto IPG strips (11 cm, pH 3-11) and isoelectric focusing was conducted at 20°C with 50 μA, for a minimum of 10 h at 50 V, 1 h at 500 V, 1 h at 1000 V and 110 min at 8000 V. The strips were afterwards incubated for 15 min in equilibration buffer containing 6 M urea, 75 mM Tris-HCL pH 8.8, 34.5% Glycerol (87%), 2% SDS, 0.002% bromophenol blue and 1.5 mM DTT and then applied on top of a SDS-PAGE gel (14 cm by 14 cm, 15%). Proteins were separated according to molecular weight in a Hoefer 600 SE RUBY chamber (3.1). For tryptic digestion, the SDS-PAGE were stained using colloidal Coomassie blue and silver staining (3.9.6 and 3.9.7).

3.9.2 1D-SDS Polyacrylamide Gel-Electrophoresis (SDS-PAGE)

Following the discontinuous tris-chloride/tris-glycine buffer systems according to (Laemmli 1970), proteins were separated in a running gel with a pH of 8.8. As standard was used, a 12.5% running gel over layered by a 4% stacking gel with a pH of 6.8. For the separation of high molecular weight proteins and complexes either gradient gels with various different compositions from minimal 3% to maximal 16% with and without stacking gel, or low percentage gels of 5% or 7% with a 3% stacking gels were applied (see list for gel composition down). Protein markers used were the pre-stained molecular weight markers Kaleidoscope (Table 3-4). The sample-running front was visualized by bromophenol blue contained in the sample-loading buffer. Gel electrophoresis in mini slap-gel chambers was conducted at 80 V until the proteins entered the running gel and continued at 100 V for approximately 90 min. Electrophoresis of larger gels (e.g. gradient gels) was performed approximately four hours. Gels were afterwards used either for immunoblotting (3.9.3) or isolated bands were prepared for mass spectrometry (3.10.1, 3.10.2, 3.10.3) by Coomassie-silver staining (3.9.6 and 3.9.7).

Stacking gel 5 mL (15 mL for big gels)		*3%*	*4%*
30% PAA	x.xx mL →	0.63 mL	0.83 mL
1 M Tris-HCl, pH 6.8	0.63 mL		
dH_2O	x.xx mL →	3.63 mL	3.43 mL
20 (w/v) % SDS	25 μL		
10% (w/v) APS	40 μL		
TEMED	5 μL		

Running gel 10 mL (30-40 mL for big gels)		*3%*	*5%*	*7.5%*	*10%*	*12.5%*	*16%*
30% PAA	x.xx mL →	0.97	1.67	2.5	3.33	4.17	5.33
2 M Tris-HCl, pH 8.8	1.86 mL						
dH_2O	x.xx mL →	7.06	6.40	5.56	4.73	3.89	2.73
20% (w/v) SDS	50 μL						
10% (w/v) APS	30 μL						
TEMED	5 μL						

SDS-Running buffer		
Tris/Base	25 mM	
Glycin	190 mM	
SDS	0.1% (w/v)	in dH_2O

3.9.3 Immunoblotting

For antibody detection, proteins previously separated on a SDS-PAGE (3.9.2) were electrophoretically transferred (blotted) to a membrane, which could be either nitrocellulose (NC)

or polyvinylidene fluoride (PVDF). PVDF is more adequate for hydrophobic proteins. For blotting, 3 mm Whatman papers and membranes were soaked in blotting buffer. PVDF membranes first had to be equilibrated in 100% methanol for 1 min at RT. A pile of one 3 mm Whatman paper, one membrane, the gel and again one 3 mm Whatman paper was prepared and embedded air was removed. The transfer occurred from the cathode to the anode at 12 V for 1 h in the semidry blotter (Trans-blot SD Semidry transfer cell, 3.1) used for proteins of 10 - 120 kDa. For high molecular weight proteins and complexes, a Hoefer TE22 Mini or TE42 Standard Tank blot system was applied see section 3.1. Wet blotting succeeded water-cooled, between 4 and 16 h depending on the application. Each method required its own buffer, which are listed down. The effectiveness of transfer was examined with Ponceau S. For washing of immunoblots 1xPBS buffer (section 3.7) was applied, in some cases completed to a 1xPBS-Tween buffer containing additionally 0.1% (v/v) Tween-20. Tween-20 is a mild non-ionic detergent used as wetting agent. Membranes were blocked for 1 h at RT with 5% low fat milk in PBS. Antibody dilutions were prepared either in PBS, PBS-Tween (PBS with 0.1% (v/v) Tween 20) or in blocking solution depending on the antibody. Membranes were incubated in primary antibody solution with agitation for 1–4 h at RT or overnight at 4°C. Then membranes were washed three times for 10 min at RT followed by incubation in a solution of horseradish peroxidase-conjugated secondary antibody for 1–2 h at RT. Membranes were washed again in PBS three times for 10 min at RT. For the enhanced chemiluminescence (ECL) reaction, ECL 1 (containing luminol) and ECL 2 (containing H_2O_2 as enhancer) solutions were mixed in a ratio of 1:1 and membranes were incubated for 2 minutes. Film exposure (3 to 30 minutes), development and fixation were performed in a dark room. For presentation and quantification films were scanned with a Bio-Rad GS-710 Calibrated Imaging Densitometer (3.1) and densitometric analysis for quantification was done using Bio-Rad Laboratories Quantity One software.

Components	*Tank blot buffer*	*Semidry blot buffer*
Tris/Base	25 mM	48 mM
Glycine	192 mM	39 mM
Methanol	20% (v/v)	20% (v/v)
20% SDS	---------	0.4% (w/v)
In dH_2O		

Ponceau S-solution	
Ponceau	0.2% (w/v)
Acetic acid	3% (v/v)
In dH_2O	

3.9.4 Quantification of Proteins by Immunoblotting

To determine, if a ZG constituent is part of the ZGC or the ZGM, a dilution series with both fractions was performed. Samples with 1-14 μg of a ZGM fraction and 140 μg of ZCG fraction were

prepared and filled up with Hepes buffer to achieve an equal volume for all samples. Then, the same amount of 3xleammli buffer was added to all tubes and samples were heated for 5 min at 95°C directly before loading onto a 12.5% SDS gel. On another gel with the same composition, samples from 0.5-12 μg of a ZGC fraction (treated as described before) were loaded together with 140 μg of a ZGM fraction. Both gels were blotted onto nitrocellulose and incubated with antibodies to GP2 (ZGM marker protein), Amylase (ZGC marker protein), ZG16p and Chymase as described in section 3.9.3. For quantification, immunoblots were scanned and ZGC to ZGM concentration ratios were measured and computed by defining the band density and the corresponding background using a GS-710 Calibrated Densitometer together with the Quantity One 4.3.1 software. The distribution of total ZG proteins (approx. 95% content proteins and 5% membrane-bound proteins) was taken into account to calculate the ratios and percentages of total protein distribution between ZGC and ZGM. Results for this experiment are shown in Chapter 4.

3.9.5 IgG Precipitation of Immunsera with Ammonium Sulfate

Serum fractions (1 mL) from antibodies were precipitated using ammonium sulfate. Samples were continuously kept at 4°C or on ice and sera obtained from different bleedings were treated separately. First, to precipitate IgG´s, one volume of serum was mixed drop by drop with one volume of a saturated ammonium sulfate solution (100% NH_4SO_4) resulting in a 50% NH_4SO_4 and centrifuged for 10 min at 10000×g. The pellet was slurred with a small self made glass pestle and washed. Washing succeeded in 1.5 mL 40% NH_4SO_4 buffer followed by a 10 min centrifugation at 10000×g. The washing step was repeated until the resulting pellet appeared snow white. The pellet was solved in 400 μL sodium phosphate (Na_2PO_4) buffer pH 7.4 by rotation for 30 min 4°C. Then the sample was dialysed overnight in 1 L 10 mM Na_2PO_4 buffer pH 7.4. Precipitates were removed by a 10 min centrifugation at 10000×g. The resulting supernatant was re-dialysed for 5 h as before and the exact volume was defined. The protein concentration was determined and IgG´s were precipitated with 100% NH_4SO_4 in a 1:1 ratio adding the solution drop by drop. The precipitate was centrifuged at 10000×g for 10 min and the pellet was resuspend in 40% NH_4SO_4 so that a final concentration of 10 μg/μL protein was obtained. Aliquots were stored at 4°C. Note: It is important to vortex antibodies directly before use when kept in an ammonium sulfate solution!

Saturated Ammonium sulfate (100% NH_4SO_4) buffer

Tris-HCl, pH 8.0	20 mM
EDTA	1 mM
NH_4SO_4	~4.1 M

40% NH_4SO_4 buffer

Mixture of 2.5 : 1 Tris-HCl, 1 mM EDTA, pH8.0 with 100% NH_4SO_4

Sodium phosphate (Na_2PO_4) buffer, pH 7.4

10 mM Na_2HPO_4, pH ~9.0

10 mM NaH_2PO_4, pH ~4.0

Buffers were titrated against each other until a pH of 7.4 was reached. For 1 L of Na_2PO_4, pH 7.4 approximately 810 mL Na_2HPO_4, pH ~9.0 were mixed with 190 mL NaH_2PO_4, pH ~4.0.

3.9.6 Staining with Colloidal Coomassie Brilliant Blue G-250

This protocol can be applied prior to silver staining for subsequent MS/MS analysis. Gels were fixed agitating for 1 h in 10% (v/v) acetic acid in 40% (v/v) methanol, followed by a washing step in distilled water. Staining was performed for 2 h in 0.12% (w/v) coomassie G250 in 20% (v/v) methanol. To wash out unbound Coomassie-G250 and visualize protein bands, gels were destained by washing in dH_2O for 1-2 min followed by several times washing in destaining solution containing 25% (v/v) methanol. Gels were then kept in dH_2O, digitalized for documentation and in some cases further processed for silver staining. For long term storage (2-4 weeks) gels were transferred into an aqueous solution containing 10% (v/v) ethanol and 20% (v/v) glycerol and were stored at 4°C.

3.9.7 Subsequent Silver Staining

Coomassie-G250´s detection limit for proteins is around 0.2–0.5 μg while with silver staining less than 1 ng of protein can be detected. To visualize low abundant proteins the following silver staining protocol was applied to coomassie stained gels.

For a subsequent silver staining, gels were washed twice with dH_2O and than fixed for 1 h in a solution of 50% (v/v) methanol, 12% (v/v) acidic acid (CH_3COOH), 0.05% (v/v) formaldehyde (60 μL from a 37% solution in 500 mL) followed by three times 20 min washing in 50% methanol. A two minutes sensitizing step was carried out in a solution of 0.02% (w/v) thiosulfate ($Na_2S_2O_3$), then gels were washed three times in dH_2O. To avoid silver oxidation, from now on all work was performed in a dark environment. For silver staining, gels were incubated for 20 – 30 min in a solution of 0.2% (w/v) $AgNO_3$ and 0.076% (v/v) formaldehyde. Formaldehyde was added freshly directly before use. After two times washing for 1 min in dH_2O gels were developed in a solution of 6% (w/v) potassium carbonate (K_2CO_3), 0.05% (v/v) formaldehyde and 0.00004% (w/v) thiosulfate ($Na_2S_2O_3$). To stop the staining, gels were transferred to a solution of 50% (v/v) methanol and 12% (v/v) acidic acid. For storage, the gels were kept in 0.1% (v/v) acidic acid containing 0.1% (w/v) sodium azid to avoid contamination.

3.10 Proteomics Methods

3.10.1 Tryptic Digestion of Proteins from Coomassie-Silver Stained Gels

Tryptic digestion and MS/MS analysis follow the protocol from (Vitorino, Lobo et al. 2004). To avoid contamination the working area was properly cleaned with 70% ethanol and all solutions applied were prepared in ddH_2O. Protein bands of stained gels were excised under a hood and each band by itself was chopped again in smaller pieces to guarantee a better excess of trypsin to the proteins trapped in the gel matrix. Samples were placed in a 96 well rack with wholes on the bottom of each well and the position of each sample was documented. This rack was fixed to a bottom rack to which a vacuum could be applied. Like this, liquids were removed from samples and collected by applying a soft vacuum in the lower rack. Gel pieces were destained twice by adding 50 μL of a 50 mM sodium thiosulfate ($Na_2S_2O_3$) and 15 mM potassium-ferrocyanite (KFeCN) solution to each well and incubation for 30 min at RT. The supernatant was removed and gel pieces were washed three times by adding 100 μL 25 mM ammonium bicarbonate (NH_4HCO_3) in 50% acetonitrile (ACN) and incubation for 30 min at RT. Followed by a final washing step with 40 μL 100% ACN for 10 min at RT. Gel pieces were dried in a SpeedVac (Thermo Savant) for 10 – 15 min. For tryptic digestion, 25 μL of 0.01 μg/μL sequence grade modified porcine trypsin in 25 mM ammonium bicarbonate were added to each sample and incubated overnight at 37°C. By addition of 30 μL of 10% (v/v) formic acid (CH_2O_2) and incubation for 30 min at RT the digestion was stopped and peptides were extracted. To increase the peptide yield, gel pieces were additionally washed twice for 30 min at RT with 50 μL 10% (v/v) formic acid with 50% (v/v) ACN. All supernatants collected were joined and lyophilised in a SpeedVac for 4 h at RT. Afterwards, pellets were resuspend in 10 μL of 50% (v/v) ACN with 0.1% (v/v) trifluoroacetic acid (TFA) and carefully vortexed.

3.10.2 Matrix Embedding of Samples from Tryptic Digestion for MS/MS Analysis

First, the MALDI target plate was washed softly in the following sequence: dH_2O, methanol, ACN and Isopropanol, afterwards, the plate was polished. Then, samples (3.10.1) were mixed 1:1 with matrix solution (saturated α-cyano-4-hydroxycinnamic acid prepared in 50% acetonitrile with 0.1% formic acid). Two times 0.5 μL of each sample mixture were spotted onto the MALDI target plate. Each sample was pipetted in duplicates and their positions were documented. In between and after sample application the plate was allowed to dry for 5 min at RT.

3.10.3 Mass Spectrometry

Peptide mass spectra were obtained on a MALDI-TOF/TOF mass spectrometer (4800 Proteomics Analyzer, Applied Biosystems, Europe, 3.1) in the positive ion reflector mode. Spectra were acquired in a mass range between 800 and 4500 Da with ca. 1500 laser shots. Up to six of the most intense ion signals per shot position (peaks) were selected excluding those coming from the matrix, trypsin autolysis, or acrylamide peaks. Trypsin autolysis peaks were used for internal calibration of the mass spectra, allowing a routine mass accuracy more than 20 ppm.

3.10.4 Liquid Chromatography Separation and Mass Spectrometry

For in solution digestion, 1 μg of ZGWash, ZGM_{washed}, or ZGM were digested using sequencing grade trypsin in a proportion of 1:20 and incubated overnight according to the manufacturer instructions. Liquid chromatography (LC) separation was performed using an Ultimate 3000 (Dionex/LC Packings, 3.1). Twenty microliters of each sample (corresponding to 1 μg of protein) were injected into a Zorbax 300SB-C18 trapping column with 5 μm particle size (3.1) using an LcPackings Probot auto sampler (3.1). The sample was washed while bound to the trapping column for 3 min with 95% buffer A (ddH_2O, 0.1% TFA) and 5% Buffer B (acetonitrile, 0.1% TFA) at a flow rate of 30 μL/min. The sample was eluted into a Zorbax 300SB-C18 capillary analytical column with 3.5 μm particle size (3.1) by reversing the flow and at a flow rate of 0.3 μL/min. A linear gradient of 5 to 55% Buffer B was run over a period of 35 min. Afterwards, the column was washed by applying a 3 min gradient from 55 to 90% Buffer B, followed by a 5 min hold at 90% Buffer B. The column was then re-equilibrated in 5% Buffer B prior to future analyses. The eluted peptides were directly deposited on 384-well MALDI plates at 20 s intervals for each spot using a Probot (3.1) adding 170 nL of matrix solution (prepared by diluting saturated α-cyano-4-hydroxycinnamic acid with 70% acetonitrile and 0.1% TFA including 10 fmol of an internal standard).

3.10.5 Mass Spectrometry Data Acquisition

Spectra were processed and analysed by the Global Protein Server Workstation (Applied BioSystems, Foster City, CA, USA), which uses internal Mascot (Matrix Science Ltd, U.K.) software for searching the peptide mass fingerprints and MS/MS data. Searches were performed against the NCBI non-redundant protein database for *Rattus norvegicus*.

3.11 Computational Method to Compile a Phylogenetic Tree

A Phylogenetic tree was compiled using BLAST pair wise alignments for proteins (BLASTP 2.2.25+) (Altschul, Madden et al. 1997; Altschul, Wootton et al. 2005) from NCBI with the following parameters: tree method: neighbour joining, maximal sequence difference 0.7. The maximum allowed fraction of mismatched bases in the aligned region between any pair of sequences. If the fraction of mismatched bases for any pair of sequences was larger than this value, both sequences were excluded from the tree generation. The accuracy of this prediction decreases as the fraction of mismatched bases increases. Hence, for larger values of *Max Seq Difference* (> 0.6) sequence grouping is often accurate, but the lengths of paths between very dissimilar sequences can be inaccurate. Double sequences were excluded prior to the tree compiling. For the tree view, the BLAST tree view tool from NCBI was chosen using the fast minimum evolution tree method.

Chapter 4 Analysis of Low Abundant Membrane-Associated Proteins from Rat Pancreatic Zymogen Granules

The exocrine pancreas served as the model that first established the role of intracellular compartments in the secretory pathway (Palade 1975), and ZG have been used as a model system to study secretory granule biogenesis and regulated secretion in general. As briefly outlined (see Introduction 1.3), the molecular mechanisms required for ZG formation at the TGN, for packaging and sorting of cargo proteins, as well as for granule fusion and exocytosis are still poorly defined reviewed in (Schrader 2004; Borgonovo, Ouwendijk et al. 2006; Dikeakos and Reudelhuber 2007; Williams, Chen et al. 2009). According to recent models (see Introduction 1.3), part of the molecular machinery required for digestive enzyme sorting, granule trafficking and exocytosis is supposed to be associated with the granule membrane (ZGM). In addition to basic research interests ZG play as well important roles in pancreatic injury and disease (Gaisano and Gorelick 2009; Husain and Thrower 2009) (see Introduction 1.1). It is well documented that mis-sorting of zymogens to lysosomes or the basolateral membrane domain can lead to acinar cell injury and pancreatic disease (*e.g.* to pancreatitis; see Introduction 1.1). Unravelling the molecular machinery that mediates the proper trafficking of potentially damaging proteases to distinct membrane domains by specific coat, adapter, and Rab proteins, is therefore of great biological and clinical importance. Thus, there is currently great interest in the identification and molecular characterization of ZG and ZGM components by conducting antibody screens, raft analyses as well as proteomics (Schmidt, Dartsch et al. 2000; Schmidt, Schrader et al. 2001; Kalus, Hodel et al. 2002; Chen, Walker et al. 2006; Berkane, Nguyen et al. 2007; Rindler, Xu et al. 2007).

As indicated (see Introduction 1.7), ZG are best suited for subcellular (and suborganellar) proteomics, as they represent abundant organelles of the exocrine pancreas, which can be easily isolated and purified due to their large size and density. In addition, their isolation yields large quantities of organelles and proteins. Furthermore, intact ZG can be lysed at pH 8 (see Figure 12 and Methods 3.8.2) and further separated into a content (ZGC) and membrane (ZGM) fraction. This reflects the physiological conditions, as the ZGC proteins become soluble in the alkaline environment of the pancreatic duct, where bicarbonate is secreted to neutralize stomach acid in the small intestine. ZGM fractions can be further purified by potassium bromide and/or carbonate treatment at pH 11 and subsequent (gradient) centrifugation to enrich transmembrane and membrane-anchored proteins (ZGM_{washed}) or peripheral ZGM proteins (ZGWash) (Hoops and Rindler 1991; Schmidt, Dartsch et al. 2000; Chen, Walker et al. 2006; Chen and Andrews 2008) (see Figure 12, Methods 3.8.2).

Our laboratory is applying various different proteomics approaches to identify new and also low abundant ZGM constituents (Figure 12). For instance, the application of doubledSDS-PAGE, an approach optimized for the analysis of hydrophobic membrane proteins (Schagger and von Jagow 1991), led to the discovery of the small GTPase Rab8A at the ZGM (Faust, Gomez-Lazaro et al. 2008). These findings were verified by immunoblotting, immunofluorescence and knock-down experiments, and our studies revealed that Rab8A has a role early on in ZG formation at the Golgi complex (Faust, Gomez-Lazaro et al. 2008).

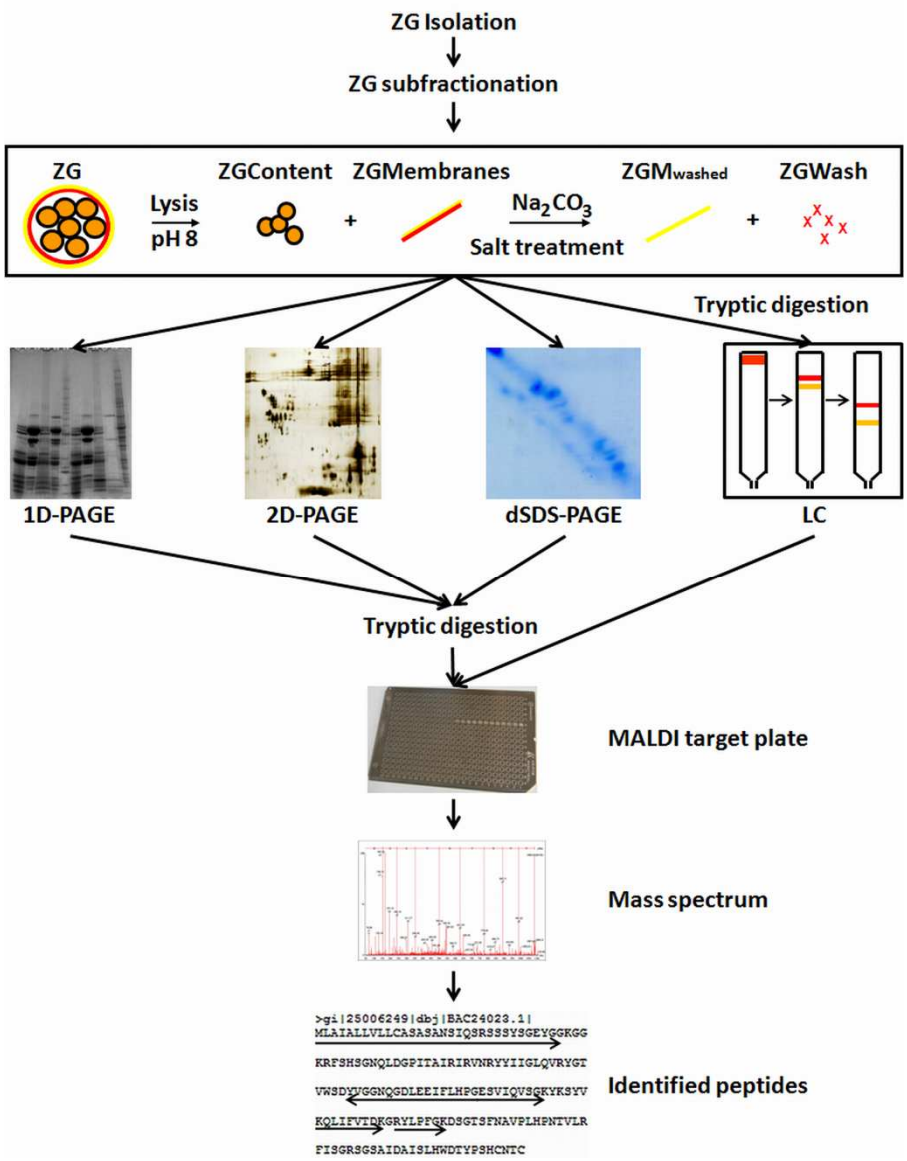

Figure 12: Methods applied by our group, for the separation of ZG and subsequent mass spectroscopic analysis of ZG subfractions

In an earlier study from our group using an old-fashioned 2D-gel electrophoresis approach applied to the ZGWash fraction, various different acidic and basic proteins were detected, *e.g.* the serpin ZG46p, GP2, the lectin ZG16p, lipase and carboxypeptidase (Schmidt, Dartsch et al. 2000). We recently continued with the further analysis of the ZGWash fraction by 2D-SDS PAGE (3.9.1) in a team approach by applying a modern and advanced set up (see Methods 3.1). We initially focused on the "basic" group of peripheral ZGM proteins (pH range 6.2-11) with about 46 spots, among which 44 were identified and assigned to 15 unique proteins by mass spectrometry (3.10.3, 3.10.5, Figure 12). The separation of the ZGWash subfraction, which was obtained by a carbonate treatment of the ZGM, was performed by two-dimensional IEF/SDS-PAGE followed by Coomassie staining. For isoelectric focusing, 300 μg of protein were separated on 11 cm IPG strips (pH 3-11NL) and on 15% polyacrylamide gels in the 2nd dimension (see Methods 3.9.2). The predicted intracellular distribution of the identified proteins is represented in the pie chart

diagram of Figure 13. The 15 unique proteins (Table 4-1) were categorized in 6 groups based on their known subcellular localization: ZGC (n=6; 38%) and ZGM (n=6; 38%) proteins, mast cell proteins (n=1; 6%), ER resident proteins (n=1; 6%), and proteins with other localizations (n=2; 12%) (Figure 13). Based on their predicted biological functions we identified 12 enzymes including 9 digestive enzymes (usually attributed to the ZGC), 2 matrix (ZG16p, syncollin) and 3 slightly acidic glycoproteins (CEL, pancreatic lipase related protein 1 and 2). Based on literature and the Protein Knowledgebase (UniProtKB), all of the identified proteins are supposed to be soluble or peripheral membrane proteins, and no transmembrane proteins or membrane-anchored proteins have been identified in the wash fraction. Furthermore, except for two cytosolic proteins (vinculin (fragment), an actin-binding protein, and ubiquitin carrier protein involved in ubiquitination/quality control) all identified proteins are supposed to be components of the secretory pathway. This further confirms the applicability of the carbonate and gel-based proteomic approach. In addition, some classical content proteins such as amylase, elastase, colipase and triacylglycerol lipase were identified in the wash fraction (Table 4-1). This can be due to a cross-contamination of the subfractions or due to the fact that the interactions established between the proteins from the different subfractions are not completely disrupted in the separation procedure. The identification of some abundant theoretical acidic proteins within the "basic" group (*e.g.* CEL, lipase related protein 1) is likely to be a result of protein degradation and/or deglycosylation.

While increased instrument sensitivity allows the identification of many more low abundant proteins, it also uncovers more potential contaminating proteins. Thus, it is important to validate the localization of proteins of interest, which in the case of ZG proteins, is mainly done by antibody-based technologies. Thus, some of the low abundant proteins identified in our approach were selected for further analysis to verify their ZG localisation.

UniProtKB	Protein name	Localization	Function
LIPR1_RAT	Pancreatic lipase related protein 1	ZGM	Lipid degradation
LIPP_RAT	Pancreatic triacylglycerol lipase	ZGM	Lipid degradation
AMYP_RAT	Pancreatic alpha-amylase	ZGC	Carbohydrate metabolism
CEL_RAT	Bile salt-activated lipase	ZGC	Lipid degradation
MCPT1_RAT	Mast cell protease I (RMCP-1) (Chymase)	Mast Cell Granules	Serine-type endopeptidase activity
CELA1_RAT	Chymotrypsin-like elastase family member 1	ZGC	Serine-type endopeptidase activity
VINC_RAT	Vinculin	Cell Membrane	Cell Adhesion
TRY3_RAT	Cationic trypsin-3	ZGC	Serine-type endopeptidase activity
RNS1B_RAT	Ribonuclease pancreatic beta-type	ZGC	RNA Endonuclease
PPIB_RAT	Peptidyl-prolyl cis-trans isomerase B	Endoplasmic Reticulum	Protein Folding
ZG16_RAT	Zymogen granule membrane protein 16	ZGM	Lectin – Sugar binding
SYCN_RAT	Syncollin	ZGM	Compound exocytosis
B2RZA9_RAT	Ubiquitin carrier protein	Cytoplasm	Protein Modification
LIPR2_RAT	Pancreatic lipase-related protein 2	ZGM	Galactolipid catabolic process
COL_RAT	Colipase	ZGM	Cofactor of pancreatic lipase

Table 4-1 Identified "basic" Proteins
In the table, functional annotation and organelle assignments were made using the UniprotKB database, additional annotation was incorporated from literature search. The diagram on the next page illustrates the intracellular distribution of the identified proteins of the wash fraction. On the basis of published data, annotations in databases or predictions based on similarity to related proteins, the identified proteins were grouped in a pie chart according to their subcellular distribution and function. The Figure is taken from Borta, Aroso et al 2010.

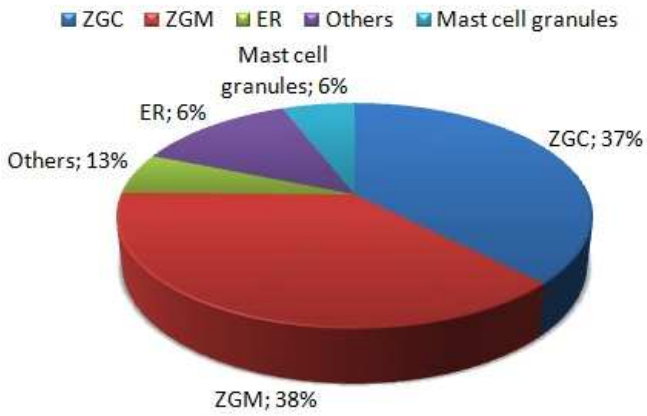

Figure 13: Diagram of the intracellular distribution of the identified proteins of the "basic group" from the wash fraction.

4.1 Rat Mast Cell Protease 1 (RMCP-1)/Chymase is a New ZGM Associated Protein

The serine protease Chymase (RMCP-1), which was so far only described in mast cell granules (Pejler and Maccarana 1994; Pejler and Berg 1995; Pejler and Sadler 1999), was identified in the ZGWash fraction by suborganellar proteomics using a 2D-SDS PAGE approach combined with tandem mass spectrometry (Figure 12). By immunoblotting of a duplicate of the 2D-gel using a specific antibody, Chymase was confirmed to be present in the ZGWash fraction (Borta, Aroso et al. 2010). Thus, the enzyme was selected for further analysis. To examine the distribution of Chymase among ZG subfractions, equal amounts of protein from the four subfractions (ZGC, ZGM, ZGM_{washed} and ZGWash) were separated on 12.5% acrylamide gels and immunoblotted using an antibody directed to Chymase (Figure 14). Furthermore, to assess a proper granule subfractionation, antibodies to the granule marker proteins Amylase, GP2, and ZG16p were used. As shown in Figure 14, immunoreactivity for Amylase was mainly found in the ZGC fraction, whereas GP2, a major GPI-anchored glycoprotein of ZG, was predominantly present in the ZGM fraction. The secretory lectin ZG16p, a peripheral ZGM protein (Cronshagen, Voland et al. 1994), was concentrated on isolated ZGM, and a major portion was liberated by carbonate treatment (Figure 14 and Figure 15 B). Interestingly, Chymase showed a very similar distribution pattern like ZG16p. The enzyme was associated with isolated ZGM, but barely detectable in the ZGC fraction. Upon carbonate-treatment, the majority of Chymase was removed from the ZGM and found in the ZGWash fraction indicating that the protein is a peripheral component of the ZGM (Figure 14). To exclude a contamination of the ZG subfractions with granules from mast cells (*e.g.* from pancreatic tissue), an antibody to Tryptase β1, a prominent mast cell marker, was applied. A lysate of rat tongue tissue, which is rich in mast cells containing RMCP-1, was used as a positive control. Both, Tryptase β1 and Chymase, were detected in lysates of rat tongue but in contrast to Chymase, Tryptaseβ1 was absent in ZG subfractions (Figure 14).

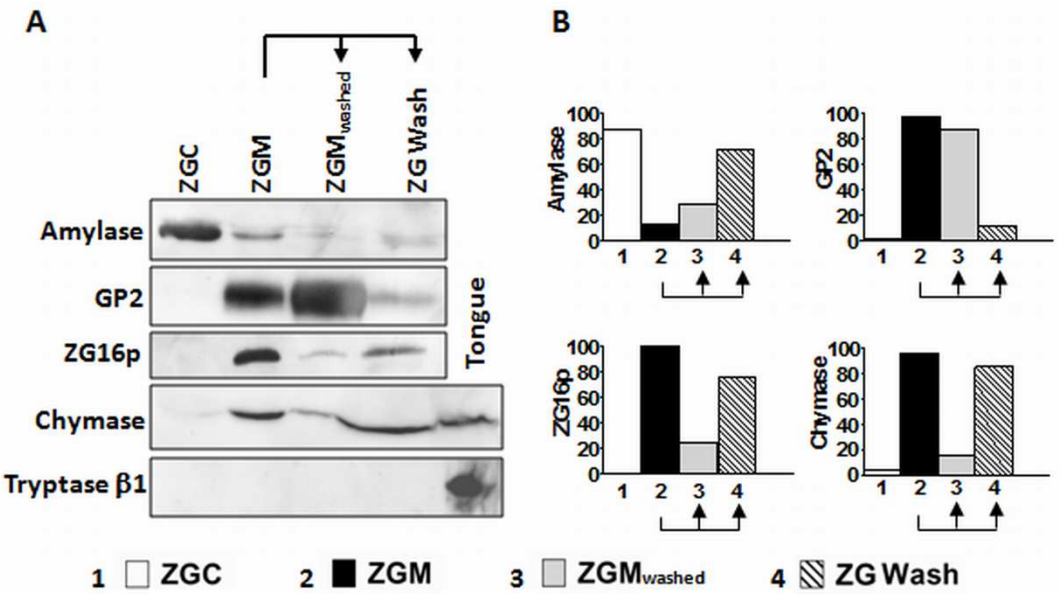

Figure 14: Chymase represents a peripheral membrane protein of rat ZG.

(**A**) Lysed granules were separated into a content (ZGC) and membrane fraction (ZGM). In addition, isolated membranes were treated with Na_2CO_3 at pH 11.5 and separated into pellet (ZGM_{washed}) and supernatant (Wash) fractions. Equal amounts of protein (20 μg) were run on 12.5% acrylamide gels, blotted onto nitrocellulose membranes and incubated with antibodies to Amylase (ZGC marker protein), GP2 (ZGM marker protein), ZG16p (peripheral ZGM marker protein), Chymase and Tryptase β1 (mast cell control). (**B**) Densitometric quantification of immunoblots shown in (**A**). The distribution of the labeling density to ZGC and ZGM (% labeling density of total ZGC + ZGM) as well as the distribution of the labeling density to ZGM_{washed} and ZGWash (% labelling density of total ZGM) is depicted (see Figure 15). Note that the overall distribution of Chymase resembles that of ZG16p, a peripheral ZGM marker protein. A lysate from rat tongue served as control for the detection of mast cell proteins.

In order to provide a quantitative approach, I performed dilution series of the ZGC and the ZGM fractions, which were analyzed by immunoblotting with specific antibodies to Chymase, Amylase, GP2 and ZG16p. The intensities of the corresponding signals were determined by densitometric measurements and the ratios of the proteins in the ZGC to ZGM fractions were calculated using these titration curves (Figure 15).

A ZGC to ZGM concentration ratio of 1:46 was calculated for Chymase, indicating an enrichment of Chymase in the membrane fraction. Interestingly, a similar concentration ratio was obtained for the secretory lectin ZG16p, a peripheral membrane protein. In contrast, Amylase was highly enriched in the ZGC fraction (about 80:1) and GP2, a GPI-anchored protein of the ZGM, was highly enriched in the ZGM fraction (about 1:93.3). The calculations take into account that approximately 95% of the total ZG proteins are constituted by content proteins and 5% by membrane-bound proteins. This implicates that about 70% of total Chymase are associated with the ZGM fraction. In contrast, only 0.06% of total Amylase is recovered in the membrane fraction, and 99.94% in the content fraction. The values for the prominently membrane-associated proteins are presumably even higher, as the proteins are partially liberated from the membranes during the isolation procedure.

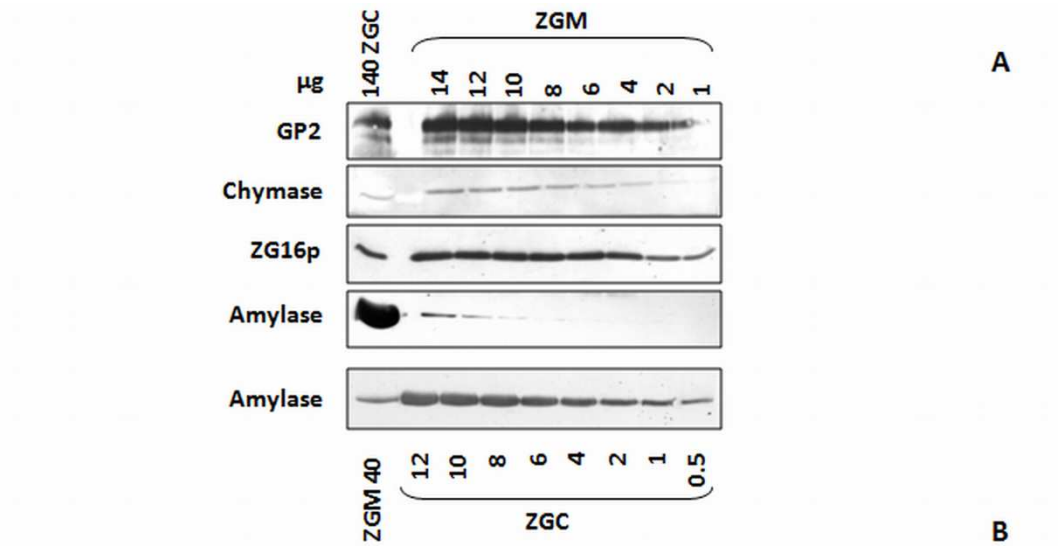

	bands compared in OD		Ratio OD	Ratio µg	Ratio of total	% of total
	ZGC µg	ZGM µg	ZGM/ZGC	ZGC : ZGM	ZGC : (ZGM*20)	in ZGM
GP2	140	1.5	1.03	1 : 93.3	1 : 4.67	82.4
Chymase	140	3	0.90	1 : 46.7	1 : 2.34	70.1
ZG16p	140	3	0.95	1 : 46.7	1 : 2.34	68.8
Amylase	0.5	40	1.04	80.0 : 1	1600 : 1	0.06

Figure 15: Determination of the ratio between the ZGC and ZGM quantities of Chymase, ZG16p, GP2 and Amylase.

(**A**) Dilution series of ZGC and ZGM subfractions were analyzed by immunoblotting. (**B**) ZGC to ZGM concentration ratios were calculated using densitometry of the corresponding signals from the immunoblots using a GS-710 Calibrated Densitometer together with the Quantity One 4.3.1 software. The distribution of total ZG proteins (approx. 95% content proteins and 5% membrane-bound proteins) was taken into account to calculate the ratios and percentages of total protein distribution between ZGC and ZGM. Note that Amylase, a classical content marker, shows 80 fold enrichment in the ZGC fraction with only 0.06% of total Amylase found within the ZGM fraction.

More stringent conditions for the isolation and subfractionation of ZG, *e.g.* a high salt buffer, recovering of ZGM in a 0.3 M/1 M sucrose gradient to avoid pelleting, and extensive washing in 100 mM $NaHCO_3$ pH 8.1, did not lead to any alteration of the distribution of Chymase and ZG16p. Only Amylase was more efficiently removed from the ZGM (Borta, Aroso et al. 2010). Thus, it can be excluded that not all of the content is solubilized and that aggregated zymogens might sediment with the membranes. The minor amount of amylase found in the ZGM fractions is as well an indicator for complete ZG lysis and solubilization of the granule content (at least of amylase-containing complexes). Furthermore, membrane-association of some content proteins was also observed by others after more stringent washing/purification conditions and gradient centrifugation (Chen, Walker et al. 2006; Rindler, Xu et al. 2007).

4.2 Chymase is Sorted to Secretory Granules in Pancreatic AR42J Cells

To examine if exogenously expressed Chymase is sorted to ZG, rat pancreatic AR42J cells were treated with the glucocorticoid dexamethasone to initiate their differentiation into acinar-like cells and the *de novo* formation of electron-opaque secretory granules containing the major pancreatic zymogens (Logsdon, Moessner et al. 1985) (see Introduction 1.7). Granule formation was usually induced 24 h after plating by the addition of 10 nM dexamethasone, and cells were processed after 2-3 days. RT-PCR with mRNA from stimulated and control AR42J cells revealed that Chymase was not endogenously expressed under our experimental conditions (Figure 16 L). It is known that AR42J cells do not express all ZG proteins found in rat pancreas (Yu, Hao et al. 2004). Thus, AR42J cells were transfected with a generated construct coding for a Chymase-YFP fusion protein (see Methods 3.5.5 and 3.6.3, Figure 16 A-C) or an YFP containing an ER-targeting signal (YFP-ER) (Figure 16 D-I) and stimulated for granule formation. After 2-3 days, cells were processed for indirect immunofluorescence (see Methods 3.7.1) using antibodies to Carboxypeptidase A (Figure 16 B, E). Dexamethasone-treatment resulted in the formation of numerous characteristic granules positive for Carboxypeptidase A. Confocal microscopy (see Methods 3.8) revealed that many of these granules showed a co-localization with Chymase-YFP (Figure 16 A, C), whereas the control YFP-ER localized mainly to the Golgi complex in AR42J cells (Figure 16 G-I), and not to secretory granules (Figure 16 D, F). As additional controls, a VSVG-GFP and YFP-GPI fusion protein were expressed in AR42J cells, but were not observed to be sorted to secretory granules. The fusion proteins were instead targeted to the plasma membrane in AR42J cells (Faust, Gomez-Lazaro et al. 2008). This shows that the YFP tag does not interfere with the protein targeting and sorting to the specific cellular compartments occurs unrestricted. Quantification by pixel-by-pixel analysis from confocal images revealed a co-localization coefficient of 77 ± 18% (n=6, 15 z-planes from each cell) for Chymase-YFP and Carboxypeptidase A (Figure 16 K). These findings demonstrate that rat mast cell Chymase enters the secretory pathway and is properly sorted to ZG in AR42J cells, an acinar model system.

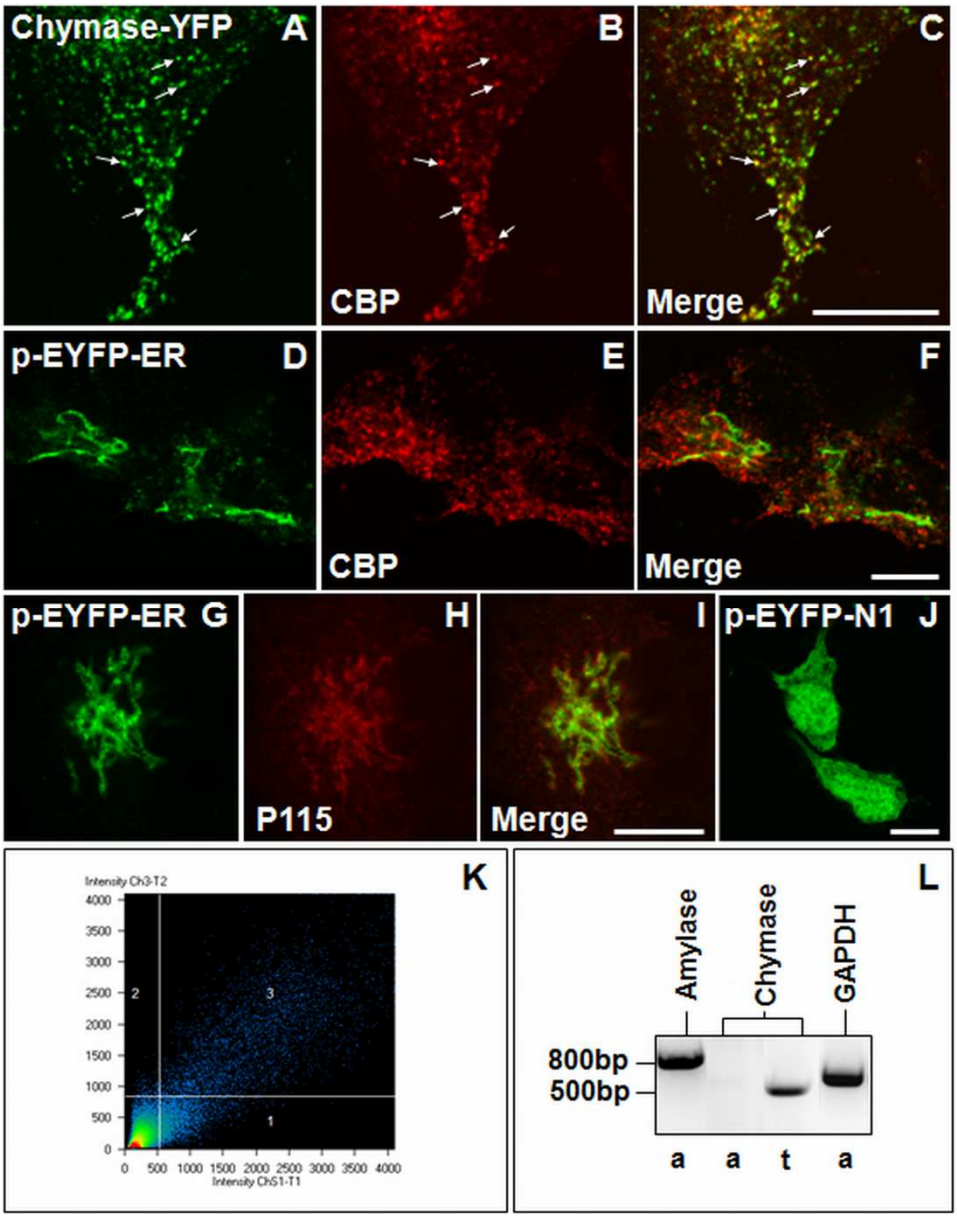

Figure 16: Chymase is targeted to zymogen granules in pancreatic acinar AR42J cells.
AR42J cells were transfected with a Chymase-YFP construct (**A**), a p-EYFP-ER construct (**D**, **G**) or a p-EYFP-N1 vector (**J**), stimulated for granule formation and processed for indirect immunofluorescence 72 hours after transfection using antibodies directed to Carboxypeptidase A (CBP) (**B**, **E**) and the Golgi marker P115 (**H**). Overlays (Merge) of the confocal images (**A**-**B**; **D**-**E**; **G**-**H**) are shown in (**C**, **F**, **I**). Arrows point to some granules showing colocalisation of Chymase-YFP and CBP. EYFP-ER localizes mainly to the Golgi complex and is not targeted to granules in AR42J cells. Cytosolic YFP (**J**) is not targeted to granules either. (**K**) Quantitative correlation analysis. Image analysis was carried out with the Zeiss LSM 510 4.0 software (Carl Zeiss MicroImaging, Inc.). The correlation plot describes the pixel colocalisation depending on their intensity in the Alexa 488 (for Chymase-YFP) and TRITC (for CBP) channels with region 3 displaying colocalising pixels, whereas regions 1 and 2 contain the non-colocalising pixels for each label, respectively. The signals below the background (indicated by the axes) in each picture were not included in the quantification of the colocalisation coefficients. An average value of 77% of colocalisation has been obtained measured from 6 cells (15 z-planes from each cell) with a standard deviation of 18%. (**L**) RT-PCR of mRNA isolated from AR42J cells (treated with 10 nM dexamethasone) (a) and from rat tongue (t) (positive control for Chymase expression). GAPDH was used as a loading control. Note that Chymase is not endogenously expressed in pancreatic acinar AR42J cells. Scale bars, 10 μm.

4.3 Chymase Locates to ZG in Rat Pancreatic Tissue

By immunohistological and ultrastructural studies which were performed in cooperation with B. Agricola (University of Marburg, Germany) the localization of endogenous Chymase to ZG in rat pancreatic tissue could be confirmed (Figure 17). For this approach (see Method 3.7.3.3), frozen sections of rat pancreas were incubated with specific antibodies directed to Chymase and to Carboxypeptidase A, a prominent granule marker protein (Figure 17 A, B). Chymase was observed to colocalize with Carboxypeptidase A over the granule region/zymogen granules surrounding the acinar lumen (Figure 17 C). As a negative control, sections were incubated with a pre-absorbed antibody and with anti-Carboxypeptidase A (Figure 17 D-F).

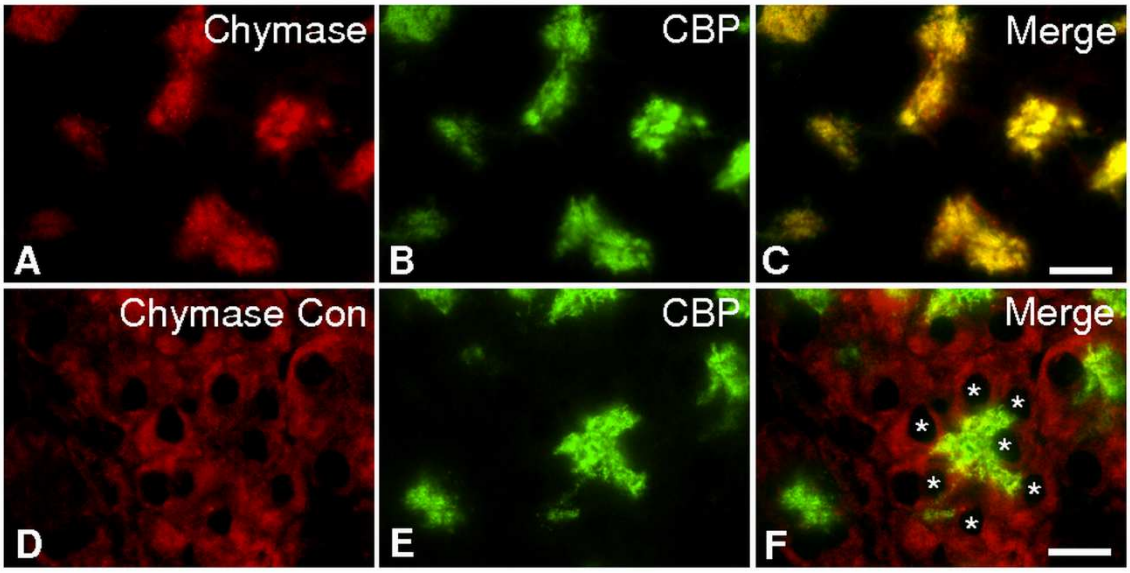

Figure 17: Immunofluorescence microscopy of rat pancreatic sections.
Cryosections of rat pancreas were incubated with antibodies specific for Chymase (**A**) and Carboxypeptidase (CBP) (**B**). (**C**) Overlay (Merge) of (**A**, **B**). (**D**, **E**) Negative control using pre-adsorbed Chymase and anti-Carboxypeptidase antibodies. (**F**) Overlay (Merge) of (**D**, **E**). Asterisks in (**F**) mark the nuclei of acinar cells. Scale bars, 10 μm.

Since immunoelectron microscopy can reveal a more precise image of the subcellular localization of a protein then immunohistology, this method was applied for further verification. Tissue samples of rat tongue and pancreas were embedded in K4M (Figure 18 A, B), and ultrathin sections were stained with antibodies to Chymase and afterward with protein A-gold (see Methods 3.8.3.5). Rat tongue tissue served as a positive control, as it is rich in mast cells and Chymase-containing granules. A prominent and uniform labeling with gold particles was observed on cytoplasmic granules (Figure 18 A). A specific gold-labeling of ZGs in pancreatic acinar cells was as well observed. The staining was less prominent, but specific for ZGs (Figure 18 B) (labeling density on ZG: 1.16±0.1 gold particles/μm^2, labeling density on control areas outside ZG: 0.18±0.8 gold particles/μm^2). This might be due to the low abundance of Chymase in ZGs and the regulation of its expression level (*e.g.* by feeding behaviour). Also, the accessibility of the protein might be reduced in highly condensed ZGs.

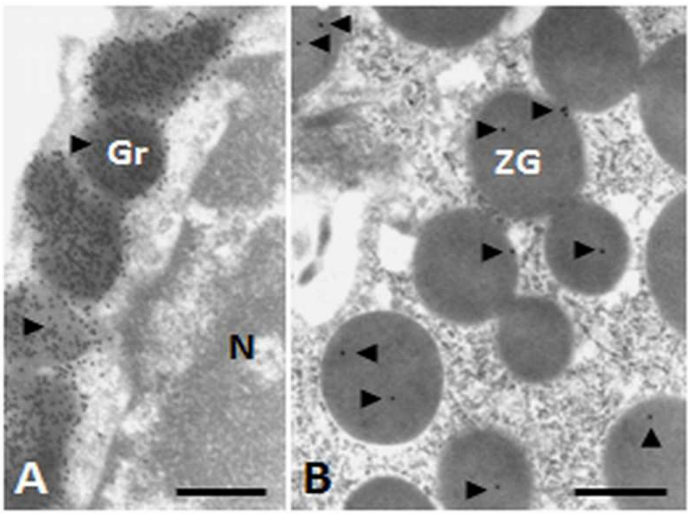

Figure 18: Chymase localizes to zymogen granules in acinar cells of the exocrine pancreas.
Tissue form rat tongue (**A**) and pancreas (**B**) was processed for immunogold electron microscopy, incubated with a polyclonal anti-Chymase antibody and visualized using 10 nm protein A gold. Arrowheads in (**B**) indicate gold particles on zymogen granules (ZG). Gr, granule of a mast cell; N, nucleus. Scale bars, 1μm. EM preparations were done with help and support of B. Agricola, University of Marburg.

4.4 Sulfated Proteoglycans are Present on the Inner Surface of the Granule Membrane

Since early electron microscopic studies revealed the existence of a fibrillar network in pancreatic juice as well as on the inner surface of the ZGM after freeze-fracture (Cabana, Hugon et al. 1981; Grondin, St-Jean et al. 1992), we examined the presence of sulfated proteoglycans in zymogen granules of pancreatic tissue by the Cupromeronic Blue (CmB) protocol (see Materials and Methods (3.7.3.4, Figure 18). This protocol has been successfully used to stain proteoglycans in secretory granules of leucocytes (Unger, Hokland et al. 1997). Interestingly, the formed CmB-proteoglycan complexes mainly appeared in ultrathin pancreatic sections, fixed-stained according to Scott (1980), as elongated small electron-dense filaments or 'prisms' underneath the granule membrane with some variation between individual granules (Figure 19 A, B). CmB-proteoglycan complexes were also observed in the intermembrane space (Figure 19 A), presumably due to a staining of proteoglycans of the extracellular matrix, and in the acinar lumen (not shown). However, no other intracellular organelles of the acinar cells were positive for proteoglycan staining. These morphological observations support our previous biochemical studies (Schmidt, Dartsch et al. 2000; Schmidt, Schrader et al. 2001) indicating that sulfated proteoglycans are components of a submembranous matrix which is associated with the inner surface of ZG (see Introduction 1.3).

When isolated ZGM and ZGM pre-treated with carbonate at pH 11 (which removes most of the peripheral components) were embedded for electron microscopy, the untreated membranes appeared overwhelmingly curved or curled (Figure 19 C). In contrast, most of the carbonate-treated membranes had a strikingly linear appearance (Figure 19 D). We assume based

on the above observations that the granule matrix might have important mechanical functions during granule formation at the trans-Golgi network (TGN) as well as for granule stability.

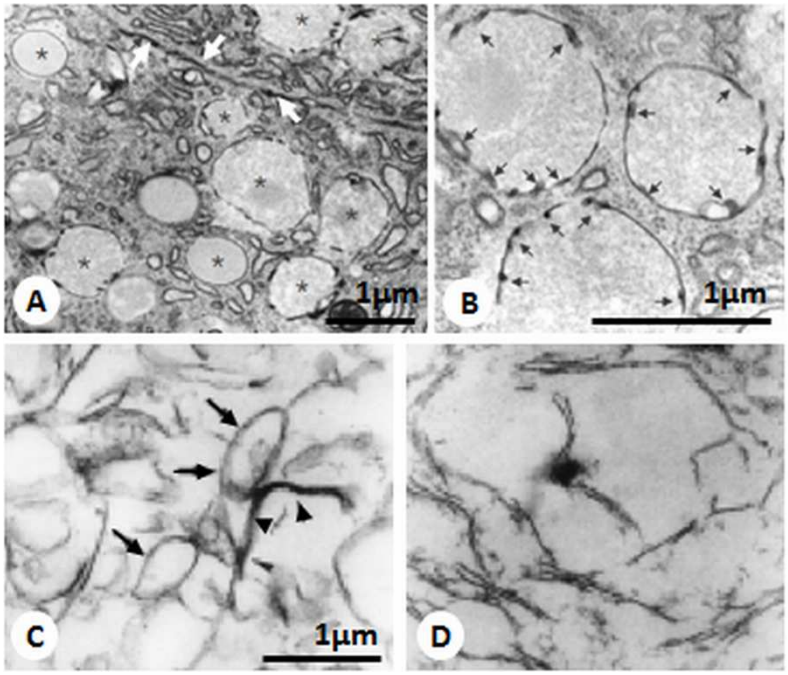

Figure 19: Pancreatic ZG possess a submembranous proteoglycan skeleton, influencing membrane curvature.

Pancreatic tissue (**A**, **B**) was stained according to the Cupromeronic Blue (Cmb) protocol and embedded for electron microscopy (3.7.3.4). (**A**, **B**) Electron dense proteoglycan complexes were found to form filaments underneath the granule membrane in acinar cells of rat pancreas (A; asterisks). In addition, Cmb staining was detected within the intracellular space (**A**, white arrows). (**B**) Higher magnification view of ZG in acinar cells of rat pancreas after Cmb staining. Arrows in (**A**) and (**B**) point to proteoglycan complexes. (**C**, **D**) ZG were isolated from rat pancreas, and membrane subfractions were prepared. Isolated membranes (ZGM) were either left untreated (**C**), or incubated with sodium carbonate to remove granule matrix components (**D**) and afterwards processed for electron microscopy. Note the strong curved (arrowheads) or curled membranes (arrows) in (**C**), in contrast to their linear appearance in (**D**). EM preparations were done with help and support of B. Agricola, University of Marburg.

4.5 Discussion to Chymase as Peripheral Protein of the ZGM

The ZG membrane has been the focus of recent proteomics studies (Chen, Walker et al. 2006; Rindler, Xu et al. 2007; Chen and Andrews 2008) as their components are supposed to contribute – at least partially – to the sorting and packaging of digestive enzymes into ZG, their apical transport, membrane fusion and regulated, Ca^{2+}-dependent secretion as well as to pancreatic and intestinal disorders. Here we report on the identification of peripheral, membrane-associated proteins of the ZGM by a suborganellar proteomic approach based on carbonate-treatment of ZGM and 2D-PAGE of the corresponding supernatant (wash) fraction. In this study we focused on the identification and characterization of a “basic” group of membrane-

associated proteins (*pI* range 6.2-11). As a verification of our approach, two previously reported peripheral (basic) ZG proteins, the secretory lectin ZG16p and Syncollin, were identified in this study. ZG16p is supposed to interact with the ZGM via its lectin domain, whereas Syncollin has been shown to interact with cholesterol and the GPI-anchored membrane glycoprotein GP2 (Kleene, Dartsch et al. 1999; Hodel, An et al. 2001; Kalus, Hodel et al. 2002). Furthermore, no transmembrane proteins or classical membrane-anchored proteins were detected. Based on bioinformatics information and published results, almost all of the identified proteins are able to enter the secretory pathway, thus confirming their interaction with the luminal side of the ZGM. The two identified cytosolic proteins Vinculin (fragment), an actin-binding protein, and Ubiquitin carrier protein involved in ubiquitination/quality control may be associated with the cytosolic side of the ZG. A novel protein, rat mast cell Chymase A, appeared to be of low abundance in the 2D-PAGE, and was thus selected for further validation of our approach. It is important to note that while increased instrument sensitivity allowed the identification of many more low abundant ZGM proteins; it also uncovered more contaminating proteins (Iwai and Inagami 1990). The confirmation of identified proteins on ZGM is thus a major and important task (Iwai and Inagami 1990).

By applying immunoblotting for the detection mast cell marker proteins, we were able to rule out that the presence of Chymase in our granule subfractions was the result of a contamination with mast cell granules/proteins. The distribution of Chymase in the granule subfractions resembled that of ZG16p, a typical peripheral ZGM marker, further confirming that Chymase is a genuine peripheral ZGM protein. In addition, its granule localization was for the first time confirmed by immunocytochemistry and morphological studies with pancreatic tissue and AR42J cells, an acinar cell model. In contrast to the biochemical data, membrane-association of Chymase appears to be less pronounced based on the ultrastructural studies. As mentioned before, this might be explained by restrictions in antibody binding. It is as well possible that Chymase interacts with membrane-associated proteoglycans which extend into the content (see below). Furthermore, we cannot rigorously exclude that the biochemical experiments exaggerate the amount of membrane-association, *e.g.* due to differential solubility of the ZG proteins in the lysis buffer. Importantly, an exogenously expressed Chymase-YFP fusion protein was targeted to ZG in pancreatic AR42J cells, whereas other fusion proteins (*e.g.* YFP-ER, Ruby-ER, VSVG-GFP, YFP-GPI) entering the secretory pathway in AR42J cells were not observed to be targeted to ZG. It should be noted that Chymase was also suggested to be a potential peripheral ZGM protein based on a recent iTRAQ quantitative proteomic analysis (Chen and Andrews 2008). Taken together, these results clearly demonstrate that Chymase is a genuine peripheral ZGM proteins and no contaminant.

Chymase has been identified as a major, highly basic chymotrypsin-like serine protease of mast cells, where it is stored in regulated secretory granules. Thus, its presence in ZGs of the exocrine pancreas is not that unusual at all. With respect to function, Chymase is likely to act as a serine protease after ZG secretion. RMCP-1 of mast cells is involved in inflammatory processes and tissue-remodelling (Leskinen, Lindstedt et al. 2003). Its capability to cleave proteins of the extracellular matrix (*e.g.* fibronectin) might be a reason for its low and regulated abundance in ZGs.

Interestingly, several known digestive enzymes, among them many lipid-interacting enzymes, were also identified in the wash subfraction. The presence of these classical content (ZGC) proteins in a ZGM fraction is usually interpreted as a contamination. However, it should be noted that these enzymes remain partially attached to the ZGM even under more stringent purification conditions (*e.g.* KBr wash before carbonate treatment) or after further purification of crude ZGM by gradient centrifugation (Chen, Walker et al. 2006; Rindler, Xu et al. 2007). Interestingly, many of the membrane-associated enzymes identified in this study in a membrane wash fraction have been predicted to be potential luminal ZGM proteins in a recent topology analysis of purified ZGM (Chen and Andrews 2008). Thus, it is very likely that the identified subset of peripheral digestive enzymes exhibits a more specific interaction with the ZGM than previously expected. Enzymes with lipid-binding properties might interact with membrane lipids to specifically associate with the ZGM. They might as well associate with lipid microdomains, which have been identified in ZGM (Schmidt, Schrader et al. 2001; Berkane, Nguyen et al. 2007). Their importance for granule biogenesis has been demonstrated in recent studies (Schmidt, Schrader et al. 2001; Gondre-Lewis, Petrache et al. 2006).

Besides Chymase, we also detected a prominent amount of RNase A at the ZGM (1:10; about 33% of total RNase A compared to 0.06% of total amylase) (not shown). Interestingly, this interaction might be mediated by the interaction of RNase A with proteoglycans, *e.g.* of a predicted *submembranous granule matrix* (Scheele, Fukuoka et al. 1994; Schmidt, Dartsch et al. 2000). We present first ultrastructural data, which reveal a submembranous localization of proteoglycans within zymogen granules using Cupromeronic Blue cytochemistry. Removal of the matrix components by carbonate treatment of granule membranes led to a loss of membrane curvature.

RNase A has been shown to interact with heparin and chondroitinsulfate (Dvorak and Morgan 1998; Dvorak and Morgan 1998), and based on these properties, a protein A-gold-RNase A technique has been developed to detect proteoglycans in cellular compartments and tissues (Dvorak and Morgan 1999). Protein A-gold-RNase A also labeled putative proteoglycans in ZG at the membrane and in the content (Dvorak and Morgan 1999). Furthermore, an interaction with proteoglycans has been described for Chymase (Pejler and Sadler 1999). This interaction is supposed to influence enzyme function (Dvorak and Morgan 1998; Pejler and Sadler 1999). The negatively charged proteoglycans in secretory granules of hematopoietic cells and mast cells are engaged in the binding of small positively charged molecules, such as histamine (Brion, Miller et al. 1992; Grimes and Kelly 1992; Castle and Castle 1998) and proteases (Lutzelschwab, Pejler et al. 1997; Huang, Sali et al. 1998), and have therefore been considered to promote the efficient packaging and concentration of secretory products (Matsumoto, Sali et al. 1995). Similarly, proteoglycans within ZGs are supposed to interact electrostatically and through specific protein-protein and carbohydrate-protein binding domains with the secretory proteins of the granule content (Scheele, Fukuoka et al. 1994; Schmidt, Dartsch et al. 2000; Schrader 2004). A potential role of Serglycin in granule formation has, however, recently been questioned (Niemann, Cowland et al. 2009). Interestingly, in a very recent study heparan sulfate containing proteoglycans have been detected in a ZGM fraction (Kumazawa-Inoue, Mimura et al. 2011). Although the core proteins could not be identified, the secretory lectin ZG16p (Kumazawa-Inoue, Mimura et al. 2011), ribonuclease, Carboxypeptidase and bile-salt activated Lipase were found to bind to

heparin by affinity chromatography (Kumazawa-Inoue, Mimura et al. 2011), whereas amylase was not found to interact (Kumazawa-Inoue, Mimura et al. 2011). ZG16p was found to bind most strongly among the ZG proteins suggesting that ZG16p may cross-link the granule heparan sulfate chains via its two carbohydrate-binding sites and facilitate the formation of the submembranous matrix (Kumazawa-Inoue, Mimura et al. 2011).

It will be a great challenge for future studies to also identify and characterize high molecular mass components such as proteoglycans and glycoproteins in ZG fractions to unveil the complex architecture and putative interactions at the granule membrane and in the granule content.

Chapter 5 Similarities in Exocrine and Neuroendocrine Biogenesis and Secretion

As mentioned in section 1.1 and Chapter 4, ZG have been used as a model system to study secretory granule biogenesis and regulated secretion in general. Also, they play important roles in pancreatic injury and disease (Gaisano and Gorelick 2009; Husain and Thrower 2009; Gomez-Lazaro, Rinn et al. 2010). As referred in section (Introduction 1.7), ZG are optimal for suborganellar proteomics as they are highly abundant in the exocrine pancreas. Due to their large size and density, they can easily be isolated and intact ZG can be further subfractionated in ZGC and ZGM (Figure 12 and 3.8.2). Furthermore, several methods were reported to remove and enrich peripheral ZGM proteins (ZGWash) as well as to enrich transmembrane and membrane-anchored proteins, consequently facilitating further analysis (Chapter 4, Hoops and Rindler 1991; Schmidt, Dartsch et al. 2000; Chen, Walker et al. 2006; Chen and Andrews 2008). Thus, significant progress has been made in the identification of proteins involved in ZG trafficking and regulated exocytosis (*e.g.* Rab proteins and effectors, and SNARE proteins) as well as in fusion events but also proton pumps, membrane channels and transporters were identified (Introduction 1.4, Gomez-Lazaro, Rinn et al. 2010). Newly identified proteins involved in ZG trafficking towards the apical plasma membrane are *e.g.* dynein, dynactin and myosin motor proeins (Chen, Walker et al. 2006; Rindler, Xu et al. 2007). Furthermore, several soluble N-ethylmaleimide-sensitive factor activating protein receptor (SNARE) proteins, Rab GTPases and aquaporins were identified and are suggested to be involved in granule docking/priming, swelling and exocytosis (Chen, Edwards et al. 2002; Cho, Sattar et al. 2002; Riedel, Antonin et al. 2002; Chen, Li et al. 2004; Faust, Gomez-Lazaro et al. 2008; Williams, Chen et al. 2009; Gomez-Lazaro, Rinn et al. 2010). In addition, proteins known to be localized in other organelles or cell types as presenillins and Chymase were identified (Chen, Walker et al. 2006; Rindler, Xu et al. 2007; Borta, Aroso et al. 2010). Interestingly, many of the proteins identified by recent proteomics approaches are also known to be involved in neuroendocrine vesicle trafficking and exocytosis. It is known that exocrine and neuroendocrine regulated secretion share some characteristics. Indeed, secretory proteins are sorted into the secretory/zymogen granules in a pH dependent manner; the membrane components of the TGN/SG/ZG are involved in the sorting process, the granules mature through the removal of non-secretory proteins in a clathrin-dependent manner and are transported to the apical plasma membrane along microtubules (Introduction 1.2). The secretion occurs in both systems upon an external stimulus and in a Ca^{2+}-dependent manner. It is widely discussed to what extent the secretion machineries of both systems may overlap.

This part of my work continues with the analysis of the ZGM and ZGWash subfraction, focusing on the identification and confirmation of low abundant, high-molecular mass and hydrophobic proteins, which possibly constitute members of exocrine and neuroendocrine secretion systems. In order to determine the proteome overlap, I started with the comparison of proteomics results of the ZG, ZGM, ZGWash and synaptic vesicles (SV) obtained during the last few years including our own results and listed the proteins found in Table 5-1. The table provides some auxiliary information about the putative functions, the type of the identified protein, the method of detection in ZG and the corresponding publication. It may as well facilitate the development of experimental approaches exploiting the information about the protein

characteristics. Thus, the table was used as a criterion for the selection of proteins for further analysis such as APP. In total, 72 proteins were found to be shared by both systems and are listed in the table, from which six are membrane channels and transporters and 12 are membrane associated proteins most likely all attached to the cytosolic side including APP, SNARE and motor proteins (*e.g.* SNAP 23 and Dynactin). Furthermore, 43 proteins are listed as being involved in trafficking, including 24 Rab proteins, but also 3 subunits of the γ-secretase complex, 8 subunits of the Vacuolar H^+-ATPase, 2 proteins which are known from the cytoplasmic active zone and one luminal ZG protein, which was identified in a rat brain lysate by 1D-MS/MS analysis.

It is important to note that the overlap of both systems, described in this table, refers solely to proteins involved in trafficking, fusion, swelling and exocytosis of ZGs and synaptic vesicles. These are either membrane associated from the cytosolic side, or are transmembrane proteins. The overlap includes only one protein known to be attached to the luminal side which is suggested to be involved in ZG sorting and packaging through its interaction with the glycoprotein scaffold on the luminal side of the ZG membrane, which is ZG16p. These findings support the theory that the secretion machineries of the exocrine and neuroendocrine system may overlap. But for many of the newly identified proteins, their existence in the ZG of the exocrine rat pancreas still has to be confirmed by alternative methods such as antibody based technologies or PCR.

Further, to identify new and low abundant ZGM constituents, a 2D-SDS PAGE was applied as shown in Chapter 4. However, the major drawback of this method is its limitation concerning the separation of hydrophobic membrane and high-molecular mass proteins. As alternative approaches to capture these special proteins, 1D-SDS-PAGE and the off gel LC-separation (3.10.4) methods were chosen. Samples which were prepared for 1D-SDS PAGE were loaded onto a 3-12.5% gradient SDS-PAGE (3.9.2) and gels were subsequently stained with Coomassie and silver (3.9.6-3.9.7). Afterwards, selected protein bands were excised and prepared for mass spectrometry by tryptic digestion (3.10.1). For LC-separation, samples of 1 μg were tryptically digested prior to separation on a HPLC system. After peptide separation, these were directly applied to a Maldi target plate for mass spectrometric analysis using an integrated LcPackings Probot auto sampler, as depicted in Figure 12. LC-MS/MS is even more suitable for the identification of high-molecular mass and hydrophobic proteins since the tryptic digestion occurs prior to separation, facilitating the identification of peptides of very low abundant proteins. Both methods have the advantage of reducing the risk of protein precipitation during the separation since the step of isoelectric focusing is spared. The major drawback of both methods is the increase in the identification of false positives, contaminations which can occur during the isolation process. This underlines the importance of further analysis to confirm eventual new ZGM and ZGM associated candidates. In general, mass spectroscopic analysis succeeded with the kind support of Prof. F. Amado, Dr. R. Vitorino (Department of Chemistry, University of Aveiro) and M. Aroso from our group.

The neuroendocrine proteins selected for further confirmation in this work are Piccolo and Synapotjanin-1 which were identified by the LC-MS/MS approach. APP was chosen based on the result obtained by the literature screen (Table 5-1) and ZG16p, which in fact represents known ZGM associated protein, was identified in a rat brain lysate by the 1D-SDS-PAGE approach.

Table 5-1 Proteins identified by proteomics approaches in exocrine ZGs and in neuroendocrine SVs. Articles about proteomics in SV used for this table: (Coughenour, Spaulding et al. 2004; Iwatsubo 2004; Burre, Beckhaus et al. 2006; Takamori, Holt et al. 2006; Burre and Volknandt 2007)

Protein Name, MW, NCBI	Biological process	Newly localized	Method of detection	Reference
Transporter & Channel:				
ATPase, Aminophospholipid transporter class I, type 8A or 8B (109499663 or 62664531)	**APLT:** not known			
Na, K-ATPase alpha-1 subunit (α1) 26.84 kDa, (205632)	**Atp1a1:** not known		LC-MS/MS	Rindler et al. 2007
Solute carrier family 1 member 3/Slc1a3, 59.7 kDa, NM_019225	**Slc1a3:** carries out Na+ dependent transport of glutamate and aspartate; may regulate neurotransmitter concentration in the CNS	ZGM		
Vesicle amine transport protein 1 homolog (VAT-1) 43.12 kDa, NM_001033683.1	**VAT-1:** not known		----------	----------
Voltage-dependent anion channel 1 (VDAC1) 30.76 kDa, NM_031353.1	**VDAC1:** mitochondrial outer membrane (MOM) channel, also at the plasma membrane, at the MOM allows diffusion of small hydrophilic molecules; in the plasma membrane it is involved in cell volume regulation and apoptosis.		iTRAQ-LC-MS/MS; 2D-MS and 1D-MS/MS	Chen et al. 2006
Voltage-dependent anion channel 2 (VDAC2) 31.75 kDa, NM_031354.1	**VDAC2:** mitochondrial outer membrane channel that allows diffusion of small hydrophilic molecules.			
Membrane associated proteins:				
Alzheimer's precursor protein (APP) 86.7kDa NP_062161.1	**APP:** Functions as a cell surface receptor and performs physiological functions on the surface of neurons relevant to neurite growth, neuronal adhesion and axonogenesis.			
Beta-actin 41.73 kDa, NM_031144.2	**Actb:** Actins are highly conserved proteins that are involved in various types of cell motility and are ubiquitously expressed in all eukaryotic cells.	ZGM associated	LC-MS/MS	Rindler et al. 2007
Guanine nucleotide-binding protein G(q)α 42.14 kDa, NP_112298.1.	**G(q)α:** involved as modulators or transducers in various transmembrane signaling systems **Gβ2:** not known			
Guanine nucleotide-binding protein Gβ2 35 kDa, 71089941				
Noc2 (Rab effector), 33.4 kDa, NP_598275.1	**Noc2:** zinc finger protein; may be involved in regulated exocytosis in endocrine and exocrine cells.			
Synaptosomal-associated protein (SNAP23) 23.2 kDa, NP_073180.1	**SNAP23:** Essential component of the high affinity receptor for the general membrane fusion machinery and an important regulator of transport vesicle docking and fusion. **SNAP29:** inhibits SNARE disassembly, implicated in synaptic transmission.			
Synaptosomal-associated protein (SNAP29) 29.1 kDa NP_446262.3				
Brain acid soluble protein 1 21.8 kDa, NP_071636.1	**Basp1:** not known yet	---------	----------	----------
Dynactin subunit 1 141.93 kDa, NP_077044.1	**Dctn1:** Required for the cytoplasmic dynein-driven retrograde movement of	ZGM		

Protein Name, MW, NCBI	Biological process	Newly localized	Method of detection	Reference
Dynein hc 1 532.52 kDa, NP_062099.3. **Myosin VIIb** 241.16 kDa, IPI00208315.	vesicles and organelles along microtubules. **Dhc1:** Cytoplasmic dynein 1 acts as a motor for the intracellular retrograde motility of vesicles and organelles along microtubules. **Myo7b:** Uncharacterized protein	associated on cytosolic side	iTRAQ-LC-MS/MS	Chen et al. 2008
Vesicular Trafficking, Transmembrane: **Ectonucleoside triphosphate diphosphohydrolase 1** (ENTP1, CD39) 57,4 kDa, NP_072109.1. **CarboxypeptidaseD** (Cpd) 152, 6 kDa, NP_036968.1. **Nicastrin** (Ncstn) 78,4 kDa, NP_777353.1. **Presinilin1** (PS-1) 52.8 kDa, NP_062036.2. **Presinilin2** (PS-2) 50.05 kDa, NP_112349.2. **Secretory carrier membrane protein 1** (SCAMP1) 24.8 kDa AF295404 **Secretory carrier membrane protein 3** (SCAMP3) 37.9 kDa, NP_001094106.1. **Vesicle-associated membrane protein 2** (synaptobrevin2) 12.7 kDa NM_012663 **Vesicle-associated membrane protein 3** (VAMP3) 11.5 kDa NP_476438.1 **Cystein string protein** 22.1 kDa, no NM number **Pantophysin** (Synaptophysin-like protein 1), 28.6 kDa, NP_006745.1 **Syntaxin 3** 33.3 kDa, NP_112386.1 **Syntaxin 6** 29.1 kDa, NP_113853.1. **Syntaxin 7** 29.8 kDa, NP_068641.2. **Syntaxin 16b** 16.0 kDa NM_001108610.1 **Transmembrane emp24 domain-containing protein** 10 24.9 kDa, NM_053467.1	**ENTP1:** Hydrolyzes ATP and ADP equally well. In the nervous system, could hydrolyze ATP and other nucleotides to regulate purinergic neurotransmission. **Cpd**: metallocarboxypeptidase, serine-type carboxypeptidase **Ncstn:** subunit of the γ-secretase complex **PS-1:** catalytic subunit of the γ-secretase complex, hydrolase **PS-2:** catalytic subunit of the γ-secretase complex, hydrolase **SCAMP1:** Functions in post-Golgi recycling pathways. Acts as a recycling carrier to the cell surface. **SCAMP3:** not known **VAMP2:** targeting and/or fusion of transport vesicles to their target membrane **VAMP3:** SNARE involved in vesicular transport from the late endosomes to the trans-Golgi network **Csp:** predominantly associated with nerve endings and synaptic vesicles, but function is unknown **SYPL1:** not known **Stx3:** Potentially involved in docking of synaptic vesicles at the CAZ **Stx6:** Involved in intracellular vesicle trafficking **Stx7:** Mediates the endocytic trafficking from early endosomes to late endosomes and lysosomes **Stx16b:** not known **Tmed10:** Involved in vesicular protein trafficking, may be involved in vesicular transport from endoplasmic reticulum to the Golgi	ZGM	iTRAQ-LC-MS/MS ---------- LC-MS/MS & iTRAQ-LC-MS/MS ---------- LC-MS/MS	Chen et al. 2008 ---------- Rindler et al. 2007 & Chen et al. 2006/8 ---------- Rindler et al. 2007 Stx7 also by Chen et al 2008

Protein Name, MW, NCBI	Biological process	Newly localized	Method of detection	Reference
Vesicular Trafficking: **Vacuolar protein sorting-associated protein 45** (VPS45) 64.9 kDa, NP_742069.1. **Exocyst complex component 4** (rSec8) 110.5 kDa, NP_446327.1	**VPS45:** expressed in brain and testis; may play a role in intracellular vesicle mediated transport **rSec8:** Component of the exocyst complex involved in the docking of exocytic vesicles with fusion sites on the plasma membrane (Golgi-to-plasma membrane vesicle trafficking)	ZGM associated ----- ZGM	LC-MS/MS -------- iTRAQ-LC-& 2D MS/MS	Rindler et al. 2007 ------- Chen et al. 2006
Vesicular Trafficking-GTPases and Effectors: **Rab-1A** 22.7 kDa, NM_031090, **B** 20.8 kDa, NM_134346.3 **Rab-2A** 23.5 kDa,NM_031718.1, **B** 24.1 kDa NM_001037645.1 **Rap-2b** 20.5 kDa NP_596901.1. **Rab-3A** 24.97 kDa, NM_013018.2, **Rab-4A** 23.9 kDa, NM_013019.2, **B** 23.6 kDa, NP_059051.1. **Rab-5A** 23.6 kDa,NM_022692.1, **B** 23.6 kDa, NM_001079936.1, **C** NM_001105840.1 **Rab-7** 23.5 kDa, NM_023950.3 **Rab-8A** 23.7 kDa NP_446450.2, **B** 23.6 kDa NP_695229.1 **Rab-10** 22.9 kDa, NP_059055.2 **Rab-14** 23.9 kDa, NP_446041.1. **Rab-18** XR_086339.1 **Ral-A** 23.5 kDa, NM_031093.2 **c-K-Ras2** 21.7 kDa, NM_031515.3 **Rac1** 21.5 kDa NM_134366.1 **Rab-11b** 24.5 kDa, NM_032617.2 **Rab-26** 28.2 kDa, NM_133580.1	**Rab-1A:** Probably required for transit of protein from the ER through Golgi compartment. Binds GTP and GDP and possesses intrinsic GTPase activity. **B:** small GTPase; involved in antagonizing the mitogenic and transforming activity of Ras **Rab-2A:** Required for protein transport from the endoplasmic reticulum to the Golgi complex **B:** not known **Rap-2b:** Involved in EGFR and CHRM3 signaling pathways through stimulation of PLCE1. **Rab-3A:** Involved in exocytosis by regulating a late step in synaptic vesicle fusion. **Rab-4A:** may play a role in intracellular recruitment of the glucose transporter GLUT4, **B:** Protein transport. Probably involved in vesicular traffic **Rab-5A:** may play a role in regulation of vesicular transport **B:** plays an important role in synaptic function by modulating the endocytosis of synaptic vesicles **C:** not known **Rab-7:** Involved in late endocytic transport. Contributes to the maturation of phagosomes **Rab-8A** and **B:** May be involved in vesicular trafficking and neurotransmitter release **Rab-10:** Not known **Rab-14:** may regulate neurotransmitter release, Involved in membrane trafficking between the Golgi complex and endosomes during early embryonic development. **Rab-18:** not known **Ral-A:** Multifunctional GTPase involved in a variety of cellular processes including gene expression, cell migration, cell proliferation, oncogenic transformation and membrane trafficking **c-K-Ras2:** Ras proteins bind GDP/GTP and possess intrinsic GTPase activity. **Rac1:** In its active state, binds to a variety of effector proteins to regulate cellular responses such as secretory processes, phagocytosis of apoptotic cells, epithelial cell polarization and growth-factor induced formation of membrane ruffles **Rab-11b:** GTPase that modulates endosomal trafficking. Acts as a major regulator of membrane delivery during cytokinesis **Rab-26:**	ZGM or peripheral	iTRAQ-LC-MS/MS ---------- LC-MS/MS For Rab8a Doubled SDS-PAGE, WB, IMF ---------- LC-MS/MS, iTRAQ-LC-MS/MS	Chen et al. 2008 --------- Rindler et al. 2007, for Rab8a also Faust et al. 2008 ---------- Rindler et al. 2007 & Chen et al. 2006/8

Protein Name, MW, NCBI	Biological process	Newly localized	Method of detection	Reference
Rab-27b 24.6 kDa NM_053459.1 **Rab-35** 23.0 kDa, NM_001013046.1	Participates in exocrine secretion: regulates the secretion of acinar granules in the parotid gland **Rab-27b:** May be involved in targeting uroplakins to urothelial apical membranes **Rab-35:** In the process of endocytosis, essential rate-limiting regulator of a fast recycling pathway back to the plasma membrane.			
Vacuolar H^+-ATPase Subunits: **H^+ -ATPase V0 subunit a1** 96.3 kDa, NP_113792.2 **H^+ -ATPase V0 subunit c** 15.8 kDa, NM_130823.2 **H^+ -ATPase V0 subunit d** 40.3 kDa, NM_001011927.1 **H^+ -ATPase V1 subunit B2** 56.6 kDa NM_057213.2 **H^+ -ATPase V1 subunit C1** 43.9 kDa, NM_001011992.1 **H^+ -ATPase V1 subunit D** 28.3 kDa, NP_955418.1. **H^+ -ATPase V1 subunit E1** 26.13 kDa, NM_198745.1 **H^+ -ATPase V1 subunit H** 50.86 kDa, NM_001013929.1	**V0a1:** Required for assembly and activity of the vacuolar ATPase. Potential role in differential targeting and regulation of the enzyme for a specific organelle **V0c:** Proton-conducting pore forming subunit of the membrane integral V0 complex of vacuolar ATPase. V-ATPase is responsible for acidifying a variety of intracellular compartments in eukaryotic cells **V1B2:** Non-catalytic subunit of the peripheral V1 complex of vacuolar ATPase **V1C1:** Subunit C is necessary for the assembly of the catalytic sector of the enzyme **V1D:** mediates acidification of intracellular organelles for processes such as protein sorting and receptor-mediated endocytosis **V1E1:** Subunit of the peripheral V1 complex of vacuolar ATPase essential for assembly or catalytic function. **V1H:** Subunit of the peripheral V1 complex of vacuolar ATPase	ZGM or peripheral	LC-MS/MS	Rindler et al. 2007
Typical ZGM associated protein newly identified in rat SV/brain				
ZG16p 16 kDa, NP_599236.2	**ZG16p:** May play a role in protein trafficking, act as a linker between the submembranous matrix on the luminal side of ZGM and aggregated secretory proteins during granule formation	newly in SV	1D-MS/MS, IMF, WB	Our un-published results
Typical SV associated proteins newly identified in ZG				
Cytosol & Cytomatrix: **Piccolo** (Aczonin), 552.7 kDa, NP_001104267.1 **Synaptojanin1** (Inositol 5-phosphatase), 172.9 kDa , NP_445928.2	**Piccolo:** scaffolding protein involved in the organization of synaptic active zones and in synaptic vesicle trafficking **Snj1:** clathrin-mediated endocytosis in the synaptic active zone (CAZ)	ZGM associated	LC-MS/MS	Our unpublished results

5.1 The High-Molecular-Mass Cytomatrix Active Zone Proteins Piccolo and Synaptojanin-1 were Identified by LC-MS/MS in a ZGWash Fraction

Piccolo (Aczonin) and Synaptojanin-1 (Snj-1) were both identified in a ZGWash fraction by LC-MS/MS analysis. Therefore, ZG were isolated and subfractionated as described in sections 3.8.1-3.8.2. One μg of the ZGWash fraction was tryptic digested and analyzed by LC-MS/MS as described in sections 3.10.4-3.10.5. In the ZGWash subfraction, Piccolo was identified with a peptide score of 9 and a total ion score of 47, while Snj-1 was identified with a peptide score of 3 and a total ion score of 54. Both proteins, when compared to Amylase (57.2 kDa) a highly abundant ZG content protein, which should appear only in miner amounts in the ZGWash fraction in LC-MS/MS (peptide score 7, total ion score 154), reveal values for very low abundant proteins or eventual contaminants.

Piccolo and Snj-1 are slightly acidic, multidomain proteins with a high molecular weight (Piccolo 552 kDa and Snj-1 173 kDa). Both proteins are known to be involved in vesicle transport either towards or from the apical plasma membrane in the cytomatrix active zone (CAZ) of nerve terminals (McPherson, Garcia et al. 1996; Wang, Kibschull et al. 1999). The CAZ is the area in which synaptic vesicles fuse with the presynaptic plasma membrane to undergo exocytosis. Also, they were found in the pancreatic β-cells as part of the endocrine secretion system (Fujimoto, Shibasaki et al. 2002; Hoy, Efanov et al. 2002).

Piccolo, as a scaffold protein in the pre-synaptic active zone, forms a complex with Bassoon involving several other proteins (Schoch and Gundelfinger 2006). It was proven to interact with Rim2 in a Ca^{2+}-dependent manner (Fujimoto, Shibasaki et al. 2002) and via Abp1 and Profilin to bind to actin organizing the exo- and endocytotic machinery (Fenster, Kessels et al. 2003; Barclay, Morgan et al. 2005; Schoch and Gundelfinger 2006; Leal-Ortiz, Waites et al. 2008). In pancreatic β-cells, it was shown that Piccolo antisense oligodeoxynucleotides inhibit insulin secretion again involving calcium (Fujimoto, Shibasaki et al. 2002). It is known that synaptic transmission is initiated when an action potential triggers neurotransmitter release from a presynaptic nerve terminal (Katz and Kopin 1969) through the opening of Ca^{2+} channels. A transient Ca^{2+} increase stimulates synaptic vesicle exocytosis after which the vesicles undergo endocytosis, recycle and refill with neurotransmitters for a new round of exocytosis (Sudhof 2004). ZG as well are released upon a regulated increase of intracellular Ca^{2+} concentration while fusing with the apical plasma membrane (Thevenod, Braun et al. 2000; Schrader 2004) but the calcium sensor has not been identified yet. Since Piccolo has the capacity to bind Ca^{2+} which induces conformational changes in the protein structure (Gerber, Garcia et al. 2001) and acts as a potential Ca^{2+} sensor in pancreatic β-cells (Fujimoto, Shibasaki et al. 2002), it cannot be excluded that this protein might also play a role in ZG exocytosis as a scaffold protein organizing ZG fusion with the apical membrane.

Synaptojanin-1 (Snj-1), also known as synaptic inositol-1, 4, 5-trisphosphate 5-phosphatase 1, is a cytosolic protein involved in clathrin-mediated endocytosis (Haffner, Takei et al. 1997). It is probably acting as a negative regulator for the interaction of the clathrin-coat and the membrane phospholipids of the vesicles, facilitating the shedding of the coat and targeting of the uncoated vesicle to its final destination (Robinson 1994; Damke 1996; De Camilli, Emr et al. 1996; Tooze 1998; Harjes and Wanker 2003). In this process, Snj-1 binds to Eps15, a clathrin coat-

associated protein, and is recruited by Endophilin to promote synaptic vesicle uncoating (Haffner, Takei et al. 1997; Verstreken, Koh et al. 2003). Ephrin, a chemirepulsant promotes Snj-1´s phosphorylation via an Ephrin receptor through which the binding to other proteins, as well as vesicle endocytosis, is inhibited (Hopper and O'Connor 2005; Irie, Okuno et al. 2005). Moreover, Snj-1s expression is not restricted to brain or pancreatic β-cells since it was also found in heart, liver, testis and muscle (Ramjaun and McPherson 1996; Nemoto, Arribas et al. 1997). In total, six different isoforms are known so far, being differently regulated throughout prenatal development. These isoforms split in two splice variants with the size of 145 kDa and 170-173 kDa, having differential membrane binding properties (Ramjaun and McPherson 1996). Appealing is the fact that through a Ca^{2+} influx in neurons, some calcium dependent phosphatases are activated which in turn activate Snj-1 increasing the endocytotic turn-over (Tojima, Akiyama et al. 2007). Hence, it is possible that Snj-1 might be involved in the clathrin-dependent removal of lysosomal proteins during ZG maturation or in the membrane recycling after zymogen secretion. Due to their roles in vesicle trafficking/recycling, both proteins were selected for further analysis in ZG.

5.2 Piccolo, a Peripheral ZG Protein? A Question still not Solved

By applying two commercial available antibodies directed to Piccolo in immunoblotting and immunofluorescence, it was not possible to obtain reliable results for Piccolo. Therefore, selected samples of ZG subfractions, AR42J cells and positive controls (brain lysate and SH-SY5Y cell lysate) were sent to the laboratory of Neurobiology of Prof. E. Gundelfinger (Leibniz Institute for Neurobiology, Magdeburg, Germany), a group which routinely works with Piccolo producing their own antibody against the protein. Here, Piccolo was detected very weakly in total ZG, ZGC and ZGM but not in ZGM_{washed} or the ZGWash fraction (Figure 20). Furthermore, it was found in the lysate of AR42J cells stimulated for granule formation with dexamethasone (+D) and controls (-D), and in positive controls (SHSY-5Y cells, rat brain), showing the characteristic antibody bands for Piccolo at 552 and ca. 65 kDa. Additionally, a strong band pattern from 0-50 kDa was detected by the antibody in ZG complete, ZGC and ZGM, probably originating from sample degradation.

Nevertheless, with the experiments performed, it is not yet possible to confirm if Piccolo is a transient part of the ZGM as suggested by LC-MS/MS analysis of the ZGWash fraction and immunoblotting of ZG fraction, or if it is a co-purification coming from vesicles of the pancreatic β-cells. Due to problems with the available antibodies, the work on this protein was at least temporally intermitted.

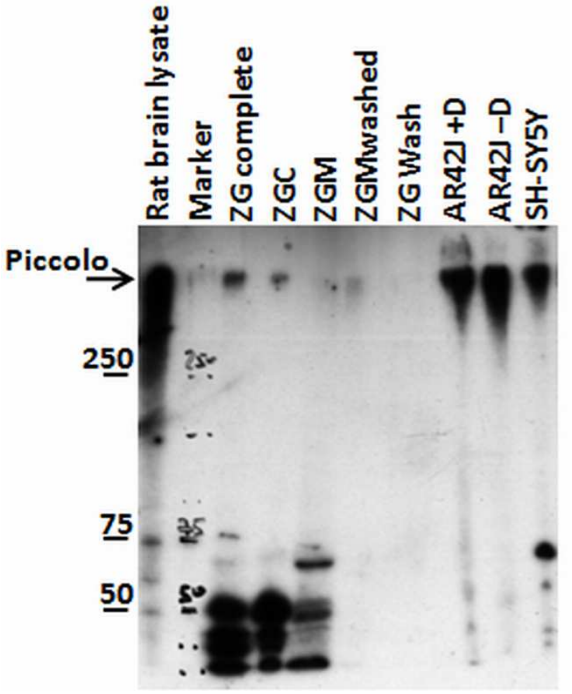

Figure 20: Piccolo seems to associate to ZG and is expressed in pancreatic AR42J cells.
Lysed granules (ZG) were separated into a content (ZGC) and membrane fraction (ZGM). In addition, isolated membranes were treated with Na_2CO_3 at pH 11.5 and separated into pellet (ZGM_{washed}) and supernatant (Wash) fractions. Equal amounts of protein (30 μg) were run on a Tris-Acetate SDS-PAGE, blotted overnight onto nitrocellulose and incubated with an antibody against Piccolo. Gel and blot were prepared by Dr. A. Fejtova (Magdeburg, Germany). Antibody specific bands appeared at approximately 65 and 550 kDa in the positive controls (rat brain and SH-SY5Y cell lysate) but also in ZG complete, ZGC, ZGM and in AR42J cells.

5.3 Synaptojanin-1 is Not a Peripheral Component of the ZGM

To confirm the detection of Snj-1 in the ZGWash fraction, immunoblot analyses were conducted with a tank blot system using nitrocellulose (3.9.3). According to the data sheet of the antibody against Snj-1, samples were not boiled but heated for 20 min at 65°C and loaded onto a 3-12.5% gradient gel. After immunoblotting, the antibody revealed a band at 145 kDa in the synaptosome fraction which was used as positive control. Only in the rat pancreatic homogenate, a very weak signal for Snj-1 was detected but not in any other samples loaded (Figure 21). Further experiments using AR42J subfractions (isolated membranes and cytosol/microsomes) and incubation of samples at 37°C overnight did not improve the detection of Snj-1.

Figure 21: Synaptojanin-1 does not localize to ZG subfractions.
Equal amounts of protein (80 μg) were run on a 3-12.5% gradient SDS-PAGE, blotted onto a nitrocellulose membrane and incubated with an antibody against Snj-1. The Snj-1 antibody shows one specific band at around 145 kDa as it is visible in the positive control of synaptosomes and in the rat pancreatic homogenate.

Immunofluorescence experiments using the Snj-1 antibody in AR42J cells stimulated for ZG formation with dexamethasone (+D) Figure 22 D-F and unstimulated controls (-D) Figure 22 A-C exhibit a weak punctate staining pattern more at the periphery of the cells. But a co-labeling

with the ZG marker Chymotrypsinogen in AR42J cells revealed that the two antibodies do not colocalize with each other (Figure 22 A-F). Rat primary neuronal cultures served as positive control for Snj-1 (Figure 22 G-L). Snj-1 as a marker for endocytotic vesicles at nerve terminals reveals a positive staining, partially colocalising with the pre-synaptic marker protein VGlut (Figure 22 G, J-K) and also with the post-synaptic marker protein PSD95 (Figure 22 I, K-L). In Figure 22 K boxed area is shown enlarged in the upper left corner of the same image. In this magnification, a stack like staining of the three proteins is shown which is marked by a white arrowhead. This stack reveals a typical staining pattern which can be found all over the neuron. In this stack, SNj-1 (green) is followed by Vglut (white) and then by PSD95 (red) placing the protein inside the cell close to the CAZ area. It can also be seen that the pre- and post-synaptic markers Vglut and PSD95 overlap but only at the border between pre- and post-synapse when fluorescence signals are difficult to separate due a limitation of resolution.

That the antibody is able to recognize Snj-1 in AR42J cells in immunofluorescence experiments but not in immunoblotting may be related to the accessibility of the epitope, as antigen recognition appears to be sensitive to denaturation.

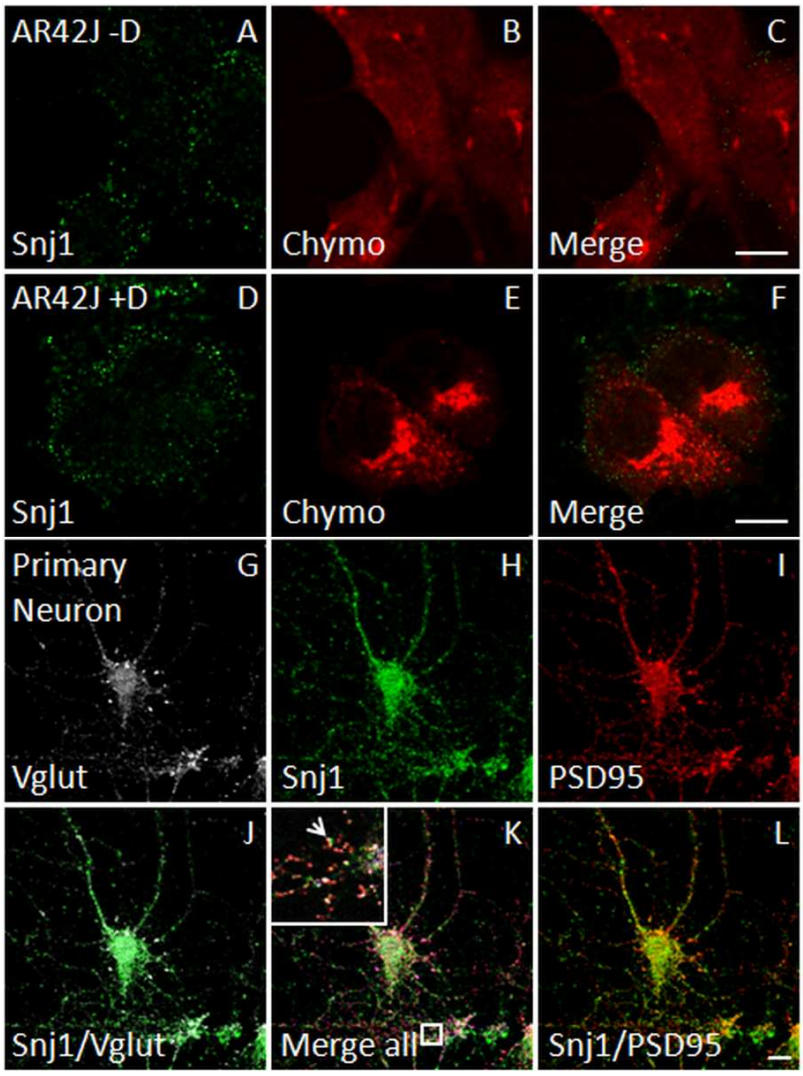

Figure 22: Synaptojanin-1 does not localize with ZG in AR42J cells.

AR42J cells stimulated for granule formation (**D**-**F**) and controls (**A**-**C**) were processed for indirect immunofluorescence after 48 h using antibodies directed to Synaptojanin-1 (Snj1) (**A**, **C**, **D**, **F**) and Chymotrypsinogen as ZG marker (Chymo) (**B**-**C**, **E**-**F**). Overlays (Merge) of images (**A**-**B**; **D**-**E**) are shown in (**C** and **F**) indicating no significant colocalisation with ZG. Pictures were obtained with an Olympus IX81 fluorescence microscope. Rat primary neurons served as positive control for the Snj-1 antibody marking endocytotic vesicles at nerve terminals (**H**, **J**-**L**). An antibody to Vglut served as pre-synaptic marker (**G**, **J** and **K**) an antibody to PSD95 as post-synaptic marker (**I**, **K** and **L**). The overlay (Merge) of images (**G**-**I**) is shown in (**K**). The overlay of (**G**-**H**) is shown in (**J**) and the overlay of (**H**-**I**) in (**L**). Images were obtained on a Confocal Zeiss LSM 510 microscope. Scale bars 10 μm

5.4 Exogenous Amyloid Beta A4 Protein Precursor (APP) is Sorted to Secretory Granules in Pancreatic AR42J Cells

Recent proteomics approaches identified the Amyloid beta A4 protein precursor (APP) in a ZGM associated subfraction (Rindler, Xu et al. 2007; Chen and Andrews 2008) together with Presenilin 1, 2 and some other subunits of the γ-secretase complex (Chen and Andrews 2008). Interestingly, all these proteins are known to be involved in neuroendocrine secretion processes (Kamal, Almenar-Queralt et al. 2001). Furthermore, APP was identified in a gene atlas about the mouse and human protein-encoding transcriptomes, in a number of tissues amongst them total pancreas but with a stronger expression in the pancreatic islets (Su, Wiltshire et al. 2004). Although it is known to be expressed in brain, (Shioi, Pangalos et al. 1995; Sandbrink, Monning et al. 1997), its expression on protein level in other tissues it still not well defined.

APP is a single-pass type 1 membrane protein known to enter the secretory pathway. In the precursor version a basolateral sorting signal was identified. APP undergoes various steps of glycosylation (Tsuchida, Shioi et al. 2001) and cleavage, especially in the endosomal-lysosomal pathway, where β-secretase generates the Aβ peptide. Soluble APP is then released into the extracellular space in a constitutive manner (Small and Gandy 2006) from where it is rapidly internalized via clathrin-coated pits. It was shown that some APP accumulates in secretory transport vesicles, leaving the late Golgi compartment returning then to the cell surface (Gandy and Greengard 1994; Selkoe 1996; Thinakaran and Koo 2008). APP binds to collagen which is inhibited by Zn^{2+}. This inhibition mediates the binding to heparin and the formation of APP homodimers (Pangalos, Efthimiopoulos et al. 1995; Brouillet, Trembleau et al. 1999; Watanabe, Sukegawa et al. 1999). Furthermore, it was proposed that APP is possibly a heparan sulfate proteoglycan core protein (Schubert, Schroeder et al. 1988). This multifunctional protein is involved, amongst other functions, in synaptic vesicle recycling (Marquez-Sterling, Lo et al. 1997), neuronal viability, polarity (Perez, Zheng et al. 1997) and migration (LoTurco and Bai 2006; Young-Pearse, Bai et al. 2007). It is reported that in APP knock-out mice, the SV density is reduced as well as the size of the CAZ, pointing towards a role in the regulation of formation and function of inter-neuronal synapses (Yang, Gong et al. 2005). It is still under discussion if this protein is involved in synaptic vesicle exocytosis as a membrane anchored receptor (McLoughlin, Irving et al. 1999). As such, it could also play a role during the exocytosis of ZG. Besides, it does not only function as a membrane-anchored receptor-like molecule, but also as a secreted derivative acting upon other cells by binding to cytomatrix components (Milward, Papadopoulos et al. 1992; Kamal, Almenar-Queralt et al. 2001; Young-Pearse, Chen et al. 2008). Regulated exocytosis implies the fusion of the vesicle membranes with the plasma membrane and the subsequent release of content to the extracellular space. It has been suggested that the core protein components of the intracellular membrane fusion machinery in the secretory granules are shared by different secretory organelles (Waters and Hughson 2000; Pfeffer 2007). Between these shared proteins are *e.g.* Rabs, Sec1/Munc18 and SNAREs (Rizo and Sudhof 2002; Burgoyne and Morgan 2007; Verhage and Toonen 2007) and eventually also APP.

Due to the proteomics results published in recent literature, its heparan binding capacity and its influence on vesicle trafficking processes, it is possible that APP might play a role in ZG

biogenesis, maturation and/or transport as well. Based on these informations, APP was selected for further analysis in ZG.

By immunoblot analysis with ZG and AR42J cell lysates from cells induced for ZG formation with dexamethasone (+D) and untreated controls (-D), using a specific antibody, APP was found weakly expressed in both AR42J cell lysate (Figure 23). However, it was neither detected in our isolated ZGs nor in the corresponding supernatant resulting from the ZG isolation (see SN3 in Figure 11, section 3.8.1). The lysates from positive controls (SH-SY5Y cells, rat brain and rat cortex) revealed a strong detection of APP (Figure 23). A specific antibody to Amylase was applied to confirm ZG enrichment and stimulation of AR42J cells.

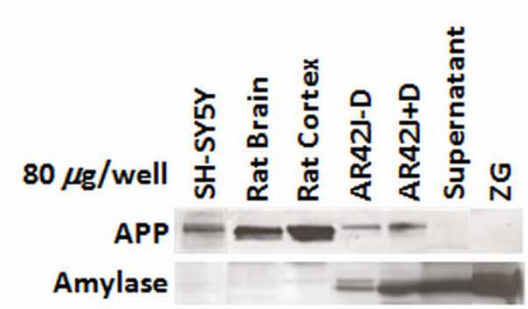

Figure 23: APP is not associated with isolated ZG.
Equal amounts of protein (80 μg) were run on a 12.5% SDS-PAGE, wet-blotted onto a nitrocellulose membrane and incubated with an antibody against APP (mc mouse 22C11). Amylase was used as control for ZG fractions. AR42J cell lysates were taken from cells induced for ZG formation for 48 h with dexamethasone (+D) and controls (-D). Lysates from SH-SY5Y cells, rat brain and cortex served as positive controls.

Although APP is expressed in AR42J cells, the localisation of the endogenous expressed protein in these cells by immunofluorescence with the specific antibody (mc mouse 22C11) was impaired probably due to an incompatibility with our immunofluorescence protocol. Nevertheless, overexpression of an APP-GFP fusion protein in AR42J cells, induced for ZG formation (Figure 24), revealed a partially cytosolic staining (Figure 24 A, E, M), but also a specific colocalisation with ER, Golgi, lysosomal and ZG marker proteins (Figure 24 A-O). AR42J cells were transfected with a generated APP-GFP construct, 24 h after transfection cells were induced for ZG formation with 10 nM dexamethasone and 72 h later, cells were processed for indirect immunofluorescence. Several organell marker antibodies were applied, which were directed to Chymotrypsinogen as ZG marker (Figure 24 B-C), Endolyn as lysosomal marker (Figure 24 F-G), PDI as ER marker (Figure 24 J-K), and p115 as Golgi marker (Figure 24 N-O). Dexamethasone-treatment resulted in the formation of numerous characteristic granules positive for Chymotrypsinogen (Figure 24 B). Quantification, using pixel-by-pixel analysis from confocal images revealed a co-localization coefficient of 18.7%±13.9 for PDI (ER marker, Figure 24 L, Q), of 29.4%±17.0 for p115 (Golgi marker, Figure 24 P, Q) and of 53.1%±21.1 for Endolyn (lysosomal marker, Figure 24 H, Q) with APP-GFP. The strongest colocalisation was observed with the ZG marker protein Chymotrypsinogen (87.9%±7.5, Figure 24 D, Q). Chymotrypsinogen and APP are both known to enter the secretory pathway colocalizing with ER and Golgi markers. This means that the actual colocalisation of APP-GFP with Chymotrypsinogen in ZG is far lower than it is represented by the values shown in Figure 24 Q. However, a clear colocalisation can be observed in ZG structures, indicating that APP-GFP is sorted to a certain extend into ZG in AR42J cells, when overexpressed (Figure 24 A-D).

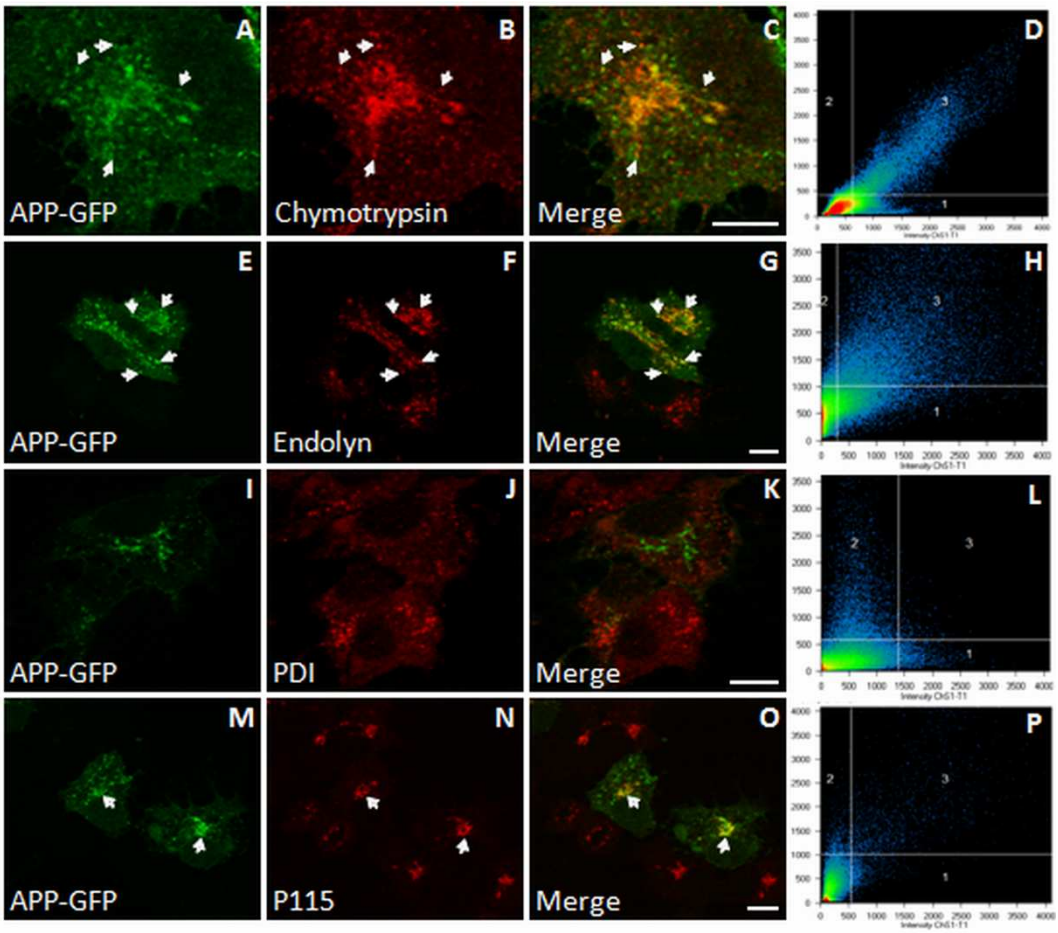

Colocalisation coefficients of Protein X with APP-GFP — **Average** — **Q**

Chymotrypsin (ZG)	87.9% ± 7.5
Endolyn (Lysosomes)	53.1% ± 21.1
PDI (ER)	18.7% ± 13.9
P115 (Golgi)	29.4% ± 17.0

Figure 24: APP-GFP is partially sorted to ZG in pancreatic AR42J cells

AR42J cells were transfected with an APP-GFP construct (**A**, **E**, **I**, **M**), stimulated for ZG formation and processed for indirect immunofluorescence 72 h after transfection. Cells were stained using antibodies directed to Chymotrypsinogen to mark ZG (**B**-**C**), the lysosomal marker Endolyn (**F**-**G**), the ER marker PDI (**J**-**K**) and the Golgi marker p115 (**N**-**O**). Overlays (merge) of confocal images (**A**-**B**; **E**-**F**; **I**-**J**, **M**-**N**) are shown in (**C**, **G**, **K**, and **O**). Arrows point to some granules, showing colocalisation of APP-GFP and Chymotrypsinogen (**C**), Endolyn (**G**) and p115 (**O**). (**D**, **H**, **L** and **P**) show the quantitative correlation analysis. Image analysis was carried out with the Zeiss LSM 510 4.0 software (Carl Zeiss MicroImaging, Inc.). The correlation plot describes the pixel colocalisation depending on their intensity in the GFP (for APP) and TRITC (for Chymotrypsinogen, Endolyn, PDI, and p115) channels with region 3 displaying colocalising pixels. Region 1 and 2 contain the non-colocalising pixels for each label, respectively. The signals below the background (indicated by the axes) in each picture were not included in the quantification of the colocalisation coefficients. (**Q**) An average value of colocalisation has been obtained measured from six cells (7 z-planes from each cell) with a standard deviation given. Scale bars, 10 μm.

5.5 The Secretory Lectin ZG16p in Rat Brain, Still a Lot to Sort Out

As mentioned in section 1.6, the secretory lectin ZG16p is expressed in several rat organs such as the exocrine pancreas but also in duodenum and colon, where ZG16p was found to localize to mucus-producing goblet cells (Cronshagen, Voland et al. 1994). However, it appears to be interconnected with diverse physiological processes such as apical sorting, wound healing and immune response (Lobler, Sass et al. 2002; Miyake, Hara et al. 2004; Kumazawa-Inoue, Mimura et al. 2011; Tateno, Yabe et al. 2011). ZG16p was suggested to represent a component of the *submembranous granule matrix* (a putative proteoglycan/glycoprotein scaffold at the luminal side of the ZGM contributing to cargo sorting, packaging and granule stability), where it was shown to interact with highly sulfated heparan proteoglycans (Kleene, Dartsch et al. 1999; Schmidt, Dartsch et al. 2000; Schrader 2004; Kumazawa-Inoue, Mimura et al. 2011). Interestingly, the protein was found in a cDNA hybridization array, 3 times upregulated after an induced brain lesion in the fornix region, during axonal regeneration, thus being associated to axonal regeneration failure (Kury, Abankwa et al. 2004). Additionally, I identified ZG16p in a crude rat brain lysate by proteomics studies using a 1D-SDS PAGE approach combined with tandem mass spectrometry in a band > 220 kDa (Figure 25). Since the mascot score for ZG16p in this band was 15, further analyses were required to confirm this result.

In the brain, ZG16p could play a role in the secretion of extracellular matrix components, or enzymes, which are responsible for the degradation of the extracellular matrix, due to its heparan binding capacity (Kumazawa-Inoue, Mimura et al. 2011). Thus, ZG16p could fulfil overlapping functions in regulated exocrine and neuroendocrine secretion systems. The extracellular matrix consists of an interwined mesh of fibrous proteins and glycosaminoglycans (GAGs) (*e.g.* heparan and chondroitin sulfate) and its formation is essential for processes like growth and wound healing. As was shown in Chapter 4 the rat mast cell protease 1 (Chymase) associates to the *submembranous matrix* of ZG and it is an extracellular matrix degrading protein. Furthermore, this enzyme was identified in rat brain (Nelson, Siman et al. 1993). Hence, Chymase might be one of the proteins dependent on ZG16p´s expression in brain, to be properly packaged and sorted. Additionally, a role of ZG16p in immune defence in brain is possible, as it was shown to bind to certain fungi (Tateno, Yabe et al. 2011), even though a binding to bacteria was not shown yet. Encouraged by the obtained result and the findings in the literature, ZG16p was selected for further analysis in rat brain on mRNA and protein level by RT-PCR, immunoblotting and immunofluorescence.

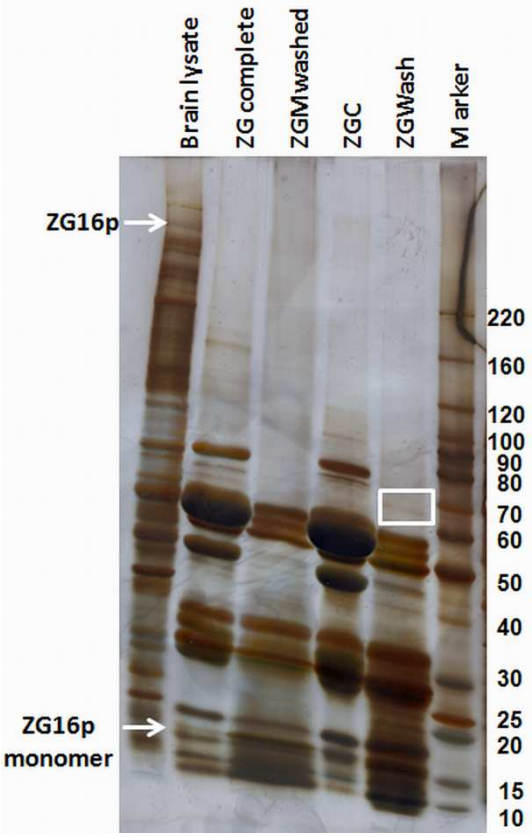

Figure 25: ZG16p identified in a rat brain lysate by 1D-MS/MS

Equal amounts of samples from rat brain lysate and ZG subfractions (40 μg) were incubated 20 min at 65°C in Laemmli buffer and run on a 3-12.5% gradient SDS-PAGE. After a Coomassie-silver staining (3.9.6-3.9.7) bands were isolated and prepared for MS/MS analysis (3.10.1-3.10.3). The band in which ZG16p was identified in rat brain was far above 220 kDa. White arrows and box mark bands in which ZG16p was identified by mass spectrometry.

5.4.1 ZG16p, a Possible New Synaptic Vesicle Constituent

To confirm the result obtained by the 1D-MS/MS approach, ZG16p´s expression on protein level in rat brain and subfractions, obtained during a synaptic vesicle isolation, were analyzed (Figure 26). Equal amounts of protein (40 μg) from the different fractions (brain lysate, cerebellum lysate, cerebellum membrane, cortex, synaptosomes, synaptic vesicles and ZG) were separated on 3-12.5% gradient gels and immunoblotted using a specific antibody directed to ZG16p (ZG16 peptide antibody). Further, to assess synaptic vesicle enrichment, a specific antibody to the synaptic vesicle resident protein synaptophysin was used. As shown in Figure 26, immunoreactivity for synaptophysin was mainly found in the enriched SV fraction and so was ZG16p, too. To provide a preliminary quantitative value for the enrichment of ZG16p in the SV fraction, intensities of the corresponding signals from rat brain lysate and SV were determined by densitometric measurements and the ratios of the protein in the brain lysate to SV fractions were calculated. Furthermore, these values were compared to the once obtained for synaptophysin in the same fractions. A brain lysate to SV concentration ratio of 1:1.8 was calculated for ZG16p, indicating an enrichment in the SV fraction (Figure 26 A and B). Interesting, a similar concentration ratio was obtained for the synaptic vesicle marker protein synaptophysin (1:1.76 enrichment in SV), confirming the enrichment of ZG16p in the SV fraction.

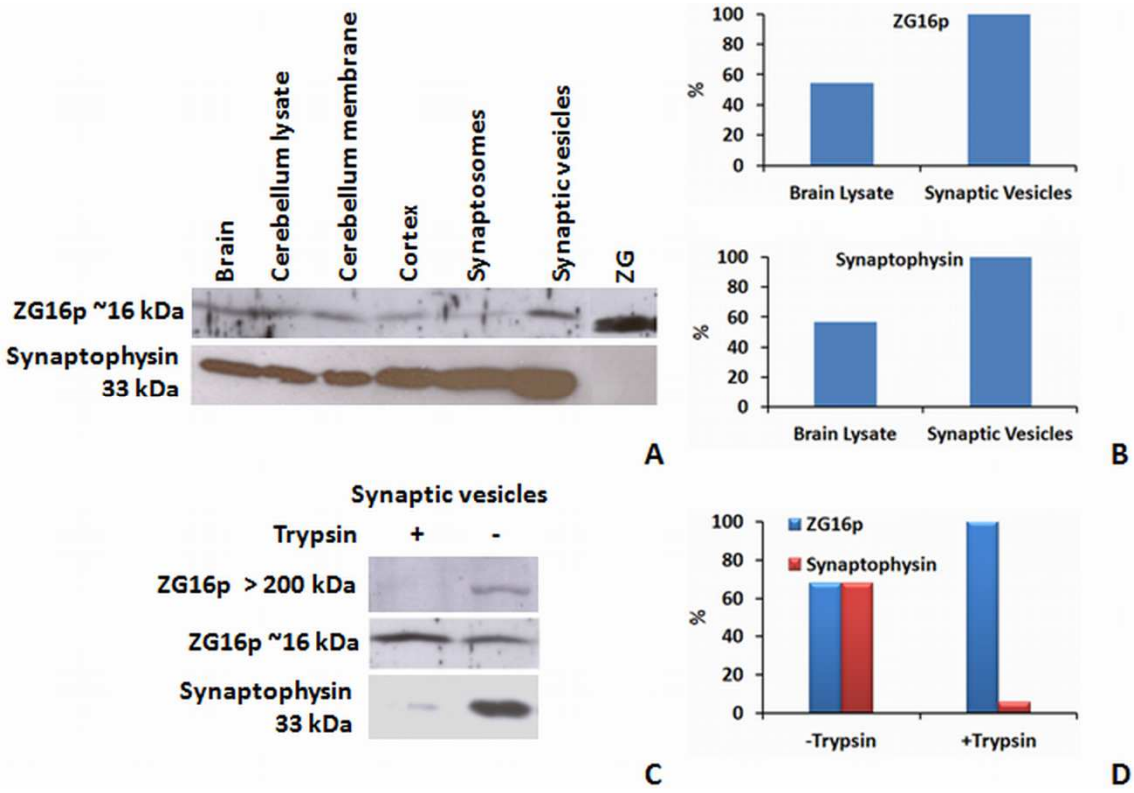

Figure 26: Immunoblot analysis of ZG16p´s expression in rat brain and synaptic vesicles.

(**A**) Synaptosomes and synaptic vesicles were isolated from total rat brain homogenate by gradient centrifugation (3.8.3). Additionally, samples from several brain regions (cerebellum lysate, cerebellum membrane and cortex) obtained during SV isolation were tested for ZG16p. Equal amounts of each sample (40 μg) were run on a 3-12.5% gradient SDS-gel, blotted onto nitrocellulose and incubated with antibodies to ZG16p (peptide antibody) and Synaptophysin, positive control for synaptic vesicle (SV) isolation. The graph in (**B**) demonstrates the enrichment of ZG16p from the whole brain to SV in comparison to Synaptophysin. (**C**) Exploiting ZG16p´s trypsin resistance, 40 μg of a SV fraction were digested overnight at 37°C and run on a 3-12.5% gradient SDS-PAGE together with an undigested control. A higher band (above 200 kDa), recognized by the ZG16 antibody as well as the SV positive control Synaptophysin disappeared after the digest, leaving only a band at ~16 kDa recognized by the ZG16 antibody, which increased in intensity. (**D**) Concentration ratios of ZG16p in SV (digested and undigested) were calculated using densitometric measures of the corresponding signals from the immunoblot using a GS-710 Calibrated Densitometer together with Quantity One 4.3.1 software.

When comparing the ZG16p band in SV to ZG, it appears that the band of ZG16p in SV is slightly higher than in ZG (Figure 26 A). Furthermore, the antibody recognizes a band > 220 kDa in the SV fraction, which could arise from a cross-reaction, or corresponds to the band found by 1D-MS/MS in the rat brain lysate (Figure 25). In previous tests performed in our laboratory, it was discovered that ZG16p is one of the few proteins that in their native and soluble form are trypsin resistent (unpublished data). This information offered the possibility to provide further proof that the bands (> 220 kDa and at ~16 kDa) correspond to ZG16p. For this purpose, 40 μg of isolated SV were digested with trypsin overnight at 37°C prior to the uptake in Laemmli buffer and were run on a 3-12.5% gradient SDS-PAGE together with an undigested control (Figure 26C). Through the trypsin digestion almost all proteins will be degraded and should disappear from the blot, and

only ZG16p should remain. By immunoblot analysis using specific antibodies directed to ZG16p (peptide antibody) and synaptophysin as a control for a successful digestion, the digested sample revealed that synaptophysin was nearly completely digested, and that the band above 220 kDa recognized by the ZG16p antibody disappeared (Figure 26 C). Interestingly, when compared to the undigested control, the ZG16p band at ~16 kDa appears more intense. The increase in intensity could be caused by the degradation of the higher molecular weight band above 220 kDa. In this band, ZG16p might be associated to a trypsin sensitive complex or high-molecular weight protein from which it is released after the tryptic digestion and accumulates as a monomer. But this topic requires further analysis in future studies. For evaluation, the intensities of the corresponding signals of ZG16p at the monomer level (~16 kDa) from digested and undigested SV were determined by densitometric measurements and the ratios of the protein bands were calculated. The remaining band in the digested SV sample revealed a concentration ratio of 1:1.35 when compared to the undigested control (Figure 26 D).

5.4.2 ZG16´s is Differentially Expressed Throughout the Brain

To further confirm the results obtained by immunoblot analysis and to specify ZG16´s expression in the different brain regions, RT-PCR experiments were employed. Total RNA from whole rat brain, different rat brain regions (hippocampus, hypothalamus, cerebellum and cortex) and pancreas was extracted as described in section 3.5.1. From each sample, 3 μg of RNA were transcribed into cDNA using MMLV reverse transcriptase (3.5.3). Equal amounts of cDNA were used to perform a semi-quantitative RT-PCR, as described in section (3.5.4). RT-PCR with mRNA from rat brain and pancreas revealed that ZG16p is expressed in rat brain, which was confirmed by sequencing (Figure 27 A). Sequencing results are presented in the appendix. By densitometric measurements of the band intensities, ZG16 mRNA revealed an approximately 2.2 fold higher expression level in rat pancreas when compared to total rat brain after normalization to the GAPDH loading control (Figure 27 A). Comparing the mRNA levels of ZG16 in the different brain regions (Figure 27 B), cerebellum revealed the highest level of mRNA (88.3%). In the cortex, the mRNA level accounted was (83.7%), in hippocampus (63.9%) and a very low level was measured in the hypothalamus region (43.8%). Pancreatic cDNA was used as positive control and was set to 100%. GAPDH was applied as internal loading control to which all values were normalized.

The differences of the ZG16 mRNA expression levels within the different brain areas can be related to the versatile compositions of cell types contained in the different brain compartments. The cerebellum consists of several types of neurons with a highly regular arrangement. Most important here are the Purkinje and granule cells and three types of axons (mossy and climbing fibers and deep nuclei). The climbing fibers represent the axons of the granule cells. The granule cells are densely packed along with interneurons, mainly Golgi cells but also with Lugaro and unipolar brush cells. The cortex is composed of the gray matter (neurons and unmyelinated fibers) and the white matter (myelinated axons interconnecting neurons). Further, it is constituted of up to six horizontal layers, each having a different connectivity and neuron composition. The hippocampus contains three main layers of cells having a different cell density

plus a varying degree of neuronal fibers, which are again dividable in at least seven subfields. The cell type composition is so complex that it will not be explained here. The hypothalamus is the link between the nervous and the endocrine system via the pituitary gland (hypophysis). It is mainly constituted of neurons releasing corticotrophin-releasing hormones and other hormones.

Although some of the cells appear in all four compartments, their ratios within the distinguishable compartments are different from each other. Furthermore, different cell densities and also the regulation of gene products vary from compartment to compartment since the tasks for each sub-brain area are different. Through its intense and tight folding (*folica cerebelli*), the cerebellum offers a much larger surface of gray matter than the cortex region and has a much higher density of neurons. All this taken together could explain the relatively strong expression of ZG16p in the cerebellum in comparison to other brain areas.

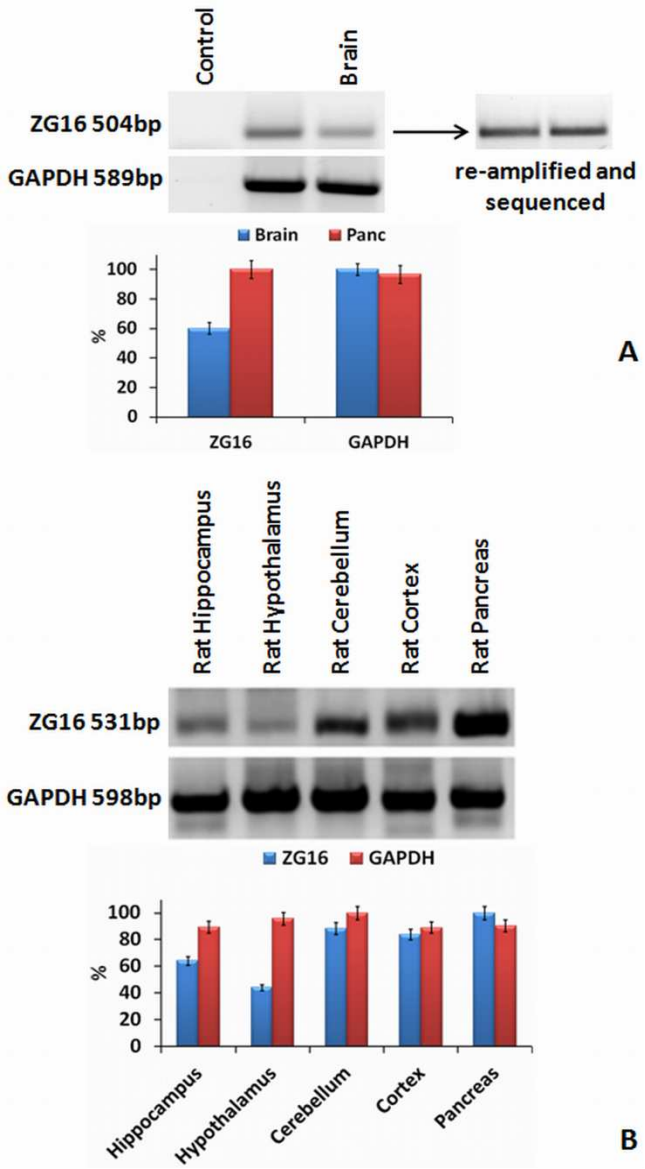

Figure 27: ZG16 mRNA distribution in rat brain.
(**A**, **B**) Total RNA extracted from rat brain tissue and special regions was transcribed into cDNA (3.5.1-3.5.3). From each sample equal amounts of cDNA (150 ng) were used for a 50 μL semi-quantitative-RT-PCR (3.5.4) with species specific primers for ZG16. GAPDH served as loading control, pancreatic cDNA served as positive control and a template-free PCR mix was used as negative control. (**A**) The band from total brain was isolated, purified, re-amplified as described in 3.5.5 and send for sequencing. The graphs in (**A** and **B**) compare the ZG16 mRNA expression levels with each other after normalization to the GAPDH control. mRNA expression ratios were calculated using densitometric values from the corresponding signals from the agarose gels using a GS-710 Calibrated Densitometer together with Quantity One 4.3.1 software.

5.4.3 ZG16 Might be Sorted to RNA Granules in Rat Primary Neurons

To determine the intracellular localisation of ZG16p, hippocampal neuronal primary cultures from rat were used in immunofluorescence experiments. After extration from rat brain, cells were seed on glass coverslips and cultured for 10-14 days. Cells were generally provided by Prof. A.L. Carvalho and Dr. S. Santos (CNC, University of Coimbra). In first immunofluorescence approaches with rat neuronal primary culture following the standard protocol, cells were permeabilised with Triton X-100. The staining, however, did not lead to a definite result due to a relatively strong background (Figure 28 A and B). To optimize the staining conditions, several antibody retrieval techniques were tested simultaneously (*e.g.* citrate buffer, glutaraldehyde and SDS). Only with SDS, a brighter staining of vesicular structure and a lower background could be observed (Figure 28 C and D). Briefly, SDS is an anionic tenside used in immunofluorescence to introduce a slight protein defolding which facilitates the access of an antibody to its antigen. It also reduces the background staining since badly cross-linked cytosolic proteins are easily washed out after the treatment. Furthermore, stained structures appeared to be the same with both methods, supporting the specificity of the ZG16 peptide antibody. In the modified protocol, cells were treated for 5 min with 1% SDS instead of 10 min with 0.2% Trition. Additional tests with both methods (0.2% Trition X-100 and 1% SDS) in our model cell line AR42J, stimulated for ZG formation, revealed that with 1% SDS the antibody recognizes the same cellular structures (ZG) as with Triton X-100. Additionally, no improvement in staining intensity was observed in this cell line (data not shown).

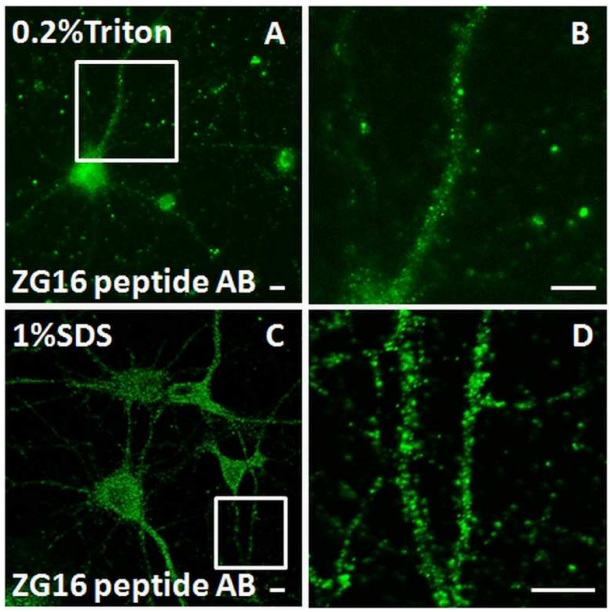

Figure 28: Staining of rat neuronal primary cells for ZG16p under different permeabilisation conditions.
Rat primary neuronal cells were either treated with 0.2% Triton X-100 for 10 min, or for 5 min with 1% SDS and subsequently immunostained with a peptide antibody against ZG16p. Cells treated with SDS revealed a much brighter staining. All images were made with a Confocal Zeiss LSM 510 microscope and associated software. Scale bars, 10 μm

After defining the conditions for immunofluorescence, localisation studies for ZG16p in rat neuronal primary cells were conducted (Figure 29) applying the modified immunofluorescence protocol for 1% SDS. Since ZG16p was found to be enriched in a SV fraction by immunoblotting (Figure 26), several subcellular marker antibodies were applied to neuronal cells stained with a ZG16p peptide antibody.

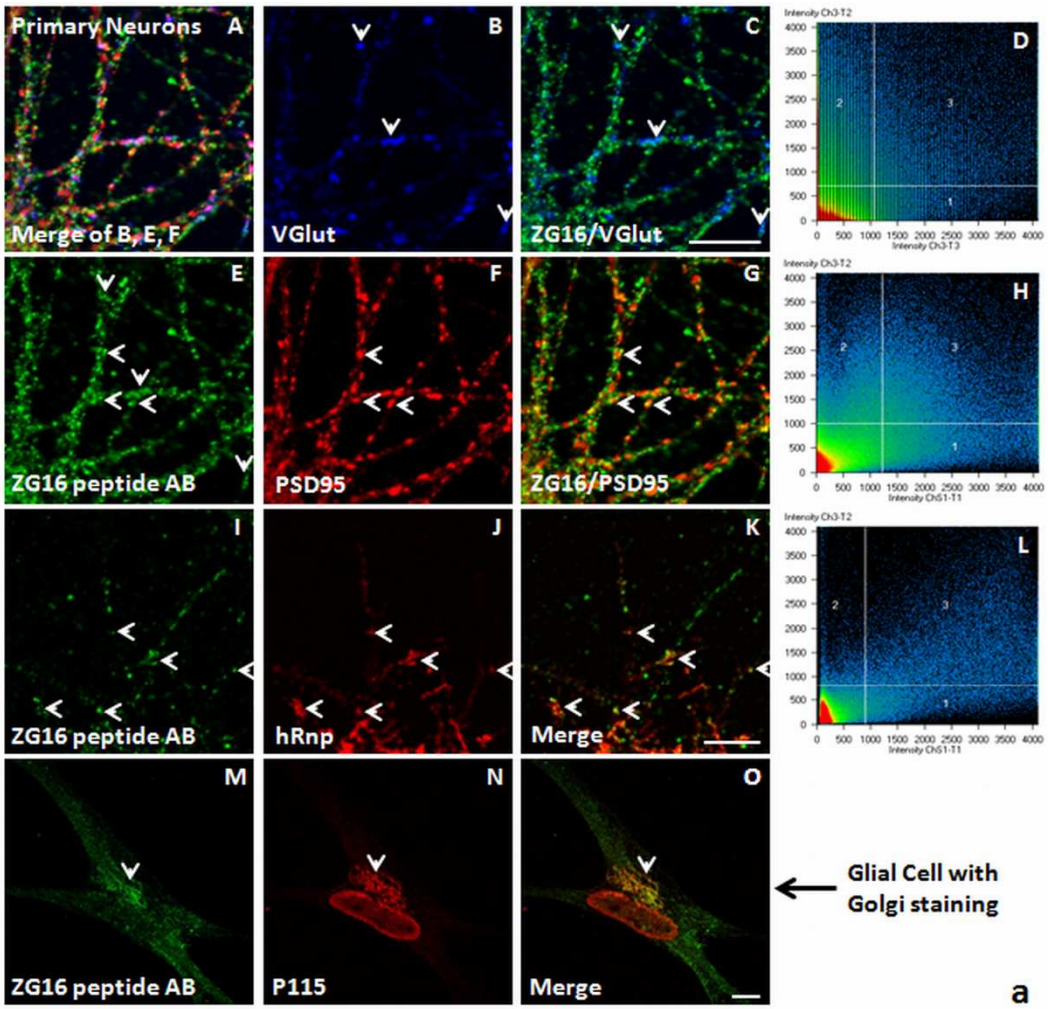

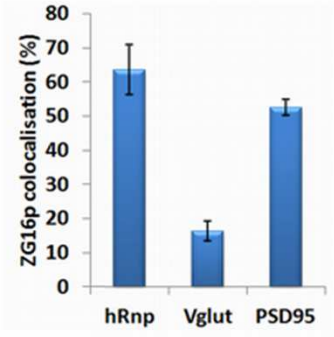

Colocalisation coefficients of Protein X with ZG16p	Average
hRnp (RNA Granules)	64.5% ± 16.9
Vglut (Pre-synapse)	16.6% ± 3.8
PSD95 (Post-synapse)	53.1% ± 2.2
Colocalisation of:	
PSD95 with Vglut	17.1% ± 2.8

b

Figure 29: Subcellular localisation of ZG16p in rat neuronal primary cells.
(**a**) Neuronal cells originating from rat brain hippocampus were cultured for 10-14 days prior to immunofluorescence labelling. Cells were stained using antibodies to ZG16p (**A**, **E**, **I** and **M** peptide AB), VGlut as pre-synaptic marker (**B**-**C**), PSD95 as post-synaptic marker (**F**, **G**), hRnP as a RNA granule marker (**J**-**K**) and p115 as a Golgi marker (**N**-**O**). Overlays (merge) of confocal images (**E** and **B**; **E** and **F**; **I** and **J**, **M** and **N**) are shown in (**C**, **G**, **K** and **O**). Areas of colocalisation are labelled with arrowheads (**B**-**O**). (**D**, **H** and **L**) show correlation plots describing the pixel colocalisation depending on their intensity in the Alexa 488 (for ZG16), TRITC (for PSD95 and hRnp), or for Alexa 647 (for Vglut) channels with region three displaying colocalising pixels in the cells. Region 1 and 2 contain the non-colocalising pixels for each label, respectively. The signals below the background (indicated by the axes) in each picture were not included in the quantification of the colocalisation coefficients. (**b**) Average values of colocalisation have been obtained measured from three cells (3 z-planes from each cell) with a standard deviation given. Image analysis was carried out with a Confocal Zeiss LSM 510 microscope and associated software. Scale bars, 10 μm.

The applied antibodies were directed to the vesicular glutamate transporter (VGlut) as a pre-synaptic marker (Figure 29**a** B-C), the post synaptic density protein (PSD95) as post-synaptic marker (Figure 29**a** F-G), but also to the human ribonucleoprotein (hRNP) as RNA granule marker (Figure 29**a** I-K). In all cases, the recognized structures are round or oval, distribute all along the cells axons and dendrites and show colocalisation with the ZG16p antibody (a staining with MAP2 to distinguish between dentrite and axon is not shown but was routinly done). Pancreatic ZG16p containes an ER-targeting signal and is known to be sorted into ZG passing through the Golgi. However, the neuronal staining with p115, a Golgi marker, was strongly outshined by the additional intense nuclei staining of p115 in neurons, impairing the evalutation of the colocalisation coefficients in these cells. Interestingly, the Golgi marker p115 revealed a prominent Golgi staining in co-isolated glial cells colocalising with ZG16p as is represented in Figure 29**a** M-O.

Quantification by pixel-by-pixel analysis from confocal images demonstrated a co-localization coefficient of 64.5%±16.9 for hRnp (RNA granules, Figure 29**a** K-L and **b**), of 16.6%±3.8 for Vglut (pre-synaptic marker, Figure 29**a** C-D and **b**) and of 53.1%±2.2 for PSD95 (post-synaptic marker, Figure 29**a** G-H and **b**) with ZG16p. PSD95 and Vglut colocalised to around 17.1%±2.8 with each other, which might be the result of a close proximity of post- and pre-synapses but maybe also due to resolution limitations as was demonstrated previously in Figure 22 K.

5.4.4 A Full-Length and a Peptide Antibody to ZG16p Confirm Each Other

For the analyses of ZG16p in different cells and tissues, two different antibodies against ZG16p were available, a peptide (produced in our laboratory) and a full-length antibody. Both were crude serum fractions from different bleedings of rabbits. The full-length antibody was kindly provided by Anson Lowe, Stanford University, USA. Prior to experiments, IgG enriched fractions of the full-length and the peptide antibody sera were prepared as described in section 3.9.5. All resulting ammonium salt precipitated IgG fractions were adjusted to a concentration of 10 μg/μL to set a standard for following experiments. The aim was to characterize and compare both antibody types in their staining specificity for ZG16p to confirm and support previous results obtained with our peptide antibody. In some experiments, the peptide antibody raised questions about its specificity and/or ZG16p binding capacities and subcellular localisation. Both antibodies and appending fractions were compared to each other in immunofluorescence (Figure 30) and immunoblotting experiments (Figure 30). In immunofluorescence experiments with dexamethasone-stimulated AR42J cells, no differences in staining specificity but in staining intensity were observed, when comparing an IgG fraction to the corresponding crude serum of the antibody (not shown). After testing various antibody dilutions from 1:100 to 1:600, the IgG fraction of the full-length antibody and the N1d serum of the peptide antibody (Figure 30) revealed to be the best suited fractions for immunofluorescence experiments. Due to limitations in the amount, no IgG fraction could be prepared from the N1d serum of the peptide antibody. Furthermore, in immunofluorescence, both antibodies revealed the same staining characteristics in dexamethasone-stimulated AR42J cells labelling zymogen granules, as depicted in Figure 30.

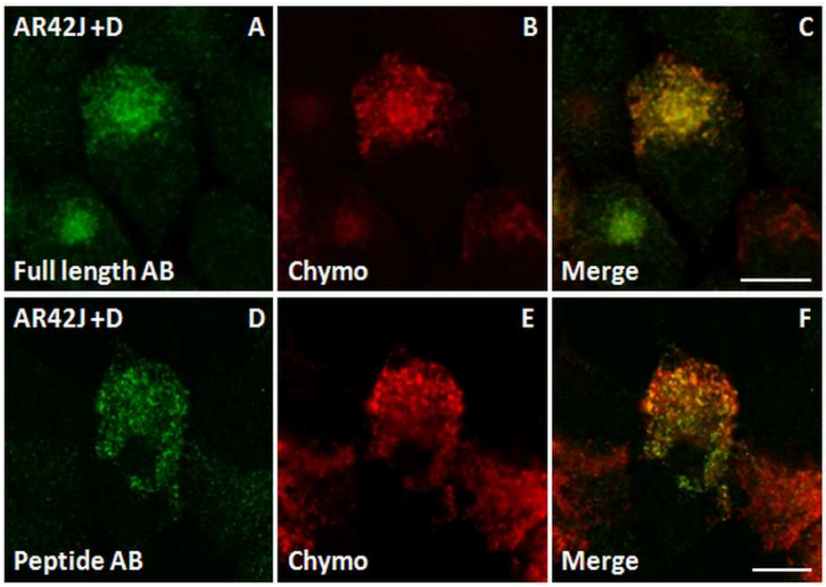

Figure 30: ZG16 full-length and peptide antibodies are both specific for ZG16p in stimulated AR42J cells
AR42J cells were induced for ZG formation with dexamethasone (+D) were immunostained either with the anti-ZG16 full-length antibody (1:400) (**A**, **C**) or with the anti-ZG16 peptide antibody (1:200) (**D**, **F**). A co-staining with the ZG marker Chymotrypsinogen is shown in (**B**-**C** and **E**-**F**). Both ZG16 antibodies reveal the same staining pattern. Images were obtained with an Olympus IX81 fluorescence microscope. Scale bars, 10 μm

In immunoblot analysis comparing all available serum antibodies and corresponding IgG fractions with each other, all recognized the ZG16p monomer at 16 kDa (Figure 31). Comparing the two different ZG16 antibodies with each other, both show the same band pattern but with different band intensities (Figure 31, yellow boxes). Furthermore, fractions belonging to the peptide antibody (N1a, N1b3 and N1d) revealed different immunoreactivities amongst each other. These variations in the immunoreactivity and band intensities are caused by different concentrations of the specific antibodies in the different bleedings. Interestingly, almost all fractions recognize a weak band appearing right on top of the 16 kDa band of approximately ~18 kDa (marked with a double arrow and red squared boxes), best visible with the N1a IgG fraction. It is possible, that this band originates from a ZG16p version before cleaving off the ER targeting signal, which would result in a protein with ~18 kDa. However, other possibilities such as antibody cross-reaction or posttranslational protein modifications can be the cause. Additionally, among the peptide antibody fractions, N1d resulted in the strongest staining, also showing bands at higher molecular weights (32 kDa, 50 kDa and 60 kDa), which are as well recognized by the full-length antibody, confirming each other's specificity. It is still under discussion, if ZG16p can form dimers which could explain the band at 32 kDa. All other bands either derive from antibody cross-reactions, or are caused by strong protein complexes containing ZG16p, which did not dissolve under the denaturing conditions. ZG16p`s strong binding capacity, to highly sulfated heparan proteoglycans of ZG was shown recently (Kumazawa-Inoue, Mimura et al. 2011). According to the authors, ZG16p recognizes the glycosaminoglycan chains and binds most strongly to heparin. Core proteins of these proteoglycans revealed molecular weights of 35-40 and 66 kDa. Further, they observed that conformational changes in the ZG16p structure only occured under stringend conditions (5 min, 98 in Laemmli buffer containing 5% mercaptoethanol).

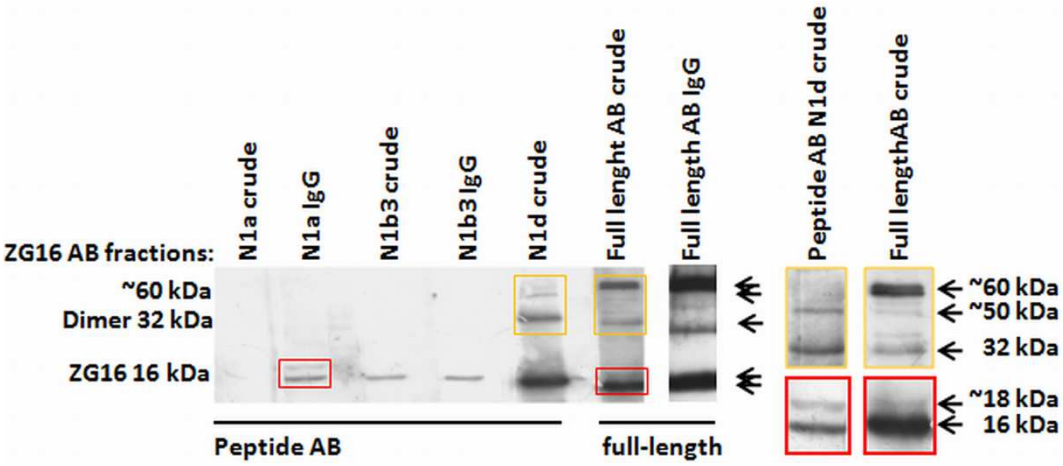

Figure 31: Immunoblot analysis of ZG16 antibody fractions

Equal amounts of total ZG (10 μg) were heated for 5 min at 95°C and run on a 12.5% SDS-gel, blotted onto a nitrocellulose. The membrane was cut in-between lanes and each lane was incubated with a different primary antibody fraction under equal conditions. Blots were developed simultaneously.

Since both ZG16p antibodies (peptide and full-length) are able to recognize the same structures (ZG) and bands in immunofluorescence and immunoblot analysis respectively, the full-length antibody was applied to rat neuronal culture and SV vesicle fractions. This allowed us to confirm the results previously obtained with the peptide antibody (data not shown).

5.5 Discussion to Proteins Identified by Proteomics Studies in Exocrine and (Neuro)Endocrine Secretion Systems

Some of the proteins identified by proteomics studies in exocrine and (neuro)endocrine secretion systems are suspected to play similar roles in both places. The scope of this part of my thesis was to identify further ZG membrane and matrix proteins of the rat ZG which might be shared by SV as well. Proteins identified by mass spectrometric methods in both systems (ZG and SV) were listed in Table 5-1 defining the proteomic overlap indicated by recent publications. Furthermore, two different approaches for the separation of ZGM and ZGM associated proteins were chosen; 1D gel-electrophoresis and as an off gel approach, liquid chromatography was applied. These approaches are better suited for the separation of hydrophobic, high-molecular-weight and membrane constituents and were combined with the tryptic digestion of proteins followed mass spectrometric analysis (Figure 12). Four proteins were selected for further analysis, based on our proteomics results and the information given by current publications about proteomics studies in ZG and SV, which were Piccolo, Snj-1, APP and ZG16p.

Nevertheless, with the experiments conducted to detect Piccolo in ZG and subfractions and also AR42J cells, it is not yet possible to confirm if Piccolo is a transient part of the ZGM as it was suggested after LC-MS/MS analysis of the ZGWash fraction. It is possible that Piccolo is a co-purification coming from vesicles of the pancreatic β-cells where it was identified previously (Fujimoto, Shibasaki et al. 2002). Since further functional studies were disabled, due to problems with the available antibodies, the work on this protein is at least temporally intermitted and results are not further discussed. However, its putative role as a Ca^{2+} sensor makes it an attractive candidate protein in ZG secretion.

In contrast, Snj-1 could be detected in immunoblot analysis in the positive control of synaptosomes and very weakly in a total lysate of rat pancreas, but not in ZG subfractions (ZGM, ZGM_{washed}, ZGWash and ZGC), or AR42J cell lysates (Figure 21). Furthermore, the Snj-1 specific antibody revealed a high sensitivity regarding the state of denaturation/folding of the protein making detection by immunoblot experiments in samples with a low Snj-1 concentration challenging. In immunofluorescence experiments, Snj-1 revealed its low expression in AR42J cells. Independent from their state of differentiation, AR42J cells show a weak punctate staining pattern close to the cells peripheries, not colocalising with the ZG marker protein Carboxypeptidase (Figure 22 A-F). Evaluating the obtained results for Snj-1, it is very unlikely that this protein is involved in ZG trafficking since in none of the experiment Snj-1 localized to ZG. Probably, Snj-1 appeared in LC-MS/MS analysis due to a co-purification, being attached to co-isolated endocytotic vesicles or membranes from ruptured vesicles constituting an impurity in the ZG preparation. The very weak positive band for Snj-1 in the pancreatic homogenate from Figure 21 is most likely caused by endosomal vesicles coming from the pancreatic β-cells in which Snj-1 was identified previously (Hoy, Maechler et al. 2002).

APP was identified in a ZGM associated subfraction by recent proteomics approaches (Rindler, Xu et al. 2007; Chen and Andrews 2008) implying a role in ZG exocytosis. In immunoblot analysis APP was not detected in ZG, or ZG subfractions, but in AR42J cell lysates (Figure 23). Probable due to an incompatibility of our immunofluorescence protocol with the APP specific antibody, endogenous APP could not be detected in AR42J cells. Conducting overexpression

experiments with an APP-GFP fusion protein in AR42J cells (Figure 24), however revealed a cytosolic staining for APP-GFP, but also a specific colocalisation with ER, Golgi and lysosomal marker proteins (Figure 24 E-O). Much more important, the strongest colocalisation was detected with Chymotrypsinogen as a ZG marker protein (Figure 24 A-C). APP is known to enter the secretory pathway due to its ER-targeting signal form where it is translocated to the trans-Golgi network. Hence, it is possible that very low amounts of endogenous APP are sorted into ZG being to low for an antibody detection. By overexpression studies it could be proven that APP is sorted into ZG where it was prevously identified by proteomics studies (Rindler, Xu et al. 2007; Chen and Andrews 2008). If this sorting to ZG is the result of a mistargeting, or relates to some physiological function remains at this state of our studies unclear. To unraveal its possible function/s in ZG might become subject of future studies.

ZG16p (16 kDa), a potential component of the submembranous matrix in ZG, was for the first time identified in a rat brain, lysate by a 1D-MS/MS approach with a very low Mascot score of 15 in a band > 220 kDa (Figure 25). With its appearance in rat brain it became an interesting candidate which might be shared by exocrine and (neuro)endocrine secretion systems and thus, ZG16p was selected for further analyses in rat brain. By semi quantitative-RT PCR (Figure 27), immunoblot analysis (Figure 26) and immunofluorescence experiments (Figure 28 and Figure 29) the expression of ZG16p could be confirmed in rat brain. In a semi-quantitative RT-PCR testing rat brain tissue for ZG16 mRNA, it was found to be expressed on mRNA level after sequencing the characteristic ZG16 cDNA band (see Appendix, Figure 27 A). In a second, semi-quantitative RT-PCR approach, different brain tissue sections were tested for the expression of ZG16 mRNA (Figure 27 B). ZG16 mRNA revealed to be expressed highest in the cerebellum but was also detected in the cortex, hypothalamus and hippocampus. Through its intense and tight folding (*folica cerebelli*), the cerebellum offers a huge surface of gray matter. Furthermore, it has a much higher density and activity of neurons then other brain regions. The higher cell activity could explain the relatively strong expression of ZG16p in the cerebellum in comparison to other brain areas. In an immunohistochemical staining of mouse brain sections with the ZG16 antibodies, it was not possible to clarify which cell types are responsible for the ZG16p expression in brain (data not shown). In addition, the question remains under which condition/s the protein is expressed or up-/down regulated in rat brain. In immunoblot experiments, ZG16p appeared enriched in a fraction of synaptic vesicles but revealed a slightly higher molecular weight (~1-2 kDa) then in ZG fractions from rat pancreas (Figure 26). However, its identity was indirectly confirmed by applying a tryptic digestion approach to a synaptic vesicle sample exploiting its protease resistance (unpublished data from our laboratory). The result demonstrated that only one protein band at approximately 16 kDa remained after digestion, while the synaptophysin control was almost completely degraded. Even though, it remains unclear why ZG16p in SV´s appears at a sightly higher molecular weigth than in ZGs. In immunofluorescence experiments with rat primary neuronal cultures originating in the hippocampus region (Figure 29 A and B), a colocalisation coefficients with several subcellular marker proteins was defined. Through a pixel-by-pixel analysis, ZG16p revealed a strong colocalisation with the RNA granule marker hRnp and the post-synaptic marker PSD95, pointing to the possibility that ZG16p might be secreted into the synaptic cleft in brain. Further, a prominent colocalisation of a ZG16p staining with the Golgi marker p115 could be observed in co-isolated glia cells. These cells surround neurons and hold them in place. They are

responsible for the supply of nutrients and oxygen to neurons, they insulate one neuron from another, destroy pathogens and remove dead neurons. It is supposed that these cells play a crucial role in neurological diseases like Alzheimer's disease, and it was proven that they are important for the regulation of neuronal repair after injury (Barres 2008). Also, it is known that ZG16p enters the secretory pathway colocalizing in parts with the Golgi marker p115. But it is not completely clear yet, if ZG16p from the exocrine pancreas is secreted into the pancreatic duct system, or if it remains attached to the ZGM or apical membrane during the exocytosis process and is recycled back via the endosomal-lysosomal pathway. In neurons, the indication points to a secretion into the synaptic cleft where ZG16p could be involved in the organisation of the post-synaptic glycocalix consisting of a variety of scaffold proteins (Cheng, Hoogenraad et al. 2006; Chen, Winters et al. 2008), or it could be part of immunologic synapses allowing the activation of a unique T-cell (Sigal 2005).

Additionally, an antibody characterisation after IgG enrichment of a full-length and a peptide anitbody directed to ZG16p demonstrated that both antibodies recognize ZGs in immunofluorescence experiments (Figure 30). In immunoblot analysis (Figure 31), both antibodies recognize the characteristic band for ZG16p at the monomer level (16 kDa) plus four additional bands at approximately 18, 32, 50 and 60 kDa in a fraction of complete zymogen granules, supporting the results obtained with the peptide antibody. It was recently demonstrated that ZG16p possesses positively-charged lysine and arginine residue cluster close to the putative sugar-binding site specifically interacting with highly sulfated heparan sulfate chains of proteoglycans at the ZGM (Kanagawa, Satoh et al. 2011; Kumazawa-Inoue, Mimura et al. 2011). The core proteins of these proteoglycans revealed, after a heparin lyase II digestion, molecular masses of 66 and 35-40 kDa. However, the core proteins itself have not been identified yet. Kumazawa-Inoue *et al.* (2011) also demonstrated that ZG16p changes its conformation only under stringend conditions (5 min, 98˚C in Laemmli buffer containing 5% mercaptoethanol). Nevertheless, in my experiment it remains demonstrated that ZG16p may still be bound to some HMW protein or complex under the denaturing conditions of the SDS-gel. A computational sequence analysis of rat ZG16p, searching for eventually unknown isoforms revealed that ZG16p does not have any isoforms. Theoretically, it is possible that both antibodies are able to recognize the ZG16p paraloge ZG16b/PAUF which is around 21 kDa in humans and has not been decribed yet in rat. A sequence alignment comparing both proteins and highlighting the binding site for the peptide antibody is added in the Appendix section. As a protease resistent protein, the eventual accumulation of ZG16p in the brain might lead to unexpected complications like in Alzheimer's disease with amyloid plaques. These last findings give a new twist for the localisation of ZG16p and its eventual role(s) in rat brain. ZG16ps` capacity to bind highly sulphated heparan chains of proteoglycans with the highest specificity for heparin, in ZG (Kumazawa-Inoue, Mimura et al. 2011) might also be relevant for the packaging of RNA in neurons, which remains to be proven by future experiments. Heparan sulfate is suggested to be involved in cell-cell recognition phenomena and in the control of cell growth while heparin is proposed to be mainly involved in defence mechanisms against bacteria and other foreign material (Nader, Chavante et al. 1999).

In very recent publications, ZG16p´s carbohydrate binding motif has been resolved and found to bind mannose/glucose-type glycans (Kanagawa, Satoh et al. 2011). ZG16p was found to bind to pathogenic fungi in the digestive system (Tateno, Yabe et al. 2011) underlining ZG16p´s

probable protective function. Hence, ZG16p is considered to contribute to immune defense by physically capturing and/or sensing pathogenic fungi (Tateno, Yabe et al. 2011). Considering the fact that ZG16p is an evolutionary highly conserved protein distributed from fishes to human (Figure 7), it might be a novel evolutionary ancient molecule required for immune defense in the digestive system (Tateno, Yabe et al. 2011). Still, its exact function/s in the exocrine pancreas and brain remain unclear and will be subject of future studies. Since ZG16p was found to be expressed in the exocrine pancreas (Cronshagen, Voland et al. 1994), and on mRNA level in the endocrine system brain (Kury, Abankwa et al. 2004), ZG16p might be the right tool to obtain new insights into the similarity of exocrine and neuroendocrine secretion and apical targeting.

Chapter 6 Modulating Zymogen Granule Formation in Pancreatic AR42J Cells

The acinar cells of the exocrine pancreas are specialized in the synthesis, mass packaging/sorting, storage and regulated secretion of a complex mixture of digestive enzymes. The variety of pancreatic digestive enzymes is packaged in a condensed and predominantly inactive form into large (approx. 1 μm in diameter) secretory organelles, so called zymogen granules (ZG), which are released by regulated apical secretion, triggered by external stimuli. ZG formation is initiated at the *trans*-Golgi network (TGN) where the regulated secretory ZG proteins co-aggregate at the mildly acidic pH and high calcium levels and condensing vacuoles/immature secretory granules are formed (Freedman and Scheele 1993; Leblond, Viau et al. 1993; Colomer, Kicska et al. 1996; Dartsch, Kleene et al. 1998). They mature by further concentration of the cargo proteins with selective removal of components not destined for regulated secretion. The mature ZG are stored at the apical pole of the acinar cells and release their cargo via exocytosis in a calcium-dependent manner upon neuronal or hormonal stimulation into the apical lumen and the pancreatic duct system. The digestive enzymes are finally activated by enterokinase via proteolytic cleavage of trypsinogen in the small intestine (Introduction 1.1).

Although the ZG has long been a model for the understanding of secretory granule biogenesis and functions, the molecular mechanisms required for ZG formation at the TGN, for packaging and sorting of cargo proteins, as well as for granule fusion and exocytosis are still poorly defined (Kleene, Dartsch et al. 1999; Schrader 2004; Dikeakos and Reudelhuber 2007; Gomez-Lazaro, Rinn et al. 2010). According to recent models, part of the molecular machinery required for digestive enzyme sorting, granule trafficking and exocytosis is supposed to be associated with the granule membrane (ZGM). In addition to basic research interests, ZG play important roles in pancreatic injury and disease (Introduction 1.1).

The understanding of ZG biogenesis requires suitable cell culture models. Pancreatic AR42J cells have been used as a model system for granule formation and pancreatic exocrine secretion. They were originally derived from a rat pancreatic tumour following exposure to azaserine (Longnecker, Lilja et al. 1979). Treatment with the synthetic glucocorticoid dexamethasone induces the differentiation of AR42J cells into exocrine, acinar-like cells and the *de novo* formation of electron-opaque secretory granules, which contain the major pancreatic zymogens (Logsdon, Moessner et al. 1985). Remarkably, long-term treatment with dexamethasone has been shown to induce transdifferentiation to hepatocytes, and loss of the acinar phenotype (Shen, Slack et al. 2000). AR42J cells display stimulated secretion of amylase in response to cholecystokinin or acetylcholine (Logsdon 1986). However, compared to acinar cells from rat pancreas, stimulated secretion in AR42J cells is suboptimal (Arvan and Castle 1987), AR42J cells are non-polarised, do not express all rat ZG proteins, and exhibit smaller ZG (Logsdon, Moessner et al. 1985).

In this chapter, we show that granule formation in AR42J cells can be modulated by altering the growth conditions in cell culture. Cultivation of AR42J cells in Panserin, a serum-free medium, resulted in enhanced induction of granule formation, expression of ZG proteins and an

increase in granule size compared to serum-containing DMEM. Our data indicate that this effect is based on the stronger stimulatory effect of Panserin on differentiation of AR42J cells. To investigate if an enhanced expression of ZG proteins is sufficient to initiate granule formation, we expressed several zymogens and ZG membrane proteins in non-stimulated AR42J cells and in constitutively secreting COS-7 cells. Neither single expression nor co-expression was sufficient to initiate granule formation in AR42J cells or granule-like structures in COS-7 cells as described for neuroendocrine cargo proteins. The importance of our findings for granule formation in exocrine cells is discussed.

6.1 Stimulation of Granule Formation in AR42J Cells by Altered Growth Conditions

To investigate the suitability of PaM for long term applications and its effect on differentiation and granule formation, AR42J cells were incubated in PaM or DMEM for 24 hours before granule formation was induced by the addition of 10 nM dexamethasone (3.6.1-3.6.2). Cells were processed for immunofluorescence after 48 and 72 hours and incubated with antibodies directed to carboxypeptidase A, a prominent granule marker protein (3.7.1, Figure 32) (Faust, Gomez-Lazaro et al. 2008). Immunofluorescence of dexamethasone-treated cells cultured in DMEM or PaM revealed the induction of numerous secretory granules positive for carboxypeptidase A under both experimental conditions (Figure 32). Interestingly, the number of cells containing granules appeared to be higher in PaM than in DMEM after dexamethasone-treatment. Furthermore, the granules in many cells appeared to be larger and occasionally more frequent than in DMEM. Quantitative analysis of the morphological observations revealed that 74.9 $\pm$ 4.9% of the dexamethasone-stimulated cells in PaM exhibited a prominent granular staining pattern compared to 62.4 $\pm$ 4.6% in DMEM (3.7.2). A stronger stimulatory activity of PaM on granule formation in AR42J cells was also visible in controls without dexamethasone. In DMEM controls, the vast majority of the cells were usually negative for carboxypeptidase, whereas about 4-8% of the cells exhibited a strong labeling of the Golgi apparatus as well as a faint staining of vesicular and/or granular structures, which might represent constitutive cargo containers, presumably due to self-stimulation (Figure 32 C). Cultivation in PaM (without dexamethasone) revealed an increase in the number of cells with a Golgi-labeling and granular staining of carboxypeptidase A further supporting its stronger stimulatory effect on differentiation, zymogen induction and granule formation. It should be noted that PaM does not contain any glucocorticoids, which may account for a stronger induction of cellular differentiation (information provided by the manufacturer). Similar observations were made when antibodies to amylase or chymotrypsinogen were used (not shown).

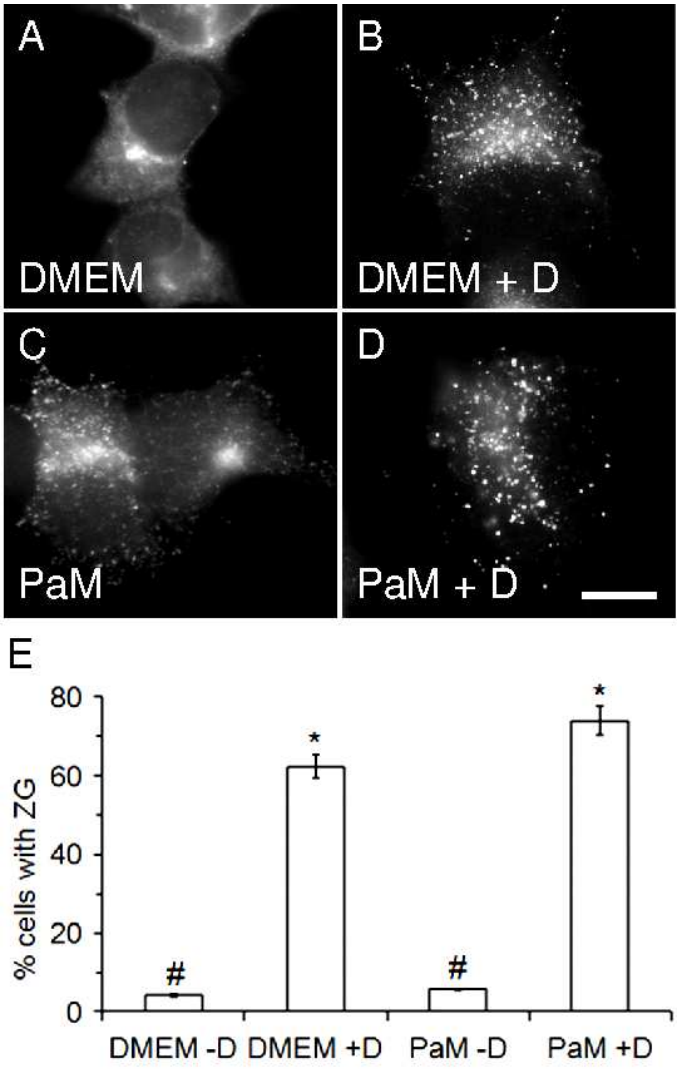

Figure 32: AR42J cells reveal a stronger ZG induction in PaM then in DMEM medium

AR42J cells were cultured in DMEM (A, B) or PaM (C, D) and stimulated for granule formation with dexamethasone (B, D), (A, C) show untreated controls. After 72 h cells were processed for immunofluorescence using an antibody directed to carboxypeptidase A. Images were acquired on an Olympus IX81 fluorescence microscope. (E) Quantitative evaluation of granule formation under the different culture conditions after 72 h. Data are from 3-4 independent experiments and are presented as means ± S.D. (*p<0.01, #p<0.05, when compared to controls). Bar, 10 µm.

Alterations in granule size were confirmed by ultrastructural studies (Figure 33). In dexamethasone-stimulated cells cultured in DMEM, electron-opaque secretory granules with a diameter of 0.1-0.5 μm were observed in 72 $\pm$ 6% of the cells. In stimulated cells cultured in PaM, secretory granules with a diameter of up to 1 µm were occasionally observed in addition to smaller ones (0.1-0.5 µm). In unstimulated controls electron-dense granular structures were mainly absent (4 $\pm$ 2% of the cells in DMEM; 12 $\pm$ 6% of the cells in PaM), but when detected were similar in size to those observed in DMEM containing dexamethasone (not shown).

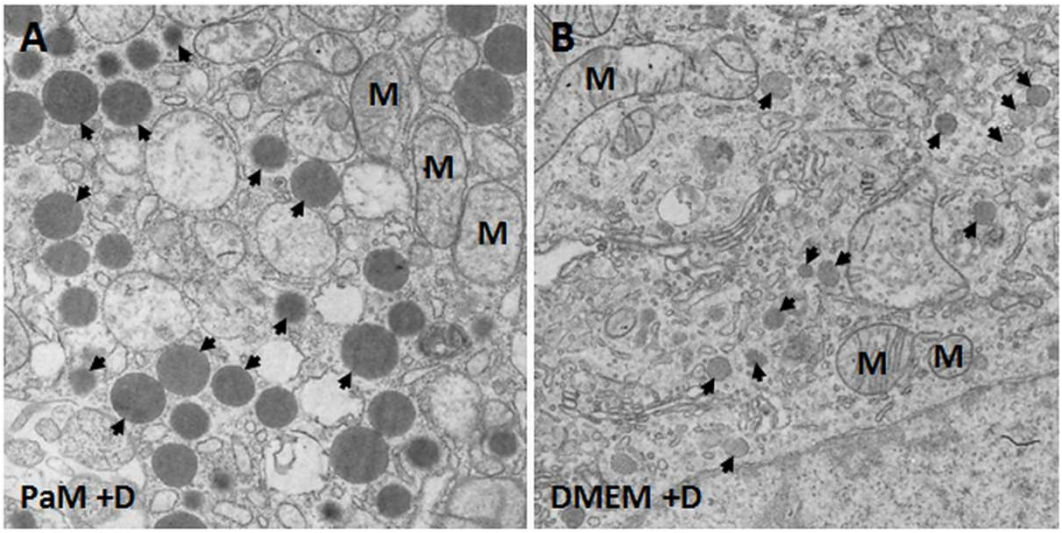

Figure 33: Stimulated AR42J cells form up to 10 times bigger granules when cultured in Panserin than in DMEM

Electron micrograph of granules in AR42J cells which were cultured in PaM (**A**) or DMEM (**B**) and induced for granule formation with dexamethasone for 72 h before being processed for electron microscopy. Arrowheads in (**A** and **B**) indicate zymogen granules. Granules in (**A**) have a diameter of up to 1 μm, while diameters of granules in (**B**) are between 0.1 – 0.5 μm. M, mitochondria. EM preparations were performed with help and support of B. Agricola, University of Marburg. Magnification of images, 1:7500.

6.2 Stimulation of Differentiation of AR42J Cells by Altered Growth Conditions

We next analyzed cellular growth, morphology and mitotic index of AR42J cells cultured in DMEM and PaM with and without dexamethasone. Cellular growth rates under the different experimental conditions were determined by cell counting over a period of 7 days. AR42J cells grown in DMEM or PaM in the absence of dexamethasone exhibited a similar growth pattern: after a phase of adaptation, cell numbers started to increased after approximately 72 hours reaching a maximum after 144 hours (Figure 34). However, cells grown in DMEM showed slightly higher growth rates compared to PaM. In contrast, cells grown in DMEM or PaM in the presence of dexamethasone showed only a slight increase in cell number due to their differentiation into acinar-like cells (Figure 34). In line with this, the mitotic index of DMEM grown control cells was slightly higher than the one of PaM grown controls (Figure 34, Pam-D). In contrast, the mitotic index of dexamethasone-induced cells was reduced to around 1% in both DMEM and PaM indicating differentiation of the cultures.

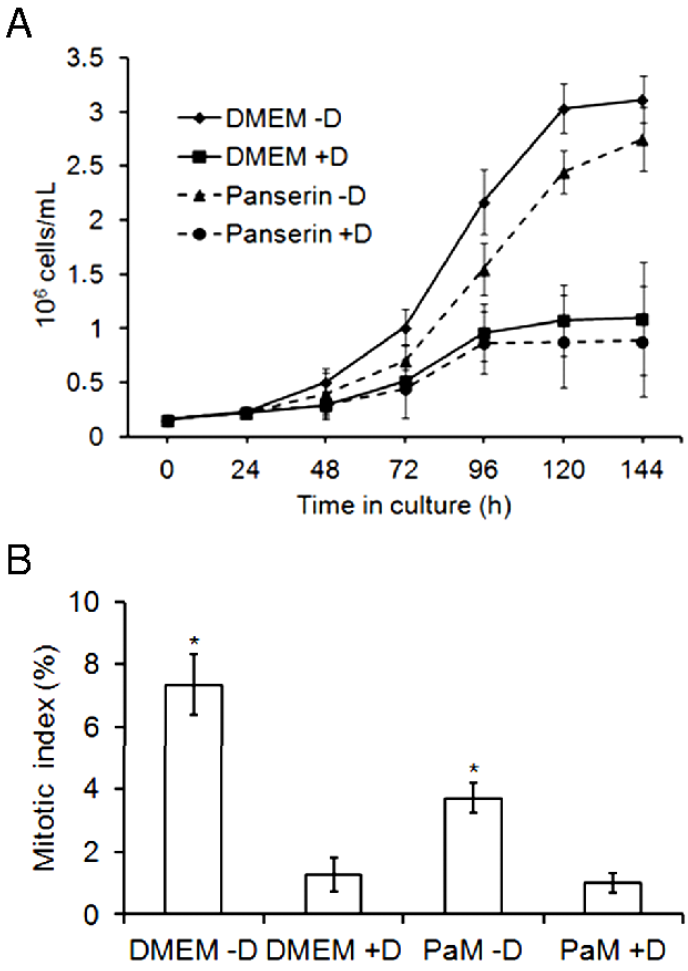

Figure 34: Growth rates and mitotic index of AR42J cells under different experimental conditions.

In (**A**) the cellular growth rates of AR42J cells cultured under different conditions (DMEM and Panserin, induced for ZG formation with dexamethasone (+D) and untreated controls (-D)) were determined by cell counting over a period of 144 h. In (**B**) the mitotic index of AR42J cells was determined after 72 h. The results of the quantitative analysis presented originate from 3-4 independent experiments and are presented as means ± S.D. (*p<0.01).

Interestingly, differentiation into acinar-like cells in the presence of dexamethasone was accompanied by alterations of cell morphology. Whereas in the absence of dexamethasone the majority of the cells grown in DMEM or PaM exhibited a spindle-like morphology, treatment with dexamethasone resulted in a prominent increase in cell size and establishment of a hexagonal, cobble-stone-like morphology (Figure 35). Cells grown in PaM plus dexamethasone appeared to be larger than the ones grown in DMEM plus dexamethasone. Furthermore, a higher percentage of apoptotic cells was observed in PaM after 72 hours of dexamethasone-stimulation. Taken together, these observations support the notion that PaM (plus dexamethasone) exerts a stronger stimulatory effect on the differentiation of AR42J cells into exocrine, acinar-like cells than stimulation in DMEM.

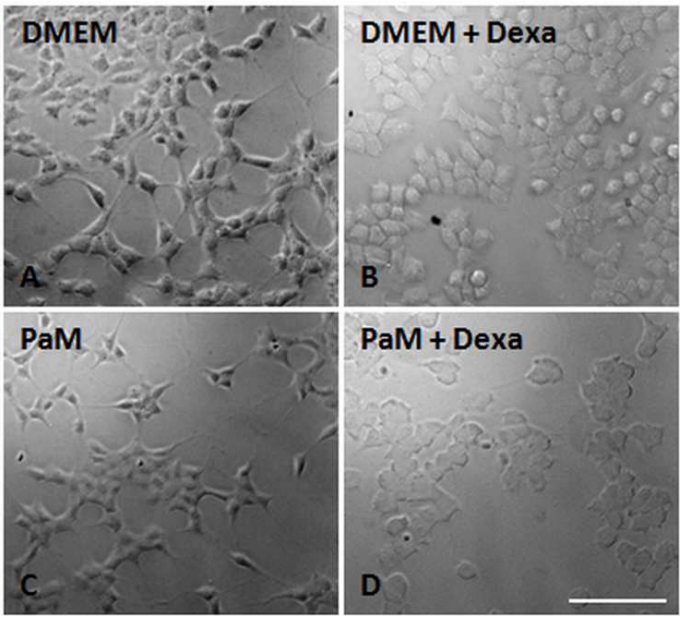

Figure 35: Alterations of AR42J cell morphology under different culture conditions.
AR42J cells were cultured under different conditions and examined by phase contrast after 72 h. Cells exhibit in the absence of dexamethasone in DMEM and PaM a spindle-like morphology (**A**, **C**). A treatment with dexamethasone resulted in a prominent increase in cell size and establishment of a hexagonal morphology (**B**, **D**). Additionally, cells grown in PaM + Dexa appeared to be larger than in DMEM +Dexa and revealed a more cobble-stone-like morphology. Scale bar 100 μm.

6.3 Enhanced Expression of ZG Membrane Proteins by Altered Growth Conditions

To investigate whether the enhanced differentiation and granule formation of AR42J cells in PaM medium was as well accompanied by an increase in the expression levels of ZG granule constituents, we performed RT-PCR and immunoblotting experiments (Figure 36). We first analyzed the mRNA expression levels of ZG markers by RT-PCR in AR42J cells grown in DMEM or PaM in the absence and presence of dexamethasone (Figure 36). The administration of dexamethasone induced the mRNA levels of typical digestive enzymes such as amylase or carboxypeptidase A in both DMEM and PaM in the presence of dexamethasone. mRNA levels were low or undetectable in the absence of dexamethasone in DMEM, but slightly increased in PaM. Interestingly, the mRNA levels of membrane markers appeared to be higher in PaM plus dexamethasone than in DMEM plus dexamethasone. The mRNA level of ZG16p, a membrane-associated secretory lectin supposed to be involved in protein sorting/membrane attachment was prominently increased in PaM (plus dexamethasone). Interestingly, the mRNA for GP2, a major GPI-anchored membrane glycoprotein, was induced in PaM (plus dexamethasone), whereas it was absent in DMEM (plus dexamethasone). The latter is consistent with published results indicating that AR42J cells do not express high levels of GP2 after dexamethasone-stimulation (Yu, Michie et al. 2004). GAPDH served as a loading control. These data indicate that cultivation of AR42J cells in PaM plus dexamethasone can be of advantage for the expression of ZG membrane and membrane-associated proteins.

The RT-PCR data were partially confirmed by immunoblotting analysis of AR42J cell lysates (Figure 36). The digestive enzymes amylase and carboxypeptidase A showed comparable protein expression levels in both DMEM and PaM in the presence of dexamethasone. Furthermore, ZG16p protein levels were slightly more increased in PaM plus dexamethasone than in DMEM plus dexamethasone. However, GP2 was barely detectable on the protein level in both PaM and

DMEM (plus dexamethasone) indicating that it is of low abundance in cell lysates. Actin served as a loading control.

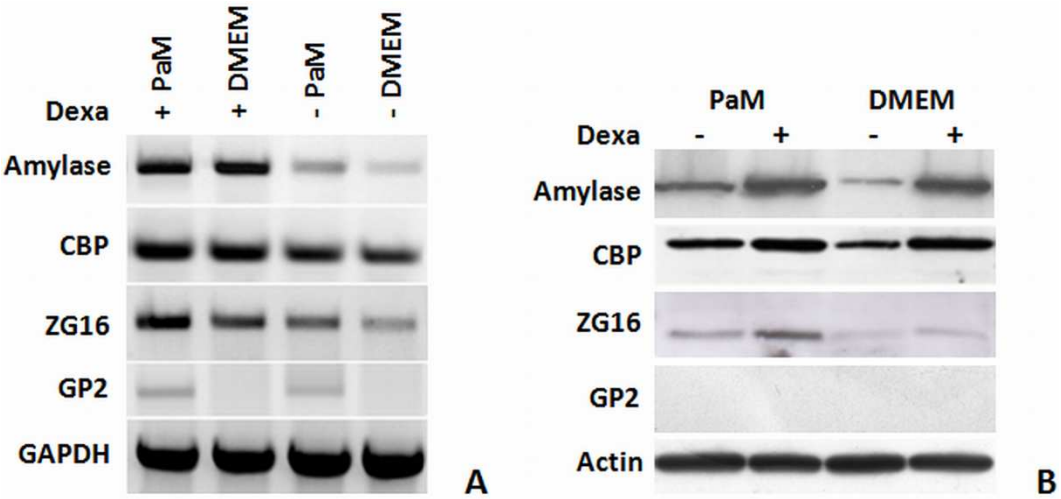

Figure 36: Expression of ZG constituents in AR42J cells under the different experimental conditions on transcription and translational level.

(**A**) For RT-PCR, total RNA was extracted from AR42J cells after 48 h cultured under four different culture conditions (see Figure 34). Total mRNA was transcribed into cDNA (3.5.1-3.5.3). Equal amounts of cDNA (150 ng) were used for a 50 μL semi-quantitative-RT-PCR with species specific primers for amylase, carboxypeptidase, ZG16 and GP2. GAPDH served as loading control. (**B**) for immunoblot analysis, equal amounts of cell lysates (20 μg) from differentially cultured AR42J cells were run on 12.5% polyacrylamide gels, blotted onto nitrocellulose and incubated with antibodies directed to amylase, carboxypeptidase A, ZG16p and GP2. An antibody to actin served as loading control.

6.4 Expression of ZG Proteins is not Sufficient to Induce Granule Formation in AR42J Cells

We assumed that an increased expression of ZG proteins as observed *e.g.* after glucocorticoid-stimulation of AR42J cells in PaM may be responsible for an increase in ZG formation and in ZG size. To test this hypothesis, we generated expression constructs encoding for amylase-YFP, trypsinogen-YFP, carboxypeptidase-Myc, GP2, and Myc-ZG16p under control of a CMV promoter (3.5.5). To examine if the exogenously expressed ZG proteins were properly sorted to ZG granules, AR42J cells were transfected by electroporation with the constructs generated and stimulated for granule formation in DMEM by adding dexamethasone. After 2-3 days, cells were processed for indirect immunofluorescence. For colocalisation studies antibodies directed to carboxypeptidase A, chymotrypsinogen, GP2 or the Myc-epitope were used (Figure 37).

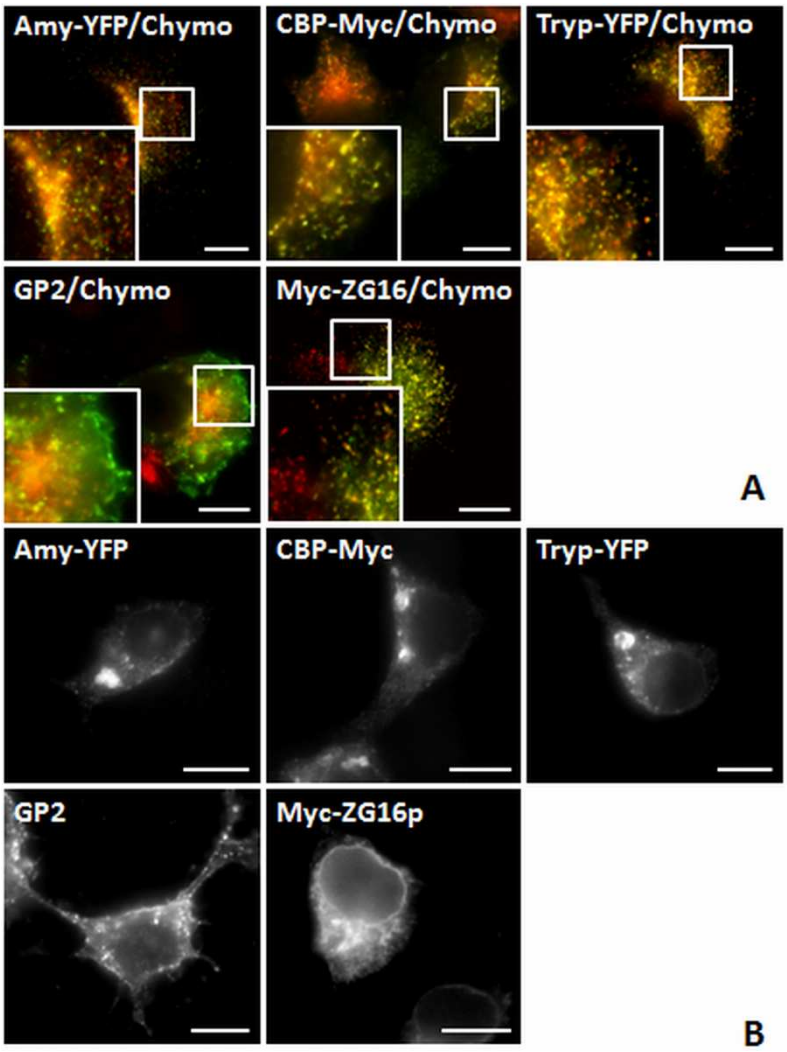

Figure 37: The expression of ZG constituents in AR42J cells does not induce or alter ZG formation.

AR42J cells transfected by electroporation with generated constructs (amylase-YFP, trypsinogen-YFP, carboxypeptidase-Myc, GP2 and Myc-ZG16p) were stimulated for granule formation in DMEM by adding dexamethasone and served as controls for the correct targeting of transfected constructs into ZG (**A**). (**B**) Represents transfected but unstimulated cells. After 2-3 days, cells were processed for indirect immunofluorescence. For colocalisation studies antibodies directed to, Chymotrypsinogen (Chymo), GP2 or the Myc-epitope were used. Images were acquired on an Olympus IX81 fluorescence microscope. Scale bars, 10 μm.

All exogenously expressed ZG proteins were observed to enter the secretory pathway in stimulated AR42J cells and were properly sorted to ZG as indicated by colocalization with appropriate ZG marker proteins (Figure 37 A). Furthermore, the ZG membrane protein GP2 exhibited a strong targeting to the plasma membrane (Figure 37). Next, we investigated whether the exogenous expression of the ZG proteins was sufficient to induce granule formation in AR42J cells in the absence of dexamethasone (Figure 37 B). The ZG content proteins amylase, trypsinogen and carboxypeptidase were detected in the Golgi apparatus, the ZG membrane associated protein ZG16p was detected in the ER of AR42J cells and the ZG membrane protein GP2 was detected at the plasma membrane, but the formation of typical granules (as seen in Figure 37 A) was not observed. Similar results were obtained when two different ZG marker proteins were co-expressed. Neither the co-expression of regulated secretory proteins (amylase, trypsinogen, and carboxypeptidase) nor the co-expression of ZG membrane proteins (ZG16p, GP2) or a combination of both resulted in the generation of ZG granules (Table 6-1). These results indicate that the overexpression of one or two ZG proteins in AR42J cells is not sufficient to induce granule formation.

Table 6-1 Combination of tested double transfections with ZG proteins in AR42J and COS-7 cells

Double transfection with		Localisation/ZG formation in AR42J		ZG like structures in
		No Dexa	10 nM Dexa	COS-7/Localisation
ZGC + ZGC	Amy-YFP/CBP-Myc	Golgi	ZG, no changes	No, ER/Golgi
	Tryp-YFP/CBP-Myc	Golgi	ZG, no changes	No, ER/Golgi
ZGC + ZGM	Amy-YFP/Myc-ZG16p	Golgi/ER	ZG, no changes	No, ER/Golgi
	CBP/Myc-ZG16p			No, ER/Golgi
	Tryp-YFP/Myc-ZG16p	Golgi/ER	ZG, no changes	No, ER/Golgi
	Amy-YFP/GP2	Golgi/Memb.	ZG/Memb., no changes	No, ER/Golgi/Memb.
	CBP-Myc/GP2			No, ER/Golgi/Memb.
	Tryp-YFP/GP2	Golgi/Memb.	ZG/Memb., no changes	No, ER/Golgi/Memb.
ZGM + ZGM	Myc-ZG16p/GP2	ER/Memb.	ZG/Memb., no changes	No, ER/Golgi/Memb.

The combinations CBP/Myc-ZG16p and CBP-Myc/GP2 could not be tested in AR42J cells due to their endogenous expression of carboxypeptidase and the available antibodies. The shortcut Memb. stands for plasma membrane.

6.5 Expression of ZG Proteins is not Sufficient to Generate Granule-Like Structures in Constitutively Secreting COS-7 Cells

As it has been demonstrated that the overexpression of (neuro)endocrine regulated cargo proteins in non-endocrine, constitutively secreting cells (*e.g.* COS-1, COS-7, NIH-3T3) is sufficient to initiate the formation of granule-like structures (Kim, Tao-Cheng et al. 2001; Huh, Jeon et al. 2003; Beuret, Stettler et al. 2004; Inomoto, Umemura et al. 2007; Stettler, Beuret et al. 2009), we as well overexpressed the exocrine ZG marker proteins in COS-7 cells, which lack a regulated secretory pathway. COS-7 cells were transfected by electroporation (3.6.3.2) with the constructs generated (3.3, 3.4, 3.5.5) and processed for immunofluorescence (3.7.1) after 24-72 hours. All exogenously expressed ZG proteins were found to label the ER and Golgi, which is typical for secretory proteins whose rate-limiting step in secretion is folding within and exit from the ER. However, no additional staining of granule-like structures or protein accumulations in post-Golgi organelles were observed as described after expression of neuroendocrine cargo proteins (Beuret, Stettler et al. 2004; Inomoto, Umemura et al. 2007; Stettler, Beuret et al. 2009). Even ZG16p, a secretory lectin supposed to act as a linker or helper protein in ZG granule sorting/formation, localised to the ER and did not induce granule-like structures (Figure 38). The ZG membrane protein GP2 was targeted to the plasma membrane due to its GPI anchor, besides the staining of the Golgi (Figure 38). Similar results were obtained when two ZG proteins were co-expressed (Table 6-1). These findings indicate that the ZG proteins tested do not possess the intrinsic information to induce the formation of granule-like structures in constitutively secreting COS-7 cells. Interestingly, this is in contrast to (neuro)endocrine cargo proteins (Beuret, Stettler et al. 2004; Inomoto, Umemura et al. 2007; Stettler, Beuret et al. 2009).

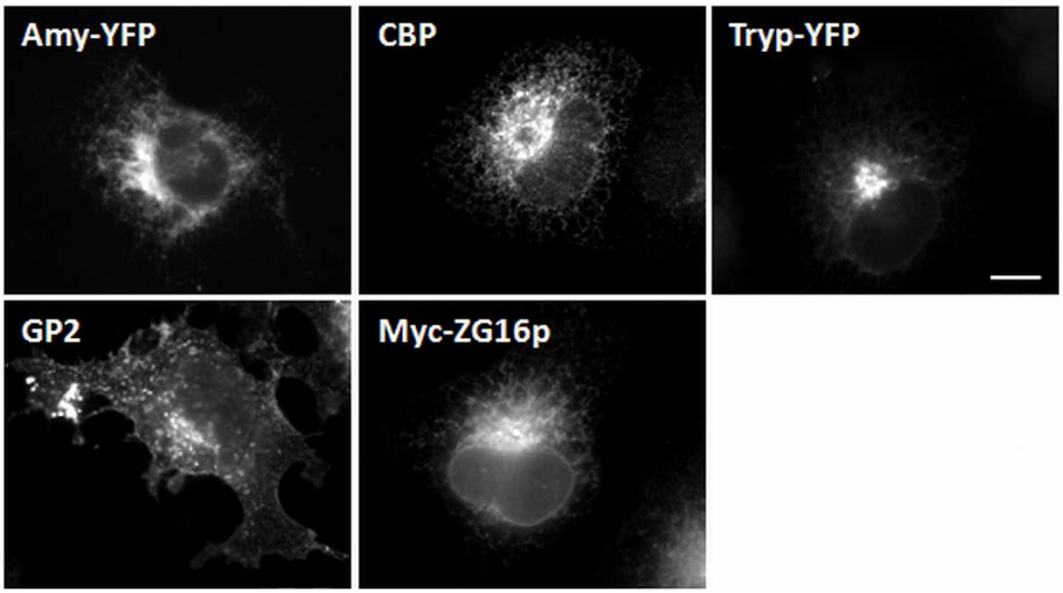

Figure 38: Expression of ZG proteins in constitutively secreting COS-7 cells.

COS-7 cells were transfected by electroporation with the following constructs: amylase-YFP, trypsinogen-YFP, carboxypeptidase, GP2 and Myc-ZG16p. After 24-72 h cells were processed for immunofluorescence using antibodies to carboryxpepetidase A, GP2 and ZG16. Images were acquired on an Olympus IX81 fluorescence microscope. Scale bar, 10 μm.

6.6 Discussion

In this study we demonstrate that granule formation in pancreatic AR42J cells can be modulated by growth conditions in cell culture. We show that cultivation of AR42J cells in Panserin 401, a serum-free medium (PaM), which includes trace elements, albumin, cholesterol, soya lipids and vitamins, but no growth or attachment factors or any insulin, promotes the induction of granule formation, the expression of ZG proteins and an increase in granule size compared to serum-containing conditions in DMEM, especially when granule-formation is stimulated by the addition of the synthetic glucocorticoid dexamethasone. These findings are important for the study of granule formation and biogenesis in AR42J cells, as available pancreatic exocrine cell models that are as well accessible to molecular manipulations are scarce.

Our data indicate that the enhanced granule formation (including granule size and protein expression) in PaM is based on its stronger stimulatory effect on the differentiation of AR42J cells towards an exocrine phenotype. Enhanced differentiation is reflected by the reduced growth rates of AR42J cells in PaM compared to DMEM, a reduction of the mitotic index, a slight increase in apoptotic cells and alterations of cell morphology including an increase in cell size and development of a hexagonal, cobble-stone-like morphology. Interestingly, secretory granules comparable in size to those of the rat exocrine pancreas are observed in PaM plus dexamethasone, whereas in DMEM plus dexamethasone they are usually smaller in size. Furthermore, in PaM the expression of ZG proteins (*e.g.* ZG16p) is increased both on the mRNA

and the protein level. Some of the proteins (*e.g.* GP-2) are absent or only weakly expressed in DMEM.

Treatment with glucocorticoids has long been shown to increase the expression of amylase in AR42J cells (Logsdon, Moessner et al. 1985), as well as ZG membrane proteins such as the SNARE proteins syntaxin-3 (Pevsner, Hsu et al. 1994; Gaisano, Huang et al. 1999), syntaxin-2 or syntaxin-4, whereas VAMP-3 and syncollin remained undetectable (Gaisano, Huang et al. 1999; Hodel and Edwardson 2000). In their induced exocrine state, AR42J cells upregulate as well the pancreatitis-associated protein 1 (PAP-1) (Lim, Song et al. 2009). Moreover, AR42J cells have the potential to differentiate into endocrine, insulin-producing cells after treatment with activin or hepatocyte growth factor (Mashima, Ohnishi et al. 1996; Mashima, Shibata et al. 1996). The AR42J-B13 clone appeared to be more susceptible to endocrine differentiation than the parent AR42J line. The differentiation capacity of AR42J cells is further underlined by their transdifferentiation into hepatocytes through long-term treatment with dexamethasone (Shen, Slack et al. 2000). This conversion is associated with the induction of the transcription factor C/EBPβ. The hepatocytes produced by the AR42J model exhibit many of the properties of true hepatocytes, expressing a range of markers including albumin, glucose-6-phosphatase, transferrin, transthyretin and the enzymes for Phase I and II detoxification (Shen, Horb et al. 2003; Shen, Burke et al. 2004). Furthermore, a transient loss of constitutive WNT3a expression, phosphorylation and depletion of β-catenin were observed before changes into the hepatocyte-like (B-13/H) cells became visible (Wallace, Marek et al. 2010).

The molecular mechanisms of ZG biogenesis and sorting of zymogens in the acinar cells of the exocrine pancreas are still incompletely understood (Kleene, Dartsch et al. 1999; Kleene, Kastner et al. 1999; Dikeakos and Reudelhuber 2007; Gomez-Lazaro, Rinn et al. 2010). It is also unclear how the size and the shape of the relatively large ZG (up to 1 μm in diameter) is regulated and maintained. Granule size might be determined by the amount of aggregated cargo proteins packaged into ZG, by the removal of non-regulated cargo proteins and membrane (constitutive-like secretion) (Arvan and Castle 1987), by granule-granule fusion during maturation (Hammel, Lagunoff et al. 2010), and by components of the granule membrane itself, *e.g.* by scaffold proteins of a submembranous matrix which contributes to granule size, stability and sorting (Schrader 2004) (Introduction 1.3). Secretory granule biogenesis in neuroendocrine cells is better understood and in contrast to exocrine ZG biogenesis, potential sorting receptors and sorting signals have been identified (*e.g.* carboxypeptidase E, secretogranin III) (Kim, Gondre-Lewis et al. 2006; Dikeakos and Reudelhuber 2007; Park, Koshimizu et al. 2009; Hosaka and Watanabe 2010; Koshimizu, Kim et al. 2010). It has also been shown that granulogenic proteins such as granins (e.g. the chromogranins A and B, secretogranin II) and prohormones/proneuropeptides (*e.g.* pro-opiomelanocortin, pro-vasopressin, pro-oxytoxin) are able to induce dense-core granule-like structures in various non-endocrine cell lines when overexpressed (Kim, Tao-Cheng et al. 2001; Huh, Jeon et al. 2003; Beuret, Stettler et al. 2004; Stettler, Beuret et al. 2009). In contrast to neuroendocrine cargo proteins, the expression of prominent ZG cargo and membrane proteins (*e.g.* amylase, procarboxypeptidase A, trypsinogen, ZG16p, GP2) alone or in combination was not sufficient to induce granule-like structures in constitutively secreting COS-7 cells. The GPI-anchored major ZG membrane protein GP2 has been found to associate with amylase and other secretory proteins in vitro, suggesting a potential role in cargo packaging or sorting (Jacob, Laine

et al. 1992; Leblond, Viau et al. 1993; Colomer, Lal et al. 1994). Furthermore, GP2 associates with the secretory lectin ZG16p and syncollin in lipid rafts and has been proposed to contribute to the formation of a submembranous matrix that functions in ZG formation and packaging (Schmidt, Schrader et al. 2001; Kalus, Hodel et al. 2002; Schrader 2004). In addition, the secretory lectin ZG16p has been suggested to act as a linker protein between aggregated ZG cargo proteins and the granule membrane/submembranous matrix (Kleene, Dartsch et al. 1999). However, these ZG proteins mainly localized to the ER or the plasma membrane in COS-7 cells. In addition, enhanced expression or co-expression of these ZG proteins in AR42J cells not stimulated for differentiation by dexamethasone was insufficient to induce granule formation. In contrast to COS-7 cells, AR42J cells possess a regulated secretion machinery. Apparently, none of the ZG cargo or membrane proteins tested was able to trigger granule formation or the formation of granule-like structures in the absence or the background of a regulated secretion machinery. However, all ZG proteins tested were properly targeted to ZG in dexamethasone-stimulated AR42J cells. Similar observations were made for GP2 after adenovirus infection of AR42J cells (Yu, Michie et al. 2004). Our findings indicate that in contrast to neuroendocrine secretion (Introduction 1.5) additional components are likely to be required for proper initiation of ZG formation. These components might include helper proteins for cargo aggregation or additional membrane components. Thus, ZG biogenesis in the exocrine pancreas is likely to require a more complex machinery, which has to ensure the packaging of a complex mixture of cargo proteins in large transport containers. We propose that an exocrine gene expression programme for the regulated secretion machinery has to be activated in pancreatic acinar cells, as exemplified by dexamethasone-treatment of AR42J cells, and that multiple components besides cargo proteins are required to perform the initial stages of exocrine granule formation.

Chapter 7 Summary and Final Conclusions

Regulated secretion is a complex and fundamental biological process through which cellular products (*e.g.* digestive enzymes, hormones and neurotransmitter) are released into the extracellular space. Digestive enzymes are synthesized, sorted and secreted by the acinar cells of the exocrine pancreas. Packed and stored in ZG at the apical plasma membrane, the enzymes are secreted into the pancreatic duct system upon a hormonal stimulus (regulated srecretion). ZG are formed at the TGN via the aggregation of zymogens in an acidic milieu, but little is known about the specific interactions of the zymogen aggregates with the TGN/ZG membranes. Under discussion are lipid microdomains and a submembranous matrix mainly consisting of a proteoglycan scaffold. A some clinical disorders derive from malfunction or interruption of this processes which can be caused by mutations leading to problems in sorting and interaction of proteins and mostly ending up in an inflammatory process known as pancreatitis.

Organeller subfractionation, combined with various gel and non-gel based methods, followed by proteomis analysis of ZG´s, helped to increase the number of ZG membrane and membrane associated constituents. Many of these new ZGM and peripheral proteins could have functions in ZG biogenesis, regulated secretion, or even after secretion into the intestinal tract in host defence. In addition, many of these proteins were found in other cells and subcellular compartments, possibly executing a similar function, which indicates a multitasking of proteins, *e.g.* in the neuroendocrine secretion system of synaptic vesicles.

One aim of my thesis was to enrich proteins of the ZG matrix (ZGWash fraction) and ZGM, by a subfractionation approach, and to identify new ZGM and ZGWash constituents using different gel electrophoretic and off-gell approches. These include 1D and 2D-SDS PAGE and liquid chromatography combinend with tryptic digestion and mass spectroscopy. Further, emphasis was put on the identification of hydrophobic, high-molecular weight (HMW) and proteoglycan binding proteins, as well as proteins identified by proteomics studies in the neuroendocrine secretion system of synaptice vesicles. Especially for the last mentioned candidates, this included a thorough literatur analysis, defining the overlap of proteins identified by proteomics studies in SV and ZG. Afterwards, the new peripheral and ZGM constituents were confirmed, localized and also characterize by immunoblotting, immunofluorescence and cell culture studies. This should help to provide new insights in their possible functions in ZG biogenesis, sorting and packaging and regulated secretion. Proteins selected for further confirmation were the proteoglycan binding protein Chymase, the HMW proteins Piccolo and Synatpojanin-1, the heparan binding protein APP, and the heparin binding ZGWash protein ZG16p which was identified in a reciprocal approach in rat brain lysate. All of them revealed low abundance in the fraction in which they were identified and were either new, or a clear confirmation was missing.

As a novel result, Chymase could be confirmed to be part of the submembranous matrix of ZG by immunoblot experiments showing a very similar distribution like ZG16p, a protein known to be part of the ZG matrix. Chymase is not endogenously expressed in AR42J cells but, overexpression experiments with a Chymase-YFP fusion protein revealed a proper targeting to ZG in AR42J cells induced for ZG formation. By electron microscopic analysis it was demonstrated that the endogenously expressed protein locates to ZG and in comparison to mast cell granules Chymase exhibited low abundance. Chymase has a proteoglycan binding capacity and is likely to

act as a serine protease after ZG secretion. Its capability to cleave proteins of the extracellular matrix (*e.g*. fibronectin), might be a reason for its low and regulated abundance in ZGs. Piccolo and Synaptojanin-1 are both members of the cytoplasmic active zone (CAZ) and were identified by LC-MS/MS analysis in the ZGWash fraction. While the work on Piccolo is temporally intermitted, it could be demonstrated, by immunoblot and immunofluorescence experiments, that Snj-1 is not a ZG constituent. APP, a multifunctional glycoprotein involved in many neuronal processes, was subsequently identified twice in the ZGM by proteomics studies (Rindler, Xu et al. 2007; Chen and Andrews 2008). By immunoblot analysis, APP was detected in AR42J cell lysates but not in ZG or corresponding subfractions. In Immunofluorescence analysis, the endogenous APP could not be detected, probably due to a incompatibility with of our protocol with the applied antibody. By overexpression experiments with the APP-GFP fusion protein in AR42J cells induced for ZG formation, the protein revealed a cytosolic staining but also colocalized in parts with the Golgi, lysosomal and ZG markers. The best colocalisation value was obtained for the ZG. As a membrane anchored receptor, APP could play a role during the exocytosis of ZG. Besides, it does not only function as a membrane-anchored receptor-like molecule, but also as a secreted derivative that acts upon other cells, as which it could use ZG as a transport vesicle.

The secretory lectin ZG16p, a well-known ZGM associated protein, was identified in a rat brain lysate by a 1D-SDS PAGE approach, followed by proteomics analysis. In subsequent RT-PCR analysis, its presence in rat brain could be confirmed by sequencing. Furthermore, a higher mRNA expression level appeared in rat cortex and the maximum was measured in cerebellum. In the rat hippocampus and hypothalamus a very weak expression was detected. By immunoblot analysis, the protein appeared to be enriched in a SV fraction. Due to problems in immunofluorescence (IMF) with the antibody staining of ZG16p in neuronal culture, different protocols for hidden antigens were tested and a strong improvement was observed by exchanging Triton X-100 against SDS. In subsequent IMF analysis of rat primary culture, ZG16p colocalized best with the RNA granule marker hRnp and at the post-synaptic marker PSD95. In brain, ZG16p can be involved in processes such as the sorting, packaging and maturation of synaptic vesicles, or RNA granules. Since it colocalized with the post synaptic marker PSD95, it might as well have a function after being released into the intracellular space, *e.g.* in immune defense by binding to pathogens or in wound healing processes (tissue regeneration). Additionally, ZG16p was found in human liver and downregulated in hepatocarcinoma, thus suggesting medically relevant functions. However, the proteins exact functions in the exocrine pancreas, brain and liver remain unclear and will be subject of future studies. ZG16p might be the right tool to obtain new insights into the similarity of exocrine and neuroendocrine secretion and apical targeting.

The results obtained by proteomics approaches revealed that the increasing sensitivity of proteomics methods does not only lead to the discovery of more and new ZG constituents, but also leads to a higher possibility of detecting contaminants caused by the method of tissue homogenisation, isolation of ZG and corresponding subfractions. For that reason, it is absolutly necessary to confirm mass spectroscopic results with further methods such as immunoblotting, immunofluorescence, knock-down, overexpression experiment and others. In addition, a thorough investigation of their biological functions is required.

Part of the last objective was to modulate and investigate ZG formation under different culture conditions. It was demonstrated that the granule formation, by culturing in the serum free

medium Panserin is slightly increased in AR42J cells not stimulated for ZG formation. In stimulated cells, granules appeared bigger and the expression of typical granules proteins was upregulated. Unraveling the role and importance of the expression of ZG proteins in ZG biogenesis and formation was the last addressed point. The overexpression of content (Amylase, Carboxypeptidase and Trypsinogen), matrix (ZG16p) and membrane (GP2) proteins in untreated AR42J cells and in constitutively secreting COS-7 cells, alone or in combination, showed that these proteins are not sufficient to initiate granule formation in AR42J cells and also not to activate an eventually existing secretion machinery in COS-7 cells. In both cell types content and matrix proteins accumulated in the ER and Golgi, while GP2 was distributed to the plasma membrane. Furthermore, no alterations in granule morphology, or number were observed in dexamethasone-stimulated AR42J cells, after overexpression of the upper mentioned ZG proteins alone or in any combination.

These findings indicate that in contrast to neuroendocrine secretion, additional components are likely to be required for proper initiation of ZG formation. These components might include helper proteins for cargo aggregation or additional membrane components. Thus, ZG biogenesis in the exocrine pancreas is likely to require a more complex machinery, which has to ensure the packaging of a complex mixture of cargo proteins in large transport containers.

Chapter 8 Future Perspectives

Besides the new insights this work provided into the composition of the ZG matrix, a number of new questions has raised. Since the components of the ZGM and the submembranous matrix (ZGWash fraction) might play important roles in the biogenesis of ZG, sorting and packing of zymogens, they are also important for the understanding and treatment of pathophysiological processes such as pancreatitis. In this context, future studies will be aimed at the further identification of ZG membrane and Wash proteins (matrix components), by proteomics approaches, and already identified new or low abundant proteins will be futher characterised by immunofluorescence and immunoelectron microscopy for intracellular localisation. Immuno pull down exeriments and siRNA knockdown studies *e.g.* with APP in AR42J cells and for ZG16p also in neuronal primary culture will help to elucidate their function and maybe also reveal further unkown ZG components. Additionally, the strong membrane association of some ZG content proteins strengthens the hypothesis of the submembranous matrix and its role in ZG formation.

For this purpose, Chymase, ZG16p and APP expressed as recombinant wild type and mutated proteins, could be used for binding assays in which their affinity to specific proteoglycans should be identified. Moreover, by cloning a tagged version of the membrane integrated part for APP, it would be possible to determine in which types of membranes APP is integrated. In addition, using specific IMF techniques (differentiated permeabilisation *e.g.* with digitonin), the exact location of the protein (if on the luminal or cytosolic side) could be determined.

Uptake experiments, with purified proteins, followed by life cell imaging for observing their pathway throughout the cell could be performed. Transcription regulation in AR42J cells stimulated for ZG formation and controls could help to determine if the expression levels are in anyway depending on the cells state of differentiation.

The expression of mutant versions of ZG16p, in which the sugar-binding motif will be altered, will help to define ZG16p's sugar binding specificity in combination with frontal affinity chromatography. By silencing of ZG16p in primary neuronal culture (or expression of ZG16p mutants), ZG16p's relevance for synaptic vesicle formation, sorting/trafficking of cargo, or acquisition of polarity (such as dendrite/axon) and synapse formation (by morphological, biochemical studies) will be evaluated. The parallel knockdown studies in pancreatic AR42J cells and primary neuronal cultures will help to elucidate putative common principles in exocrine and neuroendocrine secretion. In another approach ZG16p´s relevance in immune defence could be addressed by testing its binding ability to pathogens coming from bacteria or to bacteria itself.

References

Adler, G., G. Rohr, et al. (1982). "Alteration of membrane fusion as a cause of acute pancreatitis in the rat." *Digestive Diseases and Sciences* 27(11): 993-1002.

Ahras, M., G. P. Otto, et al. (2006). "Synaptotagmin IV is necessary for the maturation of secretory granules in PC12 cells." *The Journal of Cell Biology* 173(2): 241-251.

Altschul, S. F., T. L. Madden, et al. (1997). "Gapped BLAST and PSI-BLAST: a new generation of protein database search programs." *Nucleic Acids Research* 25(17): 3389-3402.

Altschul, S. F., J. C. Wootton, et al. (2005). "Protein database searches using compositionally adjusted substitution matrices." *The FEBS Journal* 272(20): 5101-5109.

Arvan, P. and D. Castle (1998). "Sorting and storage during secretory granule biogenesis: looking backward and looking forward." *The Biochemical Journal* 332: 593-610.

Arvan, P. and J. D. Castle (1987). "Phasic release of newly synthesized secretory proteins in the unstimulated rat exocrine pancreas." *The Journal of Cell Biology* 104(2): 243-252.

Bach, J. P., H. Borta, et al. (2006). "The secretory granule protein syncollin localizes to HL-60 cells and neutrophils." *The Journal of Histochemistry and Cytochemistry* 54(8): 877-888.

Barclay, J. W., A. Morgan, et al. (2005). "Calcium-dependent regulation of exocytosis." *Cell Calcium* 38(3-4): 343-353.

Barondes, S. H. (1988). "Bifunctional properties of lectins: lectins redefined." *Trends in Biochemical Sciences* 13(12): 480-482.

Barthel, A., W. Nickel, et al. (1995). "Sorting and budding of constitutive secretory vesicles in hepatocytes and hepatoma cells." *Advances in Enzyme Regulation* 35: 283-292.

Bates, J. M., H. M. Raffi, et al. (2004). "Tamm-Horsfall protein knockout mice are more prone to urinary tract infection: rapid communication." *Kidney International* 65(3): 791-797.

Bedoyan, J. K., R. A. Kumar, et al. (2010). "Duplication 16p11.2 in a child with infantile seizure disorder." *American Journal of Medical Genetics.* 152A(6): 1567-1574.

Berkane, A. A., H. T. Nguyen, et al. (2007). "Proteomic of lipid rafts in the exocrine pancreas from diet-induced obese rats." *Biochemical and Biophysical Research Communications* 355(3): 813-819.

Beuret, N., H. Stettler, et al. (2004). "Expression of regulated secretory proteins is sufficient to generate granule-like structures in constitutively secreting cells." *The Journal of Biological Chemistry* 279(19): 20242-20249.

Borgonovo, B., J. Ouwendijk, et al. (2006). "Biogenesis of secretory granules." *Current Opinion in Cell Biology* 18(4): 365-370.

Borta, H., M. Aroso, et al. (2010). "Analysis of low abundance membrane-associated proteins from rat pancreatic zymogen granules." *Journal of Proteome Research* 9(10): 4927-4939.

Boulatnikov, I. and R. C. De Lisle (2004). "Binding of the Golgi sorting receptor muclin to pancreatic zymogens through sulfated O-linked oligosaccharides." *The Journal of Biological Chemistry* 279(39): 40918-40926.

Bradford, M. M. (1976). "A rapid and sensitive method for the quantitation of microgram quantities of protein utilizing the principle of protein-dye binding." *Analytical Biochemistry* 72: 248-254.

Braulke, T. and J. S. Bonifacino (2009). "Sorting of lysosomal proteins." *Biochimica et Biophysica Acta* 1793(4): 605-614.

Braun, M. and F. Thevenod (2000). "Photoaffinity labeling and purification of ZG-16p, a high-affinity dihydropyridine binding protein of rat pancreatic zymogen granule membranes that regulates a K(+)-selective conductance." *Molecular Pharmacology* 57(2): 308-316.

Brion, C., S. G. Miller, et al. (1992). "Regulated and constitutive secretion. Differential effects of protein synthesis arrest on transport of glycosaminoglycan chains to the two secretory pathways." *The Journal of Biological Chemistry* 267(3): 1477-1483.

Brouillet, E., A. Trembleau, et al. (1999). "The amyloid precursor protein interacts with Go heterotrimeric protein within a cell compartment specialized in signal transduction." *The Journal of Neuroscience* 19(5): 1717-1727.

Burgoyne, R. D. and A. Morgan (2007). "Membrane trafficking: three steps to fusion." *Current Biology* 17(7): R255-258.

Burre, J., T. Beckhaus, et al. (2006). "Analysis of the synaptic vesicle proteome using three gel-based protein separation techniques." *Proteomics* 6(23): 6250-6262.

Burre, J. and W. Volknandt (2007). "The synaptic vesicle proteome." *Journal of Neurochemistry* 101(6): 1448-1462.

Butterfield, D. A. and J. B. Owen (2011). "Lectin-affinity chromatography brain glycoproteomics and Alzheimer disease: insights into protein alterations consistent with the pathology and progression of this dementing disorder." *Proteomics. Clinical Applications* 5(1-2): 50-56.

Cabana, C., J. S. Hugon, et al. (1981). "Freeze-fracture and deep-etching studies on zymogen-granule membranes of the rat pancreas." *Cell and Tissue Research* 214(2): 355-367.

Castle, D. and A. Castle (1998). "Intracellular transport and secretion of salivary proteins." *Critical Reviews in Oral Biology and Medicine* 9(1): 4-22.

Castle, J. D. (1990). "Sorting and secretory pathways in exocrine cells." *American Journal of Respiratory Cell and Molecular Biology* 2(2): 119-126.

Chanat, E. and W. B. Huttner (1991). "Milieu-induced, selective aggregation of regulated secretory proteins in the trans-Golgi network." *The Journal of Cell Biology* 115(6): 1505-1519.

Chanat, E., U. Weiss, et al. (1993). "Reduction of the disulfide bond of chromogranin B (secretogranin I) in the trans-Golgi network causes its missorting to the constitutive secretory pathways." *The EMBO Journal* 12(5): 2159-2168.

Chen, C. Y., U. Cronshagen, et al. (1997). "A novel pancreas-specific serpin (ZG-46p) localizes to the soluble and membrane fraction of the Golgi complex and the zymogen granules of acinar cells." *European Journal of Cell Biology* 73(3): 205-214.

Chen, X. and P. C. Andrews (2008). "Purification and proteomics analysis of pancreatic zymogen granule membranes." *Methods in Molecular Biology* 432: 275-287.

Chen, X. and P. C. Andrews (2009). "Quantitative proteomics analysis of pancreatic zymogen granule membrane proteins." *Methods in Molecular Biology* 528: 327-338.

Chen, X., J. A. Edwards, et al. (2002). "Dominant negative Rab3D inhibits amylase release from mouse pancreatic acini." *The Journal of Biological Chemistry* 277(20): 18002-18009.

Chen, X., C. Li, et al. (2004). "Rab27b localizes to zymogen granules and regulates pancreatic acinar exocytosis." *Biochemical and Biophysical Research Communications* 323(4): 1157-1162.

Chen, X., P. J. Ulintz, et al. (2008). "Global topology analysis of pancreatic zymogen granule membrane proteins." *Molecular & Cellular Proteomics* 7(12): 2323-2336.

Chen, X., A. K. Walker, et al. (2006). "Organellar proteomics: analysis of pancreatic zymogen granule membranes." *Molecular & Cellular Proteomics* 5(2): 306-312.

Chen, X., C. Winters, et al. (2008). "Organization of the core structure of the postsynaptic density." *Proceedings of the National Academy of Sciences of the United States of America* 105(11): 4453-4458.

Cheng, D., C. C. Hoogenraad, et al. (2006). "Relative and absolute quantification of postsynaptic density proteome isolated from rat forebrain and cerebellum." *Molecular & Cellular Proteomics* 5(6): 1158-1170.

Cho, S. J., A. K. Sattar, et al. (2002). "Aquaporin 1 regulates GTP-induced rapid gating of water in secretory vesicles." *Proceedings of the National Academy of Sciences of the United States of America* 99(7): 4720-4724.

Colomer, V., G. A. Kicska, et al. (1996). "Secretory granule content proteins and the luminal domains of granule membrane proteins aggregate in vitro at mildly acidic pH." *Journal of Biological Chemistry* 271(1): 48-55.

Colomer, V., K. Lal, et al. (1994). "Exocrine granule specific packaging signals are present in the polypeptide moiety of the pancreatic granule membrane protein GP2 and in amylase:

implications for protein targeting to secretory granules." *The EMBO Journal* 13(16): 3711-3719.

Cool, D. R., M. Fenger, et al. (1995). "Identification of the sorting signal motif within pro-opiomelanocortin for the regulated secretory pathway." *The Journal of Biological Chemistry* 270(15): 8723-8729.

Cool, D. R., E. Normant, et al. (1997). "Carboxypeptidase E is a regulated secretory pathway sorting receptor: genetic obliteration leads to endocrine disorders in Cpe(fat) mice." *Cell* 88(1): 73-83.

Coughenour, H. D., R. S. Spaulding, et al. (2004). "The synaptic vesicle proteome: a comparative study in membrane protein identification." *Proteomics* 4(10): 3141-3155.

Cronshagen, U., P. Voland, et al. (1994). "cDNA cloning and characterization of a novel 16 kDa protein located in zymogen granules of rat pancreas and goblet cells of the gut." *European Journal of Cell Biology* 65(2): 366-377.

Dahan, S., K. L. Anderson, et al. (2005). "Agonist-induced vesiculation of the Golgi apparatus in pancreatic acinar cells." *Gastroenterology* 129(6): 2032-2046.

Damke, H. (1996). "Dynamin and receptor-mediated endocytosis." *FEBS Letters* 389(1): 48-51.

Dartsch, H., R. Kleene, et al. (1998). "In vitro condensation-sorting of enzyme proteins isolated from rat pancreatic acinar cells." *European Journal of Cell Biology* 75: 211-222.

De Bie, I., M. Marcinkiewicz, et al. (1996). "The isoforms of proprotein convertase PC5 are sorted to different subcellular compartments." *The Journal of Cell Biology* 135(5): 1261-1275.

De Camilli, P., S. D. Emr, et al. (1996). "Phosphoinositides as regulators in membrane traffic." *Science* 271(5255): 1533-1539.

De Lisle, R. C. (2002). "Role of sulfated O-linked glycoproteins in zymogen granule formation." *Journal of Cell Science* 115: 2941-2952.

De Lisle, R. C. and U. Hopfer (1986). "Electrolyte permeabilities of pancreatic zymogen granules: implications for pancreatic secretion." *The American Journal of Physiology* 250: 489-496.

Delacour, D., A. Koch, et al. (2008). "Loss of galectin-3 impairs membrane polarisation of mouse enterocytes in vivo." *Journal of Cell Science* 121: 458-465.

Dikeakos, J. D. and T. L. Reudelhuber (2007). "Sending proteins to dense core secretory granules: still a lot to sort out." *Journal of Cell Biology* 177(2): 191-196.

Dittie, A. and H. F. Kern (1992). "The major zymogen granule membrane protein GP-2 in the rat pancreas is not involved in granule formation." *European Journal of Cell Biology* 58(2): 243-258.

Dodd, R. B. and K. Drickamer (2001). "Lectin-like proteins in model organisms: implications for evolution of carbohydrate-binding activity." *Glycobiology* 11(5): 71-79.

Dvorak, A. M. and E. S. Morgan (1998). "Ribonuclease-gold labels chondroitin sulphate in guinea pig basophil granules." *The Histochemical Journal* 30(8): 603-608.

Dvorak, A. M. and E. S. Morgan (1998). "Ribonuclease-gold labels heparin in human mast cell granules. New use for an ultrastructural enzyme affinity technique." *The Journal of Histochemistry and Cytochemistry* 46(6): 695-706.

Dvorak, A. M. and E. S. Morgan (1999). "Ribonuclease-gold labels proteoglycan-containing cytoplasmic granules and ribonucleic acid-containing organelles-a survey." *Histology and Histopathology* 14(2): 597-626.

Falkowski, M. A., D. D. Thomas, et al. (2010). "Complexin 2 modulates vesicle-associated membrane protein (VAMP) 2-regulated zymogen granule exocytosis in pancreatic acini." *The Journal of Biological Chemistry* 285(46): 35558-35566.

Falkowski, M. A., D. D. Thomas, et al. (2011). "Expression, localization, and functional role for synaptotagmins in pancreatic acinar cells." *American Journal of Physiology. Gastrointestinal and Liver Physiology* 301(2): G306-316.

Faust, F., M. Gomez-Lazaro, et al. (2008). "Rab8 is involved in zymogen granule formation in pancreatic acinar AR42J cells." *Traffic* 9(6): 964-979.

Fenster, S. D., M. M. Kessels, et al. (2003). "Interactions between Piccolo and the actin/dynamin-binding protein Abp1 link vesicle endocytosis to presynaptic active zones." *The Journal of Biological Chemistry* 278(22): 20268-20277.

Forsberg, E. and L. Kjellen (2001). "Heparan sulfate: lessons from knockout mice." *The Journal of Clinical Investigation* 108(2): 175-180.

Freedman, S. D. and G. A. Scheele (1993). "Regulated secretory proteins in the exocrine pancreas aggregate under conditions that mimic the trans-Golgi network." *Biochemical Biophysical Research Communications* 197(2): 992-999.

Freedman, S. D. and G. A. Scheele (1993). "Reversible pH-induced homophilic binding of GP2, a glycosyl-phosphatidylinositol-anchored protein in pancreatic zymogen granule membranes." *European Journal of Cell Biology* 61(2): 229-238.

Fujimoto, K., T. Shibasaki, et al. (2002). "Piccolo, a Ca2+ sensor in pancreatic beta-cells. Involvement of cAMP-GEFII.Rim2. Piccolo complex in cAMP-dependent exocytosis." *The Journal of Biological Chemistry* 277(52): 50497-50502.

Fukuoka, S., S. D. Freedman, et al. (1992). "GP-2/THP gene family encodes self-binding glycosylphosphatidylinositol-anchored proteins in apical secretory compartments of pancreas and kidney." *Proceedings of the National Academy of Sciences of the United States of America* 89(4): 1189-1193.

Gabius, H. J., S. Andre, et al. (2002). "The sugar code: functional lectinomics." *Biochimica et Biophysica Acta* 1572(2-3): 165-177.

Gaisano, H. Y. and F. S. Gorelick (2009). "New insights into the mechanisms of pancreatitis." *Gastroenterology* 136(7): 2040-2044.

Gaisano, H. Y., X. Huang, et al. (1999). "Snare protein expression and adenoviral transfection of amphicrine AR42J." *Biochemical and Biophysical Research Communications* 260(3): 781-784.

Gallagher, J. T., R. L. Hall, et al. (1986). "Mucus-glycoproteins (mucins) of the cat trachea: characterisation and control of secretion." *Biochimica et biophysica acta* 886(2): 243-254.

Gandy, S. and P. Greengard (1994). "Regulated cleavage of the Alzheimer amyloid precursor protein: molecular and cellular basis." *Biochemistry* 76(3-4): 300-303.

Gerber, S. H., J. Garcia, et al. (2001). "An unusual C(2)-domain in the active-zone protein piccolo: implications for Ca(2+) regulation of neurotransmitter release." *The EMBO Journal* 20(7): 1605-1619.

Gomez-Lazaro, M., C. Rinn, et al. (2010). "Proteomic analysis of zymogen granules." *Expert Review of Proteomics* 7(5): 735-747.

Gondre-Lewis, M. C., H. I. Petrache, et al. (2006). "Abnormal sterols in cholesterol-deficiency diseases cause secretory granule malformation and decreased membrane curvature." *Journal of Cell Science* 119: 1876-1885.

Gough, N. R., M. E. Zweifel, et al. (1999). "Utilization of the indirect lysosome targeting pathway by lysosome-associated membrane proteins (LAMPs) is influenced largely by the C-terminal residue of their GYXXphi targeting signals." *Journal of Cell Science* 112: 4257-4269.

Grimes, M. and R. B. Kelly (1992). "Intermediates in the constitutive and regulated secretory pathways released in vitro from semi-intact cells." *The Journal of Cell Biology* 117(3): 539-549.

Gronborg, M., J. Bunkenborg, et al. (2004). "Comprehensive proteomic analysis of human pancreatic juice." *Journal of Proteome Research* 3(5): 1042-1055.

Grondin, G., P. St-Jean, et al. (1992). "Cytochemical and immunocytochemical characterization of a fibrillar network (GP2) in pancreatic juice: possible role as a sieve in the pancreatic ductal system." *European Journal of Cell Biology* 57(2): 155-164.

Guo, X. W., D. Merlin, et al. (1997). "Purinergic agonists, but not cAMP, stimulate coupled granule fusion and Cl- conductance in HT29-Cl.16E." *The American Journal of Physiology* 273: 804-809.

Haffner, C., K. Takei, et al. (1997). "Synaptojanin 1: localization on coated endocytic intermediates in nerve terminals and interaction of its 170 kDa isoform with Eps15." *FEBS Letters* 419(2-3): 175-180.

Hajos, F. (1975). "An improved method for the preparation of synaptosomal fractions in high purity." *Brain Research* 93(3): 485-489.

Hammel, I., D. Lagunoff, et al. (2010). "Regulation of secretory granule size by the precise generation and fusion of unit granules." *Journal of Cellular and Molecular Medicine* 14(7): 1904-1916.

Han, L., M. Suda, et al. (2008). "A large form of secretogranin III functions as a sorting receptor for chromogranin A aggregates in PC12 cells." *Molecular Endocrinology* 22(8): 1935-1949.

Hansen, N. J., W. Antonin, et al. (1999). "Identification of SNAREs involved in regulated exocytosis in the pancreatic acinar cell." *The Journal of Biological Chemistry* 274(32): 22871-22876.

Harjes, P. and E. E. Wanker (2003). "The hunt for huntingtin function: interaction partners tell many different stories." *Trends in Biochemical Sciences* 28(8): 425-433.

Hase, K., K. Kawano, et al. (2009). "Uptake through glycoprotein 2 of FimH(+) bacteria by M cells initiates mucosal immune response." *Nature* 462(7270): 226-230.

Hodel, A., S. J. An, et al. (2001). "Cholesterol-dependent interaction of syncollin with the membrane of the pancreatic zymogen granule." *The Biochemical journal* 356: 843-850.

Hodel, A. and J. M. Edwardson (2000). "Targeting of the zymogen-granule protein syncollin in AR42J and AtT-20 cells." *The Biochemical Journal* 350: 637-643.

Hoops, T. C. and M. J. Rindler (1991). "Isolation of the cDNA encoding glycoprotein-2 (GP-2), the major zymogen granule membrane protein. Homology to uromodulin/Tamm-Horsfall protein." *The Journal of Biological Chemistry* 266(7): 4257-4263.

Hopper, N. A. and V. O'Connor (2005). "Ephrin tempers two-faced synaptojanin 1." *Nature Cell Biology* 7(5): 454-456.

Hosaka, M. and T. Watanabe (2010). "Secretogranin III: a bridge between core hormone aggregates and the secretory granule membrane." *Endocrine Journal* 57(4): 275-286.

Hoy, M., A. M. Efanov, et al. (2002). "Inositol hexakisphosphate promotes dynamin I- mediated endocytosis." *Proceedings of the National Academy of Sciences of the United States of America* 99(10): 6773-6777.

Hoy, M., P. Maechler, et al. (2002). "Increase in cellular glutamate levels stimulates exocytosis in pancreatic beta-cells." *FEBS Letters* 531(2): 199-203.

Huang, C., A. Sali, et al. (1998). "Regulation and function of mast cell proteases in inflammation." *Journal of Clinical Immunology* 18(3): 169-183.

Huh, Y. H., S. H. Jeon, et al. (2003). "Chromogranin B-induced secretory granule biogenesis: comparison with the similar role of chromogranin A." *The Journal of Biological Chemistry* 278(42): 40581-40589.

Husain, S. and E. Thrower (2009). "Molecular and cellular regulation of pancreatic acinar cell function." *Current Opinion in Gastroenterology* 25(5): 466-471.

Huttner, W. B., H. H. Gerdes, et al. (1991). "The granin (chromogranin/secretogranin) family." *Trends in Biochemical Sciences* 16(1): 27-30.

Huttner, W. B. and S. Natori (1995). "Regulated secretion. Helper proteins for neuroendocrine secretion." *Current Biology* 5(3): 242-245.

Huttner, W. B. and J. Zimmerberg (2001). "Implications of lipid microdomains for membrane curvature, budding and fission." *Current Opinion in Cell Biology* 13(4): 478-484.

Ikonen, E. and K. Simons (1998). "Protein and lipid sorting from the trans-Golgi network to the plasma membrane in polarized cells." *Seminars in Cell & Developmental Biology* 9(5): 503-509.

Imamura, T., M. Asada, et al. (2002). "Protection from pancreatitis by the zymogen granule membrane protein integral membrane-associated protein-1." *The Journal of Biological Chemistry* 277(52): 50725-50733.

Inomoto, C., S. Umemura, et al. (2007). "Granulogenesis in non-neuroendocrine COS-7 cells induced by EGFP-tagged chromogranin A gene transfection: identical and distinct distribution of CgA and EGFP." *The Journal of Histochemistry and Cytochemistry* 55(5): 487-493.

Iovanna, J. L. and J. C. Dagorn (2005). "The multifunctional family of secreted proteins containing a C-type lectin-like domain linked to a short N-terminal peptide." *Biochimica et Biophysica Acta* 1723(1-3): 8-18.

Irie, F., M. Okuno, et al. (2005). "EphrinB-EphB signalling regulates clathrin-mediated endocytosis through tyrosine phosphorylation of synaptojanin 1." *Nature Cell Biology* 7(5): 501-509.

Ishihara, Y., T. Sakurai, et al. (2000). "Exocytosis and movement of zymogen granules observed by VEC-DIC microscopy in the pancreatic tissue en bloc." *American Journal of Cell Physiology* 279(4): 1177-1188.

Iwai, N. and T. Inagami (1990). "Molecular cloning of a complementary DNA to rat cyclophilin-like protein mRNA." *Kidney International* 37(6): 1460-1465.

Iwatsubo, T. (2004). "The gamma-secretase complex: machinery for intramembrane proteolysis." *Current Opinion in Neurobiology* 14(3): 379-383.

Jacob, M., J. Laine, et al. (1992). "Specific interactions of pancreatic amylase at acidic pH. Amylase and the major protein of the zymogen granule membrane (GP-2) bind to immobilized or polymerized amylase." *Biochemistry and Cell Biology* 70 (10–11): 1105–14

Jamieson, J. D. and G. E. Palade (1971). "Condensing vacuole conversion and zymogen granule discharge in pancreatic exocrine cells: metabolic studies." *The Journal of Cell Biology* 48(3): 503-522.

Jeftinija, S. (2006). "The story of cell secretion: events leading to the discovery of the 'porosome' - the universal secretory machinery in cells." *Journal of Cellular and Molecular Medicine* 10(2): 273-279.

Jessen, B. A., J. S. Mullins, et al. (2003). "Assessment of hepatocytes and liver slices as in vitro test systems to predict in vivo gene expression." *Toxicological Sciences* 75(1): 208-222.

Junqueira, L.C., J. Carneiro (1996). Histology, 4. Edition, *Springer-Verlag*, Heidelberg, Berlin and New York

Kakhlon, O., P. Sakya, et al. (2006). "GGA function is required for maturation of neuroendocrine secretory granules." *The EMBO Journal* 25(8): 1590-1602.

Kalus, I., A. Hodel, et al. (2002). "Interaction of syncollin with GP-2, the major membrane protein of pancreatic zymogen granules, and association with lipid microdomains." *The Biochemical Journal* 362: 433-442.

Kamal, A., A. Almenar-Queralt, et al. (2001). "Kinesin-mediated axonal transport of a membrane compartment containing beta-secretase and presenilin-1 requires APP." *Nature* 414(6864): 643-648.

Kanagawa, M., T. Satoh, et al. (2011). "Crystal structures of human secretory proteins ZG16p and ZG16b reveal a Jacalin-related beta-prism fold." *Biochemical and Biophysical Research Communications* 404(1): 201-205.

Katz, R. I. and I. J. Kopin (1969). "Release of norepinephrine-3H and serotonin-3H evoked from brain slices by electrical-field stimulation-calcium dependency and the effects of lithium, ouabain and tetrodotoxin." *Biochemical Pharmacology* 18(8): 1835-1839.

Kelly, M. L., R. Abu-Hamdah, et al. (2005). "Patch clamped single pancreatic zymogen granules: direct measurements of ion channel activities at the granule membrane." *Pancreatology* 5(4-5): 443-449.

Kim, S. A., Y. Lee, et al. (2009). "Pancreatic adenocarcinoma up-regulated factor (PAUF), a novel up-regulated secretory protein in pancreatic ductal adenocarcinoma." *Cancer Science* 100(5): 828-836.

Kim, T., M. C. Gondre-Lewis, et al. (2006). "Dense-core secretory granule biogenesis." *Physiology* 21: 124-133.

Kim, T., J. H. Tao-Cheng, et al. (2001). "Chromogranin A, an "on/off" switch controlling dense-core secretory granule biogenesis." *Cell* 106(4): 499-509.

Kleene, R., B. Classen, et al. (2000). "SH3 binding sites of ZG29p mediate an interaction with amylase and are involved in condensation-sorting in the exocrine rat pancreas." *Biochemistry* 39(32): 9893-9900.

Kleene, R., H. Dartsch, et al. (1999). "The secretory lectin ZG16p mediates sorting of enzyme proteins to the zymogen granule membrane in pancreatic acinar cells." *European Journalof Cell Biology* 78(2): 79-90.

Kleene, R., B. Kastner, et al. (1999). "Complex formation among rat pancreatic secretory proteins under mild alkaline pH conditions." *Digestion* 60(4): 305-313.

Kleene, R., J. Zdzieblo, et al. (1999). "A novel zymogen granule protein (ZG29p) and the nuclear protein MTA1p are differentially expressed by alternative transcription initiation in pancreatic acinar cells of the rat." *Journal of Cell Science* 112: 2539-2548.

Kleinman, H. K., E. B. McGoodwin, et al. (1979). "Preparation of collagen substrates for cell attachment: effect of collagen concentration and phosphate buffer." *Analytical Biochemistry* 94(2): 308-312.

Kolset, S. O. and J. T. Gallagher (1990). "Proteoglycans in haemopoietic cells." *Biochimica et Biophysica Acta* 1032(2-3): 191-211.

Koshimizu, H., T. Kim, et al. (2010). "Chromogranin A: a new proposal for trafficking, processing and induction of granule biogenesis." *Regulatory Peptides* 160(1-3): 153-159.

Kromer, A., M. M. Glombik, et al. (1998). "Essential role of the disulfide-bonded loop of chromogranin B for sorting to secretory granules is revealed by expression of a deletion mutant in the absence of endogenous granin synthesis." *The Journal of Cell Biology* 140(6): 1331-1346.

Kumazawa-Inoue, K., T. Mimura, et al. (2011). "ZG16p, an animal homologue of {beta}-prism fold plant lectins, interacts with heparan sulfate proteoglycans in pancreatic zymogen granules." *Glycobiology*.

Kury, P., D. Abankwa, et al. (2004). "Gene expression profiling reveals multiple novel intrinsic and extrinsic factors associated with axonal regeneration failure." *The European Journal of Neuroscience* 19(1): 32-42.

Laemmli, U. K. (1970). "Cleavage of structural proteins during the assembly of the head of bacteriophage T4." *Nature* 227(5259): 680-685.

Leal-Ortiz, S., C. L. Waites, et al. (2008). "Piccolo modulation of Synapsin1a dynamics regulates synaptic vesicle exocytosis." *The Journal of Cell Biology* 181(5): 831-846.

Leblond, F. A., G. Viau, et al. (1993). "Reconstitution in vitro of the pH-dependent aggregation of pancreatic zymogens en route to the secretory granule: implication of GP-2." *Biochemical Journal* 291: 289-296.

Lee, W. K., B. Torchalski, et al. (2008). "Evidence for KCNQ1 K+ channel expression in rat zymogen granule membranes and involvement in cholecystokinin-induced pancreatic acinar secretion." *American Journal of Cell Physiology* 294(4): 879-892.

Lee, Y., S. J. Kim, et al. (2010). "PAUF functions in the metastasis of human pancreatic cancer cells and upregulates CXCR4 expression." *Oncogene* 29(1): 56-67.

Leskinen, M. J., K. A. Lindstedt, et al. (2003). "Mast cell chymase induces smooth muscle cell apoptosis by a mechanism involving fibronectin degradation and disruption of focal adhesions." *Arteriosclerosis, Thrombosis, and Vascular Biology* 23(2): 238-243.

Lim, J. W., J. Y. Song, et al. (2009). "Role of pancreatitis-associated protein 1 on oxidative stress-induced cell death of pancreatic acinar cells." *Annals of the New York Academy of Sciences* 1171: 545-548.

Lobler, M., M. Sass, et al. (2002). "Biomaterial patches sutured onto the rat stomach induce a set of genes encoding pancreatic enzymes." *Biomaterials* 23(2): 577-583.

Logsdon, C. D. (1986). "Glucocorticoids increase cholecystokinin receptors and amylase secretion in pancreatic acinar AR42J cells." *The Journal of Biological Chemistry* 261(5): 2096-2101.

Logsdon, C. D., J. Moessner, et al. (1985). "Glucocorticoids increase amylase mRNA levels, secretory organelles, and secretion in pancreatic acinar AR42J cells." *The Journal of Cell Biology* 100(4): 1200-1208.

Loh, Y. P., C. R. Snell, et al. (1997). "Receptor-mediated targeting of hormones to secretory granules: role of carboxypeptidase E." *Trends in Endocrinology and Metabolism* 8(4): 130-137.

Longnecker, D. S., H. S. Lilja, et al. (1979). "Transplantation of azaserine-induced carcinomas of pancreas in rats." *Cancer Letters* 7(4): 197-202.

LoTurco, J. J. and J. Bai (2006). "The multipolar stage and disruptions in neuronal migration." *Trends in Neurosciences* 29(7): 407-413.

Lutzelschwab, C., G. Pejler, et al. (1997). "Secretory granule proteases in rat mast cells. Cloning of 10 different serine proteases and a carboxypeptidase A from various rat mast cell populations." *The Journal of Experimental Medicine* 185(1): 13-29.

Lüllmann-Rauch, R. (2009) "Taschenbuch der Histologie" 3. Auflage, *Georg Thieme Verlag*, Stuttgart, New York

Marquez-Sterling, N. R., A. C. Lo, et al. (1997). "Trafficking of cell-surface beta-amyloid precursor protein: evidence that a sorting intermediate participates in synaptic vesicle recycling." *The Journal of Neuroscience* 17(1): 140-151.

Mashima, H., H. Ohnishi, et al. (1996). "Betacellulin and activin A coordinately convert amylase-secreting pancreatic AR42J cells into insulin-secreting cells." *The Journal of clinical investigation* 97(7): 1647-1654.

Mashima, H., H. Shibata, et al. (1996). "Formation of insulin-producing cells from pancreatic acinar AR42J cells by hepatocyte growth factor." *Endocrinology* 137(9): 3969-3976.

Matsumoto, R., A. Sali, et al. (1995). "Packaging of proteases and proteoglycans in the granules of mast cells and other hematopoietic cells. A cluster of histidines on mouse mast cell protease 7 regulates its binding to heparin serglycin proteoglycans." *The Journal of Biological Chemistry* 270(33): 19524-19531.

McLoughlin, D. M., N. G. Irving, et al. (1999). "Mint2/X11-like colocalizes with the Alzheimer's disease amyloid precursor protein and is associated with neuritic plaques in Alzheimer's disease." *The European Journal of Neuroscience* 11(6): 1988-1994.

McPherson, P. S., E. P. Garcia, et al. (1996). "A presynaptic inositol-5-phosphatase." *Nature* 379(6563): 353-357.

Milward, E. A., R. Papadopoulos, et al. (1992). "The amyloid protein precursor of Alzheimer's disease is a mediator of the effects of nerve growth factor on neurite outgrowth." *Neuron* 9(1): 129-137.

Miyake, H., S. Hara, et al. (2004). "Global analysis of gene expression profiles in ileum in a rat bladder augmentation model using cDNA microarrays." *International Journal of Urology* 11(11): 1009-1012.

Mo, L., X. H. Zhu, et al. (2004). "Ablation of the Tamm-Horsfall protein gene increases susceptibility of mice to bladder colonization by type 1-fimbriated Escherichia coli." *American Journal of Physiology. Renal Physiology* 286(4): F795-802.

Moniaux, N., H. Song, et al. (2011). "Human hepatocarcinoma-intestine-pancreas/pancreatitis-associated protein cures fas-induced acute liver failure in mice by attenuating free-radical damage in injured livers." *Hepatology* 53(2): 618-627.

Morimoto, T., S. Popov, et al. (1995). "Calcium-dependent transmitter secretion from fibroblasts: modulation by synaptotagmin I." *Neuron* 15(3): 689-696.

Nader, H. B., S. F. Chavante, et al. (1999). "Heparan sulfates and heparins: similar compounds performing the same functions in vertebrates and invertebrates?" *Brazilian Journal of Medical and Biological Research* 32(5): 529-538.

Nelson, R. B., R. Siman, et al. (1993). "Identification of a chymotrypsin-like mast cell protease in rat brain capable of generating the N-terminus of the Alzheimer amyloid beta-protein." *Journal of Neurochemistry* 61(2): 567-577.

Nelson, W. J. and C. Yeaman (2001). "Protein trafficking in the exocytic pathway of polarized epithelial cells." *Trends in Cell Biology* 11(12): 483-486.

Nemoto, T., T. Kojima, et al. (2004). "Stabilization of exocytosis by dynamic F-actin coating of zymogen granules in pancreatic acini." *The Journal of Biological Chemistry* 279(36): 37544-37550.

Nemoto, Y., M. Arribas, et al. (1997). "Synaptojanin 2, a novel synaptojanin isoform with a distinct targeting domain and expression pattern." *The Journal of Biological Chemistry* 272(49): 30817-30821.

Neuschwander-Tetri, B. A., C. J. Fimmel, et al. (2004). "Differential expression of the trypsin inhibitor SPINK3 mRNA and the mouse ortholog of secretory granule protein ZG-16p mRNA in the mouse pancreas after repetitive injury." *Pancreas* 28(4): e104-111.

Niemann, C. U., J. B. Cowland, et al. (2009). "Serglycin proteoglycan is not implicated in localizing exocrine pancreas enzymes to zymogen granules." *European Journal of Cell Biology* 88(8): 473-479.

Normant, E. and Y. P. Loh (1998). "Depletion of carboxypeptidase E, a regulated secretory pathway sorting receptor, causes misrouting and constitutive secretion of proinsulin and proenkephalin, but not chromogranin A." *Endocrinology* 139(4): 2137-2145.

Olson, L. J., G. Sun, et al. (2010). "Intermonomer interactions are essential for lysosomal enzyme binding by the cation-dependent mannose 6-phosphate receptor." *Biochemistry* 49(1): 236-246.

Ozawa, H. and K. Takata (1995). "The granin family--its role in sorting and secretory granule formation." *Cell Structure and Function* 20(6): 415-420.

Palade, G. (1975). "Intracellular aspects of the process of protein synthesis." *Science* 189(4206): 867.

Palmer, D. J. and D. L. Christie (1992). "Identification of molecular aggregates containing glycoproteins III, J, K (carboxypeptidase H), and H (Kex2-related proteases) in the soluble and membrane fractions of adrenal medullary chromaffin granules." *The Journal of Biological Chemistry* 267(28): 19806-19812.

Pangalos, M. N., S. Efthimiopoulos, et al. (1995). "The chondroitin sulfate attachment site of appican is formed by splicing out exon 15 of the amyloid precursor gene." *The Journal of Biological Chemistry* 270(18): 10388-10391.

Park, J. J., H. Koshimizu, et al. (2009). "Biogenesis and transport of secretory granules to release site in neuroendocrine cells." *Journal of Molecular Neuroscience* 37(2): 151-159.

Pearse, B. R. and D. N. Hebert (2010). "Lectin chaperones help direct the maturation of glycoproteins in the endoplasmic reticulum." *Biochimica et Biophysica Acta* 1803(6): 684-693.

Pejler, G. and L. Berg (1995). "Regulation of rat mast cell protease 1 activity. Protease inhibition is prevented by heparin proteoglycan." *European Journal of Biochemistry / FEBS* 233(1): 192-199.

Pejler, G. and M. Maccarana (1994). "Interaction of heparin with rat mast cell protease 1." *The Journal of Biological Chemistry* 269(20): 14451-14456.

Pejler, G. and J. E. Sadler (1999). "Mechanism by which heparin proteoglycan modulates mast cell chymase activity." *Biochemistry* 38(37): 12187-12195.

Perez-Vilar, J. (2007). "Mucin granule intraluminal organization." *American Journal of Respiratory Cell and Molecular Biology* 36(2): 183-190.

Perez, R. G., H. Zheng, et al. (1997). "The beta-amyloid precursor protein of Alzheimer's disease enhances neuron viability and modulates neuronal polarity." *The Journal of Neuroscience* 17(24): 9407-9414.

Pevsner, J., S. C. Hsu, et al. (1994). "Specificity and regulation of a synaptic vesicle docking complex." *Neuron* **13**(2): 353-361.

Pfeffer, S. R. (2007). "Unsolved mysteries in membrane traffic." *Annual Review of Biochemistry* 76: 629-645.

Pickett, J. A. and J. M. Edwardson (2006). "Compound exocytosis: mechanisms and functional significance." *Traffic* 7(2): 109-116.

Pimplikar, S. W. and W. B. Huttner (1992). "Chromogranin B (secretogranin I), a secretory protein of the regulated pathway, is also present in a tightly membrane-associated form in PC12 cells." *The Journal of Biological Chemistry* 267(6): 4110-4118.

Poo, M., Y. Dan, et al. (1995). "Calcium-dependent vesicular exocytosis: from constitutive to regulated secretion." *Cold Spring Harbor Symposia on Quantitative Biology* 60: 349-359.

Popov, S. V. and M. M. Poo (1993). "Synaptotagmin: a calcium-sensitive inhibitor of exocytosis?" *Cell* 73(7): 1247-1249.

Prydz, K. and K. T. Dalen (2000). "Synthesis and sorting of proteoglycans." *Journal of Cell Science* 113**:** 193-205.

Rabilloud, T. (1998). "Use of thiourea to increase the solubility of membrane proteins in two-dimensional electrophoresis." *Electrophoresis* 19(5): 758-760.

Ramjaun, A. R. and P. S. McPherson (1996). "Tissue-specific alternative splicing generates two synaptojanin isoforms with differential membrane binding properties." *The Journal of Biological Chemistry* 271(40): 24856-24861.

Raraty, M., J. Ward, et al. (2000). "Calcium-dependent enzyme activation and vacuole formation in the apical granular region of pancreatic acinar cells." *Proceedings of the National Academy of Sciences of the United States of America* 97(24): 13126-13131.

Reggio, H. A. and G. E. Palade (1978). "Sulfated compounds in the zymogen granules of the guinea pig pancreas." *The Journal of Cell Biology* 77(2): 288-314.

Riedel, D., W. Antonin, et al. (2002). "Rab3D is not required for exocrine exocytosis but for maintenance of normally sized secretory granules." *Molecular and Cellular Biology* 22(18): 6487-6497.

Rindler, M. J. (1998). "Carboxypeptidase E, a peripheral membrane protein implicated in the targeting of hormones to secretory granules, co-aggregates with granule content proteins at acidic pH." *The Journal of Biological Chemistry* 273(47): 31180-31185.

Rindler, M. J. and T. C. Hoops (1990). "The pancreatic membrane protein GP-2 localizes specifically to secretory granules and is shed into the pancreatic juice as a protein aggregate." *European Journal of Cell Biology* 53(1): 154-163.

Rindler, M. J., C. F. Xu, et al. (2007). "Proteomic analysis of pancreatic zymogen granules: identification of new granule proteins." *Journal of Proteome Research* 6(8): 2978-2992.

Rinn, C., M. Aroso, et al. (2011). The secretory lectin ZG16p. T*he Pancreapedia: Exocrine Pancreas Knowledge Base*, DOI: 10.3998/panc.2011.17

Rizo, J. and T. C. Sudhof (2002). "Snares and Munc18 in synaptic vesicle fusion." *Nature Reviews. Neuroscience* 3(8): 641-653.

Robinson, M. S. (1994). "The role of clathrin, adaptors and dynamin in endocytosis." *Current Opinion in Cell Biology* 6(4): 538-544.

Rogers, D. F. (2007). "Physiology of airway mucus secretion and pathophysiology of hypersecretion." *Respiratory Care* 52(9): 1134-1146; discussion 1146-1139.

Roussa, E., S. L. Alper, et al. (2001). "Immunolocalization of anion exchanger AE2, Na(+)/H(+) exchangers NHE1 and NHE4, and vacuolar type H(+)-ATPase in rat pancreas." *The Journal of Histochemistry and Cytochemistry* 49(4): 463-474.

Sabbatini, M. E., Y. Bi, et al. (2010). "CCK activates RhoA and Rac1 differentially through Galpha13 and Galphaq in mouse pancreatic acini." *American Journal of Physiology. Cell Physiology* 298(3): 592-601.

Sandbrink, R., U. Monning, et al. (1997). "Expression of the APP gene family in brain cells, brain development and aging." *Gerontology* 43(1-2): 119-131.

Schagger, H. and G. von Jagow (1991). "Blue native electrophoresis for isolation of membrane protein complexes in enzymatically active form." *Analytical Biochemistry* 199(2): 223-231.

Scheele, G. A., S. Fukuoka, et al. (1994). "Role of the GP2/THP family of GPI-anchored proteins in membrane trafficking during regulated exocrine secretion." *Pancreas* 9(2): 139-149.

Scheele, G. A., G. E. Palade, et al. (1978). "Cell fractionation studies on the guinea pig pancreas. Redistribution of exocrine proteins during tissue homogenization." *The Journal of Cell Biology* 78(1): 110-130.

Scheele, G. and Kern, H. F. (1993). "Cellular compartmentation, protein processing, and secretion in the exocrine pancreas. " *In The Pancreas, Biology, Pathobiology and Diseases,* Raven Press, New York, 121-150.

Schmidt, K., H. Dartsch, et al. (2000). "A submembranous matrix of proteoglycans on zymogen granule membranes is involved in granule formation in rat pancreatic acinar cells." *Journal of Cell Science* 113: 2233-2242.

Schmidt, K., M. Schrader, et al. (2001). "Regulated apical secretion of zymogens in rat pancreas. Involvement of the glycosylphosphatidylinositol-anchored glycoprotein GP-2, the lectin ZG16p, and cholesterol-glycosphingolipid-enriched microdomains." *The Journal of Biological Chemistry* 276(17): 14315-14323.

Schnefel, S., A. Profrock, et al. (1990). "Cholecystokinin activates Gi1-, Gi2-, Gi3- and several Gs-proteins in rat pancreatic acinar cells." *The Biochemical Journal* 269(2): 483-488.

Schoch, S. and E. D. Gundelfinger (2006). "Molecular organization of the presynaptic active zone." *Cell and Tissue Research* 326(2): 379-391.

Schrader, M. (2004). "Membrane targeting in secretion." *Subcellular Biochemistry* 37: 391-421.

Schubert, D., R. Schroeder, et al. (1988). "Amyloid beta protein precursor is possibly a heparan sulfate proteoglycan core protein." *Science* 241(4862): 223-226.

Scott, J. E. (1980). "Collagen-proteoglycan interactions. Localization of proteoglycans in tendon by electron microscopy." *The Biochemical Journal* 187(3): 887-891.

Scott, J. E. (1985). "Proteoglycan histochemistry--a valuable tool for connective tissue biochemists." *Collagen and Related Research* 5(6): 541-575.

Scott, J. E., C. R. Orford, et al. (1981). "Proteoglycan-collagen arrangements in developing rat tail tendon. An electron microscopical and biochemical investigation." *The Biochemical Journal* 195(3): 573-581.

Selkoe, D. J. (1996). "Cell biology of the beta-amyloid precursor protein and the genetics of Alzheimer's disease." *Cold Spring Harbor symposia on Quantitative Biology* 61: 587-596.

Shen, C. N., Z. D. Burke, et al. (2004). "Transdifferentiation, metaplasia and tissue regeneration." *Organogenesis* 1(2): 36-44.

Shen, C. N., M. E. Horb, et al. (2003). "Transdifferentiation of pancreas to liver." *Mechanisms of Development* 120(1): 107-116.

Shen, C. N., J. M. Slack, et al. (2000). "Molecular basis of transdifferentiation of pancreas to liver." *Nature Cell Biology* 2(12): 879-887.

Shioi, J., M. N. Pangalos, et al. (1995). "The Alzheimer amyloid precursor proteoglycan (appican) is present in brain and is produced by astrocytes but not by neurons in primary neural cultures." *The Journal of Biological Chemistry* 270(20): 11839-11844.

Siekevitz, P. and G. E. Palade (1966). "Distribution of newly synthesized amylase in microsomal subfractions of guinea pigs pancreas." *The Journal of Cell Biology* 30(3): 519-530.

Sigal, L. H. (2005). "Basic science for the clinician 30: The immunologic synapse." *Journal of Clinical Rheumatology* 11(4): 234-239.

Small, S. A. and S. Gandy (2006). "Sorting through the cell biology of Alzheimer's disease: intracellular pathways to pathogenesis." *Neuron* 52(1): 15-31.

Stettler, H., N. Beuret, et al. (2009). "Determinants for chromogranin A sorting into the regulated secretory pathway are also sufficient to generate granule-like structures in non-endocrine cells." *The Biochemical Journal* 418(1): 81-91.

Stoller, T. J. and D. Shields (1989). "The propeptide of preprosomatostatin mediates intracellular transport and secretion of alpha-globin from mammalian cells." *The Journal of Cell Biology* 108(5): 1647-1655.

Su, A. I., T. Wiltshire, et al. (2004). "A gene atlas of the mouse and human protein-encoding transcriptomes." *Proceedings of the National Academy of Sciences of the United States of America* 101(16): 6062-6067.

Sudhof, T. C. (2004). "The synaptic vesicle cycle." *Annual Review of Neuroscience* 27: 509-547.

Sugiya, H., M. Matsuki-Fukushima, et al. (2008). "Role of aquaporins and regulation of secretory vesicle volume in cell secretion." *Journal of Cellular and Molecular Medicine* 12(5): 1486-1494.

Svajger, U., M. Anderluh, et al. (2010). "C-type lectin DC-SIGN: an adhesion, signalling and antigen-uptake molecule that guides dendritic cells in immunity." *Cellular Signalling* 22(10): 1397-1405.

Takamori, S., M. Holt, et al. (2006). "Molecular anatomy of a trafficking organelle." *Cell* 127(4): 831-846.

Takeuchi, T. and M. Hosaka (2008). "Sorting mechanism of peptide hormones and biogenesis mechanism of secretory granules by secretogranin III, a cholesterol-binding protein, in endocrine cells." *Current Diabetes Reviews* 4(1): 31-38.

Tanne, A. and O. Neyrolles (2010). "C-type lectins in immune defense against pathogens: the murine DC-SIGN homologue SIGNR3 confers early protection against Mycobacterium tuberculosis infection." *Virulence* 1(4): 285-290.

Tartakoff, A. M., J. D. Jamieson, et al. (1975). "Studies on the pancreas of the guinea pig. Parallel processing and discharge of exocrine proteins." *The Journal of Biological Chemistry* 250(7): 2671-2677.

Tateno, H., R. Yabe, et al. (2011). "Human ZG16p recognizes pathogenic fungi through non-self polyvalent mannose in the digestive system." *Glycobiology. [Epub ahead of print]*

Thevenod, F. (2002). "Ion channels in secretory granules of the pancreas and their role in exocytosis and release of secretory proteins." *American Journal of Physiology. Cell physiology* 283(3): 651-672.

Thevenod, F., I. Anderie, et al. (1994). "Monoclonal antibodies against MDR1 P-glycoprotein inhibit chloride conductance and label a 65-kDa protein in pancreatic zymogen granule membranes." *The Journal of Biological Chemistry* 269(39): 24410-24417.

Thevenod, F., M. Braun, et al. (2000). "Molecular characterisation of pancreatic zymogen granule ion channel and regulator proteins involved in exocytosis." *Journal of Korean Medical Science:* 51-52.

Thiele, C. and W. B. Huttner (1998). "The disulfide-bonded loop of chromogranins, which is essential for sorting to secretory granules, mediates homodimerization." *The Journal of Biological Chemistry* 273(2): 1223-1231.

Thinakaran, G. and E. H. Koo (2008). "Amyloid precursor protein trafficking, processing, and function." *The Journal of Biological Chemistry* 283(44): 29615-29619.

Thorn, P., K. E. Fogarty, et al. (2004). "Zymogen granule exocytosis is characterized by long fusion pore openings and preservation of vesicle lipid identity." *Proceedings of the National Academy of Sciences of the United States of America* 101(17): 6774-6779.

Tojima, T., H. Akiyama, et al. (2007). "Attractive axon guidance involves asymmetric membrane transport and exocytosis in the growth cone." *Nature Neuroscience* 10(1): 58-66.

Tooze, J., H. F. Kern, et al. (1989). "Condensation-sorting events in the rough endoplasmic reticulum of exocrine pancreatic cells." *The Journal of Cell Biology* 109(1): 35-50.

Tooze, S. A. (1998). "Biogenesis of secretory granules in the trans-Golgi network of neuroendocrine and endocrine cells." *Biochimica et Biophysica Acta* 1404(1-2): 231-244.

Tooze, S. A., G. J. Martens, et al. (2001). "Secretory granule biogenesis: rafting to the SNARE." *Trends in Cell Biology* 11(3): 116-122.

Tsuchida, K., J. Shioi, et al. (2001). "Appican, the proteoglycan form of the amyloid precursor protein, contains chondroitin sulfate E in the repeating disaccharide region and 4-O-sulfated galactose in the linkage region." *The Journal of Biological Chemistry* 276(40): 37155-37160.

Ueda, N., H. Ohnishi, et al. (2000). "Kinesin is involved in regulation of rat pancreatic amylase secretion." *Gastroenterology* 119(4): 1123-1131.

Unger, M. L., M. Hokland, et al. (1997). "High dose IL-2-activated murine natural killer (A-NK) cells accumulate glycogen and granules, lose cytotoxicity, and alter target cell interaction in vitro." *Scandinavian Journal of Immunology* 45(6): 623-636.

Valentijn, J. A., K. Valentijn, et al. (2000). "Actin coating of secretory granules during regulated exocytosis correlates with the release of rab3D." *Proceedings of the National Academy of Sciences of the United States of America* 97(3): 1091-1095.

Verhage, M. and R. F. Toonen (2007). "Regulated exocytosis: merging ideas on fusing membranes." *Current Opinion in Cell Biology* 19(4): 402-408.

Verstreken, P., T. W. Koh, et al. (2003). "Synaptojanin is recruited by endophilin to promote synaptic vesicle uncoating." *Neuron* 40(4): 733-748.

Vitorino, R., M. J. Lobo, et al. (2004). "Identification of human whole saliva protein components using proteomics." *Proteomics* 4(4): 1109-1115.

Wagner, A. C., M. J. Wishart, et al. (1994). "GP-3, a newly characterized glycoprotein on the inner surface of the zymogen granule membrane, undergoes regulated secretion." *The Journal of Biological Chemistry* 269(12): 9099-9104.

Wallace, K., C. J. Marek, et al. (2010). "Glucocorticoid-dependent transdifferentiation of pancreatic progenitor cells into hepatocytes is dependent on transient suppression of WNT signalling." *Journal of Cell Science* 123(Pt 12): 2103-2110.

Wang, B. J. and Z. J. Cui (2007). "How does cholecystokinin stimulate exocrine pancreatic secretion? From birds, rodents, to humans." *American Journal of Physiology.* 292(2): 666-678.

Wang, X., M. Kibschull, et al. (1999). "Aczonin, a 550-kD putative scaffolding protein of presynaptic active zones, shares homology regions with Rim and Bassoon and binds profilin." *The Journal of Cell Biology* 147(1): 151-162.

Wang, Y., C. Thiele, et al. (2000). "Cholesterol is required for the formation of regulated and constitutive secretory vesicles from the trans-Golgi network." *Traffic* 1(12): 952-962.

Wasle, B. and J. M. Edwardson (2002). "The regulation of exocytosis in the pancreatic acinar cell." *Cellular Signalling* 14(3): 191-197.

Watanabe, T., J. Sukegawa, et al. (1999). "A 127-kDa protein (UV-DDB) binds to the cytoplasmic domain of the Alzheimer's amyloid precursor protein." *Journal of Neurochemistry* 72(2): 549-556.

Waters, M. G. and F. M. Hughson (2000). "Membrane tethering and fusion in the secretory and endocytic pathways." *Traffic* 1(8): 588-597.

Wendler, F., L. Page, et al. (2001). "Homotypic fusion of immature secretory granules during maturation requires syntaxin 6." *Molecular Biology of the Cell* 12(6): 1699-1709.

Wessel, D. and U. I. Flugge (1984). "A method for the quantitative recovery of protein in dilute solution in the presence of detergents and lipids." *Analytical Biochemistry* 138(1): 141-143.

Williams, J. A. (2001). "Intracellular signaling mechanisms activated by cholecystokinin-regulating synthesis and secretion of digestive enzymes in pancreatic acinar cells." *Annual Review of Physiology* 63: 77-97.

Williams, J. A., X. Chen, et al. (2009). "Small G proteins as key regulators of pancreatic digestive enzyme secretion." *American Journal of Physiology Endocrinology and Metabolism* 296(3): 405-414.

Yang, G., Y. D. Gong, et al. (2005). "Reduced synaptic vesicle density and active zone size in mice lacking amyloid precursor protein (APP) and APP-like protein 2." *Neuroscience Letters* 384(1-2): 66-71.

Yoo, S. H. (1993). "pH-dependent association of chromogranin A with secretory vesicle membrane and a putative membrane binding region of chromogranin A." *Biochemistry* 32(32): 8213-8219.

Yoo, S.H. (1995). "Purification and pH-dependent secretory vesicle membrane binding of chromogranin B." *Biochemistry* 34(27): 8680-8686.

Young-Pearse, T. L., J. Bai, et al. (2007). "A critical function for beta-amyloid precursor protein in neuronal migration revealed by in utero RNA interference." *The Journal of Neuroscience* 27(52): 14459-14469.

Young-Pearse, T. L., A. C. Chen, et al. (2008). "Secreted APP regulates the function of full-length APP in neurite outgrowth through interaction with integrin beta1." *Neural Development* 3: 15.

Yu, S., Y. Hao, et al. (2004). "Effects of GP2 expression on secretion and endocytosis in pancreatic AR4-2J cells." *Biochemical Biophysical Reseach Communications* 322(1): 320-325.

Yu, S. and A. W. Lowe (2009). "The pancreatic zymogen granule membrane protein, GP2, binds Escherichia coli Type 1 fimbriae." *Gastroenterology* 9: 58.

Yu, S., S. A. Michie, et al. (2004). "Absence of the major zymogen granule membrane protein, GP2, does not affect pancreatic morphology or secretion." *The Journal of Biological Chemistry* 279(48): 50274-50279.

Yule, D. I., C. W. Baker, et al. (1999). "Calcium signaling in rat pancreatic acinar cells: a role for Galphaq, Galpha11, and Galpha14." *The American Journal of Physiology* 276: G271-279.

Zachowski, A., J. P. Henry, et al. (1989). "Control of transmembrane lipid asymmetry in chromaffin granules by an ATP-dependent protein." *Nature* 340(6228): 75-76.

Zhou, Y. B., J. B. Cao, et al. (2007). "hZG16, a novel human secreted protein expressed in liver, was down-regulated in hepatocellular carcinoma." *Biochemical and Biophysical Research Communications* 355(3): 679-686.

Appendix

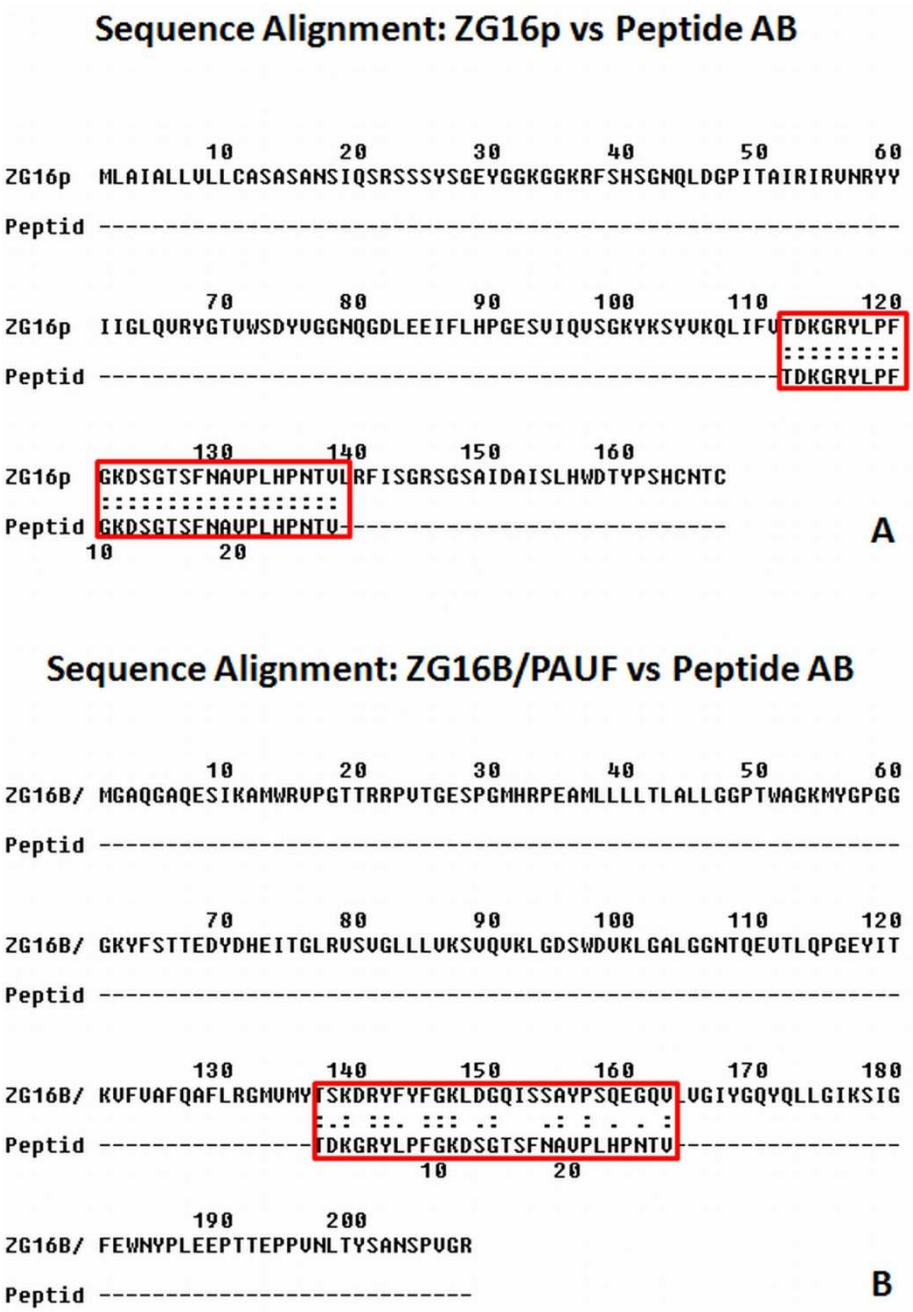

Supplementary Figure 1: Sequence alignement of ZG16p against the peptide sequence used to generate peptide antibody (red box) (A). (B) Sequence alignement of the ZG16p paralogue ZG16bp/PAUF against the peptide sequence which was used to generate the peptide antibody (red box). Due to the alignment result a recognition of PAUF by the peptide antibody can not be excluded. But based on a lower sequence agreement the recognition of PAUF is supposedly less efficient then the one of ZG16p.

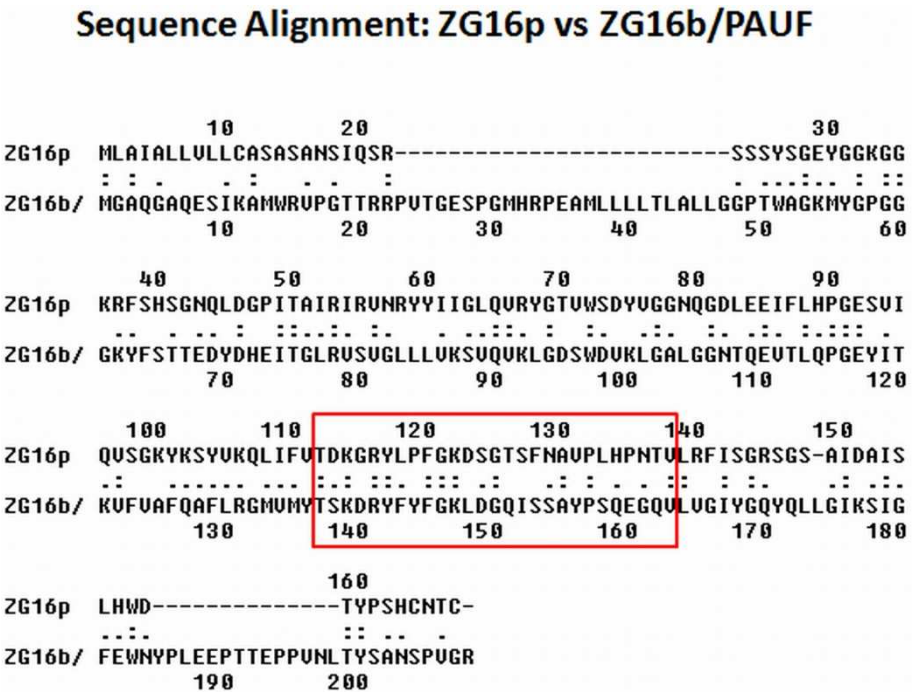

Supplementary Figure 2: Sequence alignement of ZG16p against the ZG16p paralogue ZG16bp/PAUF highlighting the recognition sequence for the peptide AB in the red box. ZG16bp/PAUF is to 30% identical (double dots) to ZG16p, 18% of amino acids are conserved substitutes (one dot) and around 14% are semi-conserved amino acids.

ZG16 from rat brain forward sequence

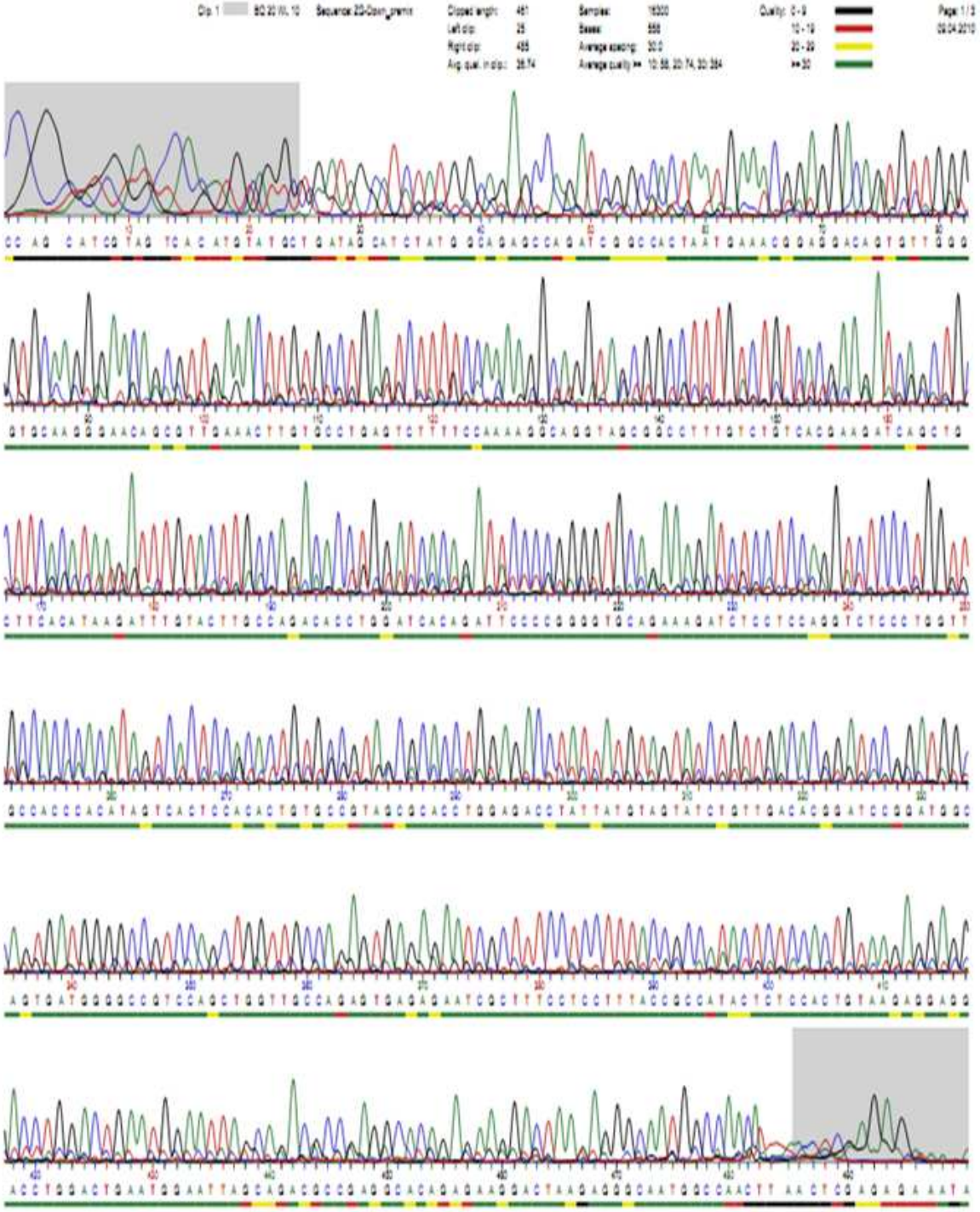

ZG16 from rat brain reverse sequence

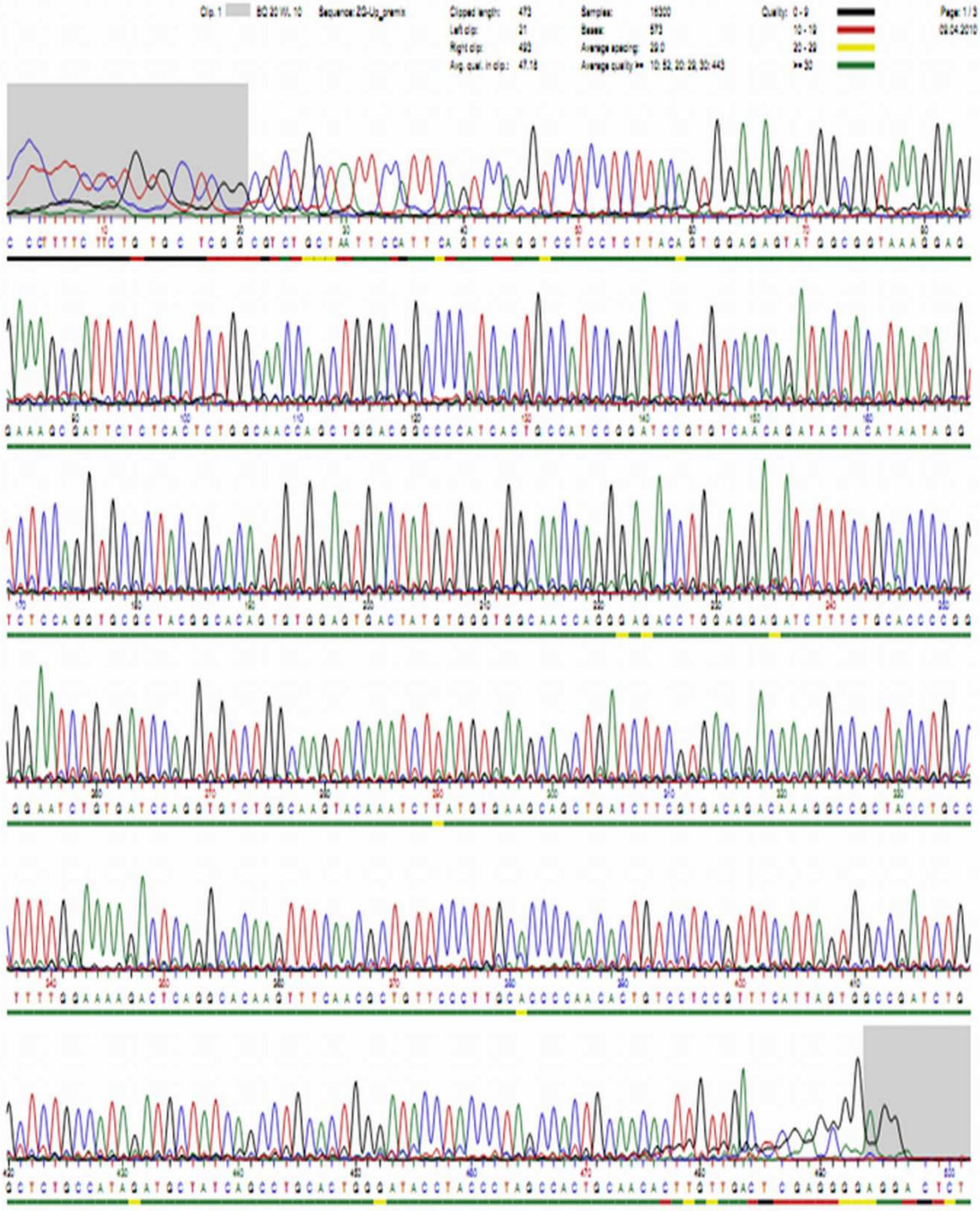

Sequence alignment of rat pancreatic ZG16 vs ZG16 obtained by PCR from rat brain

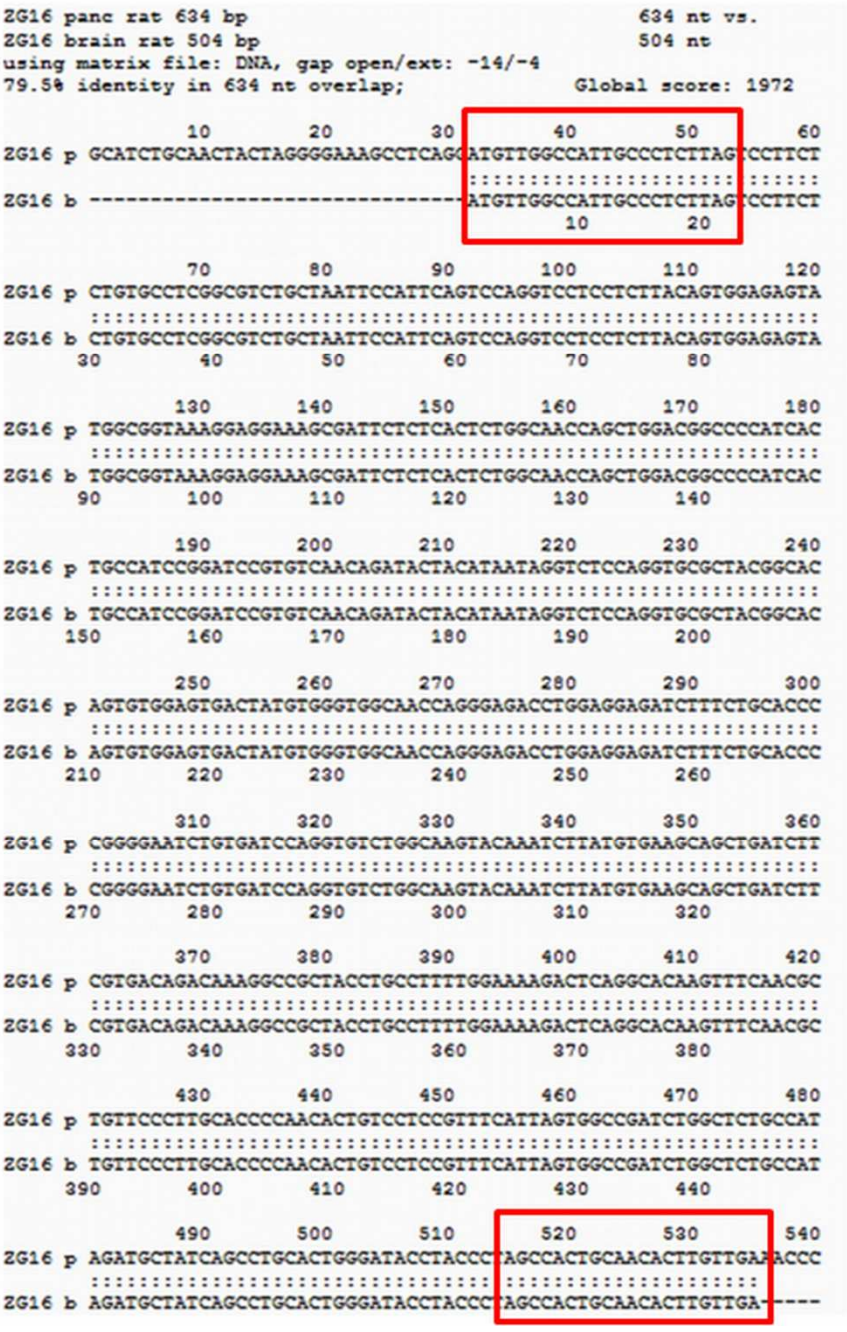

Supplementary Figure 3: Sequence alignment of rat pancreatic ZG16 mRNA versus the rat brain ZG16 mRNA/cDNA sequence. Red boxes mark primer sites.

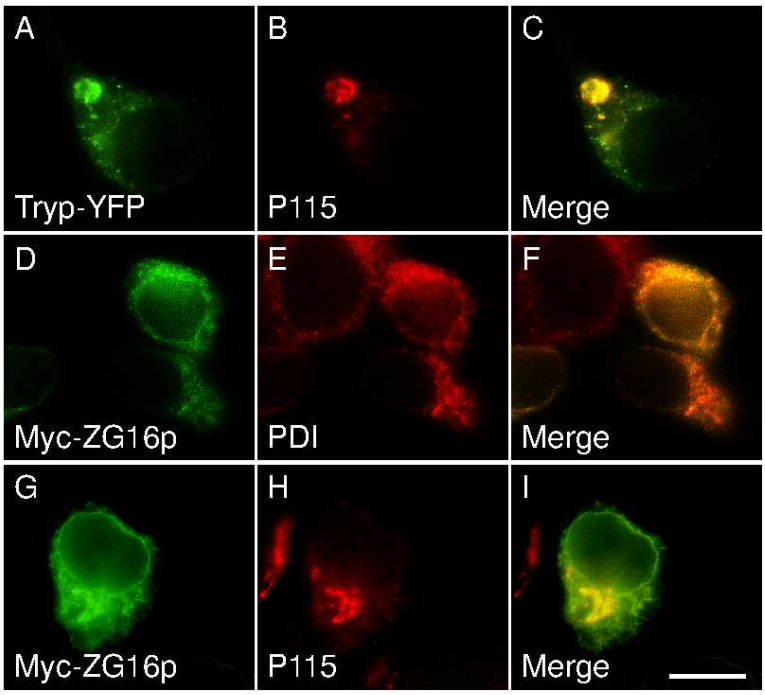

Supplementary Figure 4: Example of the localisation of the ZG protein constructs in unstimulated AR42J cells in the ER and Golgi compartment. Unstimulated AR42J cells transfected with trypsinogen-YFP, or Myc-ZG16p were processed for indirect immunofluorescence after 2-3 days in culture and labelled with antibodies directed to ZG16p, p115 as Golgi marker and PDI as ER marker. Images were acquired on an Olympus IX81 fluorescence microscope. Scale bars, 10 μm.

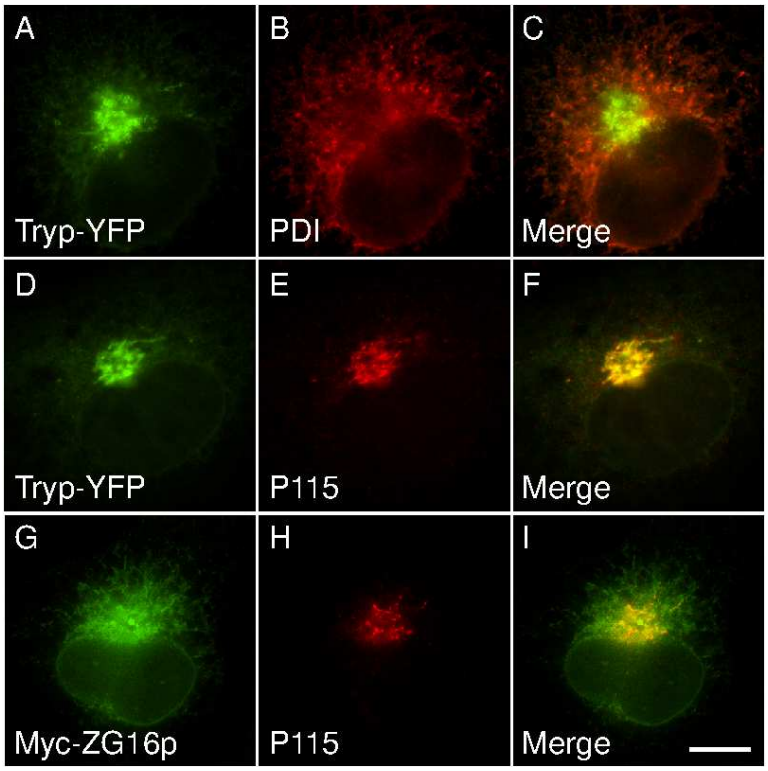

Supplementary Figure 5: Example of the localisation of the ZG protein constructs in COS-7 cells in the ER and Golgi compartment. COS7 cells transfected with trypsinogen-YFP, or Myc-ZG16p were processed for indirect immunofluorescence after 1-2 days in culture and labelled with antibodies directed to ZG16p, p115

as Golgi marker and PDI as ER marker. Images were acquired on an Olympus IX81 fluorescence microscope. Scale bars, 10 μm.

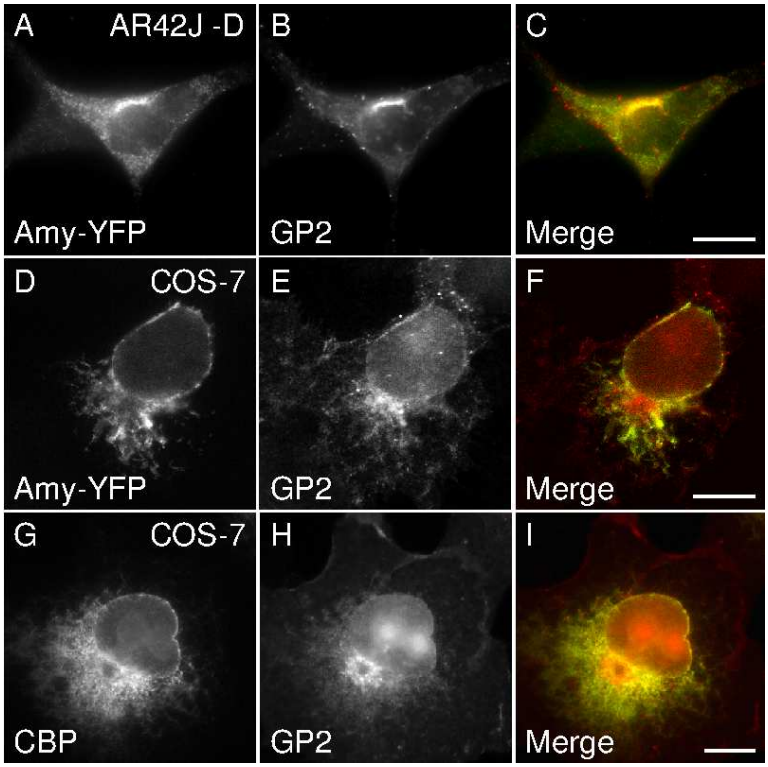

Supplementary Figure 6: Example for double transfected unstimulated AR42J and COS-7 cells. Unstimulated AR42J cells (A-C) and COS-7 cells (D-F) were double transfected with amylase-YFP and GP2 and were processed for indirect immunofluorescence after 2-3 days in culture and labelled with an antibody directed to GP2. (G-I) show double COS-7 cells double transfected with carboxypeptidase A and GP2 and were processed for indirect immunofluorescence after 2-3 days in culture and labelled with antibodies directed to GP2 and carboxypeptidase A. Images were acquired on an Olympus IX81 fluorescence microscope. Scale bars, 10 μm.

Publications Emerged From This Thesis:

Rinn C., and Schrader M. “Modulating zymogen granule formation in pancreatic AR42J cells.” (about to be submitted).

Rinn C., Aroso M., and Schrader M. The secretory lectin ZG16p. The Pancreapedia: Exocrine Pancreas Knowledge Base, DOI: 10.3998/panc.2011.17

Gomez-Lazaro M., **Rinn C**., Aroso M., and Schrader M. “Proteomic analysis of zymogen granules.” Expert Rev. Proteomics. 2010 Oct; 7 (5): 735-47.

Borta H., Aroso M., **Rinn C**., Gomez-Lazaro M., Vitorino R., Zeuschner D., Grabenbauer M., Amado F., and Schrader M. “Analysis of low abundant membrane-associated proteins from rat pancreatic zymogen granules.” J. Proteome Res. 2010 Oct 1; 9 (10): 4927-39.

Other scientific presentations

Aroso M., Gómez Lázaro M., **Rinn C.**, Vitorino R., Amado F., and Schrader M. “Suborganellar proteomics: Getting a grip on pancreatic zymogen granule membrane proteins”. 5th Portuguese ProCura Meeting on Proteomics and Mass Spectrometry; in conjunction with the 1st International Congress on Analytical Proteomics (1ST ICAP), September 30-October 3, 2009. Caparica (Lisbon), Portugal.

Rinn C., Gómez Lázaro M., Vitorino R., Amado F., and Schrader M. “Secretory granule biogenesis in exocrine and neuroendocrine cells: Same or different?” Hands-on course on Proteins and Proteomics. July 12-25, 2008. Faculdade de Ciencias e Tecnologia, Universidade Nova de Lisboa. Portugal. (Poster)

Gómez Lázaro M., **Rinn C.**, Faust F., Borta H., Vitorino R., Amado F., and Schrader M. "Suborganellar proteomics: Identification and characterization of pancreatic zymogen granule membrane proteins." 4th Annual ProCura-RNEM meeting on Proteomics and Mass Spectrometry. Nov. 10-11, 2007. Aveiro, Portugal. (BEST POSTER AWARD)

Previous Publication:

Mascarenhas J., Volkov A.V., **Rinn C**., Schiener J., Guckenberger R., Graumann P.L. “Dynamic assembly, localization and proteolysis of the Bacillus subtilis SMC complex.” BMC Cell Biol. 2005 Jun 29; 6:28.

Rahe N., **Rinn C**., Carell T. "Development of Donor/Acceptor Modified DNA Hairpins for the Investigation of Charge Hopping Kinetics in DNA" Chem. Comm. 2003, 2120-2121.